ZooKeys 1080: 1–19 (2022)
doi: 10.3897/zookeys.1080.76876
https://zookeys.pensoft.net

RESEARCH ARTICLE

A peer-reviewed open-access journal
ZooKeys
Launched to accelerate biodiversity research

A new genus of bamboo culm tarantula from Thailand (Araneae, Mygalomorphae, Theraphosidae)

Chaowalit Songsangchote[1], Zongtum Sippawat[2], Wuttikrai Khaikaew[3], Narin Chomphuphuang[4]

1 *Faculty of Forestry, Kasetsart University, Bangkok, 10900, Thailand* **2** *160 village no. 7, Mae Tho, Mueang Tak district, Tak, Thailand* **3** *5 village no. 8, Angthong sub-district, Chiang Kham district, Phayao, Thailand* **4** *Department of Entomology and Plant Pathology, Faculty of Agriculture, Khon Kaen University, Khon Kaen, Thailand*

Corresponding author: Narin Chomphuphuang (Narich@kku.ac.th)

Academic editor: Chris Hamilton | Received 21 October 2021 | Accepted 13 December 2021 | Published 4 January 2022

http://zoobank.org/EE1AD1FD-7318-4197-B0D9-2FCA537771B2

Citation: Songsangchote C, Sippawat Z, Khaikaew W, Chomphuphuang N (2022) A new genus of bamboo culm tarantula from Thailand (Araneae, Mygalomorphae, Theraphosidae). ZooKeys 1080: 1–19. https://doi.org/10.3897/zookeys.1080.76876

Abstract

Bamboo plays an important role in the animal world, including providing a nutritious food source, shelter, and habitat. Inside of bamboo culm, we discovered a new genus of tarantula, which we describe here as *Taksinus* **gen. nov.** (♂♀). Specimens of this new tarantula were collected from Mae Tho, Mueang Tak district, Tak province, in Thailand, making it geographically distant from any other arboreal genera. Genital morphology was used to diagnose its genus, which is supported by distributional data, natural history, morphological characters, and photographic illustrations of the male and female. Diagnosis of the new genus was determined by distinguishing its different characters from those of other arboreal theraphosid spiders distributed throughout Southeast Asia. This tarantula's specialization is that it lives in the stalks of the Asian bamboo *Gigantochloa* sp.

Keywords

Arboreal theraphosid, *Lampropelma*, *Melognathus*, *Omothymus*, *Phormingochilus*, *Taksinus*

Introduction

Theraphosidae Thorell, 1869, which are commonly known as tarantulas, comprises the most diverse family among Mygalomorphae Pocock, 1892, with over 1,000 species currently described (World Spider Catalog 2021). Asian tarantulas in the subfamily Ornithoctoninae Pocock, 1895, which are commonly known as earth tigers, were originally established by Pocock (1895). In this subfamily, four arboreal theraphosid genera have been recognized: *Omothymus* Thorell, 1891, *Lampropelma* Simon, 1892 *Phormingochilus* Pocock, 1895, and *Melognathus* Chamberlin, 1917. Tarantulas have not been observed to disperse aerially and thus have limited dispersal capabilities and habitat fidelities (Hendrixson et al. 2013). The type of localities and distribution of the Southeast Asian arboreal tarantula differ, as some species are restricted to a specific island; therefore, the spider's location can be used to alongside morphology to diagnose species (Gabriel and Sherwood 2019). *Lampropelma* has been found in Indonesia (Sangihe Island and Sulawesi); *Omothymus* was reported in Malaysia, Singapore, and Sumatra; *Phormingochilus* currently contains four species, which are restricted to Borneo. The type locality of *Melognathus* is unclear. It was formerly reported as "East Indies? Philippines?" (Chamberlin 1917). In this study, we report a new genus, *Taksinus* gen. nov., discovered in northern Thailand, which is geographically distant from any previous record of the Asian arboreal species (Figs 1, 2). Historically, the taxonomy of arboreal Ornithoctoninae has been based primarily on unstable taxonomic characters, resulting in highly problematic identification characters being used before 2019. Pocock (1895) distinguished the genus *Phormingochilus* from *Omothymus* based on the anterior narrowness of the sternum. In the key of the Ornithoctoninae, Raven (1985) distinguished *Phormingochilus* based on the breadth of the ocular tubercle and the low caput. He defined *Lampropelma* from *Cyriopagopus* by the presence of brush setae on the retrolateral palpal femur. Smith (1994) proposed that the genus *Phormingochilus* could be distinguished by an absence of tibial apophyses and brush setae on the retrolateral face of the palpal femur, while exhibiting twin spermathecae. Smith and Jacobi (2015) reported that *Lampropelma*, *Omothymus*, and *Phormingochilus* share the following characteristics: a wide ocular tubercle, spermathecae with twin seminal receptacles, and low caput, whereas terrestrial tarantulas, such as *Cyriopagopus* have an extremely raised caput on the carapace. Recently, Gabriel and Sherwood (2019) revised the arboreal Ornithoctoninae and proposed stable taxonomic features, which clearly delineated the subfamily Ornithoctoninae, especially based on the male palpal bulb and tibial apophyses, which remain constant and relevant for characterizing arboreal species and genera. The comparative female leg measurements and geographic distribution can be used to further elucidate these taxa. Thailand currently has two genera of the tarantula subfamily Ornithoctoninae: *Ornithoctonus* Pocock, 1892 and *Cyriopagopus* Simon, 1887 (World Spider Catalog 2021). The newly recorded arboreal *Taksinus* gen. nov. was discovered in an extraordinary habitat, namely, bamboo culms with silken retreat tubes covering the stem cavity (Fig. 1A, B). The type localities of

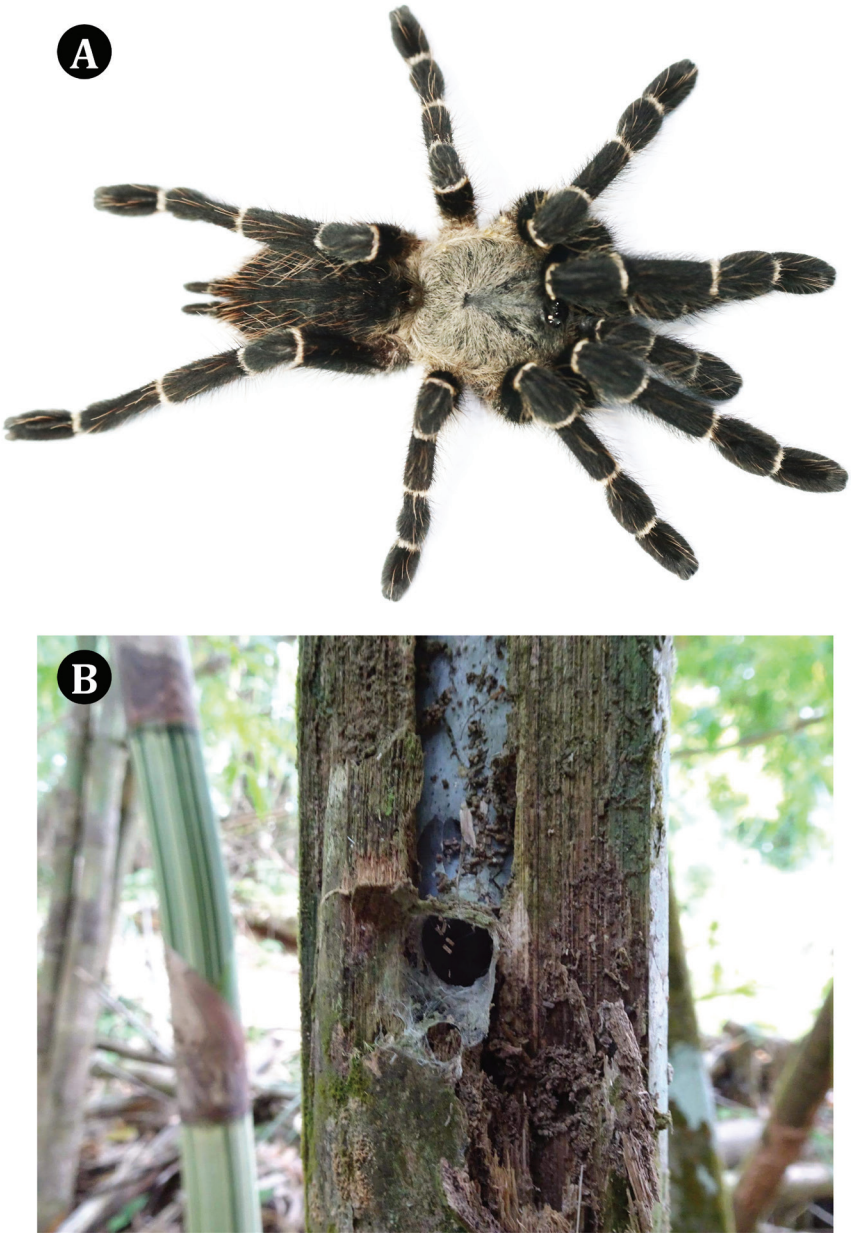

Figure 1. *Taksinus bambus* sp. nov. paratype ♀, TAK2 **A** dorsal view **B** habitat in bamboo culm.

Taksinus gen. nov. and some Southeast Asian arboreal Ornithoctoninae are shown in Figure 2. We describe and provide illustrations of the body and copulatory organs, as well as information on the natural history and morphological characteristics that distinguish the new genus from other arboreal Ornithoctoninae.

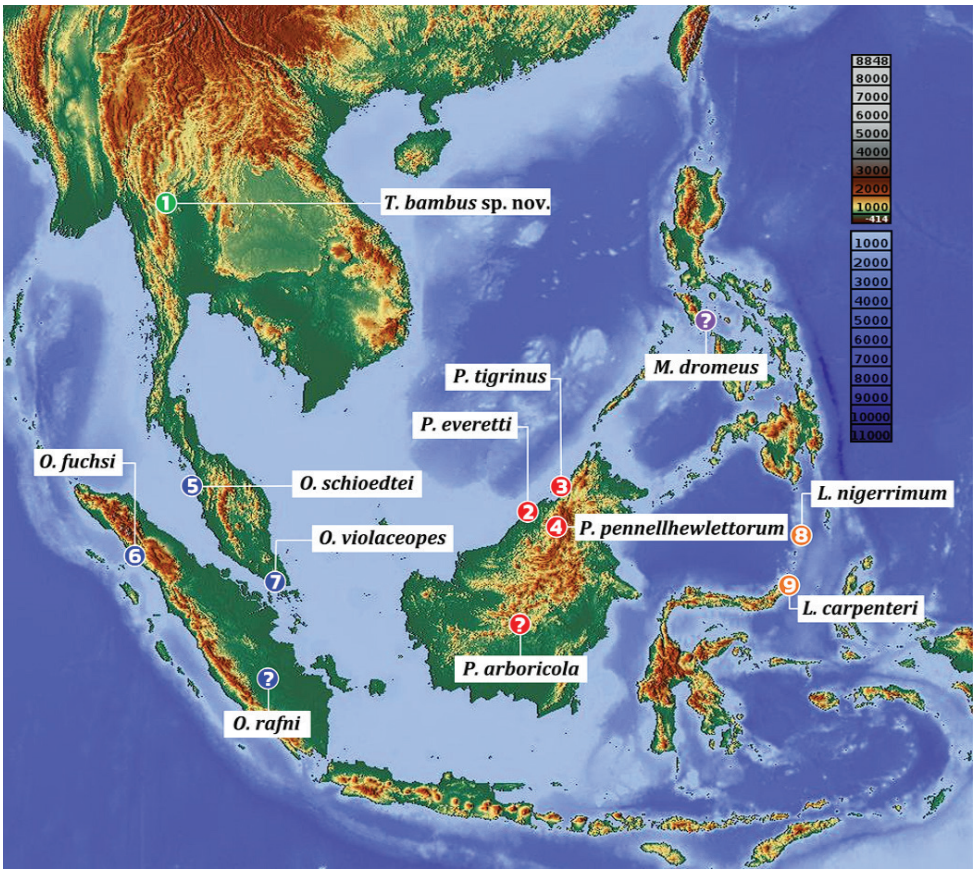

Figure 2. Distribution records of *Taksinus bambus* sp. nov. from Tak province, Thailand, and some arboreal Ornithoctoninae (Gabriel and Sherwood 2019), which demonstrate the separation of the genera by color. The topographic map of Southeast Asia and data were obtained from OpenStreetMap and OpenStreetMap Foundation OpenStreetMap (https://www.openstreetmap.org).

Materials and methods

Specimens were collected in Tak province, Thailand, on 21 July 2020. All tarantulas were preserved in 95% ethanol. Specimens were transferred to the Department of Entomology and Plant Pathology, Khon Kaen University, Khon Kaen, Thailand (ENTOKKU), for dissection and identification. The total body length, including cephalothorax and abdomen without spinnerets and appendage segments, were measured using digital vernier calipers. Diagnostic features and genitalia were photographed using a digital camera mounted to the phototube of a Nikon SMZ745T stereomicroscope, and the NIS-Elements D program was employed for measurement and counting morphology. Appendage measurements were made dorsally along the central axis of the measured structures from the left side and recorded in millimeters (mm). The length ratio of leg I–leg IV multiplied by 100 (von Wirth and Striffler

2005) was used to calculate the relation factor (RF), which was compared with data from Gabriel and Sherwood (2019) who proposed the difference between the total lengths of leg I and IV to show the distinct characteristics of *Phormingochilus*, *Lampropelma*, and *Omothymus*. The leg formula, with the leg length in decreasing order, is also provided. Unless otherwise noted, the color of the morphological character was observed in ethanol-preserved specimens. Female genitalia were dissected and cleared in 3 M aqueous KOH solution. Specimens were identified by comparing them to related species (Smith and Jacobi 2015; Gabriel and Sherwood 2019). Specimens are deposited in the Entomology Museum, Faculty of Agriculture, Khon Kaen University (**ENTOKKU**) in Khon Kaen, Thailand, and the Natural History Museum of the National Science Museum (**THNHM**) in Pathum Thani, Thailand. The following abbreviations are used in the text to describe characters: **AER** = anterior eye row; **AME** = anterior median eyes; **ALE** = anterior lateral eyes; **PER** = posterior eye row; **PME** = posterior median eyes; **PLE** = posterior lateral eyes, **MOA** = median ocular area, **PLS** = posterior lateral spinnerets; **PME** = posterior median eyes; **PMS** = posterior median spinnerets, **Fem** = femur, **Pat** = patella, **Tib** = tibia, **Met** = metatarsus, **Tar** = tarsus. The terminology for leg spines is based on Petrunkevitch (1925), with modifications proposed by Bertani (2001): **r** = retrolateral, **p** = prolateral, **d** = dorsal, and **v** = ventral. If all the spines in the apical part were apically positioned, the term "apical" would be used to refer to their position.

Other material examined

Omothymus sp. 2 ♂ Surat Thani and Chumphon, Thailand.
Omothymus sp. 1 ♀ specimen was donated from an unknown locality.
Cyriopagopus albostriatus (Simon, 1886) 2 ♀ Saraburi, Thailand.
Cyriopagopus minax (Thorell, 1897) 3 ♀ Chiang Mai, Thailand.
Cyriopagopus lividus (Smith, 1996) 1 ♂ Chanthaburi and 4 ♀ Trat, Thailand.
Cyriopagopus longipes (von Wirth & Striffler, 2005) 1 ♂ and 5 ♀ Ubon Ratchathani, Thailand.
Ornithoctonus aureotibialis von Wirth & Striffler, 2005 2 ♀ Chumphon, 2 ♀ Ranong, and 2 ♀ Krabi, Thailand.
Ornithoctonus costalis (Schmidt, 1998) 2 ♀ Phetchaburi, Thailand.

Taxonomy

Mygalomorphae Pocock, 1892
Theraphosidae Thorell, 1869
Ornithoctoninae Pocock, 1895

Included genera: *Citharognathus*, *Cyriopagopus*, *Lampropelma*, *Melognathus*, *Ornithoctonus*, *Phormingochilus*, *Taksinus* gen. nov.

***Taksinus* Songsangchote, Sippawat, Khaikaew & Chomphuphuang, gen. nov.**
http://zoobank.org/AB5E52BE-415F-415E-91AC-1155EA142B1D

Type species. *Taksinus bambus* Songsangchote, Sippawat, Khaikaew & Chomphuphuang, 2021 from Tak, Thailand.

Diagnosis. The characteristics of *Taksinus* gen. nov. that differ from *Ornithoctonus* and *Cyriopagopus* are: a low caput, a clypeus that is less than the width of the median ocular quadrangle (Fig. 6A), and spermathecae with twin seminal receptacles (Fig. 7E, F) (Raven 1985; von Wirth and Striffler 2005; Smith and Jacobi 2015). The new genus differs from *Citharognathus* by the lack of incrassate tibia and metatarsus IV. *Taksinus* gen. nov. differs from *Lampropelma* by the absence of a dense brush of hair on the retrolateral side of the femora of the front limbs (von Wirth and Striffler 2005) and males by lack of apical embolus swelling (Fig. 5A–E; see Gabriel and Sherwood 2019: 143, figs 17, 18). *Taksinus* gen. nov. can be distinguished from *Omothymus* by male palpal bulb with a gently curved embolus with rounded embolic apex (Fig. 5A–E) vs palpal bulb steep angle embolus and apex with a sharp point in *Omothymus* (Fig. 5F–J; see Gabriel and Sherwood 2019: 139, figs 1–5). *Taksinus* gen. nov. differs from *Phormingochilus* by the lack of a single megaspine on the inside of the male tibial apophyses (Fig. 4A, B; see Smith and Jacobi 2015: 41, fig. 38; Gabriel and Sherwood 2019: 142, figs 14–16), a short embolus compared to palpal bulb length (1:1) (Fig. 5A–E), and the geographic distribution of *Phormingochilus* currently restricted to Borneo.

Etymology. The generic name was named Phraya Tak (governor of Tak province), which is in honor of Taksin the Great, king of the Thonburi Kingdom, in commemoration of his early career.

Description. Carapace longer than wide, low caput. Fovea deep, straight (males) or slightly procurved (females). Clypeus short, less than width of median ocular quadrangle in males and females. Eight eyes arranged on tubercle, anterior eye row slightly procurved and the posterior row straight. Outer cheliceral on lower surface from margin with five slightly curved pad of plumose setae on the retrolateral chelicerae. Maxillae longer than wide with >155 cuspules (male) or 149–183 (females), two horizontal rows of 10–11 stout thorn-like spines on the lower half of prolateral maxillae (below suture) and one horizontal row of six stout thorn-like spines on the upper half of prolateral maxillae (above suture). Spines of varying lengths, with the longest being at the top of the series; combined to form a stridulating organ. Labium wider than long, with 75 cuspules (male) or 125 (females). Sternum longer than wide, with two pairs of ovoid sigillae; Posterior sigilla is significantly remote from the edge, middle sigilla is close to the margin, and anterior sigilla is indistinguishable. Legs: formula 1423 (males); ± Total lengths of legs I and IV = 0.48, 4123 (females) ± Total lengths of legs I and IV = 2.41–3.33, RF = 101 (males) or 90.6–93 (females). Scopulae distinct, thickly set on tarsus; ventral surface not divided. Tibial spur capped with multitude of thin, short black spines, with no single megaspine on the inside of the tibial apophyses. Palpal bulb is ellipsoid and partly concave, embolus short compared to palpal bulb length (1:1), moderately curved, rounded apex, with single retrolateral

keel. Spermathecae have twin seminal receptacles, rounded tombstone receptacles, fused in the basal region.

Distribution. Tak province, Thailand

***Taksinus bambus* Songsangchote, Sippawat, Khaikaew & Chomphuphuang, sp. nov.**
http://zoobank.org/B377A56A-9162-412D-8AF9-462759CF8F4F
Figures 1, 3, 4, 5A–E, 6–8

Type material. Thailand • ***Holotype*** 1 ♂ (TAK1); Mae Tho, Mueang Tak district, Tak province. ***Paratype*** 2 ♀ (TAK 2–3 ♀); the same data as the holotype. Specimens were deposited at ENTOKKU (holotype TAK1 ♂ and paratype TAK2 ♀ ID: ENTOKKU TAK1–2) and THNHM (paratype TAK3 ♀ ID: THNHM-Ar-00005).

Diagnosis. Same as for the genus.

Etymology. The species name *bambus* refers to the species, which was discovered in a bamboo plantation and lives in Asian bamboo stalks.

Description. Male TAK1 holotype (ENTOKKU): color in life: leg black, carapace brownish yellow. Total length (including chelicerae) 26.30 mm; cephalothorax 11.09 mm long, 7.62 mm wide, 4.40 mm high (caput); fovea 2.28 mm wide, straight, deep; cephalothorax brown, with a cover of short, whitish-yellow hairs dorsally, long whitish-yellow hairs on lateral margins; clypeus 0.23 mm; ocular tubercle 1.50 mm long, 2.59 mm wide. The anterior eye row slightly procurved and posterior row straight; eyes whitish, ALE oval and larger than the round AME; Eye sizes: AME, 0.45 mm; ALE, 0.88 mm; PLE, 0.48 mm; PME, 0.31 mm. Inter-eye distances: AME–AME, 0.62 mm; AME–ALE, 0.32 mm; AME–PME, 0.30 mm; ALE–ALE, 1.90 mm; ALE–PME, 0.34 mm; PME–PME, 1.40 mm; PME–PLE, 0.10 mm; PLE–PLE, 2.00 mm; and ALE–PLE, 0.32 mm. Chelicerae dark brown, 7.65 mm long, outer cheliceral face with short scopula edge with rows of orange-red setae, the lower surface of the outer cheliceral has five slightly curved plumose setae pads on the retrolateral chelicerae (Fig. 3A). Maxillae reddish brown, 6.06 mm long, 3.49 mm wide with >155 cuspules, covered with orange-red setae on the prolateral surface; stridulation organ consisting of stout thorn-like spines with 11 in two rows (7.4 mm from below suture) and six in one row (1.9 mm from above suture) on the prolateral maxillae (Fig. 3B). Labium brown, length 1.3 mm, width 2.0 mm, with >75 cuspules damaged and loss encompassing approximately 40% of the proximal edge (Fig. 3C). Sternum dark brown, covered with two hair types: strong dark and soft white; 6.41 mm long, 4.38 mm wide with two pairs of ovoid sigillae present near the lateral margins opposing coxa II and III. Sigilla: anterior pair absent; median pair 0.40 mm long, 0.25 mm wide, close to the sternal margin; posterior pair 0.79 mm long, 0.36 mm wide, 0.66 mm from the sternal margin. Abdomen 10.89 mm long, 7.71 wide, dark gray, black thickly hirsute laterally and ventrally. Legs: Pat, Tib, Met, and Tar dark brown. Length of legs and palpal segments are shown in Table 1, leg formula 1423. Spination: tibia II r 0–0–1 (apical), III r 0–0–2 (apical), metatarsus I v 0–0–1 (apical), II v 0–0–1 (apical), III d 0–0–1 (apical), v 0–0–1 (apical), IV d 0–0–1 (apical), v 0–0–3 (apical).

Figure 3. *Taksinus bambus* sp. nov. Holotype ♂ TAK1 **A** chelicerae, retrolateral view **B** maxilla, prolateral view **C** palpi, labium, maxilla, and coxae, ventral view. Scale bars: 1 mm.

Table 1. Legs and palp measurements (in mm) of the holotype ♂ TAK1 *Taksinus bambus* sp. nov.

	I	II	III	IV	Palp
Fem	12.98	12.23	9.28	12.66	7.84
Pat	5.69	5.50	5.40	5.91	3.92
Tib	11.94	10.14	7.30	10.44	6.77
Met	9.32	7.45	8.35	11.07	–
Tar	6.43	5.37	4.95	5.80	3.48
Total	46.36	40.69	35.28	45.88	22.01

The male tibia I spur is present and lacks a single megaspine on the inside of the tibial apophyses (Fig. 4A–D). Scopulae on metatarsi and tarsi I through IV, undivided. Tar I–IV with two claws; spinnerets covered with dark longer and thinner hairs; Posterior lateral spinnerets with three segments, basal 2.3 mm, median 1.5 mm, digitiform apical 3.0 mm; lateral median spinnerets with one segment 1.25 mm. Pedipalps reddish brown, covered with longer and thinner hairs; tibia swollen; cymbium with two lobes of light brown shaggy scopulae; bulb and embolus 1.76 mm long, dark reddish brown; palpal bulb ellipsoid and partly concave, 1.60 mm long, 1.63 mm wide; embolus moderately curved, rounded apex, with single retrolateral keel (Fig. 5A–E).

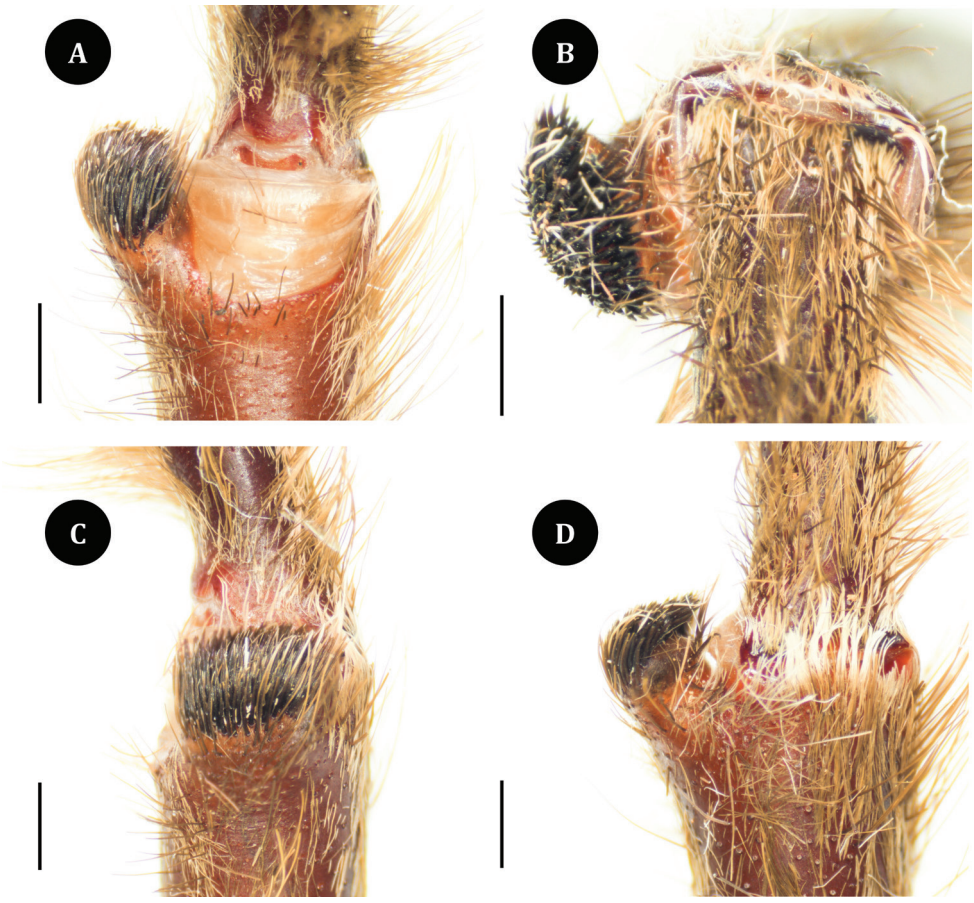

Figure 4. *Taksinus bambus* sp. nov. Holotype ♂ TAK1. Tibial apophysis **A** ventral view **B** apical view **C** prolateral view **D** dorsal view. Scale bars: 1 mm.

Paratype ♀ TAK3: total length (including chelicerae) 30.82 mm; cephalothorax 13.43 mm long, 10.39 mm wide, 2.98 mm high (caput); fovea 1.28 mm wide, slightly procurved, deep; cephalothorax brown, covered with short whitish hairs dorsally, golden yellow to yellowish-brown long hairs on lateral margins (Fig. 6A); clypeus 0.13 high; ocular tubercle 1.70 mm long, 2.92 mm wide. Anterior eyes with long hairs in front of AME and mid-posterior PME area; anterior eye row slightly procurved and posterior row straight. Eye sizes: AME, 0.45 mm; ALE, 0.71 mm; PLE, 0.54 mm; PME, 0.37 mm. Inter-eye distances: AME–AME mm, 0.47; AME–ALE, 0.41 mm; AME–PME, 0.25 mm; ALE–ALE, 1.75 mm; ALE–PME, 0.54 mm; PME–PME, 1.27 mm; PME–PLE, 0.66 mm; PLE–PLE, 1.57 mm; and ALE–PLE, 0.39 mm. Chelicerae dark brown, 6.78 mm long, outer cheliceral face with short scopula margin with rows of orange-red setae, outer cheliceral on the lower surface with five slightly curved pads of plumose setae on the retrolateral chelicerae. Maxillae reddish brown, 3.83 mm long, 2.10 mm wide with >183 cuspules, covered with orange-red setae on

Figures 5. *Taksinus bambus* sp. nov. holotype ♂ TAK1 (**A–E**) and *Omothymus* sp. ♂ (**F–J**). Palpal bulb **A** prolateral view **B** retrolateral view **C** dorsal view **D** ventral view **E** apical view **F** prolateral view **G** retrolateral view **H** dorsal view **I** ventral view **J** apical view. Scale bars: 1 mm.

the prolateral surface, labium brown, length 1.51 mm, width 2.09 mm, with >125 cuspules covering approximately 40% of the proximal edge (Fig. 6D). Sternum dark brown, covered with two types of hairs: strong dark and soft white; 5.89 mm long, 5.54 mm wide with two pairs of ovoid sigillae present near lateral margins opposite coxa II and III (Fig. 6B). Sigilla: anterior pair absent; median pair 0.35 mm long,

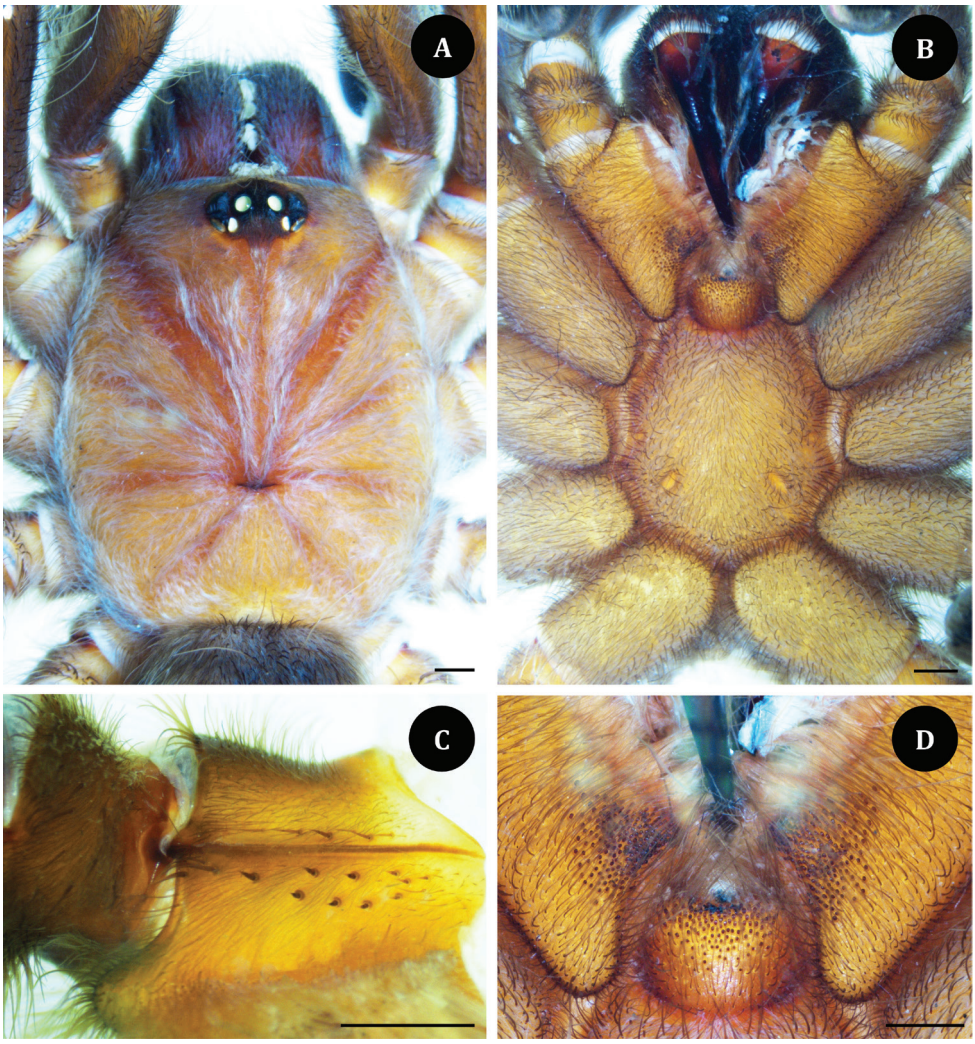

Figure 6. *Taksinus bambus* sp. nov. Paratype ♀ TAK3 (**A, B, D**) Paratype ♀ TAK2 (**C**). **A** carapace, dorsal view **B** sternum, labium, maxilla, and coxae, ventral view **C** maxilla, prolateral view **D** maxillae and labium with cuspules. Scale bars: 1 mm.

0.27 mm wide, close to the sternal margin; posterior pair 0.75 mm long, 0.32 mm wide, 0.72 mm from the sternal margin. Abdomen 15.58 mm long, 10.95 mm wide, dark gray and black thickly hirsute laterally and ventrally. Legs: Pat, Tib, Met, and Tar dark brown. Length of legs, palpal segments, and the comparative leg measurements are shown in Table 2, leg formula 4123. Spination: tibia palp r 0–0–1 (apical), p 0–0–1 (apical), r 0–0–2 (apical), I p 0–0–1 (apical), II p 0–0–1 (apical), r 0–0–1 (apical), III p 0–0–1 (apical), IV r 0–0–1 (apical), p 0–0–1 (apical), metatarsus I v 0–0–1 (apical), II v 0–0–1 (apical), III d 0–0–1 (apical), v 0–0–1 (apical), p 0–0–1 (apical), r 0–0–2 (apical), IV v 0–0–3 (apical). Scopulae on metatarsi and tarsi I through IV undivided.

Table 2. Legs and palp measurements (in mm) of paratype TAK3 ♀ *Taksinus bambus* sp. nov. from Thailand.

	I	II	III	IV	Palp
Fem	9.62	7.69	7.66	8.90	6.77
Pat	5.45	4.99	4.40	5.11	4.71
Tib	7.21	5.48	5.24	7.97	4.01
Met	5.76	4.67	5.63	8.10	–
Tar	4.20	4.21	3.84	4.57	4.81
Total	32.24	27.04	26.77	34.65	20.3

Tar I–IV with two claws; spinnerets covered with dark brown longer and thinner hairs; posterior lateral spinnerets with three segments, basal 2.03 mm, median 1.40 mm, digitiform apical 2.10 mm; lateral median spinnerets with one segment 1.21 mm. Spermathecae (Fig. 7F): paired and divided with fused in base, base 0.88 mm (left) and 1.00 mm (right) long, 1.10 mm (left) and 1.06 mm (right) wide; sclerotization heaviest apically, gradually decreasing basally.

Description. Paratype ♀ TAK2: dark brown, carapace brown. Total length (including chelicerae) 34.80 mm; cephalothorax 14.39 mm long, 11.57 mm wide, 3.16 mm high (caput); fovea 1.20 mm wide, straight, deep; cephalothorax brown, covered with short whitish hairs dorsally, golden yellow to yellowish-brown long hairs on lateral margins; clypeus 0.15 mm high; ocular tubercle 1.83 mm long, 2.70 mm wide. Anterior eyes with long hairs in front of AME and mid-posterior PME area; anterior eye row slightly procurved and posterior row straight. Eyes whitish, ALEs oval in shape, larger than the round AMEs. Eye sizes: AME, 0.44 mm; ALE, 0.69 mm; PLE, 0.59 mm; PME, 0.40 mm. Inter-eye distances: AME–AME, 0.37 mm; AME–ALE, 0.49 mm; AME–PME, 0.30 mm; ALE–ALE, 1.69 mm; ALE–PME, 0.68 mm; PME–PME, 1.20 mm; PME–PLE, 0.17 mm; PLE–PLE, 1.86 mm; and ALE–PLE, 0.50 mm. Chelicerae dark brown, 7.02 mm long, outer cheliceral face with short scopula margin with rows of orange-red setae; outer cheliceral on the lower surface with five slightly curved pad of plumose setae on the retrolateral chelicerae (Fig. 7B, C) with cheliceral needle form strikers (Fig. 7B, D). Maxillae reddish brown, 3.64 mm long, 2.21 mm wide with 149 cuspules, covered with orange-red setae on the prolateral surface, stridulation organ consisting of stout thorn-like spines with 10 in two rows (7.4 mm from below suture) and six in one row (3.0 mm from above suture) on the prolateral maxillae (Fig. 6C). Labium brown, length 2.29 mm, width 1.45 mm, with >7 cuspules damaged and lost. Sternum dark brown, covered with two types of hairs: strong dark and soft white; 6.22 mm long, 5.33 mm wide, with two pairs of ovoid sigillae present near the lateral margins opposite coxa II and III. Sigilla: anterior pair absent; median pair 0.51 mm long, 0.26 mm wide, close to the sternal margin; posterior pair 0.73 mm long, 0.32 mm wide, 0.45 mm from the sternal margin. Abdomen 18.72 mm long, 11.42 mm wide, dark gray and black thickly hirsute laterally and ventrally. Legs: Pat, Tib, Met, and Tar dark brown. Length of legs, palpal segments, and the comparative leg measurements are shown in Table 3, leg formula 4123. Spination:

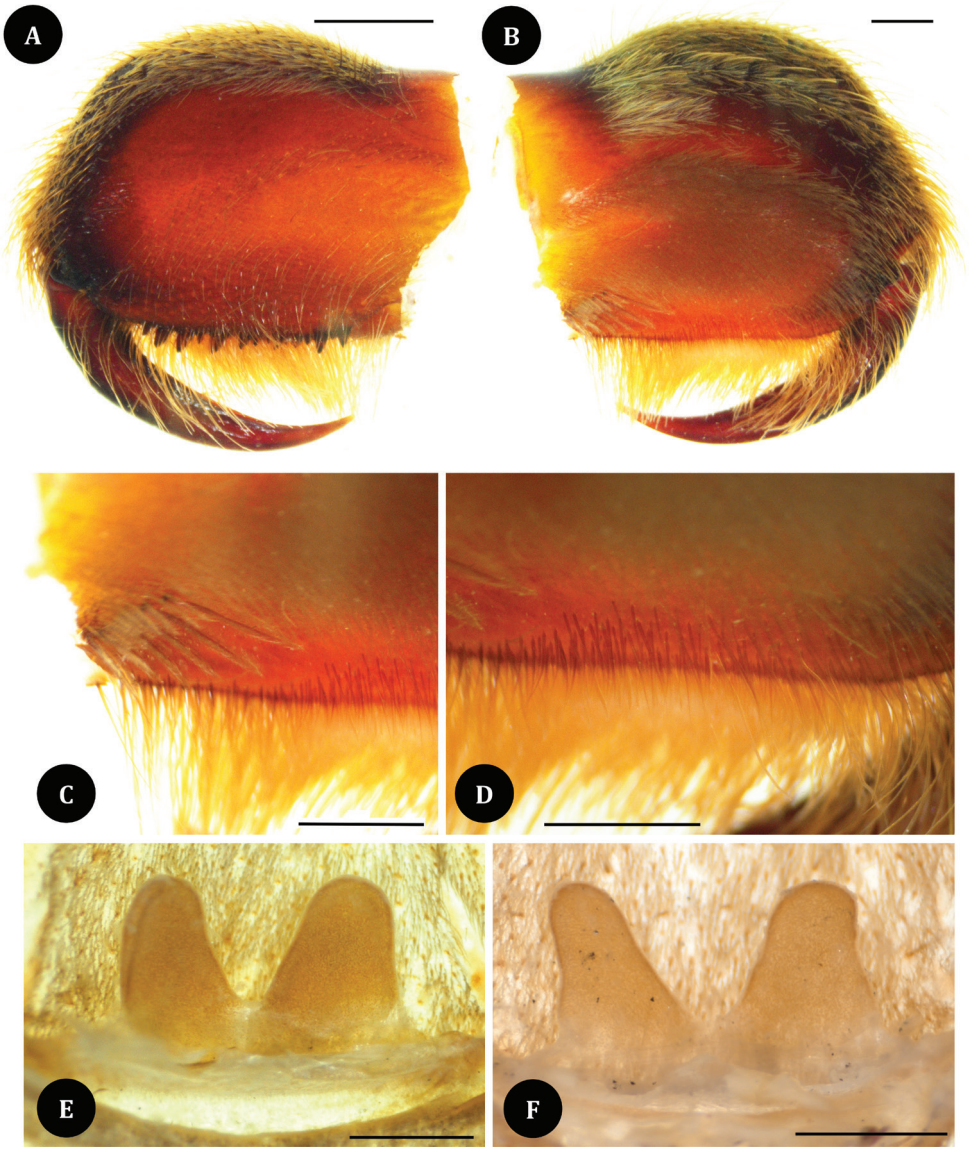

Figures 7. *Taksinus bambus* sp. nov. paratype ♀ TAK2 (**A–E**) paratype ♀ TAK3 (**F**). **A** chelicerae, prolateral view **B** chelicerae, retrolateral view **C** plumose hairs outer chelicerae, retrolateral view **D** chelicerae strikers, retrolateral view **E** spermathecae, dorsal view **F** spermathecae, dorsal view. Scale bars: 1 mm.

tibia palp r 0–0–1 (apical), p 0–0–1 (apical), r 0–0–2 (apical), I p 0–0–1 (apical), II p 0–0–1 (apical), r 0–0–1 (apical), III p 0–0–1 (apical), IV r 0–0–2 (apical), p 0–0–1 (apical), metatarsus I v 0–0–1 (apical), II v 0–0–1 (apical), III v 0–0–1 (apical), p 0–0–1 (apical), r 0–0–2 (apical), IV v 0–0–3 (apical). Scopulae on metatarsi and tarsi I through IV, undivided. Tar I–IV with two claws; spinnerets covered with dark longer

Table 3. Legs and palp measurements (in mm) of paratype TAK2 ♀ *Taksinus bambus* sp. nov. from Thailand.

	I	II	III	IV	Palp
Fem	9.33	8.46	7.08	9.67	6.59
Pat	5.07	4.04	3.6	4.58	3.39
Tib	6.66	6.37	5.33	8.25	4.23
Met	6.09	5.04	4.74	7.1	–
Tar	4.79	4.8	3.88	5.67	4.83
Total	31.94	28.71	24.63	35.27	–

and thinner hairs; posterior lateral spinnerets with three segments; basal 2.10 mm, median 1.36 mm, digitiform apical 2.19 mm; lateral median spinnerets with one segment 1.34 mm. Spermathecae (Fig. 7E): paired and divided with fused in base, base 0.90 mm (left) and 1.07 mm (right) long, 1.09 mm (left) and 1.17 mm (right) wide; sclerotization heaviest apically, gradually decreasing basally.

Distribution and natural history. Specimens were collected from villages surrounding Tak province at approximately 1,000 m elevation. The biotope consists of a mixed deciduous forest dominated by bamboo that is rarely disturbed by human activity (Fig. 8A). The new arboreal tarantula shows a surprising specialization in that it lives in the stalks of Asian bamboo (*Gigantochloa* sp.) (Fig. 8B–E). All specimens were collected from bamboo internodes in mature culms, having nest entrances approximately 2–3 cm within a silk-lined tubular burrow at the entrance located in the branch stub or at the middle of the bamboo culms. Some specimens had a secondary entrance without silk at the hole (Fig. 8B). Tarantulas do not bore bamboo stems; instead, they depend on the assistance of other animals. Bamboo is attacked by numerous animals, the most common of which are insects from the orders Coleoptera, Lepidoptera, and Diptera (Varma and Sajeev 2015). Furthermore, we hypothesized that the tarantula might occupy the empty nest of insects, such as the bamboo-nesting carpenter bee *Xylocopa*, which creates a large hole. All the tarantulas living in the bamboo culms build silken retreat tubes that cover the stem cavity (Fig. 8C–E).

Discussion and conclusion

Recently, Gabriel and Sherwood (2019) revised some arboreal Ornithoctoninae and proposed various stable morphological features that enable generic-level delineation, including the presence of the embolus rising parallel and sloping to a point at the tip, which distinguishes the genus *Omothymus* from *Phormingochilus*; embolus apical swelling in *Lampropelma* and the difference between the total lengths of leg I and IV (± 2–3 mm difference in *Phormingochilus*, ± 5 mm in *Lampropelma* and ± 10 mm in *Omothymus*) in all cases, leg I is longer than leg IV. Von Wirth and Striffler (2005) proposed a similar concept for terrestrial Ornithoctoninae called leg relation factor

Figures 8. *Taksinus bambus* sp. nov. from Tak province, Thailand **A** biotope, bamboo forests in mountainous slope areas **B** tarantula habitat in bamboo culm with entrance hole (below) and secondary entrance (upper) **C, D** tarantula in bamboo culm **E** tarantula building silk tube retreats on the cover culm **F** paratype ♀, TAK3 *T. bambus* alive.

Table 4. Comparative leg measurements of legs I and IV (female) and relation factor (RF) of arboreal Ornithoctoninae from original species descriptions or study type material.

Species (Female)	Reference from World Spider Catalog (2021) and Type material	Leg I (mm)	Leg IV (mm)	Leg formula	The total lengths of leg I minus IV in females	Relation factor (RF)
T. bambusinus sp. nov.	(paratype ENTOKKU TAK2)	31.94	35.27	4123	-3.33	90.56
T. bambusinus sp. nov.	(paratype ENTOKKU TAK3)	32.24	34.65	4123	-2.41	93.04
P. tigrinus Pocock, 1895	personal examination of this publication's reviewers (holotype BMNH 1894.6.27.1)	50.20	50.20	(1=4)23	0	100
P. tigrinus Pocock, 1895	personal examination of this publication's reviewers (holotype BMNH 1894.6.27.1)	54	53	1423	1	101.89
P. pennellhewlettorum Smith & Jacobi, 2015	*Phormingochilus pennellhewlettorum* Smith & Jacobi, 2015: 38, figs 24–40, 44–49 (holotype)	60	59	1423	1	101.7
P. everetti Pocock, 1895	*Phormingochilus everettii* Pocock, 1895: 180, pl. 10, fig. 4 (Df). (holotype BMNH 88.122)	81	79	1423	2	102.5
P. arboricola (Schmidt & Barensteiner, 2015)	*Lampropelma nigerrimum arboricola* (Schmidt & Barensteiner, 2015): 5, figs 1–4(f). (holotype)	59	57	1423	2	103.5
O. fuchsi (Strand, 1906)	*Phormingochilus fuchsi* examined by Smith, 1994: 22, fig. 16(f). (holotype MWNH 319)	71.4	65	1423	6.4	109.8
L. carpenteri (Smith & Jacobi, 2015)	*Phormingochilus carpenteri* Smith & Jacobi, 2015: 34, figs 10–16(Df). (holotype BMNH)	69.5	62	1423	7.5	112.1
O. violaceopes (Abraham, 1924)	*Lampropelma violaceopedes* (Abraham, 1924): 1108, pl. 5, figs 19–24 (holotype BMNH 1924.27.19.1.37)	90.1	80.2	1423	9.9	112.3

(RF), although Leg RF is a mathematical formula that expresses the relationship as a decimal value. We examined both methodologies and included *Taksinus* gen. nov. in our analysis, using leg measurements from original species descriptions or study type material obtained from the World Spider Catalog (2021), as shown in Table 4. The result indicated that *Taksinus* gen. nov. had the minimum difference between the total length of leg I minus IV = –3.33 to –2.41 (RF = 90.56–93.04), whereas *O. violaceopes* had the maximum height at +9.9 (RF = 112.3). According to Gabriel and Sherwood's criterion, *Taksinus* gen. nov. and *Phormingochilus* share a leg measuring range ± 2–3 mm, indicating that they belong to the same genus, although their RF are clearly dissimilar. After evaluating *Taksinus* gen. nov., we conclude that the range based on the generic number of female variations in leg I and IV length cannot be used to classify all arboreal Ornithoctoninae. Furthermore, we plot charts to show the value distribution for each species by comparing the total lengths of leg I–IV and the RF (Fig. 9). This study indicated that species on the left (red area) have a longer leg IV than their leg I (leg formula = 4123), whereas species on the right (blue area) have a longer leg I than their leg IV (leg formula = 1423). The comparative approach used in this study revealed that *Taksinus* gen. nov. appeared on the left side, with legs varying by –3.33 to –2.41 (RF = 90.56–93.04), whereas *Lampropelma* and *Omothymus* appeared on the right side with legs varying by +6.4 to +9.9 of the total length of leg I minus IV and RF greater than 100 (RF = 109–112.3). The variation in the length difference between *Phormingochilus* legs I and IV is centered on the charts, ranging from 0 to 2 (RF = 100–103.5). A visual leg length comparison of arboreal Ornithoctoninae, using

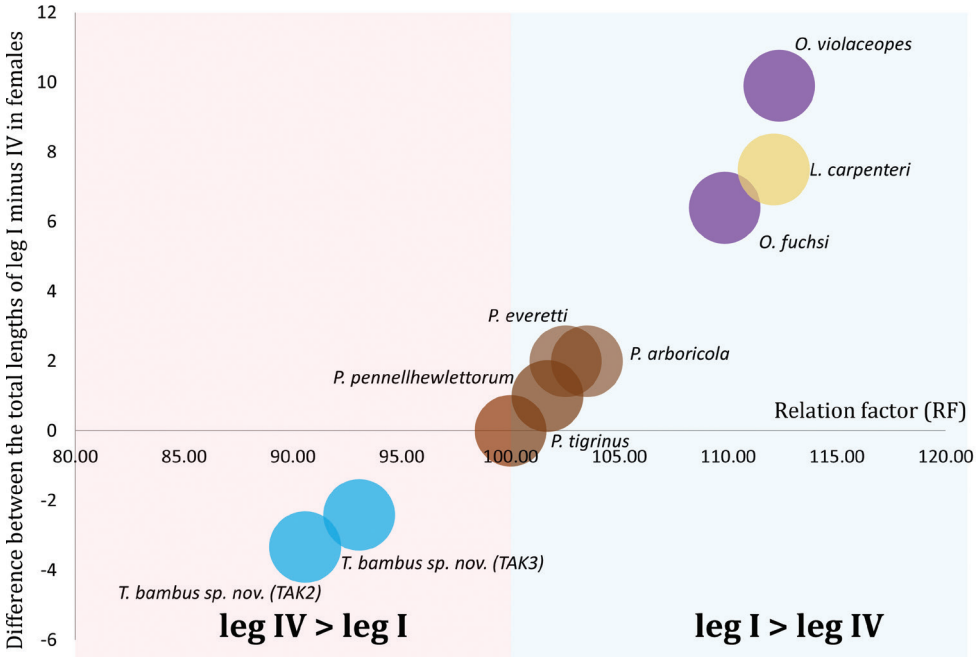

Figures 9. Scatter plot illustrating the difference between the total leg lengths I minus IV and the relation factor (RF) of arboreal Ornithoctoninae. The red area contains data indicating that species have a longer leg IV (leg formula = 4123), whereas the blue area has data indicating that species have a longer leg I (leg formula = 1423).

both methodologies is indicated in Fig. 9. Gabriel and Sherwood (2019) employed a generic number that enables rapid assessment for a defined difference of *Omothymus*, *Phormingochilus*, and *Lampropelma*, but whilst useful for those genera, *Taksinus* gen. nov. cannot be defined using this method. In contrast, the RF can be used to calculate a decimal value for leg proportions. For instance, a value greater than 100, such as *O. violaceopes* 112.3, indicates that this species has short hind legs, whereas a value less than 100 indicates that this species has long hind legs. The RF, however, was developed primarily to diagnose species rather than for higher-level delineation and needs to be further evaluated before it could be reliably used at the genus level.

Evaluation of the geographic distributions of Asia arboreal tarantula currently identified within the Ornithoctoninae subfamily—*Lampropelma*, *Omothymus*, and *Phormingochilus*, and *Taksinus* gen. nov. (Fig. 2) provided interesting data. We classified *T. bambus* in a new genus rather than *Omothymus*, which occurs in Sumatra and peninsular Malaysia due to the consistency in the morphological features of *T. bambus* sp. nov., which have a rounded, gentle curve and reduced ridges on the embolus (*Taksinus* gen. nov. Fig. 5A, B; *Omothymus* Fig. 5F–J; see Gabriel and Sherwood 2019: 139, figs 1–5), and embolus is short compared to palpal bulb length (1:1). *T. bambus* sp. nov. is closely related to *Phormingochilus* based on palpal bulb morphology (see

Gabriel and Sherwood 2019: 142, figs 9–13), with the palpal bulb's rounded apex in apical view. Based on Gabriel and Sherwood (2019), *T. bambus* sp. nov. is similar to *Phormingochilus* in terms of the total lengths of leg I and IV in females ±2.41–3.33 mm (±2–3 in *Phormingochilus*; see Gabriel and Sherwood 2019); they differ when the leg formula is calculated as the length of leg I minus that of leg IV (*Taksinus* gen. nov. are –2 to –3 while *Phormingochilus* indicated that leg I is longer with +2 to +3 of the value). Furthermore, *Phormingochilus* is found solely on Borneo Island, posing a considerable geographic barrier to northern Thailand (Fig. 2). Conclusively, our findings indicated that *Taksinus* gen. nov. showed significant differences in its morphology and comparative leg measurements compared to other Ornithoctoninae arboreal tarantulas. Nonetheless, future researchers should investigate and characterize these genera using molecular phylogenetic approaches.

Acknowledgements

We are grateful to Prof. Yupa Hanboonsong for her kindness in being a mentor of this research. Many thanks are also due to Mr Kaweesak Keeratikiat for his assistance during field collections. Special thanks are due to Mr Chawakorn Kunsete for providing the specimens used in this paper. We would like to thank Assoc. Prof. Sarawood Sungkaew for his assistance with bamboo identification. Invaluable comments were provided by Danniella Sherwood, Volker von Wirth, and Chris Hamilton who helped in significantly improving the manuscript. This research was funded by the Young Researcher Development Project of Khon Kaen University. We also acknowledge financial support from Khon Kaen University's Salt Tolerant Rice Research Group.

References

Abraham HC (1924) Some Mygalomorph Spiders from the Malay Peninsula. Proceedings of the Zoological Society of London 94: 1091–1124. https://doi.org/10.1111/j.1096-3642.1924.tb03332.x

Chamberlin RV (1917) New spiders of the family Avicolariidae. Bulletin of the Museum of Comparative Zoology. Harvard 61: 25–75.

Gabriel R, Sherwood D (2019) The revised taxonomic placement of some arboreal Ornithoctoninae Pocock, 1895 with description of a new species of *Omothymus* Thorell, 1891 (Araneae: Theraphosidae). Arachnology 18(2): 137–147. https://doi.org/10.13156/arac.2018.18.2.137

Hendrixson BE, DeRussy BM, Hamilton CA, Bond JE (2013) An exploration of species boundaries in turret-building tarantulas of the Mojave Desert (Araneae, Mygalomorphae, Theraphosidae, Aphonopelma). Molecular Phylogenetics and Evolution 66: 327–340. https://doi.org/10.1016/j.ympev.2012.10.004

Pocock RI (1895) On a new and natural grouping of some of the Oriental genera of Mygalomorphae, with descriptions of new genera and species. The Annals and Magazine of Natural History; Zoology, Botany, and Geology 15: 165–184. https://doi.org/10.1080/00222939508677863

Raven R (1985) The spider infraorder Mygalomorphae (Araneae): cladistics and systematics. Bulletin of the American Museum of Natural History 182: 1–180.

Schmidt G, Barensteiner R (2015) Ein Weibchen von *Lampropelma nigerrimum arboricola* ssp. n. aus Borneo (Araneae: Theraphosidae: Ornithoctoninae). Tarantulas of the World 143: 4–9.

Smith AM (1994) A study of the genus *Phormingochilus* with a redescription of the species described by Pocock (Araneae, Mygalomorphae, family Theraphosidae, subfamily Ornithoctinae). British Tarantula Society Journal 9: 15–22.

Smith AM, Jacobi MA (2015) Revision of the genus *Phormingochilus* with the description of three new species from Sulawesi and Sarawak and notes on the placement of the genera *Cyriopagopus*, *Lampropelma* and *Omothymus*. British. British Tarantula Society Journal 30: 25–48.

Varma RV, Sajeev TV (2015) Insect pests of bamboos in India. In: Kaushik S, Singh YP, Kumar D, Thapliyal M, Barthwal S (Eds) Bamboos in India. ENVIS Centre on Forestry, Dehradun, 227–246.

von Wirth V, Striffler BF (2005) Neue Erkenntnisse zur Vogelspinnen-Unterfamilie Ornithoctoninae, mit Beschreibung von *Ornithoctonus aureotibialis* sp. n. und *Haplopelma longipes* sp. n. (Araneae, Theraphosidae). Arthropoda 13: 2–27.

World Spider Catalog (2021) World Spider Catalog. Version 22.0. Natural History Museum Bern. http://wsc.nmbe.ch [Accessed on 2021–1–25]

ZooKeys 1080: 21–52 (2022)
doi: 10.3897/zookeys.1080.76522
https://zookeys.pensoft.net

RESEARCH ARTICLE

A peer-reviewed open-access journal
ZooKeys
Launched to accelerate biodiversity research

Seasonal and microclimatic effects on leaf beetles (Coleoptera, Chrysomelidae) in a tropical forest fragment in northeastern Mexico

José Norberto Lucio-García[1], Uriel Jeshua Sánchez-Reyes[1], Jorge Víctor Horta-Vega[1], Jesús Lumar Reyes-Muñoz[2], Shawn M. Clark[3], Santiago Niño-Maldonado[4]

1 *Tecnológico Nacional de México-Instituto Tecnológico de Cd. Victoria, Blvd. Emilio Portes Gil No. 1301, C.P. 87010. Cd. Victoria, Tamaulipas, México* **2** *Facultad de Ciencias Biológicas, Universidad Juárez del Estado de Durango. Av. Universidad S/N, Fracc. Filadelfia, 35010 Gómez Palacio, Durango, Mexico* **3** *Brigham Young University, Life Science Museum, Provo, Utah 84602, USA* **4** *Universidad Autónoma de Tamaulipas, Facultad de Ingeniería y Ciencias, Centro Universitario Victoria, C.P. 87149. Cd. Victoria, Tamaulipas, México*

Corresponding author: Santiago Niño-Maldonado (coliopteranino@hotmail.com)

Academic editor: D. D. McKenna | Received 14 October 2021 | Accepted 9 December 2021 | Published 4 January 2022

http://zoobank.org/ED0F03A2-C3FB-4CD7-9D6C-082ADD35A5C4

Citation: Lucio-García JN, Sánchez-Reyes UJ, Horta-Vega JV, Reyes-Muñoz JL, Clark SM, Niño-Maldonado S (2022) Seasonal and microclimatic effects on leaf beetles (Coleoptera, Chrysomelidae) in a tropical forest fragment in northeastern Mexico. ZooKeys 1080: 21–52. https://doi.org/10.3897/zookeys.1080.76522

Abstract

Leaf beetles (Coleoptera: Chrysomelidae) constitute a family of abundant, diverse, and ecologically important herbivorous insects, due to their high specificity with host plants, a close association with vegetation and a great sensitivity to microclimatic variation (factors that are modified gradually during the rainy and dry seasons). Therefore, the effects of seasonality (rainy and dry seasons) and microclimate on the community attributes of chrysomelids were evaluated in a semideciduous tropical forest fragment of northeastern Mexico. Monthly sampling was conducted, between March 2016 and February 2017, with an entomological sweep net in 18 plots of 20 × 20 m, randomly distributed from 320 to 480 m a.s.l. Seven microclimatic variables were simultaneously recorded during each of the samplings, using a portable weather station. In total, 216 samples were collected at the end of the study, of which 2,103 specimens, six subfamilies, 46 genera, and 71 species were obtained. The subfamily Galerucinae had the highest number of specimens and species in the study area, followed by Cassidinae. Seasonality caused significant changes in the abundance and number of leaf beetle species: highest richness was recorded in the rainy season,

with 60 species, while the highest diversity (lowest dominance and highest H' index) was obtained in the dry season. Seasonal inventory completeness of leaf beetles approached (rainy season) or was higher (dry season) than 70%, while the faunistic similarity between seasons was 0.63%. The outlying mean index was significant in both seasons; of the seven microclimatic variables analyzed, only temperature, heat index, evapotranspiration and wind speed were significantly related to changes in abundance of Chrysomelidae. Association between microclimate and leaf beetles was higher in the dry season, with a difference in the value of importance of the abiotic variables. The results indicated that each species exhibited a different response pattern to the microclimate, depending on the season, which suggests that the species may exhibit modifications in their niche requirements according to abiotic conditions. However, the investigations must be replicated in other regions, in order to obtain a better characterization of the seasonal and microclimatic influence on the family Chrysomelidae.

Keywords
Abiotic factors, community response, ecological niche, phytophagous insects, seasonal changes

Introduction

Accelerated loss of biological diversity, as well as the alterations in native ecosystems as a result of human activities, are among the most important environmental issues at a global level (Challenger and Dirzo 2009). These include land cover fragmentation, overexploitation of natural resources, pollution, and climate change (Hautier et al. 2015).

Abiotic modification produces direct effects on organisms, affecting physiology, behavior, and reproduction (Uribe-Botero 2015). Changes in precipitation and increased environmental temperature (Schaefer et al. 2008) are likely to cause alterations in abundance and even loss of species (Brook et al. 2008), as well as changes in their geographical distribution (Parmesan and Yohe 2003; Root et al. 2003). However, these responses are variable, based on the type of organism and its niche breadth (Vié et al. 2009). Therefore, changes in climatic abiotic variables are key factors in the composition and structure of biological communities, besides other ecological aspects (Pimm 2007), such as seasonal changes during wet and dry seasons (Wolda 1988; Rzedowski 2006).

An aspect of greatest influence on these communities is the microclimate (Cloudsley-Thompson 1962). This is the result of local spatial and seasonal variations in climate and has been shown to play an important role in the dynamics of metapopulations (Checa et al. 2014). Likewise, it is essential for the survival and development of the species, affecting larval diapause or growth, or indirectly modifying the availability of food resources (Currano et al. 2008; DeLucia et al. 2008). The microclimate is related to seasonal variations in the communities of phytophagous insects (Chen et al. 1999), but its specific influence has been scarcely studied.

Phytophagous insects are among the most important trophic groups that respond significantly to climatic changes. Their presence is key in natural or anthropic ecosystems, either playing a relevant role in nutrient cycling processes, or in the diet of other organisms (Iannacone and Alvariño 2006). Furthermore, their physiological processes are determined by the conditions of the environment (Régnière 2009).

Leaf beetles (Coleoptera: Chrysomelidae) constitute a model family to evaluate the seasonal effects of abiotic variation on herbivorous insect communities, since they occupy one of the first places in worldwide diversity (Santiago-Blay 1994). Most chrysomelid species exhibit phytophagous feeding habits and a close relationship with their host plants, as well as a great sensitivity to microclimatic variation (Niño-Maldonado and Sánchez-Reyes 2017). Also, they are considered to be a group with important potential for monitoring natural areas (Furth et al. 2003).

The present study was carried out in a semideciduous tropical forest (STF) fragment in the municipality of Victoria, Tamaulipas, in northeastern Mexico. The area is included in the biogeographic province of the Sierra Madre Oriental and is located within one of the 15 panbiogeographic nodes of Mexico (Morrone and Márquez 2008). Therefore, it constitutes a region with a high priority for conservation (CONABIO et al. 2007). Despite this, there are no studies in STF evaluating the effect of seasonality and microclimate on the family Chrysomelidae. It is important to recognize the factors that restrict the distribution of the species, and thus further delimit efficient conservation strategies of this important area. Based on the above, the objectives of this study were 1) to prepare a faunistic list of chrysomelid species, 2) to compare their richness, abundance, and diversity between seasons, 3) to define the abiotic variables seasonally related to the presence and abundance of the species, and 4) to delimit the breadth niche and categorize the leaf beetles as specialists or generalists, based on their variation related to the seasonal abiotic environment.

Materials and methods

Study area

The study area of semideciduous tropical forest (**STF**) is located in the Ejido Santa Ana, municipality of Victoria, in the center of the state of Tamaulipas, northeastern Mexico 23°52'4.27"N, 99°13'51.37"W and 23° 47'23.06"N, 99°18'10.22"W (DMS) (Fig. 1). It is included in the biogeographic province of the Sierra Madre Oriental (**SMO**), converging to the south with Peregrina Canyon, within the Natural Protected Area (**NPA**) "Altas Cumbres."

Two climate groups characteristic of Tamaulipas were observed in the area: 1) Semi-warm, sub-humid, with summer rains, averaging temperatures between 16.4 °C and 29.2 °C, and 2) Semi-warm, semi-dry subtype, with average temperatures from 15.1 °C to 22.9 °C. The average annual precipitation is 577 mm, with May to October as the wettest months (rainy season) and November to April having the lowest precipitation (dry season) (Gobierno del Estado 2015). Regarding the semideciduous tropical forest, it is the second richest ecosystem in plant species of the state of Tamaulipas and is located between 350 and 500 m a.s.l, comprising areas adjacent to the margin of rivers and streams. Therefore, this habitat conserves higher environmental humidity for most of the year, protecting it from sudden climatic changes, such as sudden temperature differences (García-Morales et al. 2014).

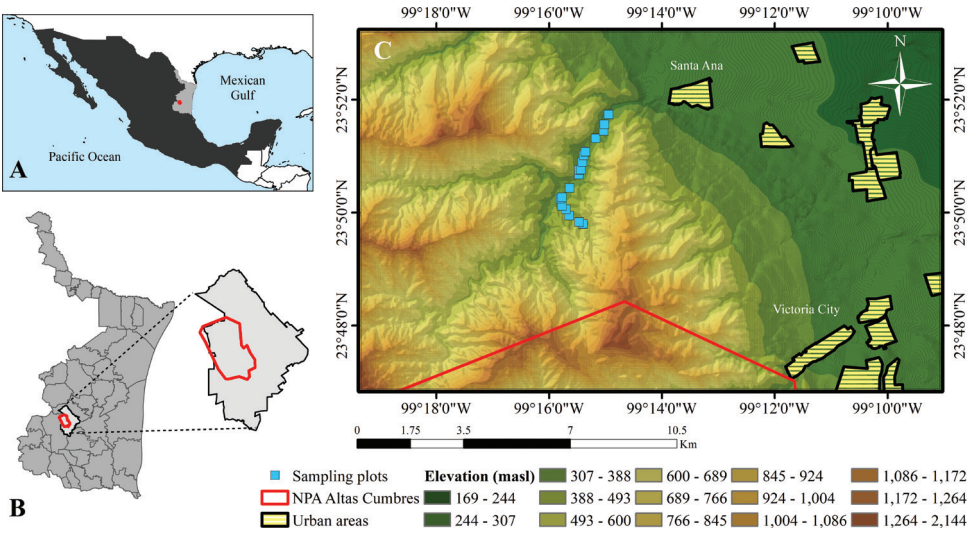

Figure 1. Location of the study area. **A** Ejido Santa Ana (red point) in Tamaulipas State, Mexico **B** NPA Altas Cumbres (red polygon) within Victoria municipality in Tamaulipas **C** Distribution of the sampling plots (blue squares) in the semideciduous tropical forest.

Sampling

A total of 18 plots measuring 20 × 20 m (400 m^2) was randomly established over an approximate land area of 5 km^2. Plots were distributed in areas of dense herbaceous and shrub vegetation, separated at least by 10 meters from the main road, in order to minimize anthropogenic influence. Each plot was measured and delimited with a 50 m tape, using trunks, trees, or branches as vertices; the center of the plot was georeferenced with a Garmin Etrex 30 GPS and then marked with a brightly colored ribbon to facilitate its location in the field.

Beetles were sampled with an entomological sweep net of 60 cm length and 40 cm rim diameter. In each plot (sample unit), 200 net beats were made, covering all the sampling area zigzagging on the understory vegetation. The contents of the net were placed inside a polyethylene bag with 70% alcohol and a collecting label data. All of the 18 plots were sampled from 10:00 to 17:00 hours, once a month, from March 2016 to February 2017.

Sample bags were processed in the Entomology Laboratory of the Facultad de Ingeniería y Ciencias, Universidad Autónoma de Tamaulipas. Each sample was placed in a tray with water, plant debris were then removed using entomological forceps, and the insect specimens were afterwards placed in small bottles with 70% alcohol. Later, the contents of each bottle were analyzed in a Petri dish, using a stereoscopic microscope to identify the specimens; chrysomelids were dried on absorbent paper and mounted in opaline triangles, following the methodology of Triplehorn and Johnson (2005). Taxonomic determination of subfamilies was carried out using the keys of Triplehorn and Johnson (2005), while genera and/or species were identified by consulting various

authors (Wilcox 1972; Scherer 1983; White 1993; Flowers 1996; Riley et al. 2002; Staines 2002), as well as by comparison with previously identified specimens.

Microclimatic variables were recorded using a Kestrel 3500 portable meteorological station, with which the following variables were evaluated: maximum wind speed (m/s), average wind speed (m/s), temperature (°C), relative humidity (%), heat index (°C), dew point (°C) and evapotranspiration (°C). Abiotic data collection was carried out in each plot, simultaneously with the sampling of leaf beetles (once a month for each plot, during the period from March 2016 to February 2017).

Data analysis

Statistical differences in abundance and number of species between seasons were calculated with a non-parametric Mann-Whitney test and a diversity permutation test, respectively. Both analyses were conducted using PAST 3.17 software (Hammer et al. 2017).

Seasonal estimated richness was determined using Chao 1, Chao 2, Jackknife 1 and ACE non-parametric estimators. These indices are recommended for the minimum estimate of richness and useful as a complementary measure in biodiversity analyzes (Gotelli and Colwell 2011). Chao 1 considers the abundance of rare species (singletons and doubletons). Chao 2 is robust for presence-absence data. Jackknife 1 is a conservative index based on incidence data of those species found only in a single sample, while ACE is an index that considers the abundance of species represented by 1–10 individuals (Magurran 2004). The estimators were calculated by means of 100 randomizations without replacement in the software EstimateS 9.1.0 (Colwell 2013), based on the abundance of the recorded species. In addition, the Clench model was used to calculate the estimated species richness, following the methods proposed by Jiménez-Valverde and Hortal (2003). This procedure was performed in STATISTICA 8.0 (StatSoft, Inc. 2007).

Alpha diversity was estimated using Shannon's entropy index (**H'**) and Simpson's dominance index (**D**). Both values were transformed to the effective number of species (true diversity), through the Hill numbers of order (**q**) 1 and 2, respectively (Jost 2006). To measure beta diversity, the Bray-Curtis similarity index was used, which relates the abundance of the shared species with the total abundance in two samples. Therefore, it constitutes a robust measure for the analysis of biotic similarity between communities (Magurran 2004). All diversity analyses were carried out with PAST software.

Association between leaf beetle species and the environmental abiotic variables, as well as the measure of niche breadth, were calculated with the Outlying Mean Index (**OMI**). This index identifies the niche of the species, or marginality, according to the average distance between the abiotic resources used by each species (centroid) with respect to the total resources available (microclimate) in the area. It gives a more even weight to all sampling units, including those with a low number of species or individuals (Dolédec et al. 2000). First, the OMI assesses the contribution of the abiotic variables to the niche separation of the species by computing a Principal Component Analysis, and higher correlation values (loadings) are interpreted at each of the most

important axes. Then, a total Inertia (**InerO**) value is obtained, which is a measure proportional to the average marginality of the species and represents a quantification of the influence of environmental variables on the separation of the species niche. Lastly, the analysis decomposes the inertia associated with the distribution of a species (**InerO**) into three main parameters: Marginality, Tolerance (**T1**), and Residual Tolerance (**T2**) (Dolédec et al. 2000).

Marginality represents the deviation of the environmental conditions used by a species with respect to the average environment for the entire study area. Species with high OMI values have marginal niches (occur in atypical habitats, and are influenced by a specific subset of environment variables), while those with low values have non-marginal niches (common species occurring in typical habitats, without a specific response to environment variables). Tolerance (T1) measures the dispersion of the assessment units that contain a species along an environmental gradient (the range of habitat of the species), and it is analogous to the concept of niche breadth: high tolerance values represent greater niche breadth, and the species are distributed in habitats with widely variable conditions (generalist); contrarily, low tolerance values indicate a smaller niche width where a species is distributed in habitats with a limited range of conditions (specialists). Finally, T2 is defined as the variance in the species niche that is not considered by the marginality axes, and it is useful for determining the reliability of a set of environmental conditions for the definition of the niche of each species (Dolédec et al. 2000).

Statistical significance of the OMI was determined with a Monte Carlo test, in which the observed marginalities are compared with 10,000 random permutations, in order to reject the null hypothesis that species are equally distributed in relation to (not influenced by) environmental variables (Dolédec et al. 2000). All OMI analyses were carried out in ADE-4 software (Thioulouse et al. 1997), and they were calculated separately for the rainy and dry seasons. Data input consisted of a matrix with the abundances of each of the species in each month/season and a matrix with the values of the seven environmental variables registered in each of the sampling plots. Ordination graphics of centroids and loadings were generated in the same software and later exported to CorelDRAW X3 to be edited. Environmental ranges of species were calculated for each of the significant variables using the Kriging interpolation technique, which is a geostatistical method that quantifies spatial autocorrelation for the prediction and generation of continuous surfaces (Murillo et al. 2012). Procedures were carried out in ArcGis 10.2.2 (ESRI 2014).

Results

Overall response of leaf beetles in the semideciduous tropical forest

During the study, 2,103 specimens of Chrysomelidae were obtained, involving six subfamilies, 47 genera and 71 species (Appendix 1: Table A1). Galerucinae were most abundant (1,628 specimens = 77%), followed by Cassidinae (410 = 19.44%). Among the other four subfamilies, only 65 specimens (3%) were collected throughout the year,

being 36 in Eumolpinae, 14 in Criocerinae, nine in Chrysomelinae, and six in Cryptocephalinae. Regarding total richness, Galerucinae represented 51% (36 species), Cassidinae 17% (12 species), Eumolpinae 11% (eight species), Chrysomelinae 8% (six species), Criocerinae 7% (five species), and Cryptocephalinae 6% (four species).

Species that dominated in abundance in the study area were *Centralaphthona diversa* (Baly, 1877) (629 individuals), *Monomacra bumeliae* (Schaeffer, 1905) (528 individuals), *Heterispa vinula* (Erichson, 1847) (311 individuals), and *Margaridisa* sp. 1 (147 individuals), which together represent 77% (1,615 individuals) of the total abundance recorded. In addition, the community included 67 species with very low abundances, from which 25 (37%) correspond to singletons and nine to doubletons (13%). The dominance value (D) in the study area was 0.1998, which represents a true diversity (1/D) of 5.005. For the Shannon index (H'), a value of 2.221 was registered, with true diversity (e^H) of 9.217.

Seasonal variation

Seasonal differences in abundance of the leaf beetle community were statistically significant (Mann-Whitney U = 4039; $p \leq 0.0001$). The highest number of specimens was recorded during the rainy season (1,242 specimens, involving 41 genera), followed by the dry season (861, involving 30 genera). According to the permutation test, significant differences were also found in the number of species and diversity. Highest species richness was recorded in the rainy season. In contrast, the lowest dominance and highest diversity were obtained in the dry season (Table 1).

Estimated species richness according to the non-parametrical estimators in the rainy season ranged between 85 and 100 species; therefore, the observed richness represents between 59.66 and 69.96% of completeness. For the dry season, the estimated richness varied from 48 to 56 species, indicating a completeness from 70.49 to 82.85% (Table 2). Inventory reliability with Clench's model was higher during the dry season, with a completeness of 81% and a lower slope value, compared with the rainy season (Table 2).

The best represented subfamily during the rainy season was Galerucinae (943 specimens, 32 species), followed by Cassidinae (260, 11 species). This same pattern was reflected in the dry season: Galerucinae with 685 specimens (21 species), followed by Cassidinae with 150 specimens (7 species). The remainder of the subfamilies had lower abundances and number of species for both seasons (Table 3).

Faunistic similarity according to the Bray-Curtis index was 0.63%. A high proportion of the species composition shared between seasons involved Galerucinae, including *Acrocyum dorsale* Jacoby, 1885, *C. diversa*, *Epitrix* sp. 1, *Margaridisa* sp. 1,

Table 1. Diversity permutation test for species richness and alpha diversity of leaf beetles between seasons.

	Season		
	Rainy	**Dry**	**p**
Observed species richness	60	40	0.0132
Simpson index (D)	0.228	0.175	0.0001
Shannon index (H´)	2.062	2.232	0.0229

Table 2. Chrysomelid estimated species richness and sampling completeness during the rainy and dry seasons.

Estimator	Rainy	% of completeness	Dry	% of completeness
Chao 1	97.53	61.52	55.11	72.58
Chao 2	90.44	66.34	56.74	70.49
Jack 1	85.76	69.96	55.88	75.64
Ace	100.56	59.66	48.28	82.85
Clench model (slope)	0.1561	–	0.077	–
Clench model (estimated richness)	82	73	50	81

% was obtained on the basis of observed species richness.

Table 3. Number of specimens and species registered by subfamily and season in the semideciduous tropical forest.

	Season			
	Rainy		Dry	
Subfamily	Specimens	Species	Specimens	Species
Galerucinae	943	32	685	21
Cassidinae	260	11	150	7
Eumolpinae	25	7	11	5
Criocerinae	7	3	7	2
Chrysomelinae	5	5	4	3
Cryptocephalinae	2	2	4	2

and *Monomacra bumeliae*. The proportion was also high for Cassidinae, involving *Brachycoryna pumila* Guérin-Méneville, 1844, *Helocassis crucipennis* (Boheman, 1855), and *Heterispa vinula* (Erichson, 1847).

Response of Chrysomelidae to seasonal microclimatic variation

The OMI analysis for the rainy season indicated a significant deviation between the abiotic conditions used by the leaf beetles and the average total microclimatic conditions (Monte Carlo test, $p = 0.047$). Of the 60 species registered in this season, only six showed a significant association. *Centralaphthona diversa* and *M. bumeliae* obtained low marginality values, which represents a wider niche breadth, and they were thus considered to be generalist species (Table 4); abundance of these species was equally distributed in almost all samples (Fig. 2). The rest of the species presented high marginality and lower tolerance values, which indicates a smaller niche breadth, and they were therefore categorized as specialists. *Labidomera suturella* Guérin-Méneville, 1838 was the species with the highest marginality and the lowest tolerance, followed by *Walterianella* sp. 1, *Zenocolaspis inconstans* (Lefèvre, 1878) and *Alagoasa trifasciata* (Fabricius, 1801) (Table 4). The aforementioned species had lower abundance, 1–15 specimens, in a minor number of samples (Fig. 2).

In the case of the dry season, marginality was significant (Monte Carlo test, $p = 0.017$) for only seven of the 40 registered species. Two were considered as generalists, with low marginality values; of these, *B. pumila* presented the highest tolerance, while

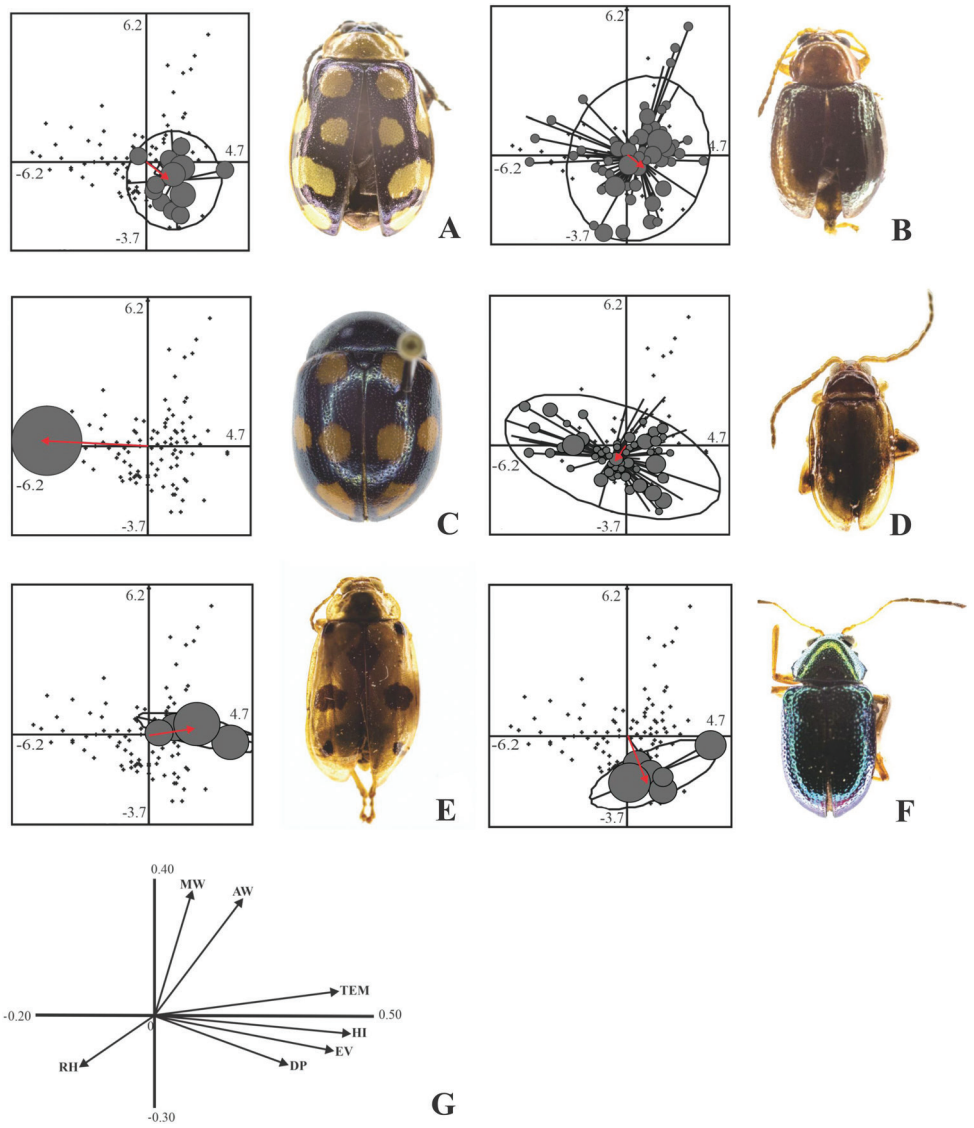

Figure 2. Individual dispersion of leaf beetle species whose association for microclimatic variables was significant in the rainy season **A** *Alagoasa trifasciata* **B** *Centralaphthona diversa* **C** *Labidomera suturella* **D** *Monomacra bumeliae* **E** *Walterianella* sp. 1 **F** *Zenocolaspis inconstans*. At each species panel: the gray circles represent the presence of the species in the sample, and the size of the circle is proportional to its abundance; straight lines represent vectors and indicate the dispersion of the species from the average position (centroid) towards each of the evaluation units where it was recorded; and ellipses represent the concentration of 95% of the specimens of the species. **G** canonical correlation values (loadings) between microclimatic variables and the abundance of Chrysomelidae. Abbreviations: MW: Maximum wind speed, AW: average wind speed, Tem: temperature, RH: relative humidity, HI: heat index, DP: dew point, Ev: evapotranspiration.

Table 4. Parameters of the Outlying Mean Index (OMI) for the significant species of Chrysomelidae ($p < 0.05$) from each season. Values for the non-significant species are presented in Appendix 1: Tables A2, A3. Key: InerO: Total Inertia, T1: Tolerance, T2: Residual tolerance, *p*: probability.

Season	Species	InerO	OMI	T1	T2	*p*
Rainy	*Alagoasa trifasciata* (Fabricius, 1801)	5.199	2.521	0.9	1.778	0.0037
Rainy	*Centralaphthona diversa* (Baly, 1877)	6.011	0.2003	2.14	3.671	0.0168
Rainy	*Labidomera suturella* Guérin-Méneville, 1838	23.86	23.86	7.889E-31	-7889-31	0.0409
Rainy	*Monomacra bumeliae* (Schaeffer, 1905)	6.991	0.4444	1.699	4.894	0.0007
Rainy	*Walterianella* sp. 1	7.257	5.25	1.494	0.512	0.0193
Rainy	*Zenocolaspis inconstans* (Lefèvre, 1878)	6.561	4.146	0.233	2.182	0.0172
Dry	*Acallepitrix* sp. 7	8.299	6.09	0.423	1.786	0.0169
Dry	*Alagoasa trifasciata* (Fabricius, 1801)	7.092	6.523	0.038	0.530	0.0469
Dry	*Brachycoryna pumila* Guérin-Méneville, 1838	9.761	2.114	5.087	2.56	0.0258
Dry	*Centralaphthona diversa* (Horn, 1889)	8.056	0.2969	2.788	4.971	0.0415
Dry	*Chaetocnema* sp. 1	10.03	6.778	1.714	1.539	0.0083
Dry	*Epitrix* sp. 1	7.5	3.023	1.432	3.045	0.0073
Dry	*Syphrea* sp. 1	11.29	9.965	0.204	1.12	0.0106

C. diversa showed the lowest marginality (Table 4). Abundance of both species was uniformly distributed in almost all samples (Fig. 3). The other five chrysomelids had high marginality and low tolerance values (specialists): the highest marginality and lowest tolerance occurred in *A. trifasciata*, and it was consequently the species most specialized to microclimatic conditions during the dry season in the semideciduous tropical forest. In descending order, *Syphrea* sp. 1, *Chaetocnema* sp. 1, *Acallepitrix* sp. 7, and *Epitrix* sp. 1 (Table 4) were species recorded in few samples, with abundances between four and 18 specimens (Fig. 3).

Heat index, evapotranspiration and temperature were the microclimatic variables most related with the abundance of leaf beetle species during the rainy season and were represented in Axis 1 of the OMI analysis (Eigenvalue = 4.9077, inertia = 55.74%). In Axis 2 (Eigenvalue = 2.6344, inertia = 29.92%) the most important variable was the average wind speed (Table 5). For the dry season, evapotranspiration, temperature, and heat index in Axis 1 (Eigenvalue = 7.9982, inertia = 75.67%) were the microclimatic variables most associated with the changes in abundance of leaf beetles. Maximum wind speed had the highest correlation in Axis 2 (Eigenvalue = 1.7084, inertia = 0.1616%) (Table 5).

The association of the species with the environmental variables was determined based on the positions of the centroids and their closeness with respect to Axes 1 and 2. Those species that were located very close to the origin of both axes were considered to be related to average microclimatic values. For the rainy season, *A. trifasciata* and *Z. inconstans*, were related with low values of average wind speed (1.06–2.12 m/s), as well as high values of heat index (39.61–43.89 °C), evapotranspiration (27.24–29.02 °C) and temperatures (30.47–35.42 °C). *Walterianella* sp. 1 presented a similar microclimatic pattern, with a positive correlation with Axis 1 (high values of heat index from 43.89 to 48.18 °C, evapotranspiration from 24.24 to 29.02 °C, and temperature from 32.94 to 35.42 °C), although it was associated with average to high

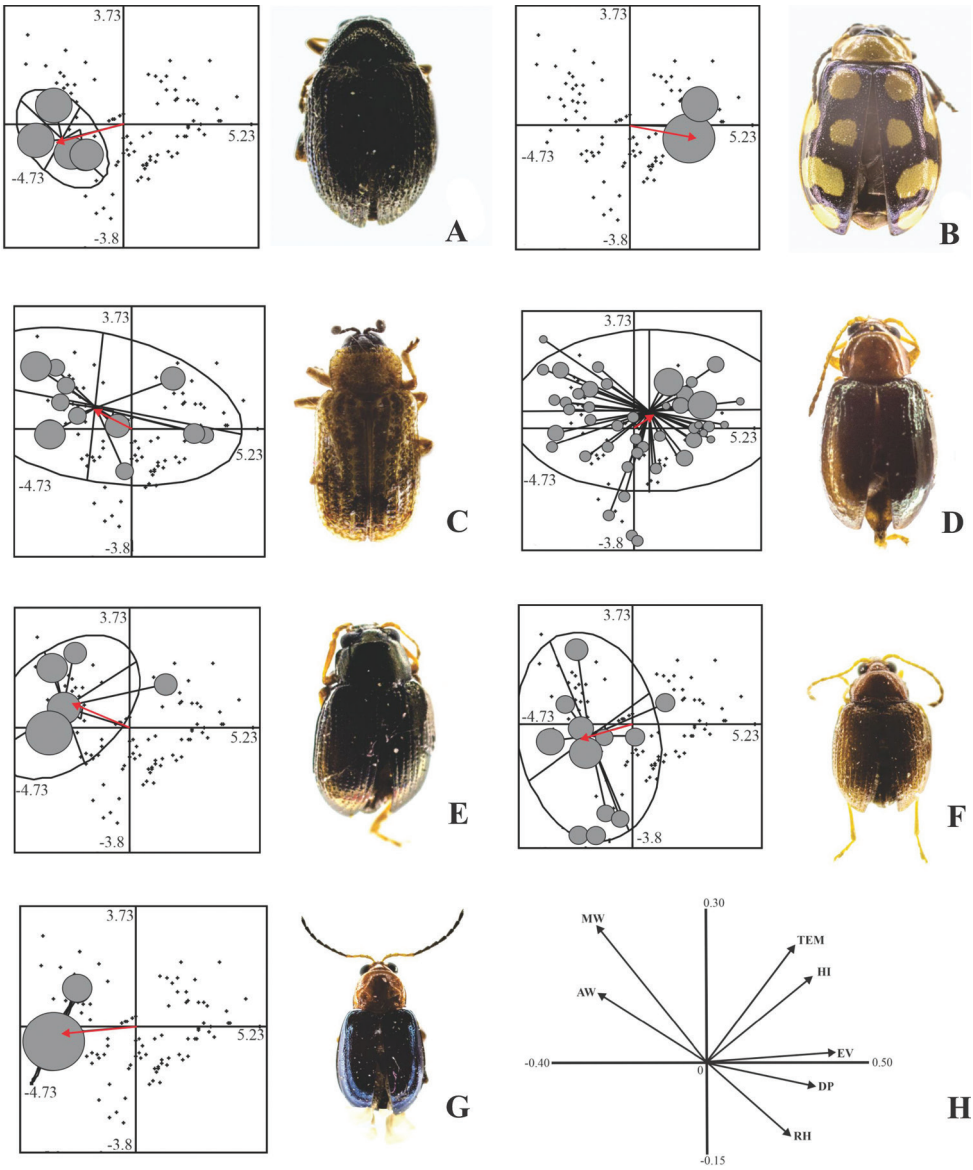

Figure 3. Individual dispersion of leaf beetle species whose association for microclimatic variables was significant in the dry season **A** *Acallepitrix* sp. 7 **B** *Alagoasa trifasciata* **C** *Brachycoryna pumila* **D** *Centralaphthona diversa* **E** *Chaetocnema* sp. 1 **F** *Epitrix* sp. 1 **G** *Syphrea* sp. 1. At each species panel: tiny, black dots represent the sampling units; gray circles represent the presence of the species in the sample, and the size of the circle is proportional to its abundance; straight lines represent vectors and indicate the dispersion of the species from the average position (centroid, pointed to by the red arrow) towards each of the sampling units where it was recorded; and ellipses represent the concentration of 95% of the specimens of the species. **H** canonical correlation values (loadings) between microclimatic variables and the abundance of Chrysomelidae. Abbreviations: MW: Maximum wind speed, AW: average wind speed, Tem: temperature, RH: relative humidity, HI: heat index, DP: dew point, Ev: evapotranspiration.

Table 5. Canonical correlation values (loadings) between the seven microclimatic variables and the abundance of chrysomelid species during both seasons. Significant values are marked (*).

	Rainy season		Dry season	
Microclimatic variables	Axis 1	Axis 2	Axis 1	Axis 2
Maximum wind speed (m/s)	0.075	0.299	-0.274	0.271*
Average wind speed (m/s)	0.136	0.301*	-0.278	0.143
Temperature (°C)	0.345*	0.042	0.375*	0.192
Relative humidity (%)	-0.084	-0.201	0.2481	-0.119
Heat Index (°C)	0.380*	-0.040	0.371*	0.154
Dew Point (°C)	0.275	-0.173	0.368	-0.001
Evapotranspiration (°C)	0.345*	-0.091	0.413*	0.035

values of wind speed (2.12–4.24 m/s). In the case of *L. suturella*, this species was located in areas with lower values of heat index (18.20–22.48 °C), evapotranspiration (16.60–18.37 °C), and temperature (18.10–20.57 °C), but higher wind speed (1.06–2.12 m/s). Lastly, *C. diversa* and *M. bumeliae* did not follow a specific pattern in relation to the significant variables in any axis since they were at the origin of the niche dispersion (Fig. 4).

During the dry season, the average distribution of *Syphrea* sp. 1, *Acallepitrix* sp. 7, and *Epitrix* sp. 1 was correlated with areas of lower evapotranspiration (13–16.82 °C), temperature (16.30–19.69 °C) and heat index (16.60–22.20 °C) in Axis 1. Similarly on Axis 2, these species predominated under conditions of low to average maximum wind speed (1.42–2.84 m/s). *Chaetocnema* sp. 1 occurred in conditions of low evapotranspiration (13–14.91 °C) and low temperature (21.39–23.09 °C), as well as low heat index (19.40–22.20 °C), but this species was associated with high values of maximum wind speed (1.42–2.13 m/s). *Alagoasa trifasciata* was the species with the lowest tolerance value; so, its centroid was positioned in areas with high evapotranspiration values (22.56–24.47 °C), high temperature (24.79–26.49 °C), high heat index (30.60–33.40 °C), and low maximum wind speed (0–0.71 m/s). Finally, the centroid of the distribution of *B. pumila* and *C. diversa* was significantly associated with average microclimatic conditions, since their distribution included areas with high and low values for the heat index, as well as for the other variables (Fig. 5).

Discussion

Faunistic inventory and chrysomelid biodiversity

Prior to this study, 2,660 species of Chrysomelidae had been recorded from Mexico (Niño-Maldonado and Sánchez-Reyes 2017) and 257 from the state of Tamaulipas (Niño-Maldonado et al. 2014). Accordingly, results in the STF of the study area represent 2.7% of the leaf beetle biodiversity reported for the country, and 27.6% for the state. Our study revealed *Diachus chlorizans* (Suffrian, 1852) as a new country record for Mexico, and *Diabrotica biannularis* Harold, 1875 as a new state record for

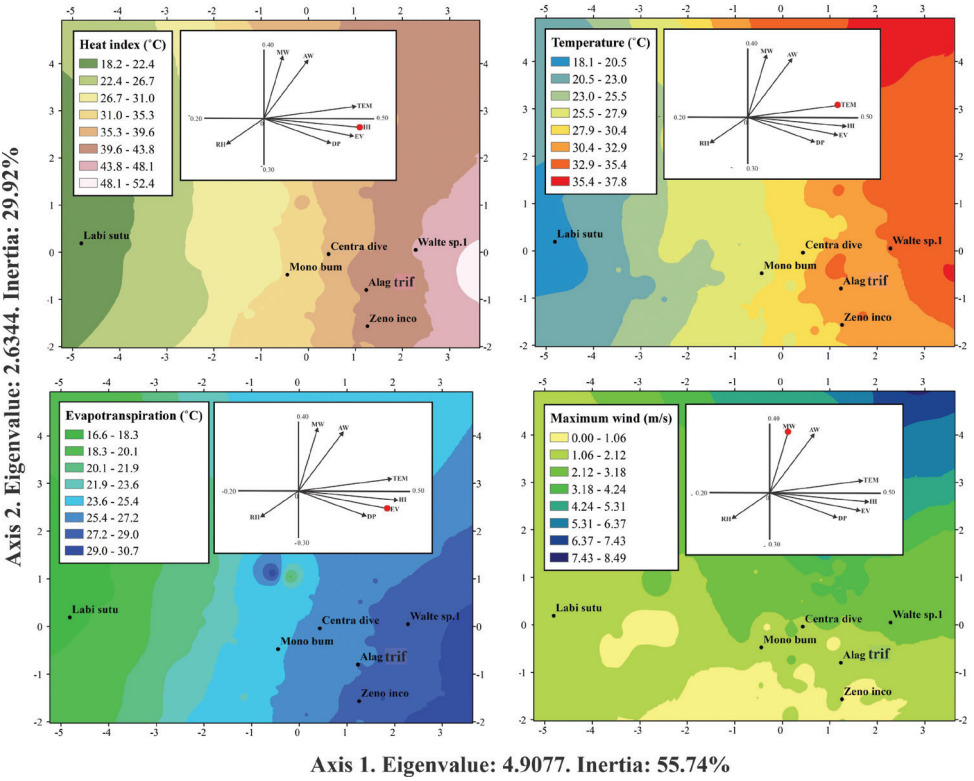

Figure 4. Environmental ranges of leaf beetles during the rainy season. Abbreviations: Labi sutu (*Labidomera suturella*), Centra dive (*Centralaphthona diversa*), Mono bume (Monomacra bumeliae), Walte sp. 1 (*Walterianella* sp. 1), Alag trif (*Alagoasa trifasciata*), Zeno inco (*Zenocolaspis inconstans*).

Tamaulipas. These records were previously published in preliminary works from the study area (Lucio-Garcia et al. 2019).

The number of taxa recorded in this research is lower compared to similar studies in northeastern Mexico, such as those conducted at El Cielo Biosphere Reserve (RBEC) (Niño-Maldonado et al. 2005), the Cañón de la Peregrina (CDP) (Sánchez-Reyes et al. 2014) and the Sierra de San Carlos (SDSC) (Sánchez-Reyes et al. 2016a). Niño-Maldonado et al. (2005) reported 105 species in different elevational strata of STF. Lower values were found in two fragments of this vegetation in the Peregrina Canyon, where 85 (Sánchez-Reyes et al. 2014) and 37 species (Martínez-Sánchez 2016) were recorded. Other patches of STF were evaluated in the Cañón del Novillo (21 species) and Cerro El Diente (five species), also in Tamaulipas. The lower number in the present study can be attributed to the spatial scale and number of environments evaluated in these other investigations, which are greater compared to the STF of this work. For example, analyzing elevation gradients, different types of vegetation or biogeographic islands with extreme conservation status may result in the observed differences in fauna. On basis of the aforementioned numbers, the chrysomelid richness for the current

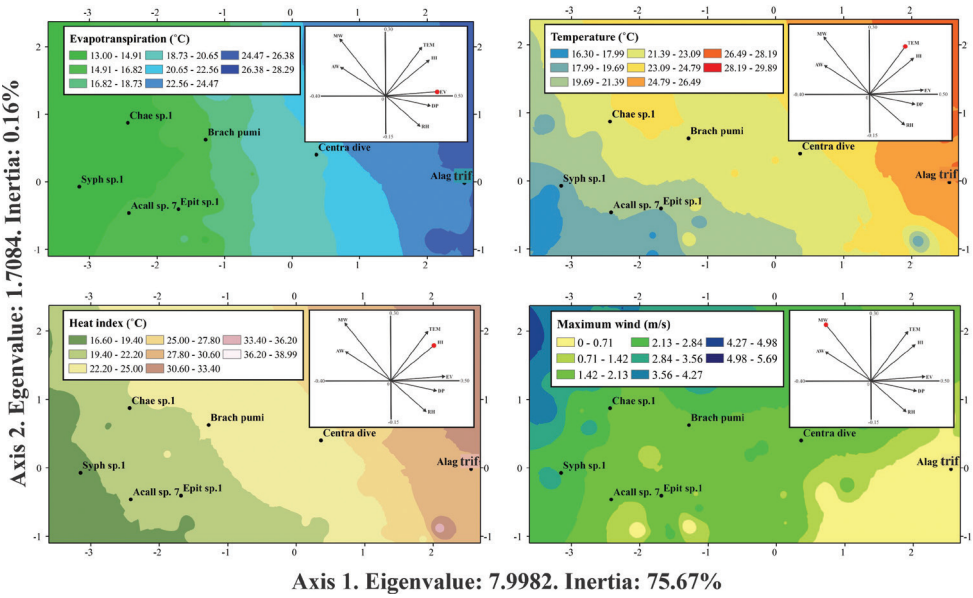

Figure 5. Environmental ranges of leaf beetles during the dry season. Abbreviations: Chae sp. 1 (*Chaetocnema* sp. 1), Syph sp. 1 (*Syphrea* sp. 1), Acall sp. 7 (*Acallepitrix* sp. 7), Brach pumi (*Brachycoryna pumila*), Epit sp. 1 (*Epitrix* sp. 1), Centra dive (*Centralaphthona diversa*), Alag trif (*Alagoasa trifasciata*).

research is above other STF fragments in northeastern Mexico, and it represents 68.2% of the most biodiverse site. Regarding true diversity, the numbers of equally dominant (1/D) and typical (e^H) species in this study were lower than those observed in Peregrina Canyon (Sánchez-Reyes et al. 2014), although they were higher than those observed in STF fragments from Cañón del Novillo (Martínez-Sánchez 2016) or Cerro El Diente (Sánchez-Reyes et al. 2015b).

Galerucine dominance as observed in our study has also been reported in other studies in northeastern Mexico (Niño-Maldonado et al. 2005; Furth 2009; Furth 2013; Sánchez-Reyes et al. 2013; Sánchez-Reyes et al. 2014; Bouzan et al. 2015; Flinte et al. 2017; Lucio-García et al. 2019, 2020), and this may be due to the subfamily's high number of species (Riley et al. 2002), with specimens found in all ecosystems during most parts of the year (Furth 2013; Sánchez-Reyes et al. 2013). In contrast, the subfamily composition of this study is quite different from that in tropical forests. In the Chamela region, on the Pacific side of Mexico, 49 species of Cassidinae were listed (Noguera 1988).

As a whole, the aforementioned results highlight the great importance of the study area, since it was possible to find a large percentage of species within a smaller expanse when compared to larger space-temporal gradients or natural protected areas. This can be attributed to the geographic location of the studied STF within a region with a high conservation priority (CONABIO et al. 2007). The area, although adjacent to the Altas Cumbres Natural Protected Area, constitutes a mosaic with fragments of different durations since last disturbance, and this may favor the presence of a complex

community of species (Sánchez-Reyes et al. 2017). Furthermore, the STF is one of the ecosystems with the highest biodiversity of plants (Rzedowski 2006; García-Morales et al. 2014), and it is one of the most important in terms of chrysomelid species richness in Mexico (Noguera 1988; Burgos-Solorio and Anaya-Rosales 2004; Niño-Maldonado et al. 2005; Lucio-García et al. 2019). The combination of environmental factors in the STF results in a great diversification of plants, providing a wide range of food resources, which could lead to the high number of leaf beetles in this plant community in Tamaulipas and other states of Mexico.

Seasonal variation

On a temporal scale, the chrysomelid community followed a seasonal pattern, where the rainy season was the most favorable for the presence of this group in the study area. Increase in abundance and species richness during this season has also been found in numerous studies worldwide, including studies in Tamaulipas and other parts of Mexico (Petitpierre et al. 2000; Esker et al. 2002; Burgos-Solorio and Anaya-Rosales 2004; Koji and Nakamura 2006; Furth 2009; Martínez-Sánchez et al. 2009; Furth 2013; Sánchez-Reyes et al. 2015b; Sánchez-Reyes et al. 2016a; Sandoval-Becerra et al. 2016; Şen and Gök 2016; Miwa and Meinke 2017; Lucio-García et al. 2019). Results of the richness estimators support these patterns, because the percentage of completeness during rains is lower when compared to the dry season. Thus, in certain areas, the highest activity of chrysomelids is restricted to the rainy season, while inactivity increases during drought conditions (Noguera 1988; Furth 2013). This is due to the association of chrysomelids with the quality and availability of their host plants (Řehounek 2002; Şen and Gök 2016), which are some of the most important elements in their diet (Ávila and Postali-Parra 2003), as well as with the abundance of young foliage (Basset and Samuelson 1996), variables that are increased during the period of highest rainfall. In addition, there is more vegetation cover producing shade, creating microenvironments that could be more favorable to maintaining a high population density (Hill and Hill 2001), with the climatic conditions of humidity necessary for the adult beetles to emerge and fly (Yanes-Gómez and Morón 2010).

However, in other geographic regions, such as the subtropical areas of Brazil, the highest abundance has occurred in the dry season, specifically within the subfamilies Galerucinae, Cassidinae and Chrysomelinae (Linzmeier and Ribeiro-Costa 2008; Flinte et al. 2011; Bouzan et al. 2015; Flinte et al. 2017). In addition, in some areas of northeastern Mexico, greater numbers of species and specimens have also been recorded during the dry season (Sánchez-Reyes et al. 2014). These discrepancies can be attributed to the climatic and biogeographic differences between plant communities. For example, in cloud forests, dry periods are shorter and less intense, causing a favorable increase in specimens of some Coleoptera families (Pedraza et al. 2010). Although soil moisture and precipitation are reduced in these areas, the cloudiness in the form of mist reduces evaporation, providing water during periods of low rain; in consequence, marked deficiency of humidity in these forests is rare. In other tropical forests near the

study area, the dry season is not as severe, for example in the Peregrina Canyon, where a higher abundance of adult chrysomelids often occurs concentrated in refuges during this season, while the larval stages are more abundant during the rains (Sánchez-Reyes et al. 2014). On the contrary, differences in geographic position, latitude and elevation influence the contrast that exists between the dry and rainy seasons in other fragments of the same type of vegetation in northeastern Mexico. In the study area, there are well-defined periods of high temperature and precipitation, in addition to a non-continuous flow of water currents during the year, which lead to a more severe dry season. Similar and more extreme cases exist in tropical dry forests from the south or Pacific coast of Mexico, where the plants lose their leaves completely during the dry season, resulting in a notable absence of chrysomelids (Noguera 1988). Likewise, these climatic variations and their effects on the phenology of the host plants are probably the main drivers of the temporal dynamics in these beetles (Flinte et al. 2017).

Unlike other investigations where the greatest diversity also occurs in the wet season (Sánchez-Reyes et al. 2016a), in this work, the low abundance and species richness resulted in a high diversity in the dry season, by decreasing the dominance and increasing the effective number of species (Magurran 2004). Therefore, the dry season is of great importance for the chrysomelid community in the STF of the study area, since the prevailing conditions increase the evenness of the chrysomelid community. Species may exploit food resources in a more efficient way during this season, achieving a balance in their populations and reducing the dominance of most species, thus suggesting an adaptation of Chrysomelidae to acute drought conditions. This could be noted also when observing the high percentage of faunistic similarity between seasons, which indicates that most of the leaf beetles are the same in both periods. Therefore, it is possible that their resource acquirement changes and consequently their abundances are modified during the seasonal variations. Moreover, 31 species were registered exclusively for the rainy season, while only 11 for the dry season. Together, these results highlight the relevance of areas where there is a marked temporal or seasonal heterogeneity, since it can generate unique species compositions.

Response of Chrysomelidae to seasonal microclimatic changes

In this research, the niches of chrysomelid species were examined by means of the Outlying Mean Index. This showed that the variations in the abundance of leaf beetles were significantly related to the microclimatic changes in each season. Factors that influence the distribution of phytophagous insects are a combination of geographic and environmental elements (Wąsowska 2004; Andrew and Hughes 2005; Lassau et al. 2005; Baselga and Jiménez-Valverde 2007). It has also been shown that leaf beetles present different degrees of association with the microclimatic conditions of the habitats where they develop (Sánchez-Reyes et al. 2016b; Sandoval-Becerra et al. 2017), and this is demonstrated in our study. However, the variation explained by the analysis and the correlation values of the variables were higher in the dry season, suggesting a stronger association between the microclimate and the chrysomelid community with

respect to the rainy season. This can be attributed to more heterogeneous environment values during low precipitation months. For example, in tropical forests it has been observed that lower microclimatic variability occurs through the rainy season (Checa et al. 2014; Sánchez-Reyes et al. 2019), which could be due to a higher homogeneity in the vegetation structure. Therefore, chrysomelid populations are more variable in relation to the seasonal microclimate prevailing during the dry season, so that the effects, particularly of precipitation, determine strong positive or negative responses in these insects (Pinheiro et al. 2002); this pattern also occurs in other phytophagous groups, such as Curculionidae or Cicadidae (Novotny et al. 1999; Silva et al. 2017).

Significant microclimatic variables were very similar between seasons (environmental temperature, heat index, evapotranspiration and, to a lesser extent, wind speed), although there were differences in the order of importance and in their contribution to the variations in abundance of leaf beetles. In the rainy season, the most important variable to characterize the niche of the species was the heat index, which is considered to be a combination of humidity and temperature in the same value and represents the thermal sensation (Lee and Brenner 2015). In physiological terms, phytophagous insects must accumulate a certain amount of heat to be able to hatch and accelerate their development rate, thereby increasing the number of generations (Marco 2001; Mejía 2005). However, in the dry season, the variable of greatest importance was evapotranspiration. Such variation can be attributed to the environmental humidity stress to which the host plants are exposed after rainfall, modifying the moisture content of leaves and stems and thereby affecting feeding patterns of chrysomelids. This suggests that direct effects on trophic networks may occur during drought periods, which influence the development of phytophagous insects, particularly due to desiccation (Martínez et al. 2010; Anderson et al. 2016).

A similar set of microclimatic variables has been associated with Chrysomelidae in other works, specifically temperature, heat index, maximum wind speed and evapotranspiration (Stewart et al. 1996; Flinte and Valverde de Macedo 2004; Isard et al. 2004; Baselga and Jiménez-Valverde 2007; Linzmeier and Ribeiro-Costa 2013; Aneni et al. 2014; Sánchez-Reyes et al. 2016b; Oliveira et al. 2017; Sandoval-Becerra et al. 2017). There are other studies where the most important abiotic variables were solar radiation, precipitation, relative humidity, photoperiod and condensation point (Flinte and Valverde de Macedo 2004; Isard et al. 2004; Linzmeier and Ribeiro-Costa 2013). It should be mentioned that differences compared to the present study arise due to various factors, including the type of study, geographic location, ecosystems evaluated and method for measuring microclimatic variables, as well as the specific response of taxa to the variables.

Regarding the individual response of leaf beetles to the variables, it was observed that only 11 of the 71 species registered a significant variation between their niche and the average microclimatic conditions in the STF. It has been observed that the number of chrysomelid species that present a significant relationship with abiotic parameters is variable, although previous studies have focused on the effect of disturbance (Sandoval-Becerra et al. 2017) and elevation gradients (Sánchez-Reyes et al. 2016b).

The study of chrysomelid species associated with abiotic variables has been useful in recognizing part of their biology and ecology, specifically their reproductive cycle or their potential for biological control (Stewart et al. 1996; Flinte and Valverde de Macedo 2004; Isard et al. 2004; Oliveira et al. 2017). Also, such study has been applied to know their niches (Sánchez-Reyes et al. 2015a) and to identify indicator species of conservation status (Ohsawa and Nagaike 2006) or disturbance (Sandoval-Becerra et al. 2017). Other studies have focused on the influence of climate in the distribution of species (Sánchez-Reyes et al. 2016b; Wang et al. 2017). The present work, on the other hand, is one of the first to address the influence of microclimatic variation on Chrysomelidae from a seasonal perspective.

Specifically, in the dry season, seven significant species were recorded, while in the rainy season there were only six. In both seasons, *C. diversa* was categorized as a generalist species, since it presented a low marginality and a high tolerance, which indicates a wide distribution in the study area associated with average microclimatic values. This response is similar to that observed in the same and other species within the genus, but in different areas (Sánchez-Reyes et al. 2016b; Sandoval-Becerra et al. 2017). The second common species in both seasons was *A. trifasciata* although it was categorized as a specialist due to high marginality and low tolerance values. A similar response pattern was previously recorded in the Sierra de San Carlos for this species (Sánchez-Reyes 2014). Association between variables and *A. trifasciata* was higher in the dry season, since the marginality parameters were higher, while the tolerance values were lower; that is, the distribution of *A. trifasciata* appears to be more restricted during the dry conditions. The rest of the species demonstrated seasonal differences. For example, during the rainy season, *L. suturella* presented the highest marginality value and had a low tolerance to the microclimatic environment; similar responses were observed in *Walterianella* sp. 1 and *Z. inconstans*. In the dry season, *Syphrea* sp. 1 was the species with the lowest tolerance, followed by *Chaetocnema* sp. 1, *Acallepitrix* sp. 7, *Epitrix* sp. 1 (Galerucinae), and *B. pumila* (Cassidinae). However, some of these species also occurred throughout the year, despite being significantly associated with only one season. The above observations provide evidence that leaf beetles have seasonal modifications in their niche requirements. Influence of the microclimate may be more important in the rainy season, while in the dry season (or vice versa) the variables that determine niches are different, or they may have a non-significant contribution to the distribution of the species (Basset et al. 1992; Martínez et al. 2010; García-Atencia et al. 2015). These seasonal changes may be associated with the synchronization of the reproductive cycles of the phytophagous insects, particularly depending on the precipitation and temperature provided by the forest structure, which is not constant throughout the year and tends to be increasingly variable (Basset et al. 1992; Soler et al. 2002; García-Atencia et al. 2015).

The broad microclimatic tolerance of *C. diversa* and the abiotic specialization of *A. trifasciata* represent a first approach to the analysis of the generalized environmental response of chrysomelids, even though both have been documented in other studies. In this way, it is probable that the behavior of the species is similar and constant in other

geographical areas, which would allow the use of such taxa in environmental monitoring. New studies on chrysomelid niches would allow us to elucidate these effects. It is also important to recognize that phytophagous insects and specialist taxa with a small niche breadth could be negatively influenced by the possible effects of climate change (Williams et al. 2007; Dormann et al. 2008; Hill et al. 2011), which will impact the structure and functioning of the communities (Hegland et al. 2009; Stuble et al. 2013; Luna-Castellanos et al. 2017). Effects extend to plant-insect interactions (mutualism, predation, competition, etc.), either due to phenological changes (synchronization in the interaction) or distribution of species (Hódar et al. 2004; Luna-Castellanos et al. 2017), with some species even being susceptible to local extinction (Tscharntke et al. 2002; Petermann et al. 2010). Furthermore, the present results and similar evidence suggest that climate variability can lead to significant biodiversity losses (Parmesan et al. 1999; Hill et al. 2002; Konvicka et al. 2003; Wilson et al. 2007). However, despite having knowledge about possible consequences, little information is available on the effects that the changing microclimate can have on biodiversity, its populations, biological communities, and the ecosystems that harbor them.

Conclusions

The study of seasonal and microclimatic changes on species and communities is a topic of great importance in conservation ecology. Community attributes of the family Chrysomelidae and the beetles' response to microclimatic variation were evaluated for the first time from a seasonal perspective, in a semideciduous tropical forest fragment of northeastern Mexico. Overall, the observed results were similar to those from other faunistic studies of leaf beetles, although the number of species ranked third within tropical forest areas of the state of Tamaulipas. Seasonality induced significant changes in the parameters of abundance, diversity and faunistic composition in the chrysomelid community. The highest number of specimens and species were recorded in the rainy season, while the lowest dominance and highest diversity occurred in the driest period.

In this study, it was shown that Chrysomelidae were significantly associated with the microclimatic variation among seasons. However, the strength of this association and the number of significant species were different for each season. Changes in the abundance of the leaf beetles were influenced by the heat index, temperature, evapotranspiration, and average wind speed, reflected by specific conditions required for each species. Microclimatic and seasonal assessment could be useful for the evaluation of climate change, since niche analysis enables detection of specialized or vulnerable species, which are associated with a delimited set of environmental conditions. This characterization of the microclimate niche of Chrysomelidae from a seasonal perspective was conducted here for the first time in northeastern Mexico. However, additional studies are warranted to determine if the observed patterns are different when evaluating other abiotic factors or when evaluating other plant communities.

Acknowledgements

Financial support for this study was granted by the Consejo Nacional de Ciencia y Tecnología (CONACYT-Mexico) (Doctoral scholarship No. 401277), as well as by the Programa del Mejoramiento del Profesorado (PROMEP) of the Universidad Autónoma de Tamaulipas. Sugeidi San Juanita Siaz Torres provided field support, measuring microclimatic variables during the sampling period. Sergio A. Terán Juárez collaborated in the photography and editing of chrysomelid images. We acknowledge support provided by the authorities from Ejido Santa Ana, Victoria, Tamaulipas, who authorized the fieldwork during the sampling period.

References

Anderson MC, Zolin CA, Sentelhas PC, Hain CR, Semmens K, Yilmaz MT, Gao F, Otkin JA, Tetra R (2016) The evaporative stress index as an indicador of agricultural drought in Brazil: An assessment based on crop yield impacts. Remote Sensing of Environment 174: 82–99. http://dx.doi.org/10.1016/j.rse.2015.11.034

Andrew NR, Hughes L (2005) Diversity and assemblage structure of phytophagous Hemiptera along a latitudinal gradient: predicting the potential impacts of climate change. Global Ecology and Biogeography 14: 249–262. https://doi.org/10.1111/j.1466-822x.2005.00149.x

Aneni TI, Aisagbonhi CI, Iloba BN, Adaigben VC, Ogbebor CO (2014) Influence of weather factors on seasonal population dynamics of *Coelaenomenodera elaeidis* (Coleoptera: Chrysomelidae) and its natural enemies in NIFOR, Nigeria. American Journal of Plant Sciences 5: 42–47. https://doi.org/10.4236/ajps.2014.51007

Ávila CJ, Postali-Parra JR (2003) Leaf consumption by *Diabrotica speciosa* (Coleoptera: Chrysomelidae) adults on different host plants. Scientia Agricola 60: 789–792. https://doi.org/10.1590/s0103-90162003000400028

Baselga A, Jiménez-Valverde A (2007) Environmental and geographical determinants of beta diversity of leaf beetles (Coleoptera: Chrysomelidae) in the Iberian Peninsula. Ecological Entomology 32: 312–318. https://doi.org/10.1111/j.1365-2311.2007.00880.x

Basset Y, Samuelson GA (1996) Ecological characteristics of an arboreal community of Chrysomelidae in Papua New Guinea. In: Jolivet PHA, Cox ML (Eds) Chrysomelidae Biology. Volume 2: Ecological Studies. SPB Academic Publishing. Netherlands, 243–262.

Basset Y, Aberlenc HP, Delvare G (1992) Abundance and stratification of foliage arthropods in a lowland rain forest of Cameroon. Ecological Entomology 17: 310–318. https://doi.org/10.1111/j.1365-2311.1992.tb01063.x

Bouzan MA, Flinte M, Valverde-Macedo M, Ferreira-Monteiro R (2015) Elevation and temporal distributions of Chrysomelidae in southeast Brazil with emphasis on the Galerucinae. ZooKeys 547: 103–117. https://doi.org/10.3897/zookeys.547.9723

Brook WB, Sodhi NS, Bradshaw CJA (2008) Synergies among extinction drivers under global change. Trends in Ecology and Evolution 23: 453–460. https://doi.org/10.1016/j.tree.2008.03.011

Burgos-Solorio A, Anaya-Rosales S (2004) Los crisomelinos (Coleoptera: Chrysomelidae: Chrysomelinae) del estado de Morelos. Acta Zoológica Mexicana 20: 39–66. https://doi.org/10.21829/azm.2004.2031581

Challenger A, Dirzo R (2009) Factores de cambio y estado de la biodiversidad. In: CONABIO (Ed.) Capital natural de México, vol. 2: Estado de conservación y tendencias de cambio. CONABIO, Mexico, 37–73.

Checa MF, Rodriguez J, Willmott KR, Liger B (2014) Microclimate variability significantly affects the composition, abundance, and phenology of butterfly communities in a highly threatened Neotropical dry forest. Florida Entomologist 97: 1–13. https://doi.org/10.1653/024.097.0101

Chen J, Saunders SC, Crow TR, Naiman RJ, Brosofske KD, Mroz GD, Brookshire BL, Franklin JF (1999) Microclimate in forest ecosystem and landscape ecology. BioScience 49: 288–297. https://doi.org/10.2307/1313612

Cloudsley-Thompson JL (1962) Microclimates and the distribution of terrestrial arthropods. Annual Review of Entomology 7: 199–222. https://doi.org/10.1146/annurev.en.07.010162.001215

Colwell RK (2013) EstimateS: Statistical estimation of species richness and shared species from samples. Version 9.1.0. http://purl.oclc.org/estimates

Comisión Nacional para el Conocimiento y Uso de la Biodiversidad (CONABIO), Comisión Nacional de Áreas Naturales Protegidas y The Nature Conservancy, Programa México, Pronatura (2007) Sitios prioritarios terrestres para la conservación de la biodiversidad.

Currano ED, Wilf P, Wing SL, Labandeira CC, Lovelock EC, Royer DL (2008) Sharply increased insect herbivory during the Paleocene-Eocene Thermal Maximum. Proceeding of the National Academy of Sciences of the United States of America 105: 1960–1964. https://doi.org/10.1073/pnas.0708646105

De-Lucia EH, Casteel CL, Nabity PD, O'Neill BF (2008) Insects take a bigger bite out of plants in a warmer, higher carbon dioxide world. Proceeding of the National Academy of Sciences of the United States of America 105: 1781–1782. https://doi.org/10.1073/pnas.0712056105

Dolédec S, Chessel D, Gimaret-Carpentier C (2000) Niche separation in community analysis: a new method. Ecology 81: 2914–2927. https://doi.org/10.2307/177351

Dormann CF, Schweiger O, Arens P, Augenstein I, Aviron ST, Bailey D (2008) Prediction uncertainty of environmental change effects on temperate European biodiversity. Ecology Letters 11: 235–244. https://doi.org/10.1111/j.1461-0248.2007.01142.x

Esker PD, Obrycki J, Nutter FW (2002) Temporal distribution of *Chaetocnema pulicaria* (Coleoptera: Chrysomelidae) populations in Iowa. Journal of Economic Entomology 95: 739–747. https://doi.org/10.1603/0022-0493-95.4.739

ESRI (2014) ArcGIS Desktop: versión 10.2.2. Redlands, California. Environmental Systems Research Institute.

Flinte V, Valverde de Macedo M (2004) Biology and seasonality of *Fulcidax monstrosa* (F.) (Chrysomelidae: Chlamisinae). The Coleopterists Bulletin 58: 457–465. https://doi.org/10.1649/629

Flinte V, De Freitas S, Valverde de Macedo M, Ferreida-Monteiro R (2011) Altitudinal and temporal distribution of *Plagiometriona* Spaeth, 1899 (Coleoptera, Chrysomelidae,

Cassidinae) in a tropical forest in southeast Brazil. ZooKeys 157: 15–31. https://doi.org/10.3897/zookeys.157.1179

Flinte V, Abejanella A, Daccordi M, Ferreida RM, Valverde-de Macedo M (2017) Chrysomelinae species (Coleoptera, Chrysomelidae) and new biological data from Rio de Janeiro, Brazil. ZooKeys 720: 5–22. https://doi.org/10.3897/zookeys.720.13963

Flowers RW (1996) La subfamilia Eumolpinae (Coleoptera: Chrysomelidae) en América Centra. Revista de Biología Tropical, Publicación especial 2: 1–60.

Furth DG (2009) Flea beetle diversity of the Sierra Tarahumara, Copper Canyon, Mexico (Chrysomelidae: Alticinae). In: Jolivet P, Schmitt M, Santiago-Blay J (Eds) Research on Chrysomelidae Volume 2. Koninklijke Brill. Leiden, The Netherlands, 131–151. https://doi.org/10.1163/ej.9789004152045.1-299.46

Furth DG (2013) Diversity of Alticinae in Oaxaca, Mexico: a preliminary study (Coleoptera, Chrysomelidae). In: Jolivet P, Santiago-Blay J, Schmitt M (Eds) Research on Chrysomelidae 4. ZooKeys, 1–32. https://doi.org/10.3897/zookeys.332.4790

Furth DG, Longino JT, Paniagua M (2003) Survey and quantitative assessment of flea beetle diversity in a Costa Rican rainforest (Coleoptera: Chrysomelidae: Alticinae). In: Furth DG (Ed.) Special topics in leaf beetle biology. Proceedings of the 5th International Symposium on the Chrysomelidae. Pensoft Publishers. Bulgaria, 1–23. https://agris.fao.org/agris-search/search.do?recordID=US201300259237

García-Atencia S, Martínez-Hernández N, Pardo-Locarno LC (2015) Escarabajos fitófagos (Coleoptera: Scarabaeidae) en un fragmento de bosque seco tropical del departamento del Atlántico, Colombia. Revista Mexicana de Biodiversidad 86: 754–763. https://doi.org/10.1016/j.rmb.2015.07.009

García-Morales LJ, Estrada-Castillón AE, García-Jiménez J, Villarreal-Quintanilla JA, Cantú-Ayala C, Jurado-Ybarra E, Vargas-Vázquez VA (2014) Florística y vegetación del Área Natural Protegida Altas Cumbres, Tamaulipas, México. In: Correa SA, Horta JV, García-Jiménez J, Barrientos-Lozano L (Eds) Biodiversidad tamaulipeca Vol. 2. Instituto Tecnológico de Ciudad Victoria. Tamaulipas, Mexico, 15–73.

Gobierno del Estado (2015) Decreto Gubernamental mediante el cual se aprueba el programa de manejo del Área Natural Protegida "Altas Cumbres", localizada en los municipios de Jaumave y Victoria, Tamaulipas. Órgano del Gobierno Constitucional del Estado Libre y Soberano de Tamaulipas. Periódico Oficial del Estado de Tamaulipas. Tomo CXL. Secretaria General de Gobierno. Cd Victoria, Mexico, 2–75.

Gotelli NJ, Colwell RK (2011) Chapter 4. Estimating species richness. In: Magurran AE, McGill BJ (Eds) Biological diversity: frontiers in measurement and assessment. Oxford University Press. New York, USA, 39–54.

Hammer O, Harper DAT, Ryan PD (2017) PAST: Paleontological statistics software package for education and data analysis. Palaeontologia Electronica 4: 1–9. http://palaeo-electronica.org/2001_1/past/issue1_01.htm

Hautier Y, Tilman D, Isbell F, Seabloom EW, Borer ET, Reich PB (2015) Anthropogenic environmental changes affect ecosystem stability via biodiversity. Science 348: 336–340. https://doi.org/10.1126/science.aaa1788

Hegland SJ, Nielsen A, Lázaro A, Bjerknes AL, Totland O (2009) How does climate warming affect plant-pollinator interactions? Ecology Letters 12: 184–95. https://doi.org/10.1111/j.1461-0248.2008.01269.x

Hill J, Griffiths H, Thomas C (2011) Climate change and evolutionary adaptations at species range margins. Annual Review of Entomology 56: 143–149. https://doi.org/10.1146/annurev-ento-120709-144746

Hill JK, Thomas CD, Fox R, Telfer MG, Willis SG, Asher J, Huntley B (2002) Responses of butterflies to twentieth century climate warming: implications for future ranges. Proceedings of the Royal Society B-Biological Sciences 269: 2163–2171. https://doi.org/10.1098/rspb.2002.2134

Hill JL, Hill RA (2001) Why are tropical rain forests so species rich? Classifying, reviewing, and evaluating theories. Progress in Physical Geography 25: 326–354. https://doi.org/10.1191/030913301680193805

Hódar JA, Zamora R, Peñuelas J (2004) El efecto del cambio global en las interacciones planta-animal. In: Valladares F (Ed.) Ecología del bosque mediterráneo en un mundo cambiante. Ministerio de Medio Ambiente, EGRAF S. A., Madrid, 248 pp.

Iannacone J, Alvariño L (2006) Diversidad de la artropofauna terrestre en la Reserva Nacional de Junín, Perú. Ecología Aplicada 5: 171–174. https://doi.org/10.21704/rea.v5i1-2.332

Isard SA, Spencer JL, Mabry TR, Levine E (2004) Influence of atmospheric conditions on high-elevation flight of western corn rootworm (Coleoptera: Chrysomelidae). Environmental Entomology 33: 650–656. https://doi.org/10.1603/0046-225x-33.3.650

Jiménez-Valverde A, Hortal J (2003) Las curvas de acumulación de especies y la necesidad de evaluar la calidad de los inventarios biológicos. Revista Ibérica de Aracnología 8: 151–161.

Jost L (2006) Entropy and diversity. Oikos 113: 363–375. https://doi.org/10.1111/j.2006.0030-1299.14714.x

Koji S, Nakamura K (2006) Seasonal fluctuation, age structure, and annual changes in a population of *Cassida rubiginosa* (Coleoptera: Chrysomelidae) in a natural habitat. Annals of the Entomological Society of America 99: 292–299. https://doi.org/10.1603/0013-8746(2006)099[0292:sfasaa]2.0.co;2

Konvicka M, Maradova M, Benes J, Fric Z, Kepka P (2003) Uphill shifts in distribution of butterflies in the Czech Republic: effects of changing climate detected on a regional scale. Global Ecology and Biogeography 12: 403–410. https://doi.org/10.1046/j.1466-822x.2003.00053.x

Lassau SA, Hochuli DF, Cassis G, Reid CAM (2005) Effects of habitat complexity on forest beetle diversity: do functional groups respond consistently? Diversity and Distribution 11: 73–82. https://doi.org/10.1111/j.1366-9516.2005.00124.x

Lee D, Brenner T (2015) Perceived temperature in the course of climate change: an analysis of global heat index from 1979 to 2013. Earth System Science Data 7(2): 193–202. https://doi.org/10.5194/essd-7-193-2015

Linzmeier AM, Ribeiro-Costa CS (2008) Seasonality and temporal structuration of Alticini community (Coleoptera, Chrysomelidae, Galerucinae) in the Araucaria Forest of Parana, Brazil. Revista Brasileira de Entomología 52: 289–295. https://doi.org/10.1590/s0085-56262008000200009

Linzmeier AM, Ribeiro-Costa CS (2013) Seasonal pattern of Chrysomelidae (Coleoptera) in the state of Paraná, southern Brazil. Biota Neotropica 13: 154–162. https://doi.org/10.1590/s1676-06032013000100018

Lucio-Garcia JN, Niño-Maldonado S, Coronado-Blanco JM, Horta-Vega JV, Reyes-Muñoz JL, Sánchez-Reyes UJ (2019) Diversidad de Chrysomelidae (Coleoptera) en un fragmento de bosque tropical subcaducifolio del noreste de México. Entomología mexicana 6: 348–355.

Lucio-García JN, Sánchez-Reyes UJ, Horta-Vega JV, Coronado-Blanco JM, Reyes-Muñoz JL, Niño-Maldonado S (2020) Especies de Galerucinae (Coleoptera: Chrysomelidae) asociadas a fragmentos de bosque tropical del estado de Tamaulipas. Entomología Mexicana 7: 286–293.

Luna-Castellanos F, Cuautle M, Feria-Arroyo TP, Castillo-Guevara C (2017) Effects of climatic change in the interaction plant-ant: a mini review on thermal tolerance. Mexican Journal of Biotechnology 2: 81–88. https://doi.org/10.29267/mxjb.2017.2.1.81

Magurran AE (2004) Measuring biological diversity. Blackwell Science Ltd. United Kingdom, 256 pp.

Marco V (2001) Modelación de la tasa de desarrollo de insectos en función de la temperatura. Aplicación al manejo integrado de plagas mediante el método de grados-días. Aracnet (Bol. S.E.A.) 7: 147–150. http://sea-entomologia.org/PDF/BOLETIN_28/B28-038-147.pdf

Martínez N, García S, Sanjuán S, Gutiérrez MJ, Contreras C (2010) Composición y estructura de la fauna de escarabajos (Insecta: Coleoptera) atraídos por trampas de luz en La Reserva Ecológica de Luriza, Atlántico, Colombia. Boletín de la Sociedad Entomológica Aragonesa 47: 373–381. https://dialnet.unirioja.es/servlet/articulo?codigo=3718541

Martínez-Sánchez I (2016) Bioecología de Chrysomelidae (Coleoptera) en los Cañones de la Libertad y el Novillo, Victoria, Tamaulipas. Phd Thesis, Universidad Autónoma de Tamaulipas, Instituto de Ecología Aplicada, Mexico.

Martínez-Sánchez I, Niño-Maldonado S, Barrientos-Lozano L, Horta-Vega JV (2009) Dinámica poblacional de Chrysomelidae (Coleoptera) en un gradiente altitudinal en tres municipios del estado de Hidalgo, México. Tecno INTELECTO 6: 1–4.

Mejia M (2005) Calentamiento global y la distribución de plagas. Boletín de la NAPPO (Ontario, Canada), 2 pp.

Miwa K, Meinke LJ (2017) Seasonality of *Colaspis crinicornis* (Coleoptera: Chrysomelidae) and its injury potential to corn in southeastern Nebraska. Journal of Economic Entomology 111: 209–217. https://doi.org/10.1093/jee/tox325

Morrone JJ, Márquez J (2008) Biodiversity of Mexican terrestrial arthropods (Arachnida and Hexapoda): a biogeographical puzzle. Acta Zoológica Mexicana 24: 15–41. https://doi.org/10.21829/azm.2008.241613

Murillo D, Ortega I, Carrillo JD, Pardo A, Rendon J (2012) Comparación de métodos de interpolación para la generación de mapas de ruido en entornos urbanos. Ingenierías USBMed 3: 62–68. https://doi.org/10.21500/20275846.265

Niño-Maldonado S, Sánchez-Reyes UJ (2017) Taxonomía de insectos. Orden Coleoptera. Familia Chrysomelidae. In: Cibrián-Tovar D (Ed.) Fundamentos de entomología forestal. Red de salud forestal – Redes temáticas de la Comisión Nacional de Ciencia y Tecnología (CONACYT), Mexico, 304–310.

Niño-Maldonado S, Riley EG, Furth DG, Jones RW (2005) Coleoptera: Chrysomelidae: In: Sánchez-Ramos G, Reyes-Castillo P, Dirzo R (Eds) Historia natural de la Reserva de la Biósfera El Cielo, Tamaulipas, México. Universidad Autónoma de Tamaulipas, Mexico, 417–422.

Niño-Maldonado S, Romero-Nápoles J, Sánchez-Reyes UJ, Jones RW, González-De-León EI (2014) Inventario preliminar de Chrysomelidae (Coleoptera) de Tamaulipas, México. In: Correa-Sandoval J, Horta-Vega V, García-Jiménez J, Barrientos-Lozano L (Eds) Biodiversidad Tamaulipeca Vol. 2, No. 2. Tecnológico Nacional de México, Instituto Tecnológico de Ciudad Victoria, Mexico, 121–132.

Noguera FA (1988) Hispinae y Cassidinae (Coleoptera: Chrysomelidae) de Chamela, Jalisco, México. Entomología Mexicana 77: 277–311.

Novotny V, Basset Y, Auga J, Boen W, Dal C, Drozd P, Kasbal M, Isua B, Kutil R, Manumbor M, Molem K (1999) Predation risk for herbivorous insects on tropical vegetation: a search for enemy-free space and time. Austral Ecology 24: 477–483. https://doi.org/10.1046/j.1440-169x.1999.00987.x

Ohsawa M, Nagaike T (2006) Influence of forest types and effects of forestry activities on species richness and composition of Chrysomelidae in the central mountainous region of Japan. Biodiversity and Conservation 15: 1179–1191. https://doi.org/10.1007/978-1-4020-5208-8_8

Oliveira D, Freire-Zilch KC, Hintz FC, Köhler A (2017) Populational fluctuation and distribution of *Epitrix* sp. Foudras (Coleoptera: Chrysomelidae) in the organic tobacco management in Santa Cruz do Sul, RS, Brazil. American Journal of Plant Sciences 8: 3285–3294. https://doi.org/10.4236/ajps.2017.812221

Parmesan C, Yohe G (2003) A globally coherent fingerprint of climate change impacts across natural systems. Nature 421: 37–42. https://doi.org/10.1038/nature01286

Parmesan C, Ryrholm N, Stefanescu C, Hill JK, Thomas CD, Descimon H, Huntley B (1999) Poleward shifts in geographical ranges of butterfly species associated with regional warming. Nature 399: 579–583. https://doi.org/10.1038/21181

Pedraza M, Márquez J, Gómez-Anaya JA (2010) Estructura y composición de los ensambles estacionales de coleópteros (Insecta: Coleoptera) del bosque mesófilo de montaña en Tlanchinol, Hidalgo, México, recolectados con trampas de intercepción de vuelo. Revista Mexicana de Biodiversidad 81: 437–456. https://doi.org/10.22201/ib.20078706e.2010.002.234

Petermann JS, Muller CB, Weigelt A, Weisser WW, Schmid B (2010) Effect of plant species loss on aphid parasitoid communities. Journal of Animal Ecology 79: 709–720. https://doi.org/10.1111/j.1365-2656.2010.01674.x

Petitpierre E, Bastazo G, Blasco-Zumeta J (2000) Crisomélidos (Coleoptera: Chrysomelidae) de un sabinar de *Juniperus thurifera* L. en los Monegros (Zaragoza, NE, España). Sociedad Entomológica Aragonesa 27: 53–61.

Pimm SL (2007) Biodiversity: climate change or habitat loss – which will kill more species? Current Biology 18: 117–119. https://doi.org/10.1016/j.cub.2007.11.055

Pinheiro F, Diniz I, Coelho RD, Bandeira MPS (2002) Seasonal pattern of insect abundance in the Brazilian cerrado. Austral Ecology 27: 132–136. https://doi.org/10.1046/j.1442-9993.2002.01165.x

Régnière J (2009) Predicción de la distribución continental de insectos a partir de la fisiología de las especies. Unasylva 60: 37–42. http://www.fao.org/3/i0670s/i0670s09.pdf

Řehounek J (2002) Comparative study of the leaf beetles (Coleoptera: Chrysomelidae) in chosen localities in the district of Nymburk. Acta Universitatis. Palackianae Olomucensis Facultas Rerum Natturalium Biologica 40: 123–130.

Riley EG, Clark SM, Flowers RW, Gilbert AJ (2002) Chrysomelidae Latreille 1802. In: Arnett RH, Thomas MC, Skelley PE, Frank JH (Eds) American Beetles. Polyphaga: Scarabaeoidea through Curculionoidea. Vol 2. CRC Press LLC. Boca Raton, FL, 617–691.

Root TL, Price JT, Hall KR, Schneider SH, Rosenzweing C, Pounds AJ (2003) Fingerprints of global warming on wild animals and plants. Nature 421: 57–60. https://doi.org/10.1038/nature01333

Rzedowski J (2006) Vegetación de México. 1ra. Edición digital. Comisión Nacional para el Conocimiento y Uso de la Biodiversidad, Mexico, 504 pp. https://doi.org/10.2307/1219727

Sánchez-Reyes UJ (2014) Análisis y distribución de Chrysomelidae (Coleoptera) en la Sierra de San Carlos, Tamaulipas. MS Thesis, Instituto Tecnológico de Cd. Victoria. Tamaulipas, Mexico, 31(1): 10–22. https://doi.org/10.21829/azm.2015.311499

Sánchez-Reyes UJ, Niño-Maldonado S, Barrientos-Lozano L, Banda-Hernández JE, Medina-Puente A (2013) Galerucinae (Coleoptera: Chrysomelidae) del Cañón de la Peregrina, Victoria, Tamaulipas, México. Entomología Mexicana 12: 1517–1522.

Sánchez-Reyes UJ, Niño-Maldonado S, Jones RW (2014) Diversity and altitudinal distribution of Chrysomelidae (Coleoptera) in Peregrina Canyon, Tamaulipas, Mexico. ZooKeys 417: 103–132. https://doi.org/10.3897/zookeys.417.7551

Sánchez-Reyes UJ, Niño-Maldonado S, Barrientos-Lozano L, Jones RW, Sandoval-Becerra FM (2015a) Análisis del nicho ecológico de Cryptocephalinae (Coleoptera: Chrysomelidae) en la Sierra de San Carlos, Tamaulipas, México. Entomología Mexicana 2: 526–532.

Sánchez-Reyes UJ, Niño-Maldonado S, Meléndez-Jaramillo E, Gómez-Moreno VC, Banda-Hernández JE (2015b) Riqueza de Chrysomelidae (Coleoptera) en el Cerro el Diente, San Carlos, Tamaulipas, México. Acta Zoológica Mexicana 31: 10–22. https://doi.org/10.21829/azm.2015.311499

Sánchez-Reyes UJ, Niño-Maldonado S, Barrientos-Lozano L, Clark SM, Jones RW (2016a) Faunistic patterns of leaf beetles (Coleoptera, Chrysomelidae) within elevational and temporal gradients in Sierra de San Carlos, Mexico. ZooKeys 611: 11–56. https://doi.org/10.3897/zookeys.611.9608

Sánchez-Reyes UJ, Niño-Maldonado S, Barrientos-Lozano L, Sandoval-Becerra FM (2016b) Influencia del clima en la distribución de Chrysomelidae (Coleoptera) en el Cañón de la Peregrina, Tamaulipas, México. Entomología Mexicana 3: 467–473.

Sánchez-Reyes UJ, Niño-Maldonado S, Barrientos-Lozano L, Treviño-Carreón J (2017) Assessment of land use-cover changes and successional stages of vegetation in the Natural Protected Area Altas Cumbres, Northeastern Mexico, using Landsat satellite imagery. Remote Sensing 9: 1–33. https://doi.org/10.3390/rs9070712

Sánchez-Reyes UJ, Niño-Maldonado S, Barrientos-Lozano L, Clark SM, Treviño-Carreón J, Almaguer-Sierra P (2019) Microclimate niche requirements ofleaf beetles (Chrysomelidae: Coleoptera) inasuccessional gradient oflow thorn forest innortheastern Mexico. Journal of Insect Conservation 23: 503–524. https://doi.org/10.1007/s10841-019-00140-2

Sandoval-Becerra FM, Sánchez-Reyes UJ, Niño-Maldonado S, Horta-Vega JV (2016) Patrones de actividad de Cassidinae Gyllenhal, 1813 (Coleoptera: Chrysomelidae) en el sendero interpretativo El Tepalo, Chapala, Jalisco. Entomología mexicana 3: 488–494.

Sandoval-Becerra FM, Niño-Maldonado S, Sánchez-Reyes UJ, HortaVega JV, Venegas-Barrera CS, Martínez-Sánchez I (2017) Respuesta de la comunidad de Chrysomelidae (Coleoptera) a la variación microclimática en un fragmento de bosque de encino del noreste de México. Entomología Mexicana 4: 421–427.

Santiago-Blay JA (1994) Paleontology of leaf beetles: In: Jolivet PH, Cox ML, Petitpierre E (Eds) Novel aspects of the biology of Chrysomelidae. Kluwer Academic Publishers, Dordrecht, 1–68. https://doi.org/10.1007/978-94-011-1781-4_1

Schaefer HC, Jetz W, Böhning-Gaese K (2008) Impact of climate change on migratory birds: community reassembly versus adaptation. Global Ecology and Biogeography 17: 38–49. https://doi.org/10.1111/j.1466-8238.2007.00341.x

Scherer G (1983) Diagnostic key for the Neotropical Alticinae genera. Entomologische Arbeiten aus dem Museum G. Frey 31/32: 2–89.

Şen I, Gök A (2016) Seasonal activity of adult leaf beetles (Coleoptera: Chrysomelidae, Orsodacnidae) occurring in Kovada Lake and Kızılda˘g National Parks in Isparta Province (Turkey). Biología 71: 593–603. https://doi.org/10.1515/biolog-2016-0062

Silva JO, Leal CRO, Espirito-Santo MM, Morais HC (2017) Seasonal anddiel variations intheactivity ofcanopy insect herbivores differ betweendeciduous andevergreen plant species inatropical dry forest. Journal of Insect Conservation 21: 667–676. https://doi.org/10.1007/s10841-017-0009-9

Soler JM, García-Mari F, Alonso D (2002) Evolución estacional de la entomofauna auxiliar en cítricos. Boletin Sanidad Vegetal Plagas 28: 133–149. https://doi.org/10.4995/thesis/10251/5952

Staines C (2002) The New World tribes and genera of hispines (Coleoptera: Chrysomelidae: Cassidinae). Proceedings of the Entomological Society of Washington 104: 721–784.

StatSoft Inc (2007) STATISTICA: data analysis software system, version 8.0. www.statsoft.com

Stewart CA, Emberson RM, Syrett P (1996) Temperature effects on the alligator weed flea-beetle *Agasicles hygrophila* (Coleoptera: Chrysomelidae): implications for biological control in New Zealand. In: Moran VC, Hoffman JH (Eds) Proceedings of the IX International Symposium on Biological Control of Weeds. University of Cape Town. South Africa, 393–398.

Stuble KL, Pelini SL, Diamond SE, Fowler DA, Dunn RR, Sanders NJ (2013) Foraging by forest ants under experimental climatic warming: a test at two sites. Ecology and Evolution 3: 482–491. https://doi.org/10.1002/ece3.473

Thioulouse J, Chessel D, Dolédec S, Olivier JM (1997) ADE-4: a multivariate analysis and graphical display software. Stat Comput 7: 75–83. https://doi.org/10.1023/A:1018513530268

Triplehorn CA, Johnson NF (2005) Borror and DeLong´s Introduction to the Study of Insects. Seventh Edition. Thomson Brooks/Cole, Learning Inc. United States of America, 864 pp.

Tscharntke T, Steffan-Dewenter I, Kruess A, Thies TC (2002) Characteristics of insect populations on habitat fragments: a mini review. Ecological Research 17: 229–239. https://doi.org/10.1046/j.1440-1703.2002.00482.x

Uribe-Botero E (2015) El cambio climático y sus efectos en la biodiversidad en América Latina. Comisión Económica para América Latina y el Caribe, Naciones Unidas. Santiago, 84 pp.

Vié JC, Hilton-Taylor C, Stuart SN (2009) Wildlife in a changing world – an analysis of the 2008 IUCN Red List of threatened species. Ingoprint. Barcelona, España, 180 pp. https://doi.org/10.2305/IUCN.CH.2009.17.en

Wang C, Hawthorne D, Qin Y, Pan X, Li Z, Zhu S (2017) Impact of climate and host availability on future distribution of Colorado potato beetle. Scientific Reports 7: 1–9. https://doi.org/10.1038/s41598-017-04607-7

Wąsowska M (2004) Impact of humidity and mowing on chrysomelid communities (Coleoptera, Chrysomelidae) in meadows of the Wierzbanówka valley Pogórze Wielickie hills, Southern Poland. Biologia Bratislava 59: 601–611.

White RE (1993) A revision of the subfamily Criocerinae (Chrysomelidae) of North America north of Mexico. United States Department of Agriculture, Agricultural Research Service. Technical Bulletin 1805, 158 pp.

Wilcox JA (1972) A review of the North American Chrysomelinae leaf beetles (Coleoptera: Chrysomelidae). University of the State of New York. State Education Department. State Museum and Science Service. Bulletin 421, 37 pp.

Williams PH, Araújo MB, Rasmont P (2007) Can vulnerability among British bumblebee (*Bombus*) species be explained by niche position and breadth? Biological Conservation 138: 493–505. https://doi.org/10.1016/j.biocon.2007.06.001

Wilson RJ, Gutiérrez D, Gutiérrez J, Monserrat VJ (2007) An elevational shift in butterfly species richness and composition accompanying recent climate change. Global Change Biology 13: 1873–1887. https://doi.org/10.1111/j.1365-2486.2007.01418.x

Wolda H (1988) Insect seasonality: Why? Annual Review of Ecology and Systematics 19: 1–18. https://doi.org/10.1146/annurev.es.19.110188.000245

Yanes-Gómez G, Morón MA (2010) Fauna de coleópteros Scarabaeoidea de Santo Domingo Huehuetlán, Puebla, México. Su potencial como indicadores ecológicos. Acta Zoológica Mexicana 26: 123–145. https://doi.org/10.21829/azm.2010.261683

Appendix 1

Table A1. Taxonomic checklist of Chrysomelidae by season in a fragment of semideciduous tropical forest from northeastern Mexico (March 2016 to February 2017).

Taxon		Rainy season	Dry season
	N	N	N
CRIOCERINAE Latreille, 1807	**14**		
Tribe Lemini Heinze, 1962			
Lema sp. 1	5	–	5
Lema sp. 2	2	2	–
Lema sp. 3	2	–	2
Neolema sp. 1	2	2	–
Oulema sp. 1	3	3	–
CASSIDINAE Gyllenhal, 1813	**410**		
Tribe Chalepini Weise, 1910			
Baliosus sp. 1	1	1	–
Brachycoryna pumila Guérin-Méneville, 1844	34	17	17

Taxon		Rainy season	Dry season
	N	N	N
Chalepus digressus Baly, 1885	1	–	1
Heterispa vinula (Erichson, 1847)	311	209	102
Octotoma intermedia Staines, 1989	3	3	–
Sumitrosis inaequalis (Weber, 1801)	2	2	–
Tribe Cassidini Gyllenhal, 1813			
Agroiconota vilis (Boheman, 1855)	1	1	–
Charidotella sexpunctata (Fabricius, 1781)	3	2	1
Helocassis clavata (Fabricius, 1798)	12	5	7
Helocassis crucipennis (Boheman, 1855)	37	16	21
Microctenochira punicea (Boheman, 1855)	4	3	1
Microctenochira varicornis (Spaeth, 1926)	1	1	–
CHRYSOMELINAE Latreille, 1802	**9**		
Tribe Chrysomelini Latreille, 1802			
Calligrapha ancoralis Stål, 1860	1	1	–
Calligrapha fulvipes Stål, 1859	1	–	1
Deuterocampta atromaculata Stål, 1859	1	1	–
Labidomera suturella Chevrolat, 1844	3	1	2
Plagiodera semivittata Stål, 1860	2	1	1
Plagiodera thymaloides Stål, 1860	1	1	–
GALERUCINAE Latreille, 1802	**1628**		
Tribe Galerucini Latreille, 1802			
Coraia subcyanescens (Schaeffer, 1906)	8	8	–
Tribe Luperini Chapuis, 1875			
Acalymma sp. 1	1	1	–
Cyclotrypema furcata (Olivier, 1808)	23	23	–
Diabrotica biannularis Harold, 1875	1	1	–
Gynandrobrotica lepida (Say, 1835)	8	1	7
Paratriarius curtisii (Baly, 1886)	1	1	–
Tribe Alticini Newman, 1835			
Acallepitrix sp. 1	1	–	1
Acallepitrix sp. 2	1	1	–
Acallepitrix sp. 3	2	2	–
Acallepitrix sp. 4	3	–	3
Acallepitrix sp. 5	11	5	6
Acallepitrix sp. 6	9	2	7
Acallepitrix sp. 7	8	4	4
Acallepitrix sp. 8	2	2	–
Acrocyum dorsale Jacoby, 1885	30	17	13
Acrocyum sp. 1	2	–	2
Alagoasa bipunctata (Chevrolat, 1834)	8	5	3
Alagoasa trifasciata (Fabricius, 1801)	19	15	4
Alagoasa sp. 1	1	1	–
Asphaera abdominalis (Chevrolat, 1835)	1	1	–
Asphaera nigrofasciata Jacoby, 1885	1	1	–
Centralaphthona diversa (Baly, 1877)	692	440	252
Centralaphthona sp. 1	1	1	–
Chaetocnema sp. 1	19	6	13
Disonycha stenosticha Schaefer, 1931	1	–	1
Epitrix sp. 1	28	10	18
Heikertingerella sp. 1	24	21	3
Longitarsus sp. 1	7	4	3
Longitarsus sp. 2	16	1	15
Margaridisa sp. 1	147	16	131
Monomacra bumeliae (Schaeffer, 1905)	528	336	192
Phyllotreta aeneicollis (Crotch, 1873)	1	1	–
Syphrea sp. 1	8	2	6

Taxon		Rainy season	Dry season
	N	N	N
Syphrea sp. 2	5	5	–
Walterianella sp. 1	9	8	1
Walterianella sp. 2	1	1	–
CRYPTOCEPHALINAE Gyllenhal, 1813	**6**		
Tribe Cryptocephalini Gyllenhal, 1813			
Cryptocephalus umbonatus Schaeffer, 1906	1	–	1
Diachus chlorizans (Suffrian, 1852)	1	1	–
Tribe Clytrini Lacordaire, 1848			
Babia distinguenda Jacoby, 1889	1	1	–
Smaragdina agilis (Lacordaire, 1848)	3	–	3
EUMOLPINAE Hope, 1840	**36**		
Tribe Eumolpini Hope, 1840			
Brachypnoea sp. 1	3	1	2
Brachypnoea sp. 2	5	1	4
Colaspis freyi (Bechyné, 1950)	1	1	–
Colaspis melancholica Jacoby, 1881	13	12	1
Colaspis townsendi Bowditch, 1921	1	1	–
Xanthonia sp. 1	3	–	3
Zenocolaspis inconstans (Lefèvre, 1878)	8	7	1
Tribe Typophorini Chapuis, 1874			
Paria sp. 1	2	2	–
71 species Totals	**2103**	**1242**	**861**

Table A2. Outlying Mean Index parameters for chrysomelid species in the rainy season. Key: InerO = Total inertia, OMI = Marginality index, T1 = Tolerance, T2 = Residual tolerance, *p* = probability; significant values in bold.

Species	InerO	OMI	T1	T2	P
Acallepitrix sp. 2	3.76	3.76	0.00	0.00	0.55
Acallepitrix sp. 3	11.91	5.64	3.86	2.42	0.16
Acallepitrix sp. 5	5.74	2.92	0.82	2.00	0.09
Acallepitrix sp. 6	11.66	7.62	2.35	1.69	0.08
Acallepitrix sp. 7	3.88	0.23	0.99	2.67	0.96
Acallepitrix sp. 8	3.72	3.03	0.10	0.59	0.42
Acalymma sp. 1	4.56	4.56	0.00	0.00	0.47
Acrocyum dorsale	6.33	0.54	2.01	3.78	0.24
Agroiconota vilis	1.51	1.51	0.00	0.00	0.91
Alagoasa bipunctata	3.45	0.85	0.97	1.63	0.70
Alagoasa trifasciata	**5.20**	**2.52**	**0.90**	**1.78**	**0.00**
Alagoasa sp. 1	2.29	2.29	0.00	0.00	0.78
Asphaera abdominalis	2.29	2.29	0.00	0.00	0.78
Asphaera nigrofasciata	5.57	5.57	0.00	0.00	0.40
Babia distinguenda	9.82	9.82	0.00	0.00	0.23
Brachycoryna pumila	5.14	0.95	2.58	1.62	0.25
Brachypnoea sp. 1	5.83	5.83	0.00	0.00	0.37
Brachypnoea sp. 2	0.75	0.75	0.00	0.00	0.97
Calligrapha fulvipes	3.05	3.05	0.00	0.00	0.65
Centralaphthona diversa	**6.01**	**0.20**	**2.14**	**3.67**	**0.02**
Centralaphthona sp. 1	0.94	0.94	0.00	0.00	0.96
Chaetocnema sp. 1	5.46	1.58	0.81	3.08	0.43
Charidotella sexpunctata	2.52	1.27	0.62	0.63	0.79
Colaspis freyi	4.30	4.30	0.00	0.00	0.49
Colaspis melancholica	7.96	7.96	0.00	0.00	0.31
Colaspis townsendi	3.33	1.00	0.24	2.08	0.40

Species	InerO	OMI	T1	T2	P
Coraia subcyanescens	4.61	0.57	0.42	3.62	0.78
Cyclotrypema furcata	3.25	0.37	0.70	2.18	0.58
Diabrotica biannularis	2.22	2.22	0.00	0.00	0.81
Diachus chlorizans	0.59	0.59	0.00	0.00	0.98
Deuterocampta atromaculata	3.05	3.05	0.00	0.00	0.65
Epitrix sp. 1	4.62	3.55	0.37	0.70	0.07
Gynandrobrotica lepida	20.23	20.23	0.00	0.00	0.06
Heikertingerella sp. 1	6.29	0.11	1.29	4.89	0.96
Helocassis clavata	9.99	1.93	6.06	2.00	0.22
Helocassis crucipennis	5.12	1.61	0.46	3.05	0.09
Heterispa vinula	6.06	0.09	1.30	4.68	0.21
Labidomera suturella	**23.86**	**23.86**	**1.83**	**0.00**	**0.04**
Lema sp. 2	6.01	4.36	0.80	0.85	0.26
Longitarsus sp. 1	17.20	5.69	10.66	0.85	0.07
Longitarsus sp. 2	2.53	2.53	0.00	0.00	0.75
Margaridisa sp. 1	5.40	0.16	2.07	3.17	0.86
Microctenochira punicea	2.59	1.41	0.38	0.80	0.59
Microctenochira varicornis	9.80	9.80	0.00	0.00	0.23
Monomacra bumeliae	**6.99**	**0.44**	**1.70**	**4.85**	**0.00**
Neolema sp. 1	5.55	5.45	0.00	0.10	0.18
Octotoma sp. 1	4.60	1.23	1.88	1.50	0.66
Oulema sp. 1	3.75	2.72	0.08	0.94	0.49
Paratriarius curtisii	2.62	2.62	0.00	0.00	0.71
Paria sp. 1	8.16	2.32	3.98	1.86	0.56
Phyllotreta aeneicollis	6.34	6.34	0.00	0.00	0.35
Plagiodera semivittata	4.00	4.00	0.00	0.00	0.53
Plagiodera thymaloides	3.15	3.15	0.00	0.00	0.65
Sumitrosis inaequalis	3.17	0.35	0.64	2.18	0.97
Sumitrosis sp. 1	1.24	1.24	0.00	0.00	0.94
Syphrea sp. 1	1.70	0.60	0.01	1.08	0.92
Syphrea sp. 2	3.41	3.20	0.04	0.16	0.44
***Walterianella* sp. 1**	**7.26**	**5.25**	**1.49**	**0.51**	**0.02**
Walterianella sp. 2	2.62	2.62	0.00	0.00	0.71
Zenocolaspis inconstans	**6.56**	**4.15**	**0.23**	**2.18**	**0.02**

Table A3. Outlying Mean Index parameters for chrysomelid species in the dry season. Key: InerO = Total inertia, OMI = Marginality index, T1 = Tolerance, T2 = Residual tolerance, p = probability; significant values in bold.

Species	InerO	OMI	T1	T2	P
Acallepitrix sp. 1	7.86	7.86	0.00	0.00	0.41
Acallepitrix sp. 4	5.76	2.15	0.23	3.38	0.41
Acallepitrix sp. 5	5.63	0.90	3.16	1.58	0.45
Acallepitrix sp. 6	6.31	0.46	2.41	3.43	0.80
***Acallepitrix* sp. 7**	**8.30**	**6.09**	**0.42**	**1.79**	**0.02**
Acrocyum dorsale	8.21	0.25	3.58	4.38	0.72
Acrocyum sp. 1	14.37	7.55	4.42	2.40	0.10
Alagoasa trifasciata	**7.09**	**6.52**	**0.04**	**0.53**	**0.05**
Alagoasa sp. 1	4.47	1.72	0.68	2.07	0.52
Brachycoryna pumila	**9.76**	**2.11**	**5.09**	**2.56**	**0.03**
Brachypnoea sp. 1	9.51	0.65	4.61	4.25	0.95
Brachypnoea sp. 2	12.33	12.33	0.00	0.00	0.10
Calligrapha fulvipes	5.45	5.45	0.00	0.00	0.56
Centralaphthona diversa	**8.06**	**0.30**	**2.79**	**4.97**	**0.04**
Chaetocnema sp. 1	**10.03**	**6.78**	**1.71**	**1.54**	**0.01**

Species	InerO	OMI	T1	T2	P
Chalepus digressus	12.80	12.80	0.00	0.00	0.09
Charidotella sexpunctata	9.42	9.42	0.00	0.00	0.22
Colaspis townsendi	5.85	5.85	0.00	0.00	0.52
Cryptocephalus umbonatus	0.83	0.83	0.00	0.00	0.98
Disonycha stenosticha	8.31	8.31	0.00	0.00	0.32
***Epitrix* sp. 1**	**7.50**	**3.02**	**1.43**	**3.05**	**0.01**
Gynandrobrotica lepida	4.94	1.29	0.25	3.41	0.24
Heikertingerella sp. 1	5.75	0.88	2.31	2.57	0.76
Helocassis clavata	6.28	0.57	4.26	1.45	0.58
Helocassis crucipennis	8.65	1.95	5.37	1.33	0.13
Heterispa vinula	7.04	0.23	1.79	5.02	0.15
Labidomera suturella	3.43	1.30	0.78	1.34	0.82
Lema sp. 1	8.29	1.54	4.25	2.50	0.82
Lema sp. 3	2.29	2.29	0.00	0.00	0.89
Longitarsus sp. 1	5.51	2.46	0.09	2.96	0.34
Longitarsus sp. 2	5.79	0.13	0.20	5.47	0.88
Margaridisa sp. 1	7.69	0.13	3.27	4.29	0.96
Microctenochira punicea	2.93	2.93	0.00	0.00	0.76
Monomacra bumeliae	6.20	0.16	2.86	3.18	0.08
Plagiodera thymaloides	5.72	5.72	0.00	0.00	0.54
Smaragdina agilis	5.31	0.53	1.71	3.07	0.97
***Syphrea* sp. 1**	**11.29**	**9.97**	**0.20**	**1.12**	**0.01**
Walterianella sp. 1	5.72	5.72	0.00	0.00	0.54
Xanthonia sp. 1	4.60	2.42	0.23	1.95	0.36
Zenocolaspis inconstans	4.25	4.25	0.00	0.00	0.69

ZooKeys 1080: 53–97 (2022)
doi: 10.3897/zookeys.1080.74286
https://zookeys.pensoft.net

RESEARCH ARTICLE

A peer-reviewed open-access journal
ZooKeys
Launched to accelerate biodiversity research

Three cryptic *Anaplecta* (Blattodea, Blattoidea, Anaplectidae) species revealed by female genitalia, plus seven new species from China

Jing Zhu[1], Jiawei Zhang[1], Xinxing Luo[1], Zongqing Wang[1], Yanli Che[1]

1 *College of Plant Protection, Southwest University, Beibei, Chongqing 400715, China*

Corresponding author: Yanli Che (shirleyche2000@126.com)

Academic editor: F. Legendre | Received 11 September 2021 | Accepted 30 November 2021 | Published 4 January 2022

http://zoobank.org/86DAAF2D-C098-452B-B3EA-51D84EB5855E

Citation: Zhu J, Zhang J, Luo X, Wang Z, Che Y (2022) Three cryptic *Anaplecta* (Blattodea, Blattoidea, Anaplectidae) species revealed by female genitalia, plus seven new species from China. ZooKeys 1080: 53–97. https://doi.org/10.3897/zookeys.1080.74286

Abstract

Morphological characteristics, including male and female genitalia, combined with DNA barcodes were used to identify 470 *Anaplecta* specimens sampled from China. Ten *Anaplecta* species are new to science, including three cryptic species: *A. paraomei* Zhu & Che, **sp. nov.**, *A. condensa* Zhu & Che, **sp. nov.**, and *A. longihamata* Zhu & Che, **sp. nov.**, which are distinguished mainly by their female genitalia. The other seven new species are as follows: *A. bicruris* Zhu & Che, **sp. nov.**, *A. spinosa* Zhu & Che, **sp. nov.**, *A. ungulata* Zhu & Che, **sp. nov.**, *A. anomala* Zhu & Che, **sp. nov.**, *A. serrata* Zhu & Che, **sp. nov.**, *A. bombycina* Zhu & Che, **sp. nov.**, and *A. truncatula* Zhu & Che, **sp. nov.** This study illustrates that differences in female genitalia can be used to distinguish among species of *Anaplecta*. The female genitalia of 19 Chinese *Anaplecta* species are described and illustrated in this paper.

Keywords

ABGD, *Anaplecta omei*, cryptic species, DNA barcodes, female genitalia

Introduction

The genus *Anaplecta*, has been attributed to the superfamily Blattoidea (Djernæs 2018) based on molecular studies (Djernaes et al. 2015; Wang et al. 2017; Bourguignon et al. 2018). In previous studies, body color and veins were usually used to distinguish

Anaplecta species (Shelford 1906; Rehn 1916). However, intraspecific variations in costal veins and cross veins of the medio-radia as well as in body color were found, which reduces the value of these characteristics for morphology-based identification (Bruijning, 1948). Almost forty years later, and as for other cockroaches, male genitalia were gradually adopted as the main characters to identify species of *Anaplecta* (Roth 1990, 1996; Lucañas 2016; Deng et al. 2020) .

Deng et al. (2020) established eight *Anaplecta* species from China with the aid of DNA barcodes, which successfully solved several problems in identification. Males and females were difficult to match if only based on morphological characters, and there was intraspecific variation in male genitalia. After careful examination, we found that the samples of *Anaplecta omei* examined in Deng (2020) belong to a complex species containing three species (*A. omei*, *A. paraomei* sp. nov., and *A. condensa* sp. nov.; see below); Deng (2020) had treated the differences in male genitalia as intraspecific variation of *Anaplecta omei*. We re-examined all the samples that had been identified as *Anaplecta omei*, and found some subtle differences in the samples from Libo, Dushan, Mt. Wuliang, and other regions, differences that could either reflect intraspecific variations or interspecific differences.

Therefore, it is necessary to find new morphological characters to identify *Anaplecta* species. Although female genitalia were considered to have fewer useful morphological characters in the taxonomy of cockroaches, Aldrich et al. (2004) successfully identified four *Cryptocercus* species based on female genitalia. Female genitalia have also been used in the identification of *Cryptocercus* (Wang et al. 2015; Bai et al. 2018). Meanwhile, female genitalia of other cockroaches were gradually described in detail and used to distinguish species in Ectobiidae (Bohn et al. 2010; Anisyutkin 2013), Blaberidae (Anisyutkin 2014, 2016), or Blattidae (Grandcolas et al. 2014).

In the present study, we use DNA barcodes combined with morphological characteristics, including male and female genitalia, to comprehensively analyze and identify 470 samples of *Anaplecta*, and to determine whether the samples from Libo, Dushan, Mt. Wuliang should be treated as cryptic species.

Materials and methods

Morphological study

We examined 470 *Anaplecta* specimens, including 165 females. The measurements are based on examined specimens. The genitalia were soaked in 10% NaOH at 65 °C for 30–35 minutes, then rinsed with distilled water. All segments were dissected and observed in glycerol with a Motic K400 stereomicroscope or a Leica M205A stereomicroscope. Photographs were taken with a Leica M205A stereomicroscope, and edited with Adobe Photoshop CS6. All type materials are deposited at the Institute of Entomology, College of Plant Protection, Southwest University, Chongqing, China (**SWU**).

The terminology for body, male, and female genitalia mainly follows McKittrick (1964), Roth (1990), Wang et al. (2016), and Deng et al. (2020). Terminology for veins follows Li et al. (2018).

Abbreviations in this paper are as follows:

CuA cubitus anterior;
CuP cubitus posterior;
L1, L2, L3 sclerites of the left phallomere;
L2d L2 dorsal;
L2v L2 ventral;
L2vm median sclerite;
M media;
R1, R2, R3 sclerites of the right phallomere.

PCR amplification and sequencing

A total of 38 specimens was used for COI sequencing in this study. Total DNA was extracted from the muscles of the thorax and legs according to the Hipure Tissue DNA MiniKit. Primers for polymerase chain reaction (PCR) were COI-F3 (5'-CAACYAATCATAAAGANATTGGAAC-3') and COI-R3 (5'-TAAACTTCTGGRTGACCAAARAATCA-3'). The thermal cycling conditions were as follows: initial denaturation 2 min at 98 °C, followed by 35 cycles of 10 s at 98 °C, 10 s, annealing at 49–50 °C, 15 s extension at 72 °C, and a final extension of 2 min at 72 °C; the samples were then held at 8 °C. The PCR products were sequenced by Tsingke (Beijing, China). All sequences were deposited in GenBank with the following accession numbers OL790028-OL790065 (Table 1).

Species delimitation and distance analyses

A total of 58 COI sequences was analyzed: 38 sequences of *Anaplecta* species in this study, 17 published sequences of *Anaplecta*, 3 sequences of *Periplaneta* Burmeister, 1838 (as outgroup) downloaded from GenBank (Table 1). All COI sequences were aligned using MEGA 7.0 and adjusted visually after translation into amino acid sequences. Genetic divergence values were quantified based on the Kimura 2-parameter (K2P) distance model (Kimura, 1980). Maximum Likelihood (ML) method was implemented in IQ-TREE (Nguyen et al. 2015) with the GTR+I+G model selected by PartitionFinder v.2.1.1 according to the corrected Akaike Information Criterion (AICc) (Lanfear et al. 2017), and nodal support values were estimated using 1000 bootstrap replicates. We then performed the Automatic Barcode Gap Discovery (ABGD; Puillandre et al. 2012) molecular species delimitation method to provide auxiliary evidence for distinguishing species. As a simple, quick, and efficient method, ABGD is available

Table 1. Samples used in species delimitation.

Species	Location	Voucher number	Accession Number
A. bicruris sp. nov.	Mt. Jianfengling, Hainan	SH1(♂)	OL790029
A. bicruris sp. nov.	Mt. Jianfengling, Hainan	SH2(♂)	OL790030
A. bicruris sp. nov.	Mt. Jianfengling, Hainan	ZJFL4(♀)	OL790036
A. spinosa sp. nov.	Mt. Limu, Hainan	N1(♂)	OL790028
A. spinosa sp. nov.	Mt. Limu, Hainan	ZLMS2(♀)	OL790038
A. ungulata sp. nov.	Xishuangbanna, Yunnan	SP1(♂)	OL790031
A. ungulata sp. nov.	Xishuangbanna, Yunnan	ZYRC3(♀)	OL790053
A. ungulata sp. nov.	Pu'er, Yunnan	ZMZH1(♂)	OL790048
A. anomala sp. nov.	Mt. Wuliang, Yunnan	SP2(♂)	OL790032
A. anomala sp. nov.	Mt. Wuliang, Yunnan	ZWLS1(♀)	OL790050
A. serrata sp. nov.	Xishuangbanna, Yunnan	SP2_2(♂)	OL790033
A. serrata sp. nov.	Xishuangbanna, Yunnan	ZLMC1(♀)	OL790047
A. serrata sp. nov.	Naban River, Yunnan	ZGMS1(♂)	OL790046
A. bombycina sp. nov.	Pu'er, Yunnan	MZH1(♀)	OL790037
A. bombycina sp. nov.	Xishuangbanna, Yunnan	ZSXZ1(♂)	OL790049
A. bombycina sp. nov.	Xishuangbanna, Yunnan	SP3(♂)	OL790034
A. bombycina sp. nov.	Xishuangbanna, Yunnan	ZYRC2(♀)	OL790052
A. longihamata sp. nov.	Mt. Wuliang, Yunnan	SP4(♂)	OL790035
A. longihamata sp. nov.	Mt. Wuliang, Yunnan	ZWLS2(♀)	OL790051
A. paraomei sp. nov.	Dushan, Guizhou	GZ2(♂)	OL790039
A. paraomei sp. nov.	Dushan, Guizhou	DS4_2(♀)	OL790045
A. paraomei sp. nov.	Dushan, Guizhou	GZ5(♂)	OL790041
A. paraomei sp. nov.	Dushan, Guizhou	GZ6(♀)	OL790042
A. condensa sp. nov.	Libo, Guizhou	GZ4(♂)	OL790040
A. condensa sp. nov.	Libo, Guizhou	GZ10(♀)	OL790043
A. condensa sp. nov.	Guiping, Guangxi	GX8(♂)	OL790044
A. truncatula sp. nov.	Chengbu, Hunan	HNSY1(♂)	OL790054
A. truncatula sp. nov.	Chengbu, Hunan	HNSY2(♀)	OL790055
A. omei	Mt. Jingyun, Chongqing	CQ2(♂)	OL790056
A. omei	Mt. Jingyun, Chongqing	CQ5(♀)	OL790057
A. omei	Guiping, Guangxi	GX7(♂)	OL790058
A. omei	Nanjing, Jiangsu	♂	MT800287
A. corneola	Mt. Yinggeling, Hainan	YGL1(♀)	OL790063
A. corneola	Mt. Jianfengling, Hainan	♂	MT800293
A. corneola	Mount Wuyi, Fujian	♂	MT800296
A. cruciata	Mengla, Yunnan	ML3(♀)	OL790061
A. cruciata	Mengla, Yunnan	♂	MT800303
A. cruciata	Mengla, Yunnan	♂	MT800304
A. basalis	Mengla, Yunnan	ML4(♀)	OL790060
A. basalis	Xishuangbanna, Yunnan	♂	MT800305
A. basalis	Xishuangbanna, Yunnan	♂	MT800309
A. nigra	Motuo, Xizang	♂	MT800306
A. staminiformis	Mt. Diaoluo, Hainan	DLS3(♀)	OL790062
A. staminiformis	Mt. Diaoluo, Hainan	♀	MT800297
A. staminiformis	Mt. Limu, Hainan	♂	MT800299
A. arcuata	Mt. Limu, Hainan	ZLMS1(♀)	OL790065
A. arcuata	Baoting, Hainan	♂	MT800307
A. arcuata	Baoting, Hainan	♂	MT800308
A. strigata	Pu'er, Yunnan	MZH(♀)	OL790064
A. strigata	Mt. Jianfengling, Hainan	♂	MT800291
A. strigata	Menglun, Yunnan	♂	MT800292
A. furcata	Mt. Dayao, Guangxi	♂	MT800301
A. furcata	Mt. Dayao, Guangxi	♂	MT800302
A. bicolor	Mengla, Yunnan	ML5(♀)	OL790059
A. bicolor	Xishuangbanna, Yunnan	♂	MT800310

Species	Location	Voucher number	Accession Number
Periplaneta americana	Indiana, USA		KC617846
Periplaneta fuliginosa	Buenos Aires, Argentina		KM577133
Periplaneta australasiae	China		KF640069

as a web interface (https://bioinfo.mnhn.fr/abi/public/abgd/abgdweb.html) and was used with default settings, using the Jukes-Cantor (JC69) and p distance model with relative gap width (X = 1.0).

Results

Morphological delimitation based on external morphology and male genitalia

Observing the external morphological characters and male genitalia of 470 samples of *Anaplecta*, we could easily identify 17 morphospecies. We found there were some differences in the samples from Libo (GZ4), Dushan (GZ2), Mt. Wuliang (SP4), and other regions where samples were initially identified as *Anaplecta omei*. In terms of color, the sample from Libo (GZ4) was grayish brown while those from other regions were mostly yellowish brown (CQ2, GZ2, SP4) (Figs 1A, B, 10A, B, 11A, B, 12A, B). Two samples (CQ2, SP4) have only one paraproct extended backwards, with dense spines on a curly posterior margin, or both paraprocts extended (GZ4), or neither (GZ2) extended. The subgenital plate is sub-rectangular in CQ2 and GZ4 or sub-trapezoidal in SP4 and GZ2. In male genitalia, the L3 has a long uncinate part (SP4) or not (CQ2, GZ2, GZ4), R1 is bifurcated (CQ2, GZ2) or not (SP4, GZ4), R2 consists of three (CQ2, GZ2, SP4) or four (GZ4) sclerites (Figs 1E–I, 10G–K, 11G–K, 12G–K). Due to the instability in body color (Bruijning, 1948) and the intraspecific variations in male genitalia (Deng et al. 2020), it would be premature to use them to distinguish species. Therefore, we have treated them as intraspecific variations of *A. omei*, as in Deng (2020).

Phylogenetic analysis based on COI and MOTUs estimations

In this study, we acquired 38 COI sequences of *Anaplecta* species. The ML phylogenetic tree showed that males and females of the same morphospecies form monophyletic groups (Fig. 2). Most specific clades have 100 bootstrap values, except *A. strigata* (B = 86), *A. omei* (B = 94), and *A. corneola* (B = 87), indicating that the same morphospecies we identified were well clustered. The relatively low bootstrap values may be caused by the large geographical distances and lack of transitional population. In addition, ABGD analysis produced 20 MOTUs with prior intraspecific divergence (P) = 0.004642, 0.007743, 0.012915, 0.021544, and 0.035938, 17 morphospecies were detected as a single MOTU, but GZ2, GZ5, GZ6, DS4_2, formed one branch, SP4 and ZWLS2 formed a second,

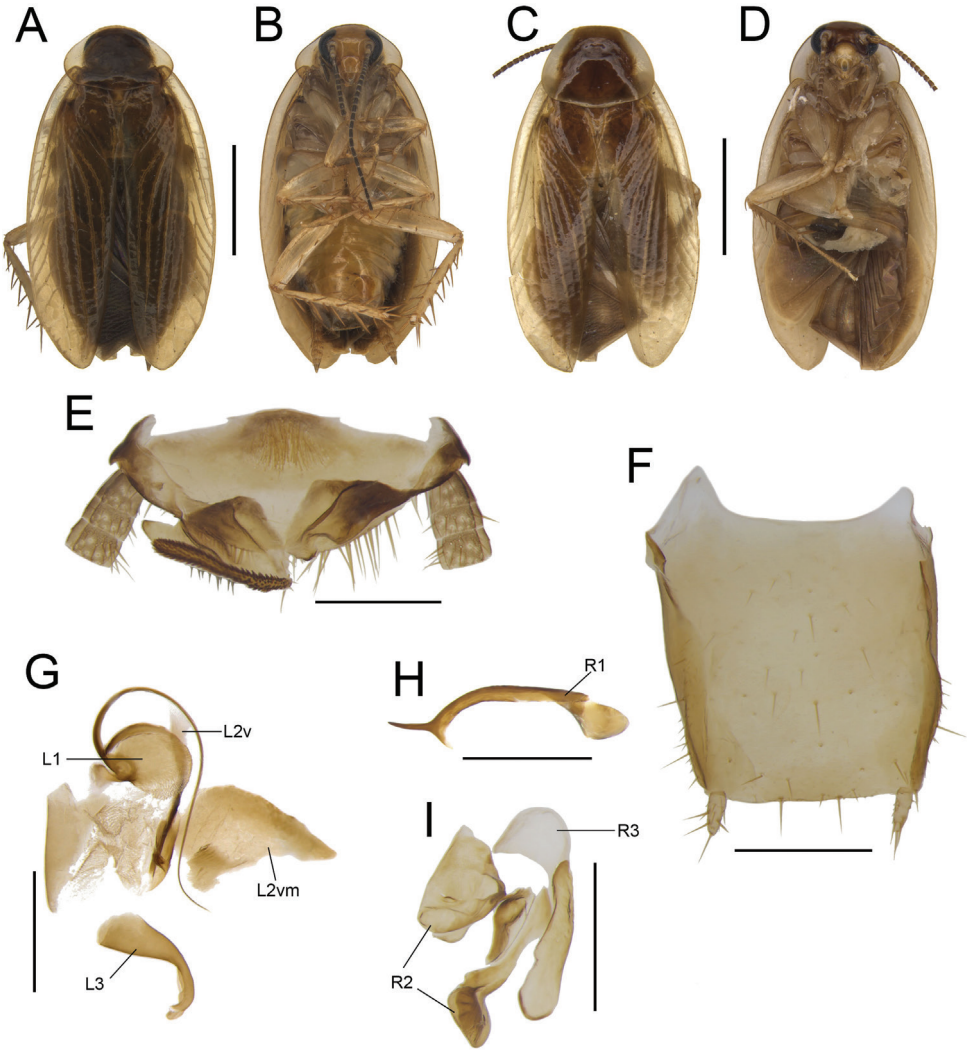

Figure 1. A, B, E–I *Anaplecta omei* Bey-Bienko, 1958 (CQ2), male SWU-B-B-A060315 **C, D** *Anaplecta condensa* Zhu & Che, sp. nov. paratype (GX8), male SWU-B-B-A060126 **A, C** habitus, dorsal view **B, D** habitus, ventral view **E** supra-anal plate, ventral view **F** subgenital plate, dorsal view **G** left phallomere, dorsal view **H, I** right phallomere, ventral view. Scale bars: 2 mm (**A–D**); 0.5 mm (**E–I**). Abbreviations: **L1, L2, L3** sclerites of the left phallomere, **L2v** L2 ventral, **L2vm** median sclerite, **R1, R2, R3** sclerites of the right phallomere.

and GZ4, GX8, and GZ10 formed a third branch; all were distinct from *A. omei* but more closely related than the other species. The K2P genetic distance between the 38 individuals ranged from 0 to 27.4% (Suppl. material 1: Table S1).

Establishment of ten new species based on molecular and morphological data

The results of species delimitation by ABGD were nearly consistent with those by morphological identification (Fig. 2), except 13 samples, which were initially identified as *A. omei*

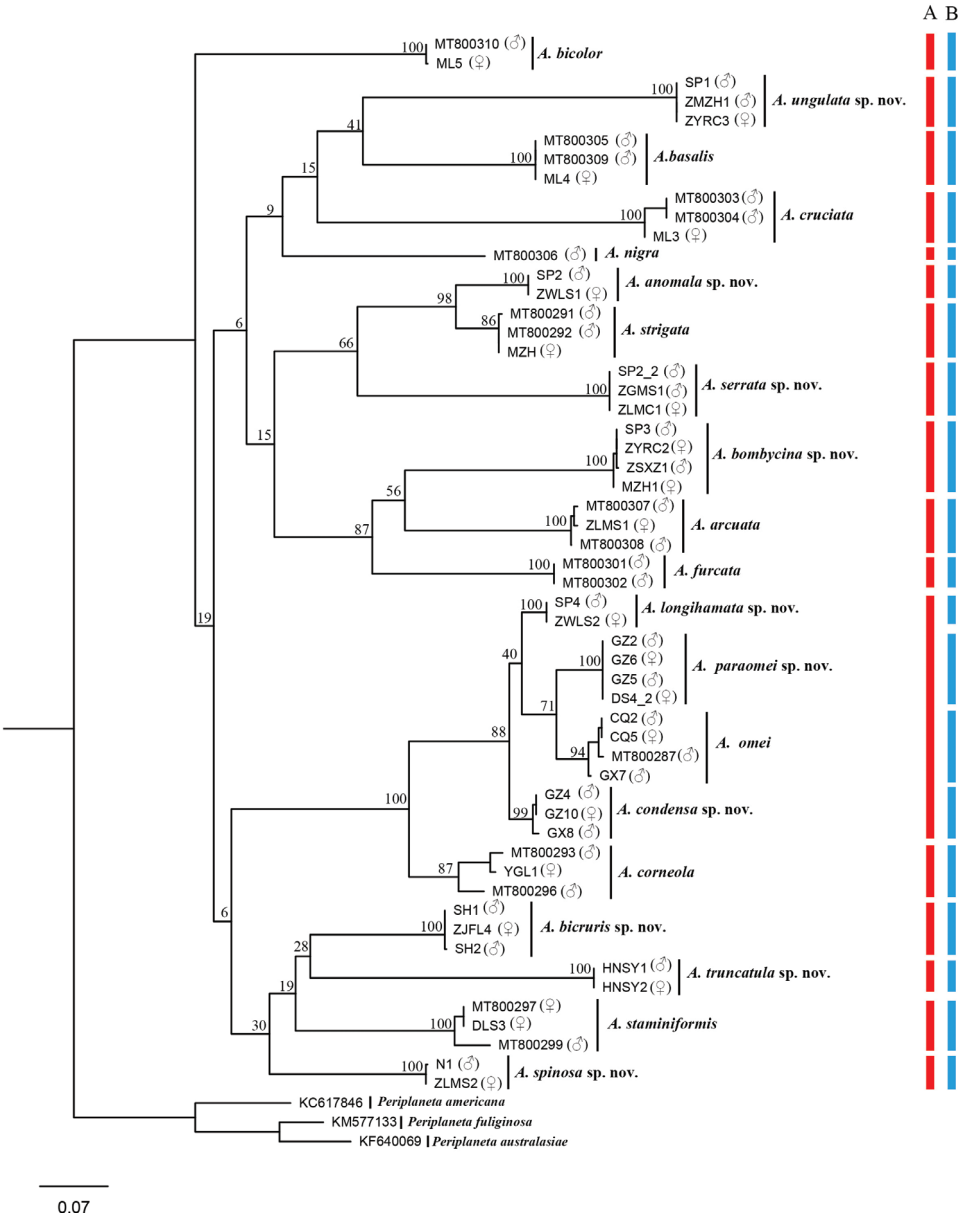

Figure 2. Maximum Likelihood tree derived from COI sequences analyzed with a GTR+I+G model and with 1000 bootstrap replicates. The numbers at nodes are bootstrap values, the sex of the specimens is given in brackets (we checked the voucher specimens of the published sequences to determine whether they were males or females), the red bar indicated morphospecies, the blue bar indicated MOTUs in ABGD (P = 0.0046).

based on external morphological characters and male genitalia, that were divided into 4 MOTUs. But it was insufficient and challenging to distinguish the 13 samples based on the characteristics of male genitalia. Therefore, we examined the females of all *Anaplecta* species from China carefully (except *A. furcata*, *A. malayensis*, *A. simplex*, and *A. arisanica*,

for which no female specimen was available), and found there were significant differences among their female genitalia. The sample from Mt. Wuliang (ZWLS2) has a robust and long first valvifer arm, while the first valvifer arm of others (CQ5, GZ10, DS4_2) are short and curled. The sample from Libo (GZ10) has a small and filamentous intercalary sclerite, while the intercalary sclerite of others (ZWLS2, CQ5, DS4_2) are strip-shaped or sheet-like. The anterior arch of the sample from Dushan (DS4_2) has a hip-shaped posterior margin, while that from Mt. Wuliang (ZWLS2) has two transverse finger-like protrusions, and that of CQ5 and GZ10 are smooth. The shape of the basivalvulae are also varied (Fig. 16). Ultimately, we discerned 20 *Anaplecta* species among our 470 samples, including ten new species, using both morphological characteristics and molecular data. The ten new species are *Anaplecta bicruris* sp. nov., *A. spinosa* sp. nov., *A. ungulata* sp. nov., *A. anomala* sp. nov., *A. serrata* sp. nov., *A. bombycina* sp. nov., *A. truncatula* sp. nov., *A. longihamata* sp. nov., *A. paraomei* sp. nov., and *A. condensa* sp. nov.

Diagnosis of the genus

The characteristics of the external structure and male genitalia are given in Deng et al. (2020) and are therefore not repeated here. Female genitalia: paratergites connected to crosspiece by membrane. First valvifer arm usually short, fused with crosspiece. Anterior margin of anterior arch with weakly sclerotized protrusions, and the shape of basivalvula is always irregular. Spermathecal plate almost merged with basivalvula. Subgenital plate symmetrical. Intersternal fold always simple, sheet-like.

Distribution

North America, South America, Africa, Asia, Oceania (Beccaloni, 2014).

Key to species of *Anaplecta* in China

1 Disk of pronotum bicolored **2**
– Disk of pronotum unicolored **6**
2 Disk of pronotum without longitudinal markings **3**
– Disk of pronotum with longitudinal markings **4**
3 Tegmina yellowish brown, 1/3 of the base black (except the lateral margins). ..... ***A. basalis* Bey-Bienko, 1969**
– Tegmina completely yellowish brown (except the lateral margins)..... ..... ***A. bicolor* Deng & Che, 2020**
4 Disk of pronotum yellowish brown, with two symmetrical brown markings (Fig. 3C) ..... ***A. bicruris* Zhu & Che, sp. nov.**
– Disk of pronotum dark brown, with a yellowish brown longitudinal stripe or line on the middle..... **5**

5 Tegmina unicolored ..... ***A. strigata* Deng & Che, 2020**
– Tegmina bicolored, 1/3 of the base darker than remaining parts (except lateral margins and anal field) (Fig. 7E) ..... ***A. anomala* Zhu & Che, sp. nov.**
6 Tegmina with obvious markings **7**
– Tegmina without obvious markings **9**
7 Tegmina yellowish brown, with a nearly oval brown spot at CuP (Fig. 6E) ... . ***A. ungulata* Zhu & Che, sp. nov.**
– Tegmina yellowish brown, with a subrectangular black spot at base (e.g. Fig. 9E) **8**
8 R1 needle-shaped (Fig. 9J) ..... ***A. truncatula* Zhu & Che, sp. nov.**
– R1 arc-shaped ..... ***A. nigra* Deng & Che, 2020**
9 Male paraprocts with dense spines on curly posterior margin (e.g. Figs 1E, 10G) **10**
– Male paraprocts not as above **13**
10 Intercalary sclerite small, nearly filamentous (Fig. 16G, H .... ***A. condensa* Zhu & Che, sp. nov.**
– Intercalary sclerite large, strip-shaped or sheet-like **11**
11 Right first valvifer arm long, lateral edges folded up (Fig. 16A, B)..... ..... ***A. longihamata* Zhu & Che, sp. nov.**
– Right first valvifer arm short, lateral edges not folded up **12**
12 The posterior margin of anterior arch hip-shaped (Fig. 16D, E)..... ..... ***A. paraomei* Zhu & Che, sp. nov.**
– The posterior margin of anterior arch smooth (Fig. 16J, K) .... ***A. omei* Bey-Bienko, 1958**
13 L1 with a long and curved filamentary structure (e.g. Figs 4I, 8I) **14**
– L1 with a short and robust uncinate structure..... ..... ***A. cruciata* Deng & Che, 2020**
14 R1 degraded or merged with L2vm..... **15**
– R1 well developed, not merged with L2vm **18**
15 Male paraprocts specialized, strip-shaped, with spines on posterior margin (Fig. 4G) ..... ***A. spinosa* Zhu & Che, sp. nov.**
– Male paraprocts unspecialized **16**
16 The apex of L2v bifurcated, sheet-like **17**
– The apex of L2v not bifurcated, shaped like '3' (Fig. 8I) .... ***A. bombycina* Zhu & Che, sp. nov.**
17 One sclerite of R2 serrated (Fig. 5J) ..... ***A. serrata* Zhu & Che, sp. nov.**
– All sclerites of R2 without serration ..... ***A. arcuata* Deng & Che, 2020**
18 R1 curved **19**
– R1 straight, cylinder-shaped..... ***A. staminiformis* Deng & Che, 2020**
19 R1 highly sclerotized horn-shaped ..... ***A. corneola* Deng & Che, 2020**
– R1 sightly sclerotized arc-shaped..... ***A. furcata* Deng & Che, 2020**

***Anaplecta bicruris* Zhu & Che, sp. nov.**
http://zoobank.org/A05B9533-A9AF-4226-935C-05DF6F6F5693
Figures 3, 13A–C

Type material. ***Holotype*:** China • male; Hainan Prov., Ledong County, Mt. Jianfengling; 18°42.63'N, 108°52.75'E; 940–1000 m; 24 June 2020; Yong Li, Jing Zhu leg.; SWU-B-B-A060001.

***Paratypes*:** China • 1 male; same data as holotype; SWU-B-B-A060002 • 1 male and 3 females; Hainan Prov., Ledong County, Mt. Jianfengling; 18°42.63'N, 108°52.75'E; 940–960 m; 23 June 2020; Yong Li, Jing Zhu leg.; SWU-B-B-A060003 to 060006 • 5 males; Hainan Prov., Ledong County, Mt. Jianfengling; 18°42.58'N, 108°52.57'E; 940–1000 m; 23 June 2020; Rong Chen, Li-Kang Niu leg.; SWU-B-B-A060007 to 060011.

Diagnosis. This species is similar to *A. corneola* Deng & Che, 2020, but can be distinguished as follows: 1) L2vm stamen-shaped with sharp bifurcation in *A. bicruris* sp. nov., while simple, sheet-like in *A. corneola*; 2) R1 absent in *A. bicruris* sp. nov., while horn-shaped in *A. corneola*; 3) the protrusion of anterior arch horn-shaped in *A. bicruris* sp. nov., while that of *A. corneola* nearly cylindrical; and 4), basivalvula with a backward extension in *A. corneola*, while only curled in *A. bicruris* sp. nov.

Etymology. The specific epithet is derived from the Latin word *bicruris*, meaning that L2vm is bifurcated.

Measurements (mm). Male: pronotum length × width: 1.40–1.49 × 1.84–2.05, tegmina length: 4.97–5.66, overall length: 6.16–6.85. Female: pronotum length × width: 1.34–1.47 × 1.86–2.21, tegmina length: 5.01–5.53, overall length: 6.23–6.75.

Description. ***Coloration*.** Body light yellowish brown, face yellowish brown (Fig. 3A, B). Antennae brown, maxillary palpus pale brown (Fig. 3D). Pronotum and tegmina light yellowish brown, lateral edges pale or hyaline, pronotum with two symmetrical brown markings (Fig. 3C, E). Hind wings infuscate, costal field and appendicular field darker than remaining parts (Fig. 3F). Abdominal sterna, legs, and cerci yellowish brown (Fig. 3B).

***Head and thorax*.** The distance between antennal sockets slightly narrower than interocular space. Fifth maxillary palpus nearly oval, slightly thicker and wider than others (Fig. 3D). Pronotum nearly sub-elliptical, posterior margin slightly straight (Fig. 3C). Tegmina with slightly indistinct veins; radius posterior veins of hind wings slightly indistinct, without transverse veins between M and CuA (Fig. 3E, F). Front femur Type B_2 (Fig. 3B). Pulvilli absent, tarsal claws symmetrical.

***Male genitalia*.** Supra-anal plate with sheet-like paraprocts (Fig. 3G). Subgenital plate slightly asymmetrical, the left margin longer than the right and both margins upcurved near the middle; the interstylar margin smooth and curved. Styli medium, length ~ 1/4 of interstylar space (Fig. 3H). L1 small, fan-shaped with a curved and long filamentary structure. L2v slender and curved. L2vm brush-like with a sharp bifurcation. L3 hook-like, stubby with apical part blunt (Fig. 3I). R2 irregular, weakly sclerotized; one of R2 with dense tiny punctuations. R3 slightly curved, sheet-like (Fig. 3J).

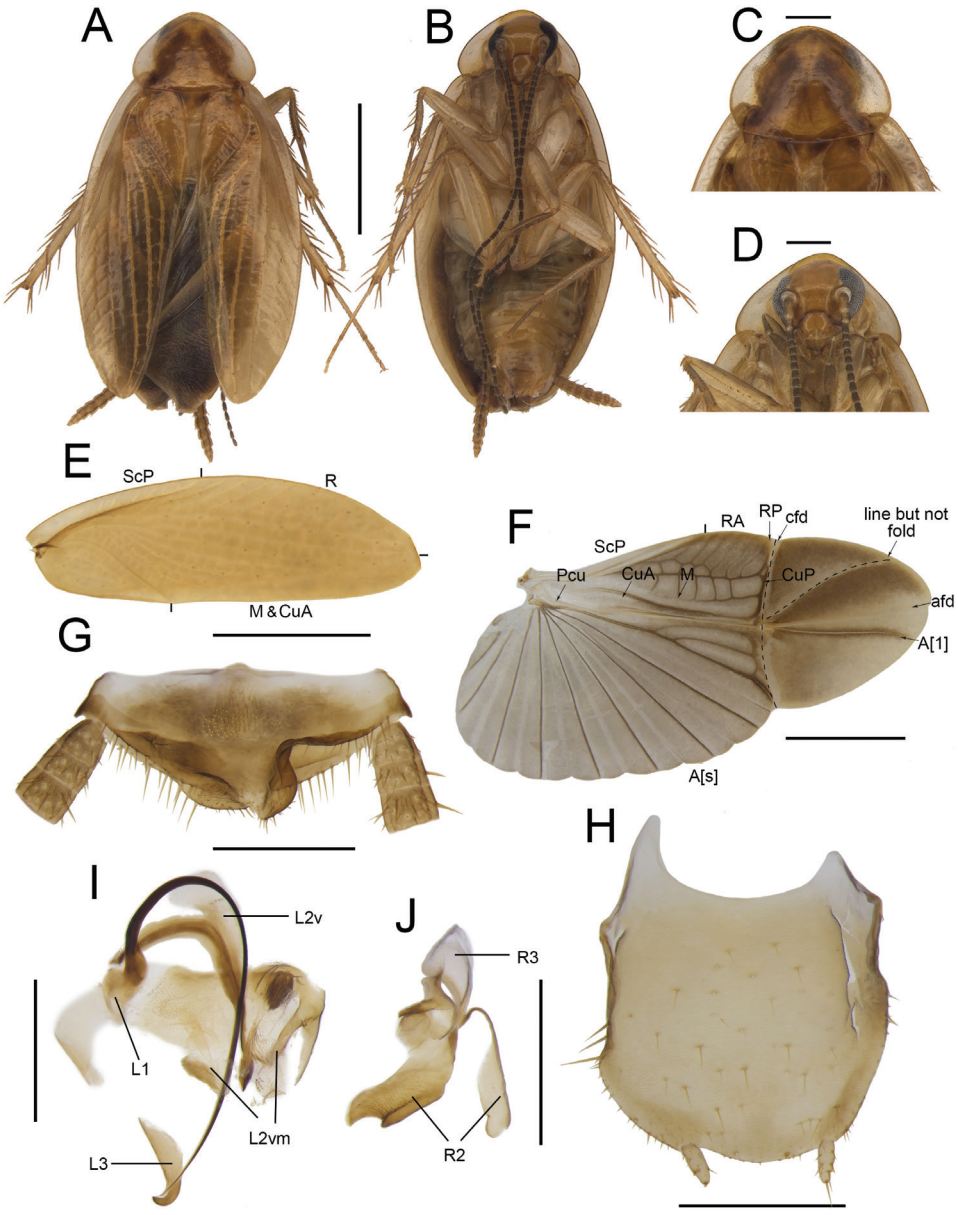

Figure 3. *Anaplecta bicruris* Zhu & Che, sp. nov. holotype, male SWU-B-B-A060001 **A** habitus, dorsal view **B** habitus, ventral view **C** pronotum, dorsal view **D** head, ventral view **E** tegmina **F** wings **G** supra-anal plate, ventral view **H** subgenital plate, dorsal view **I** left phallomere, dorsal view **J** right phallomere, ventral view. Scale bars: 2 mm (**A–F**); 0.5 mm (**G–J**). Abbreviations: **afd** anal fold, **A[1]** the anterior one of the anal vein, **A[s]** the other element of vannal vein, **cfd** cubitus fold, **CuA** cubitus anterior, **CuP** cubitus posterior, **L1, L2, L3** sclerites of the left phallomere, **L2v** L2 ventral, **L2vm** median sclerite, **M** media, **Pcu** postcubitus, **R** radius, **RA** radius anterior, **RP** radius posterior, **R2, R3** sclerites of the right phallomere, **ScP** subcostal posterior.

***Female genitalia*.** Supra-anal plate nearly symmetrical. Paraprocts broad, not extending to the posterior margin of supra-anal plate. Intercalary sclerite slender, slightly curved. First valve curved. Second valve small, basally fused. Third valve broad. The anterior margin of anterior arch slightly sclerotized, with a horn-shaped protrusion; lateral area with dense tiny punctuation (Fig. 13A, B). Basivalvula irregular, anterior margin curled upward, right lateral deeply concave, lateral area with dense punctuations (Fig. 13A). Spermatheca slightly sclerotized at base. Laterosternal shelf slightly sclerotized, lateral margin slightly curved, with dense spinules at base (Fig. 13C).

Distribution. China (Hainan).

Anaplecta spinosa Zhu & Che, sp. nov.

http://zoobank.org/F0AC2430-A023-4921-AA28-77432A9457B8
Figures 4, 13D–F

Type material. ***Holotype*:** China • male; Hainan Prov., Qiongzhong County, Mt. Limu; 19°10.57'N, 109°43.77'E; 650 m; 20 June 2020; Yong Li, Jing Zhu, leg.; SWU-B-B-A060012.

***Paratypes*:** China • 1 male and 1 female; same data as holotype; SWU-B-B-A060013 and 060014.

Diagnosis. This species is slightly similar to *A. anncajanoae* Lucañas, 2016, but can be distinguished from the latter by the spines on the left phallomere. It is also similar to *A. cruciata* Deng & Che, 2020 in body color and size, but can be distinguished as follows: 1) sclerites of the left phallomere spinous in *A. spinosa* sp. nov., while spineless in *A. cruciata*; 2) one of R2 with dense punctuations in *A. spinosa* sp. nov., while *A. cruciata* without; 3) anterior margin of anterior arch with a long horn-shaped protrusion in *A. spinosa* sp. nov., that of *A. cruciata* blunter and rounder; and 4) basivalvula nearly triangular in *A. spinosa* sp. nov., while nearly rectangular in *A. cruciata*.

Etymology. The specific epithet is derived from the Latin word *spinosus*, referring to the left phallomere that is spiny.

Measurements (mm). Male: pronotum length × width: 1.19–1.38 × 1.80–1.89, tegmina length: 4.12–4.28, overall length: 5.10–5.57. Female: pronotum length × width: 1.30 × 1.92, tegmina length: 4.29, overall length: 5.55.

Description. *Coloration*. Body dark brown, face dark brown, terminal of clypeus and labrum yellowish brown (Fig. 4A, B). Antennae brown, maxillary palpus pale brown (Fig. 4D). Pronotum and tegmina dark brown, lateral edges hyaline (Fig. 4C, E). Hind wings infuscate, costal field and appendicular field darker than remaining parts (Fig. 4F). Center of abdominal sterna yellow, gradually darkening to dark brown to edges. Legs and cerci yellowish brown (Fig. 4B).

***Head and thorax*.** The distance between antennal sockets slightly narrower than interocular space. Fifth maxillary palpus nearly oval, slightly thicker and wider than others (Fig. 4D). Pronotum nearly sub-parabolic, anterior and posterior margins straight (Fig. 4C). Tegmina with slightly indistinct veins; radius posterior veins of hind

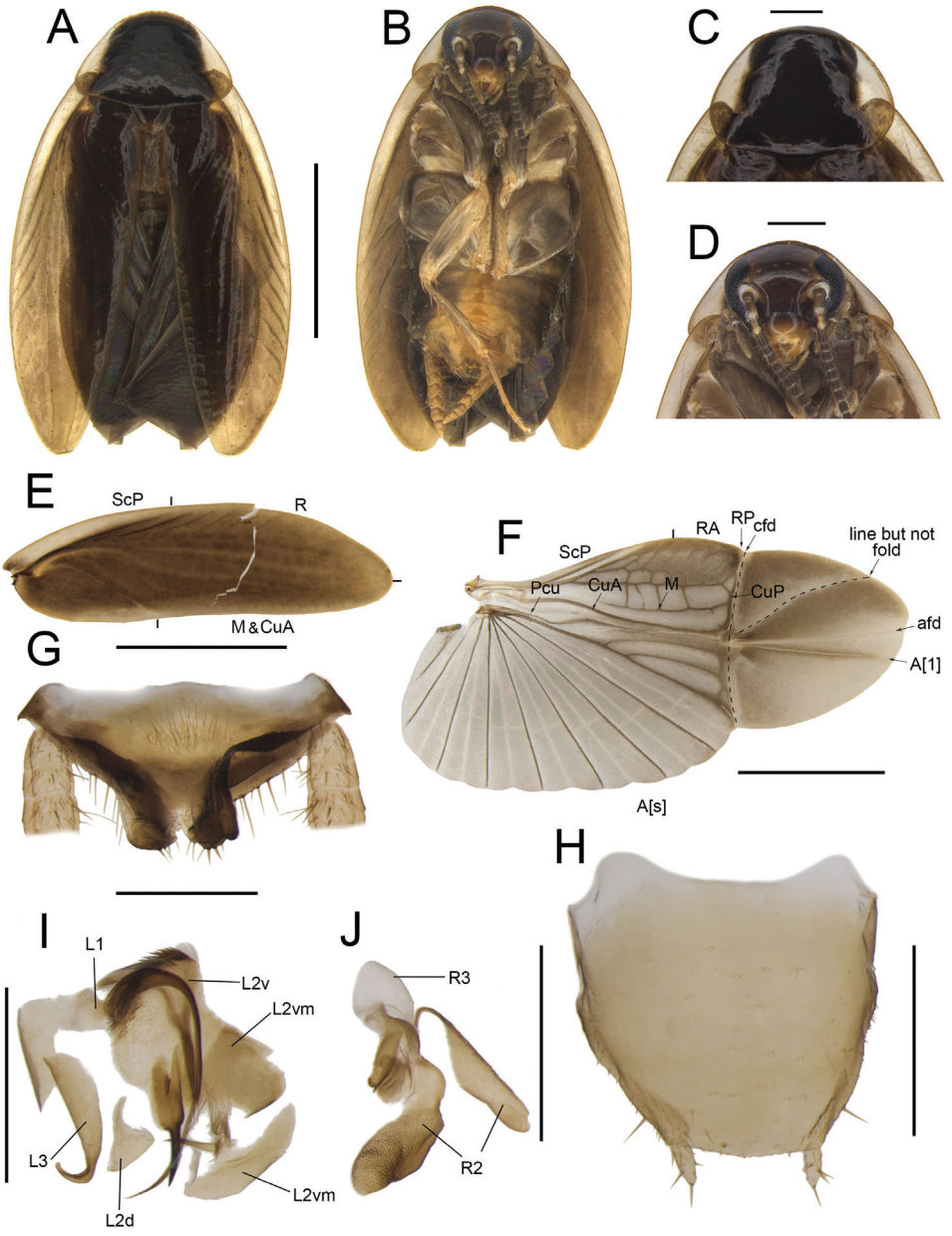

Figure 4. *Anaplecta spinosa* Zhu & Che, sp. nov. holotype, male SWU-B-B-A060012 **A** habitus, dorsal view **B** habitus, ventral view **C** pronotum, dorsal view **D** head, ventral view **E** tegmina **F** wings **G** supra-anal plate, ventral view **H** subgenital plate, dorsal view **I** left phallomere, dorsal view **J** right phallomere, ventral view. Scale bars: 2 mm (**A–F**); 0.5 mm (**G–J**). Abbreviations: **afd** anal fold, **A[1]** the anterior one of the anal vein, **A[s]** the other element of vannal vein, **cfd** cubitus fold, **CuA** cubitus anterior, **CuP** cubitus posterior, **L1, L2, L3** sclerites of the left phallomere, **L2d** L2 dorsal, **L2v** L2 ventral, **L2vm** median sclerite, **M** media, **Pcu** postcubitus, **R** radius, **RA** radius anterior, **RP** radius posterior, **R2, R3** sclerites of the right phallomere, **ScP** subcostal posterior.

wings slightly indistinct, with one discontinuous or no transverse veins between M and CuA (Fig. 4E, F). Front femur Type B_2. Pulvilli absent, tarsal claws symmetrical.

***Male genitalia*.** Supra-anal plate symmetrical. Both paraprocts extend into a strip, with spines on posterior margins (Fig. 4G). Subgenital plate sub-trapezoidal, the center of anterior and interstylar margins straight. Styli medium, length ~ 1/4 of interstylar space (Fig. 4H). L1 fan-shaped, with a curved and long filamentary structure. Terminal of L2v needle-like. L2d small. L2vm with brush-like structure and tapering at terminal. L3 robust, hook-like, apical part enlarged and slightly sharp (Fig. 4I). R2 irregular, weakly sclerotized; one of R2 with dense punctuations. R3 slightly curved, sheet-like (Fig. 4J).

***Female genitalia*.** Supra-anal plate nearly symmetrical. Paraprocts broad, not extending to the posterior margin of supra-anal plate. Intercalary sclerite strip-shaped, slightly curved. First valve robust, with inward protrusions. Second valve small, basally fused. Third valve broad. The anterior margin of anterior arch slightly sclerotized, with a long horn-shaped protrusion, lateral area with dense tiny punctuations (Fig. 13D, E). Basivalvula broad, the right lateral deeply concave, lateral area with dense punctuations (Fig. 13D). Spermatheca slightly sclerotized at base. Laterosternal shelf slightly sclerotized, lateral margin slightly curved, with dense spinules at base (Fig. 13F).

Distribution. China (Hainan).

Anaplecta serrata Zhu & Che, sp. nov.

http://zoobank.org/5C843FC5-E328-43DB-95F0-61DF51C8B0DD
Figures 5, 13G–I

Type material. ***Holotype*:** China • male; Yunnan Prov., Xishuangbanna, Shangyong Town; 21°16.80'N, 101°31.80'E; 870 m; 7 July 2020; Du-Ting Jin, Rong Chen leg.; SWU-B-B-A060015.

***Paratypes*:** China • 4 males and 2 females; same data as holotype; SWU-B-B-A060016 to 060021 • 1 male; Yunnan Prov., Jinghong City, Nabanhe Nature Reserve; 22°14.08'N, 100°36.29'E; 1080 m; 3 July 2020; Du-Ting Jin, Yi-Shu Wang, leg.; SWU-B-B-A060022.

Diagnosis. This species is similar to *A. cruciata* Deng & Che, 2020 in body color and size, but can be distinguished as follows: 1) R2 serrated in *A. serrata* sp. nov., while that of *A. cruciata* without serration; 2) anterior margin of anterior arch with a sheet-like protrusion in *A. serrata* sp. nov.; while the protrusions of *A. cruciata* nearly Y-shaped; and 3) basivalvula extremely curled in *A. serrata* sp. nov., while slightly in *A. cruciata*.

Etymology. The specific epithet is derived from the Latin word *serratus*, in reference to the serrated lateral edges of R2.

Measurements (mm). Male: pronotum length × width: 1.12–1.25 × 1.67–1.85, tegmina length: 3.93–4.46, overall length: 5.06–5.53. Female: pronotum length × width: 1.07–1.19 × 1.67–1.69, tegmina length: 4.02–4.06, overall length: 5.00–5.09.

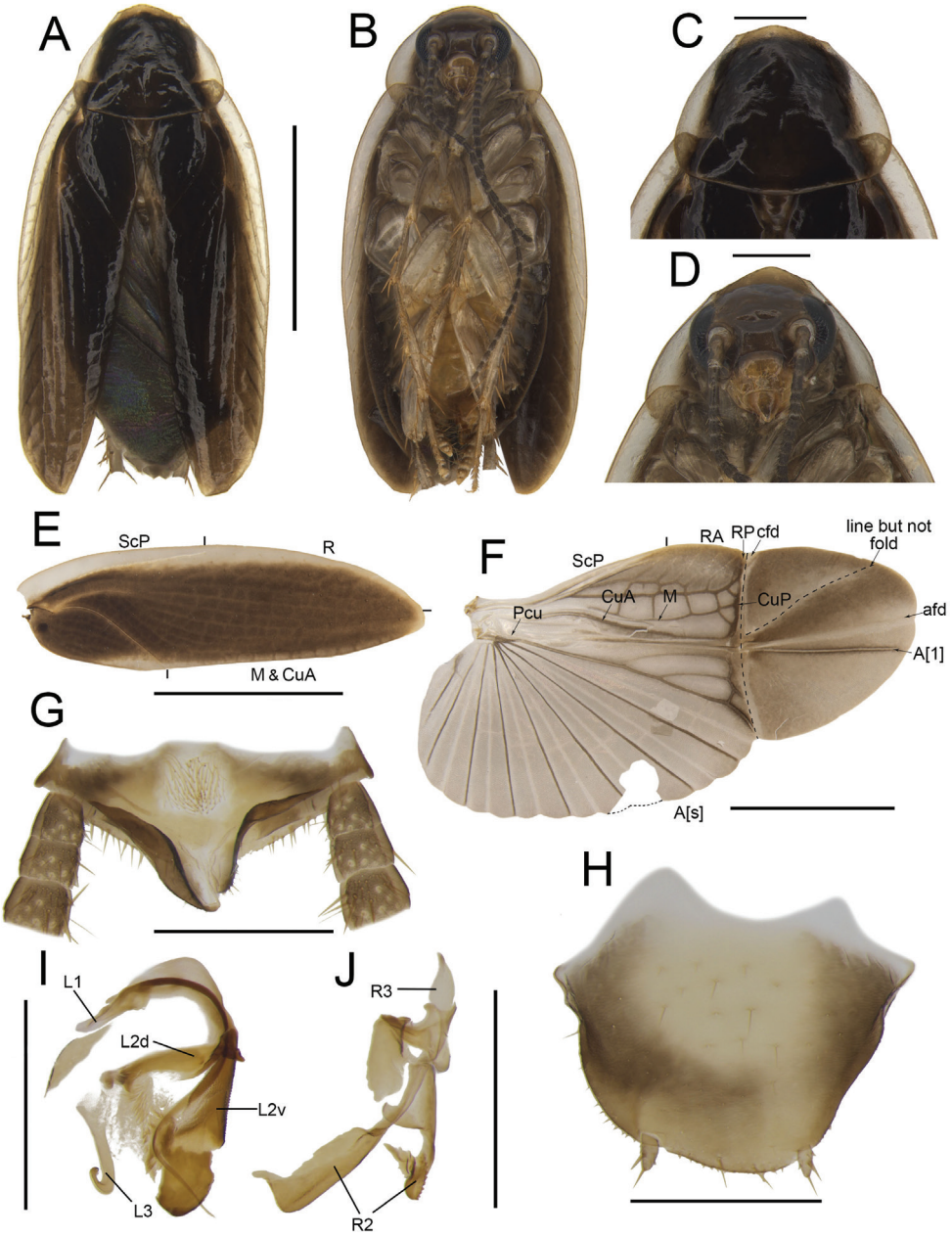

Figure 5. *Anaplecta serrata* Zhu & Che, sp. nov. holotype, male. SWU-B-B-A060015 **A** habitus, dorsal view **B** habitus, ventral view **C** pronotum, dorsal view **D** head, ventral view **E** tegmina **F** wings **G** supra-anal plate, ventral view **H** subgenital plate, dorsal view **I** left phallomere, dorsal view **J** right phallomere, dorsal view. Scale bars: 2 mm (**A–F**); 0.5 mm (**G–J**). Abbreviations: **afd** anal fold, **A[1]** the anterior one of the anal vein, **A[s]** the other element of vannal vein, **cfd** cubitus fold, **CuA** cubitus anterior, **CuP** cubitus posterior, **L1, L2, L3** sclerites of the left phallomere, **L2d** L2 dorsal, **L2v** L2 ventral, **L2vm** median sclerite, **M** media, **Pcu** postcubitus, **R** radius, **RA** radius anterior, **RP** radius posterior, **R2, R3** sclerites of the right phallomere, **ScP** subcostal posterior.

Description. ***Coloration*.** Body dark brown, face dark brown, terminal of clypeus and labrum yellowish brown (Fig. 5A, B). Antennae and maxillary palpus brown (Fig. 5D). Pronotum and tegmina dark brown, lateral edges nearly hyaline (Fig. 5C, E). Hind wings infuscate, costal field and appendicular field darker than remaining parts (Fig. 5F). Center of abdominal sterna yellow, gradually darkening to dark brown to edges. Legs and cerci pale yellowish brown (Fig. 5B).

***Head and thorax*.** The distance between antennal sockets slightly narrower than interocular space. Fifth maxillary palpus nearly triangular, slightly thicker and wider than others (Fig. 5D). Pronotum sub-elliptical, anterior margin straight, posterior margin arcuate (Fig. 5C). Tegmina with slightly indistinct veins, radius posterior veins of hind wings slightly indistinct, with one transverse veins between M and CuA (Fig. 5E,F). Front femur Type B_2 (Fig. 5B). Pulvilli absent, tarsal claws symmetrical.

***Male genitalia*.** Paraprocts bifurcated at the base: filamentary part short, another part sheet-like (Fig. 5E). Subgenital plate almost symmetrical, anterior margin concave, interstylar margin convex. Styli short, the distance between them long (Fig. 5H). L1 narrow, with a curved and long filamentary structure; L2v broad, folded in the middle. L2d elongated with a sharp horn. L3 small, uncinate part extremely bent (Fig. 5I). R2 irregular, weakly sclerotized; one of R2 with sharp apex, another serrated. R3 slightly curved, sheet-like (Fig. 5J).

***Female genitalia*.** Supra-anal plate nearly symmetrical. Paraprocts broad, not extending to the posterior margin of supra-anal plate. Intercalary sclerite strip-shaped. First valve long. Second valve small, basally fused. Third valve broad. The anterior margin of anterior arch slightly sclerotized, extending forward into a sheet-like protrusion, with wavy depressions. Basivalvula broad, extremely curled, with dense punctuations (Fig. 13G, H). Laterosternal shelf slightly sclerotized, lateral margin slightly curved (Fig. 13I).

Distribution. China (Yunnan).

Anaplecta ungulata Zhu & Che, sp. nov.

http://zoobank.org/9A65A093-36A6-4701-AE54-65F305E8AB2B
Figures 6, 14A–C

Type material. ***Holotype*:** China • male; Yunnan Prov., Xishuangbanna, Dadugang Village; 21°59.06'N, 101°64.40'E; 870 m; 14 July 2020; Rong Chen, Li-Kang Niu leg.; SWU-B-B-A060023.

***Paratypes*:** China • 10 males and 1 female; same data as holotype; SWU-B-B-A060024 to 060034 • 2 males; Yunnan Prov., Xishuangbanna, Ya'nuo Village; 21°59.70'N, 101°6.02'E; 1212 m; 14 July 2020; Du-Ting Jin, Yi-Shu Wang leg.; SWU-B-B-A060035 and 060036 • 12 males and 5 females; Yunnan Prov., Xishuangbanna, Dadugang Village; 22°16.52'N, 100°55.02'E; 1100 m; 15 July 2020; Rong Chen, Du-Ting Jin leg.; SWU-B-B-A060037 to 060053 • 1 male; Yunnan Prov., Pu'er City, Meizi Lake; 22°44.24'N, 100°58.32'E; 1400 m; 16 July 2020; Du-

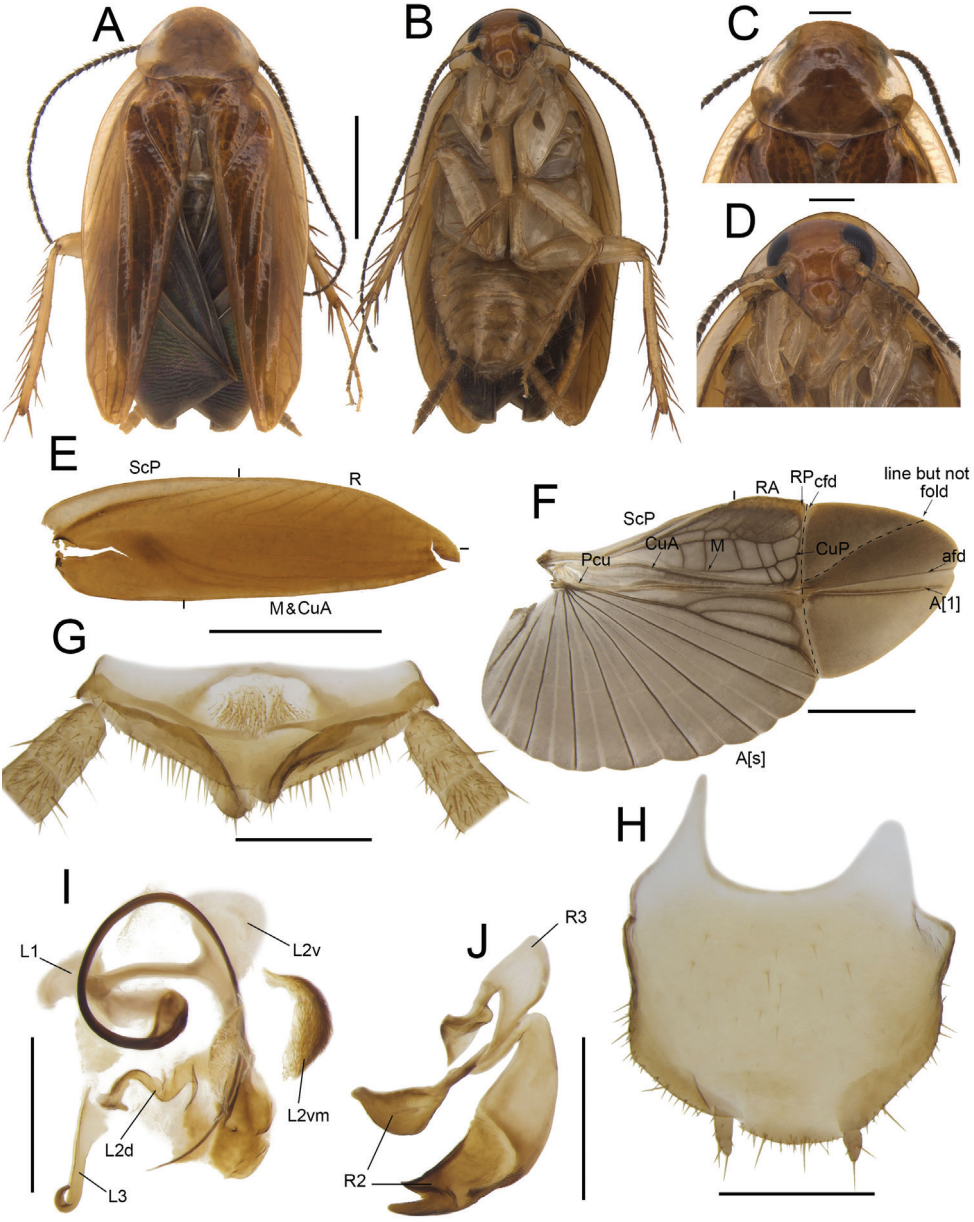

Figure 6. *Anaplecta ungulata* Zhu & Che, sp. nov. holotype, male SWU-B-B-A060023 **A** habitus, dorsal view **B** habitus, ventral view **C** pronotum, dorsal view **D** head, ventral view **E** tegmina **F** wings **G** supra-anal plate, ventral view **H** subgenital plate, dorsal view **I** left phallomere, dorsal view **J** right phallomere, dorsal view. Scale bars: 2 mm (**A–F**); 0.5 mm (**G–J**). Abbreviations: **afd** anal fold, **A[1]** the anterior one of the anal vein, **A[s]** the other element of vannal vein, **cfd** cubitus fold, **CuA** cubitus anterior, **CuP** cubitus posterior, **L1, L2, L3** sclerites of the left phallomere, **L2d** L2 dorsa,l **L2v** L2 ventral, **L2vm** median sclerite, **M** media, **Pcu** postcubitus, **R** radius, **RA** radius anterior, **RP** radius posterior, **R2, R3** sclerites of the right phallomere, **ScP** subcostal posterior.

Ting Jin, Li-Kang Niu, leg.; SWU-B-B-A060054 • 1 male, Yunnan Prov., Pu'er City, Meizi Lake; 22°45.27'N, 100°59.60'E; 1365 m; 17 July 2020; Rong Chen, Yi-Shu Wang, leg.; SWU-B-B-A060055.

Diagnosis. This species can be easily separated from other species by its hoof-shaped right phallomere, and the vestibular sclerite with two serrated and curved long spines.

Etymology. The specific epithet is derived from the Latin word *ungulatus*, referring to the apex of R2 shaped like a pig or horse hoof.

Measurements (mm). Male: pronotum length × width: 1.40–1.47 × 1.95–2.00, tegmina length: 5.31–5.94, overall length: 6.77–7.23. Female: pronotum length × width: 1.21–1.44 × 1.97–2.03, tegmina length: 5.63–5.80, overall length: 6.62–7.11.

Description. ***Coloration.*** Body yellowish brown, face yellowish brown (Fig. 6A, B). Antennae brown, maxillary palpus pale brown (Fig. 6D). Pronotum and tegmina yellowish brown, lateral edges nearly hyaline, tegmina with a slightly darker marking at the base of mediocubital field (Fig. 6C, E). Hind wings infuscate, costal field and appendicular field darker than remaining parts (Fig. 6F). Abdominal sterna, cerci, and legs yellowish brown (Fig. 6B).

Head and thorax. The distance between antennal sockets slightly narrower than interocular space. Fifth maxillary palpus nearly triangular, slightly thicker and wider than others (Fig. 6D). Pronotum sub-elliptical, anterior margin slightly curved and posterior margin straight (Fig. 6C). Tegmina with slightly indistinct veins; the radius posterior veins of hind wings slightly indistinct, with one or two transverse veins between M and CuA (Fig. 6E, F). Front femur Type B_2. Pulvilli absent, tarsal claws symmetrical.

Male genitalia. Paraprocts bifurcated at the base: the upper part strip-shaped, approximately the length of paraprocts, the rest sheet-like (Fig. 6G). Subgenital plate asymmetrical, the left margin longer and slender than the right, the interstylar margin curved. The length of styli ~ 1/4 of interstylar space (Fig. 6H). L1 strip-shaped, with extremely curved and long filamentary structure. L2v with a right-angled bifurcation. L2d irregular. L2vm curls and thickens in a crescent shape, with dense spines. L3 slender, apical part extremely bent (Fig. 6I). R2 irregular, weakly sclerotized; one of R2 diverging into two sharp horns at apex. R3 slightly curved, sheet-like (Fig. 6J).

Female genitalia. Supra-anal plate nearly symmetrical. Paraprocts broad, extending to the posterior margin of supra-anal plate. Intercalary sclerite strip-shaped. First valve tubular, with inward protrusions. Second valve small, basally fused. Third valve broad. The anterior margin of anterior arch protrudes in the shape of two triangles. Irregularly shaped basivalvula with dense punctuations, posterior margin curled. The base of vestibular sclerite nearly hyaline, posterior margin bifurcated into two highly sclerotized spines (Fig. 14A, B). Laterosternal shelf nearly hyaline (Fig. 14C).

Distribution. China (Yunnan).

***Anaplecta anomala* Zhu & Che, sp. nov.**
http://zoobank.org/27360C71-7C4F-4174-ADC2-95AC115BE34D
Figures 7, 14D–F

Type material. ***Holotype*:** China • male; Yunnan Prov., Pu'er City, Mt. Wuliang; 24°38'N, 100°44'E; 1232 m; 21 July 2020; Li-Kang Niu, Rong Chen, leg.; SWU-B-B-A060056.

***Paratypes*:** China • 11 males and 5 females; same data as holotype; SWU-B-B-A060057 to 060072.

Diagnosis. This species is slightly similar to *A. falcifer* Hebard, 1925 but differs in the coloration of pronotum and tegmina. It is also similar to *A. strigata* Deng & Che, 2020 in body color and pronotum, but can be distinguished as follows: 1) the base of the tegmina almost black, while *A. strigata* mostly uniform dark yellowish brown; 2) L2d nearly rectangular in *A. anomala* sp. nov., while slightly bent in *A. strigata*; and 3) anterior margin of anterior arch with a finger-like protrusion, while the protrusion of *A. strigata* nearly wavy.

Etymology. The specific epithet is derived from the Latin word *anomalus*, referring to the left phallomere being different from other species.

Measurements (mm). Male: pronotum length × width: 1.20–1.42 × 1.68–1.95, tegmina length: 4.52–5.49, overall length: 5.94–6.54. Female: pronotum length × width: 1.29 × 1.97, tegmina length: 4.67–5.13, overall length: 5.91–6.22.

Description. ***Coloration*.** Body dark brown, face brown, terminal of clypeus and labrum yellowish brown (Fig. 7A, B). Antennae and maxillary palpus brown (Fig. 7D). Pronotum dark brown, middle part lighter, lateral edges nearly hyaline (Fig. 7C). Tegmina dark brown, lateral edges nearly hyaline, 1/3 of the base darker than remaining parts (except for anal field) (Fig. 7E). Hind wings infuscate, costal field and appendicular field darker than remaining parts (Fig. 7F). Abdominal sterna, legs, and cerci pale yellowish brown (Fig. 7B).

***Head and thorax*.** The distance between antennal sockets slightly narrower than interocular space. Fifth maxillary palpus nearly oval, slightly thicker and wider than others (Fig. 7D). Pronotum sub-elliptical, anterior and posterior margins nearly straight (Fig. 7C). Tegmina with slightly indistinct veins; radius posterior veins of hind wings slightly indistinct, without transverse veins between M and CuA (Fig. 7E, F). Front femur Type B_2 (Fig. 7B). Pulvilli absent, tarsal claws symmetrical.

***Male genitalia*.** Paraprocts bifurcated at the base: the upper part strip-shaped, length ~ 1/2 of paraprocts, the rest sheet-like (Fig. 7G). Subgenital plate slightly asymmetrical, the left margin slightly wider than the right, the interstylar margin extremely convex. Styli short, the distance between them long (Fig. 7H). L1 fan-shaped, with a curved and long filamentary structure. L2v handle-shaped, with a sharp horn. L2d an approximate rectangle. L2vm with a curled and thickened sclerite, crescent-like with dense spines. L3 medium, hook-like, apical part enlarged and slightly sharp (Fig. 7I). R2 irregular, weakly sclerotized, one of R2 sheet-like, with sharp apex. R3 slightly curved, sheet-like (Fig. 7J).

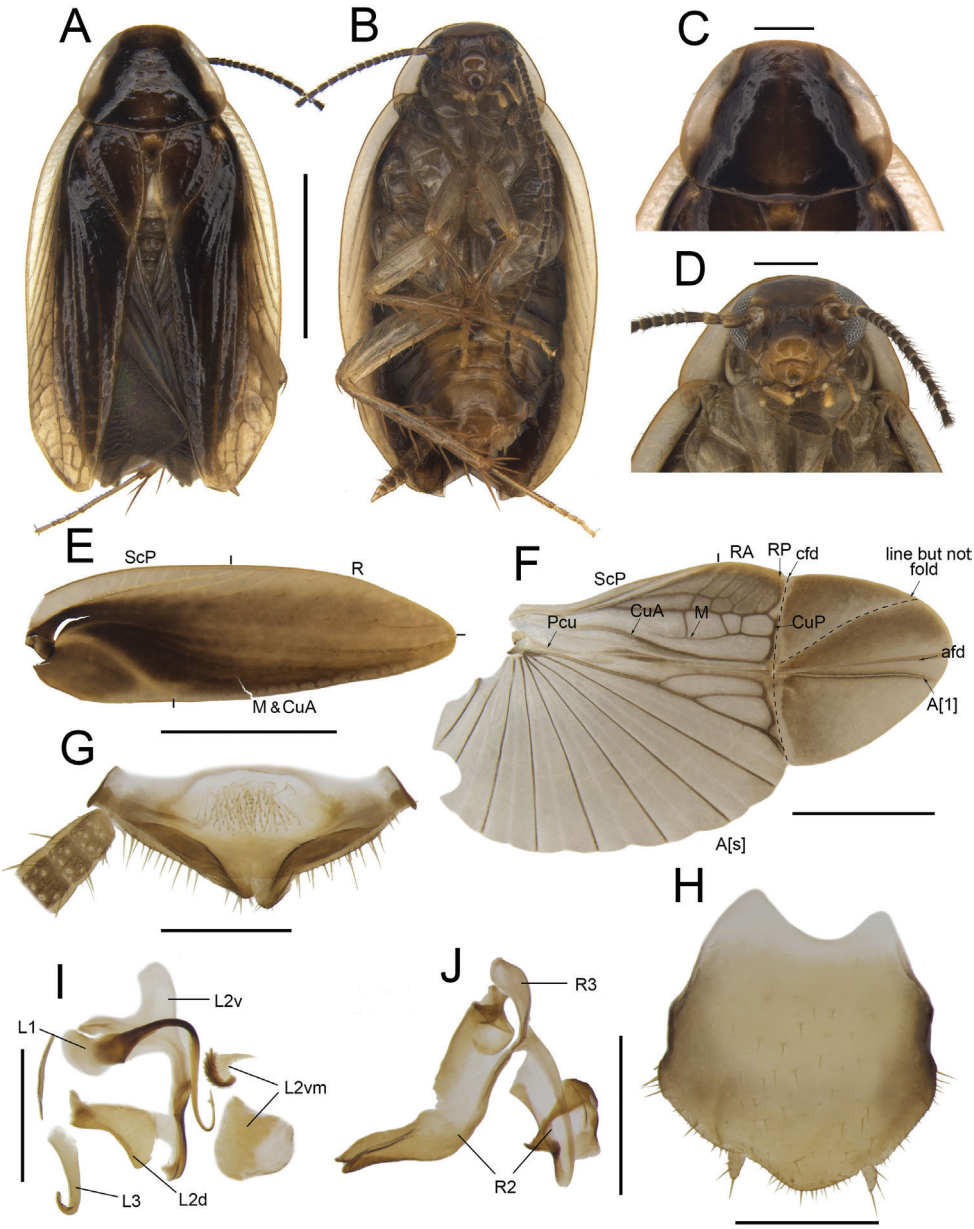

Figure 7. *Anaplecta anomala* Zhu & Che, sp. nov. holotype, male SWU-B-B-A060056 **A** habitus, dorsal view **B** habitus, ventral view **C** pronotum, dorsal view **D** head, ventral view **E** tegmina **F** wings **G** supra-anal plate, ventral view **H** subgenital plate, dorsal view **I** left phallomere, dorsal view **J** right phallomere, dorsal view. Scale bars: 2 mm (**A–F**); 0.5 mm (**G–J**). Abbreviations: **afd** anal fold, **A[1]** the anterior one of the anal vein, **A[s]** the other element of vannal vein, **cfd** cubitus fold, **CuA** cubitus anterior, **CuP** cubitus posterior, **L1, L2, L3** sclerites of the left phallomere, **L2d** L2 dorsal, **L2v** L2 ventral, **L2vm** median sclerite, **M** media, **Pcu** postcubitus, **R** radius, **RA** radius anterior, **RP** radius posterior, **R2, R3** sclerites of the right phallomere, **ScP** subcostal posterior.

***Female genitalia*.** Supra-anal plate nearly symmetrical. Paraprocts broad, not extending to the posterior margin of supra-anal plate. Intercalary sclerite slender. First valve tubular. Second valve small, basally fused. Third valve broad. The anterior margin of anterior arch slightly sclerotized, with a finger-like protrusion. Basivalvula broad, nearly triangle, anterior and posterior margin slightly curled (Fig. 14D, E). Vestibular sclerite sheet-like. Laterosternal shelf slightly sclerotized, lateral margin nearly straight (Fig. 14F).

Distribution. China (Yunnan).

Anaplecta bombycina Zhu & Che, sp. nov.

http://zoobank.org/678DC628-4480-4498-9490-9EF66660E8A5
Figures 8, 14G–I

Type material. ***Holotype*:** China • male; Yunnan Prov., Xishuangbanna, Dadugang Village; 22°16.52'N, 100°55.02'E; 1100 m; 15 July 2020, Rong Chen, Du-Ting Jin leg.; SWU-B-B-A060073.

***Paratypes*:** China • 4 males and 3 females; same data as holotype; SWU-B-B-A060074 and 060080 • 1 female; Yunnan Prov., Pu'er City, Meizi Lake; 22°45.27'N, 100°59.60'E; 1365 m; 17 July 2020; Rong Chen, Yi-Shu Wang, leg.; SWU-B-B-A060081 • 2 female; Yunnan Prov., Xishuangbanna, Ji'nuozu Village; 22°02.44'N, 101°1.81'E; 1100 m; 13 July 2020; Li-Kang Niu, Yi-Shu Wang leg.; SWU-B-B-A060082 and 060083 • 3 males and 1 female; Yunnan Prov., Xishuangbanna, Dadugang Village, 21°59.06'N, 101°64.40'E; 870 m; 14 July 2020; Rong Chen, Li-Kang Niu leg.; SWU-B-B-A060084 to 060087.

Diagnosis. This species can be easily separated from other species by dark brown tegmina and the extremely slender filamentous structure in the male genitalia.

Etymology. The specific epithet is derived from the Latin word *bombycinus*, referring to the slender filamentous structure with which L1 is connected.

Measurements (mm). Male: pronotum length × width: 1.35× 1.57, tegmina length: 4.70, overall length: 6.08. Female: pronotum length × width: 1.42 × 1.68, tegmina length: 4.95, overall length: 6.26.

Description. ***Coloration*.** Body dark brown, face brown (Fig. 8A, B). Antennae and maxillary palpus brown (Fig. 8D). Pronotum and tegmina dark brown, lateral edges hyaline (Fig. 8C, E). Hind wings infuscate, costal field and appendicular field darker than remaining parts (Fig. 8F). Abdominal sterna, legs, and cerci yellowish brown (Fig. 8B).

***Head and thorax*.** The distance between antennal sockets narrower than interocular space. Fifth maxillary palpus nearly triangular, slightly thicker and wider than others (Fig. 8D). Pronotum a semicircle, anterior margin arcuate, posterior margin straight (Fig. 8C). Tegmina with slightly indistinct veins; radius posterior veins of hind wings slightly indistinct, without transverse veins between M and CuA (Fig. 8E, F). Front femur Type B_2 (Fig. 8B). Pulvilli absent, tarsal claws symmetrical.

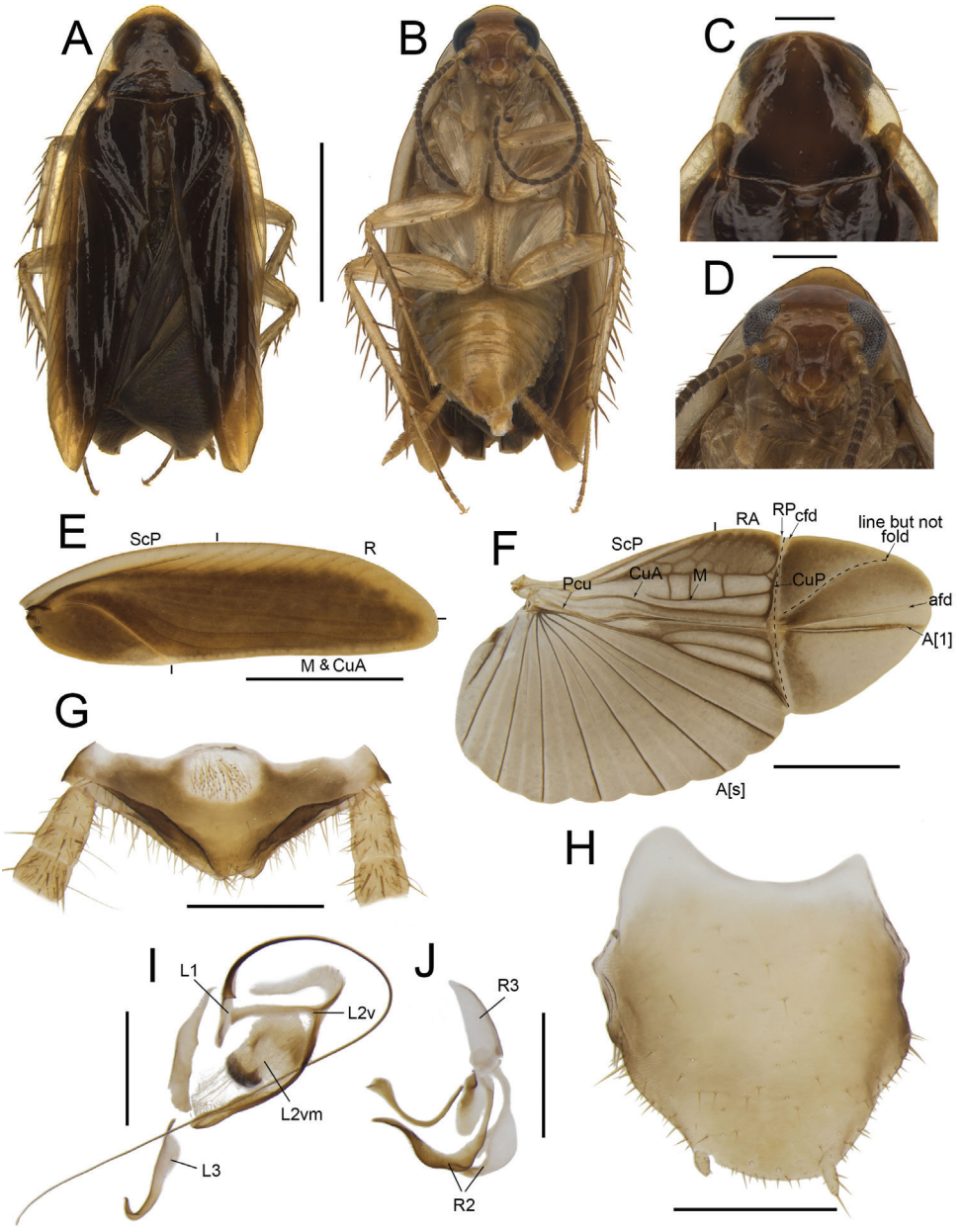

Figure 8. *Anaplecta bombycina* Zhu & Che, sp. nov. holotype, male SWU-B-B-A060073 **A** habitus, dorsal view **B** habitus, ventral view **C** pronotum, dorsal view **D** head, ventral view **E** tegmina **F** wings **G** supra-anal plate, ventral view **H** subgenital plate, dorsal view **I** left phallomere, dorsal view **J** right phallomere, dorsal view. Scale bars: 2 mm (**A–F**); 0.5 mm (**G–J**). Abbreviations: **afd** anal fold, **A[1]** the anterior one of the anal vein, **A[s]** the other element of vannal vein, **cfd** cubitus fold, **CuA** cubitus anterior, **CuP** cubitus posterior, **L1, L2, L3** sclerites of the left phallomere, **L2v** L2 ventral, **L2vm** median sclerite, **M** media, **Pcu** postcubitus, **R** radius, **RA** radius anterior, **RP** radius posterior, **R2, R3** sclerites of the right phallomere, **ScP** subcostal posterior.

***Male genitalia*.** Supra-anal plate with sheet-like paraprocts (Fig. 8G). Subgenital plate asymmetrical, the left margin wider than the right, the interstylar margin convex, skewed to right. The left stylus smaller than the right, the distance between them long (Fig. 8H). L1 small, with a curved and very slender filamentary structure. L2v shaped like '3'. L2vm sheet-like, with dense spines. L3 medium, uncinate part with sharp apex (Fig. 8I). R2 irregular, weakly sclerotized. R3 sheet-like (Fig. 8J).

***Female genitalia*.** Supra-anal plate nearly symmetrical. Paraprocts broad, extending to the posterior margin of supra-anal plate. Intercalary sclerite strip-shaped, slightly curved. First valvifer slender. First valve robust. Second valve small, basally fused. Third valve broad. The anterior margin of anterior arch protrudes in the shape of lungs with curved edges (Fig. 14G, H). Basivalvula broad, kidney shaped, posterior margin curled, with spines at left lateral (Fig. 14G). Vestibular sclerite small. Laterosternal shelf slightly sclerotized, lateral margin slightly curved (Fig. 14I).

Distribution. China (Yunnan).

Anaplecta truncatula Zhu & Che, sp. nov.

http://zoobank.org/B81FCCEA-D820-4488-B570-82F40719F8F9
Figures 9, 15A–C

Type material. ***Holotype*:** China • male; Hunan Prov., Shaoyang City, Baimaoping Town; 26°24.90'N, 110°36.04'E; 564 m; 19–21 August 2020; Lu Qiu, leg.; SWU-B-B-A060088.

***Paratypes*:** China • 5 males and 3 females; same data as holotype; SWU-B-B-A060089 to 060096.

Diagnosis. This species is similar to *A. japonica* Asahina, 1977 in body color and tegmina marking, but may be distinguished from the latter by the straight interstylar margin, Since *A. japonica* was described by external structures lacking genitalia, a comparison of this part is impossible. It is also similar to *A. nigra* Deng & Che, 2020, but can be distinguished as follows: 1) subgenital plate sub-rectangular in *A. truncatula* sp. nov., while *A. nigra* fan-shaped; 2) R1 needle-shaped in *A. truncatula* sp. nov., while arc-shaped in *A. nigra*; 3) anterior margin of anterior arch with a strip-shaped protrusion in *A. truncatula* sp. nov., while the protrusion of *A. nigra* triangular; and 4) vestibular sclerite with two long spines in *A. nigra*, *A. truncatula* sp. nov. without.

Etymology. The specific epithet is derived from the Latin word *truncatulus*, referring to the truncated end of the bifurcation of the paraprocts.

Measurements (mm). Male: pronotum length × width: 1.28–1.37 × 1.98–2.05, tegmina length: 5.21–5.24, overall length: 6.23–6.32. Female: pronotum length × width: 1.37–1.48 × 1.97–2.13, tegmina length: 5.37–5.46, overall length: 6.58–6.70.

Description. ***Coloration*.** Body pale yellowish brown, face yellow (Fig. 9A, B). Antennae and maxillary palpus brown (Fig. 9D). Pronotum yellowish brown,

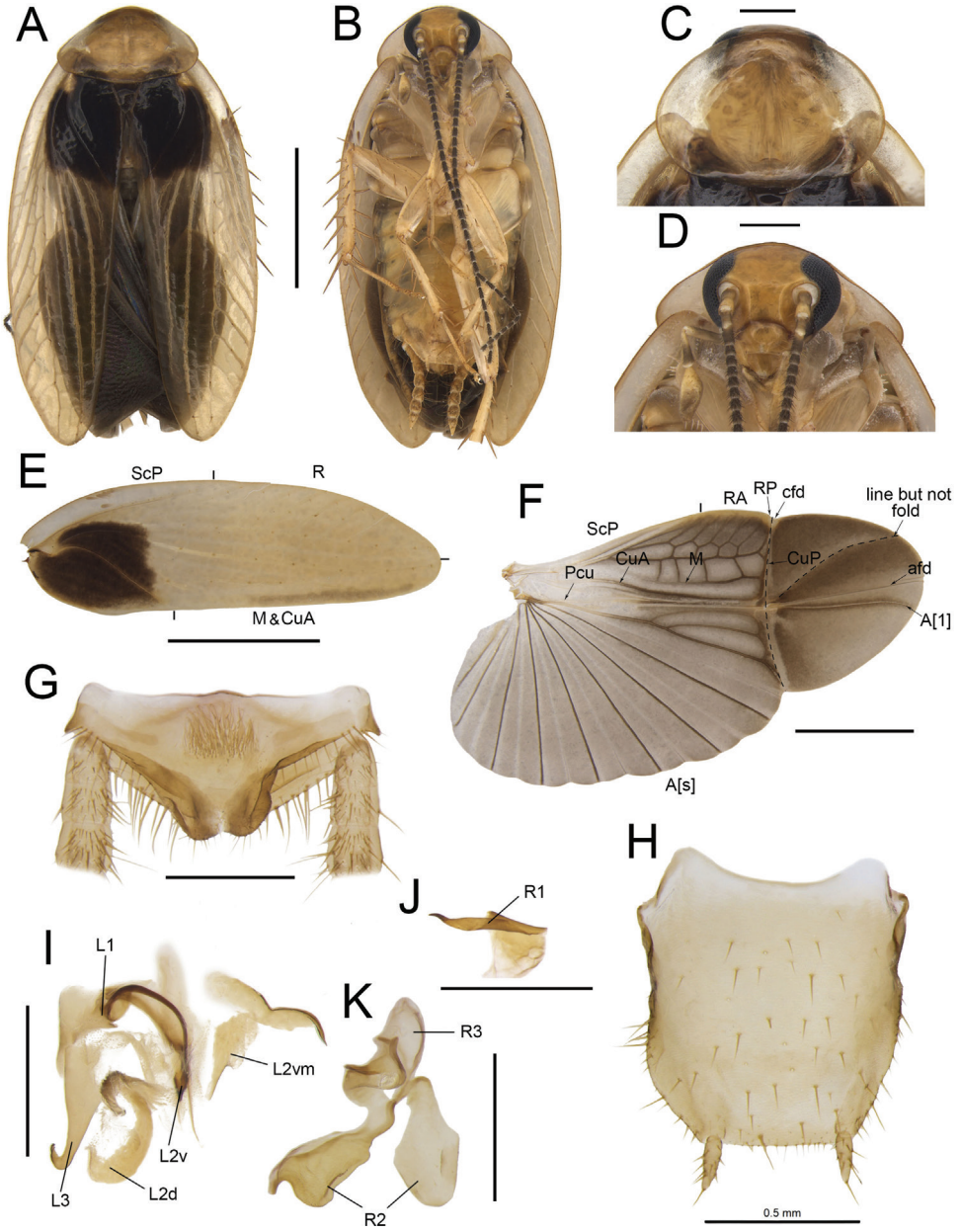

Figure 9. *Anaplecta truncatula* Zhu & Che, sp. nov. holotype, male SWU-B-B-A060088 **A** habitus, dorsal view **B** habitus, ventral view **C** pronotum, dorsal view **D** head, ventral view **E** tegmina **F** wings **G** supra-anal plate, ventral view **H** subgenital plate, dorsal view **I** left phallomere, dorsal view **J–K** right phallomere, dorsal view. Scale bars: 2 mm (**A–F**); 0.5 mm (**G–K**). Abbreviations: **afd** anal fold, **A[1]** the anterior one of the anal vein, **A[s]** the other element of vannal vein, **cfd** cubitus fold, **CuA** cubitus anterior, **CuP** cubitus posterior, **L1, L2, L3** sclerites of the left phallomere, **L2d** L2 dorsal, **L2v** L2 ventral, **L2vm** median sclerite, **M** media, **Pcu** postcubitus, **R** radius, **RA** radius anterior, **RP** radius posterior, **R1, R2, R3** sclerites of the right phallomere, **ScP** subcostal posterior.

lateral edges hyaline (Fig. 9C). Tegmina light yellowish brown, lateral edges pale or hyaline, 1/3 of the base black (Fig. 9E). Hind wings infuscate, costal field and appendicular field darker than remaining parts (Fig. 9F). Abdominal sterna, legs, and cerci yellow (Fig. 9B).

Head and thorax. The distance between antennal sockets narrower than interocular space. Fifth maxillary palpus nearly triangular, slightly thicker and wider than others (Fig. 9D). Pronotum subelliptic, posterior margin straight, lateral margin protruding and arc-shaped (Fig. 9C). Tegmina with indistinct veins, the radius posterior veins of hind wings distinct, no transverse veins between M and CuA (Fig. 9E, F). Front femur Type B_2 (Fig. 9B). Pulvilli absent, tarsal claws symmetrical.

Male genitalia. Paraprocts bifurcated at the base: the strip-shaped part truncated, the rest sheet-like (Fig. 9G). Subgenital plate sub-rectangular, the center of anterior slightly concave, interstylar margin straight. Styli long, length ~ 1/2 of interstylar space (Fig. 9H). L1 small, with curved and long filamentary structure. L2v bifurcated, with sharp apex. L2d narrow, nearly meniscus-shaped. L2vm sheet-like, irregular. L3 robust, uncinate part slightly sharp (Fig. 9I). R1 needle-shaped, the proximal part sharply tapered and highly sclerotized (Fig. 9J). R2 irregular, weakly sclerotized. R3 slightly curved, sheet-like (Fig. 9K).

Female genitalia. Supra-anal plate nearly symmetrical. Paraprocts broad, not extending to the posterior margin of supra-anal plate. Intercalary sclerite short, nearly spindle-shaped. Right first valvifer finger-like. First valve robust. Second valve small, basally fused. Third valve broad. The anterior margin of anterior arch slightly sclerotized, with a bifurcated strip-shaped protrusion (Fig. 15A, B). Basivalvula irregular, posterior margin and center with dense punctuations, the left of anterior margin extending back, connecting to crosspiece by membrane (Fig. 15A). Laterosternal shelf slightly sclerotized, lateral margin slightly curved, with dense spinules at lateral base (Fig. 15C).

Distribution. China (Hunan).

Anaplecta longihamata Zhu & Che, sp. nov.

http://zoobank.org/648EBFA2-6972-4528-8C00-886A256949C3
Figures 10, 16A–C

Type material. ***Holotype*****:** China • male; Yunnan Prov., Pu'er City, Mt. Wuliang; 24°38'N, 100°44'E; 1232 m, 21 July 2020; Li-Kang Niu, Rong Chen leg.; SWU-B-B-A06097.

Paratypes**:** China • 1 male and 1 female; same data as holotype; SWU-B-B-A06098 and 06099 • 2 males; Yunnan Prov., Xishuangbanna, Dadugang Village; 21°59.06'N, 101°64.40'E; 870 m; 14 July 2020; Rong Chen, Li-Kang Niu leg.; SWU-B-B-A06100 and 060101 • 2 males; Yunnan Prov., Xishuangbanna, Dadugang Village; 22°16.52'N, 100°55.02'E; 15 July 2020; Rong Chen, Du-Ting Jin leg.; SWU-B-B-A060102 and 060103.

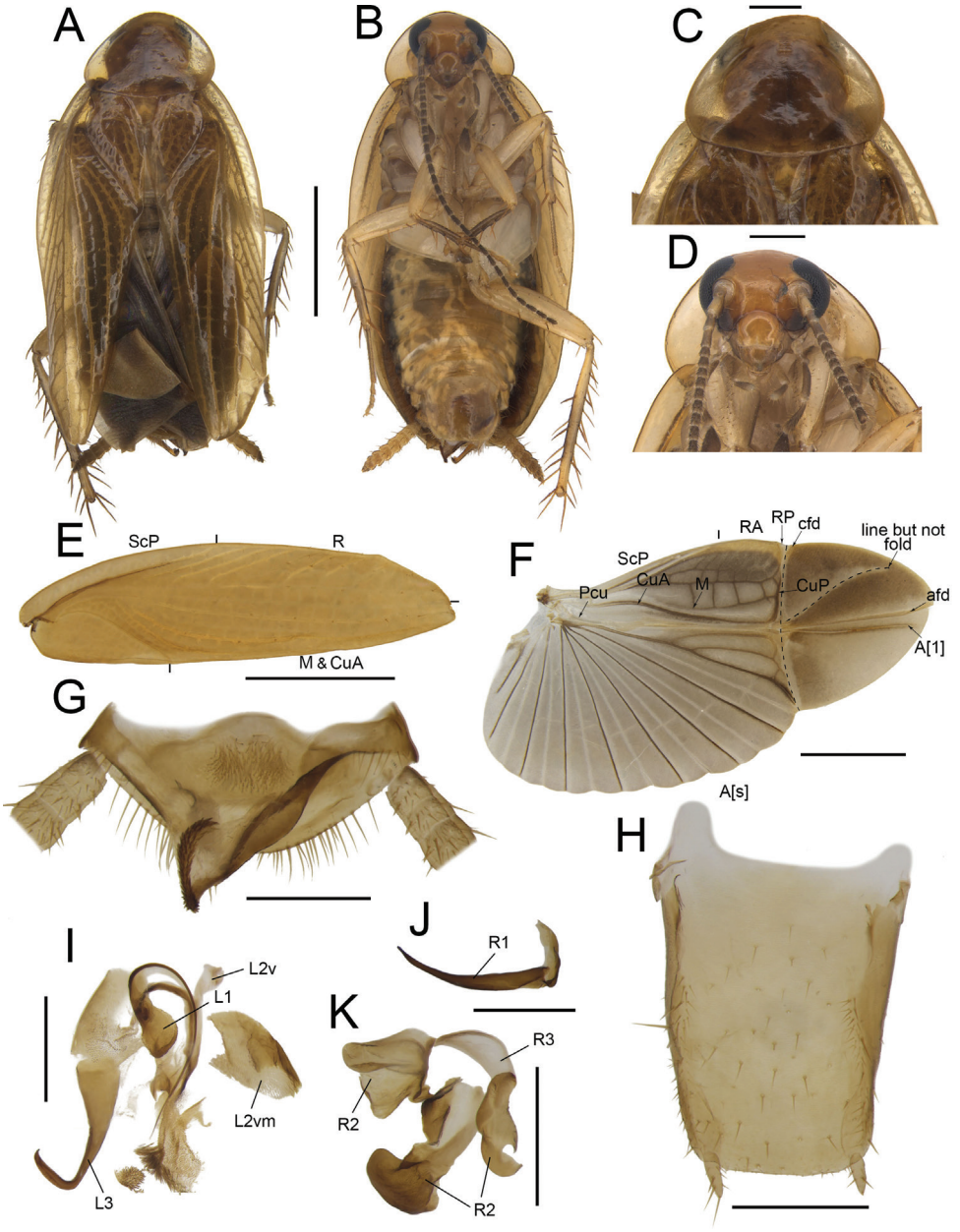

Figure 10. *Anaplecta longihamata* Zhu & Che, sp. nov. holotype (SP4), male SWU-B-B-A06097 **A** habitus, dorsal view **B** habitus, ventral view **C** pronotum, dorsal view **D** head, ventral view **E** tegmina **F** wings **G** supra-anal plate, ventral view **H** subgenital plate, dorsal view **I** left phallomere, dorsal view **J, K** right phallomere **J** dorsal view **K** ventral view. Scale bars: 2 mm (**A–F**); 0.5 mm (**G–K**). Abbreviations: **afd** anal fold, **A[1]** the anterior one of the anal vein, **A[s]** the other element of vannal vein, **cfd** cubitus fold, **CuA** cubitus anterior, **CuP** cubitus posterior, **L1, L2, L3** sclerites of the left phallomere, **L2v** L2 ventral, **L2vm** median sclerite, **M** media, **Pcu** postcubitus, **R** radius, **RA** radius anterior, **RP** radius posterior, **R1, R2, R3** sclerites of the right phallomere, **ScP** subcostal posterior.

Measurements (mm). Male: pronotum length × width: 1.39–1.53 × 1.94–2.03, tegmina length: 5.17–5.76, overall length: 6.57–7.09. Female: pronotum length × width: 1.42 × 1.92, tegmina length: 5.12, overall length: 6.43.

Diagnosis. This species is similar to *A. omei* Bey-Bienko, 1958, but can be distinguished as follows: 1) right paraproct long hooked in *A. longihamata* sp. nov., while sheet-like in *A. omei*; 2) R1 bifurcated in *A. omei*, while unbranched in *A. longihamata* sp. nov.;3) anterior arch with two transversely finger-like protrusions in *A. longihamata* sp. nov., while *A. omei* without; and 4) first valvifer arm lateral edges folded up in *A. longihamata* sp. nov., while not folded in *A. omei* .

Etymology. The specific epithet is derived from the Latin words *longi* and *hamatus*, referring to the right paraproct extended backward in a long hook shape.

Description. ***Coloration.*** Body yellowish brown, face yellowish brown (Fig. 10A, B). Antennae and maxillary palpus brown (Fig. 10D). Pronotum yellowish brown, lateral edges hyaline (Fig. 10C). Tegmina light yellowish brown, lateral edges pale (Fig. 10E). Hind wings infuscate, costal field and appendicular field darker than remaining parts (Fig. 10F). Abdominal sterna, legs, and cerci yellowish brown (Fig. 10B).

Head and thorax. The distance between antennal sockets slightly narrower than interocular space. Fifth maxillary palpus nearly oval, slightly thicker and wider than others (Fig. 10D). Pronotum subelliptic, anterior and posterior margins nearly straight (Fig. 10C). Tegmina with slightly indistinct veins; radius posterior veins of hind wings slightly indistinct, without transverse veins between M and CuA (Fig. 10E, F). Front femur Type B_2 (Fig. 10B). Pulvilli absent, tarsal claws symmetrical.

Male genitalia. Supra-anal asymmetrical, the left paraproct sheet-like, right paraproct extending backward, hooked, and curled at apex with dense spines (Fig. 10G). Subgenital plate sub-rectangular, the center of anterior and interstylar margins nearly straight. Styli long, length about 1/4 of interstylar space (Fig. 10H). L1 subelliptic, thickened at anterior edge, with a curved and long filamentary structure connected. L2v curved, bifurcated at the apex, with a sharp horn. L2vm sheet-like. L3 extremely robust, with long uncinate part and bent at right angles (Fig. 10I). R1 needle-shaped, the proximal part slightly curved (Fig. 10J). R2 irregular, weakly sclerotized, one of R2 with small protrusions. R3 broad, sheet-like (Fig. 10K).

Female genitalia. Supra-anal plate nearly symmetrical. Paraprocts broad, extending to the posterior margin of supra-anal plate. Intercalary sclerite short, sheet-like. Right first valvifer arm extremely robust, lateral edges folded up, fused with crosspiece (Fig. 16A). First valve robust. Second valve small, basally fused. Third valve broad. The anterior margin of anterior arch slightly sclerotized, with a hook-shaped protrusion, hind edge with two transversely finger-like protrusions. Basivalvula irregular, anterior edge curly. Vestibular sclerite sheet-like (Fig. 16A, B). Laterosternal shelf slightly sclerotized, lateral margin nearly straight (Fig. 16C).

Distribution. China (Yunnan).

***Anaplecta paraomei* Zhu & Che, sp. nov.**
http://zoobank.org/D8AD2528-06E2-4980-A090-6CC1089F3256
Figures 11, 16D–F

Type material. ***Holotype*:** China • male; Guizhou Prov., Dushan County; 25°45.60'N, 107°33.03'E; 7 June 2019; Lu Qiu, Wen-Bo, Deng, leg.; SWU-B-B-A060104.

***Paratypes*:** China • 12 males and 4 females, same data as holotype; SWU-B-B-A060105 and 060120.

Diagnosis. This species is very similar to *A. omei*, but can be distinguished as follows: 1) the paraprocts not extending backward in *A. paraomei* sp. nov., while left paraproct extending backward in *A. omei*; 2) the apex of R1 nearly symmetrical in *A. paraomei*, while asymmetrical in *A. omei*; 3) intercalary sclerite nearly strip-shaped in *A. paraomei*, while spindle-shaped in *A. omei*; and 4) posterior margin of anterior arch hip-shaped in *A. paraomei* sp. nov., while smooth in *A. omei*.

Etymology. The Latin word *para* means similar, referring to its close resemblance to *A. omei*.

Measurements (mm). Male: pronotum length × width: 1.29–1.35 × 2.00–2.09, tegmina length: 5.24–5.53, overall length: 6.15–6.57. Female: pronotum length × width: 1.44 × 2.09, tegmina length: 5.31, overall length: 6.23

Description. ***Coloration*.** Body yellowish brown, face yellow (Fig. 11A, B). Antennae and maxillary palpus brown (Fig. 11D). Pronotum and tegmina yellowish brown, lateral edges hyaline (Fig. 11C, E). Hind wings infuscate, costal field and appendicular field darker than remaining parts (Fig. 11F). Abdominal sterna, legs, and cerci yellow brown (Fig. 11B).

***Head and thorax*.** The distance between antennal sockets narrower than interocular space. Fifth maxillary palpus nearly oval, slightly thicker and wider than others (Fig. 11D). Pronotum subelliptic, anterior and posterior margins nearly straight, lateral margin protruding and arc-shaped (Fig. 11C). Tegmina with slightly indistinct veins, radius posterior veins of hind wings slightly indistinct, with one transverse vein between M and CuA (Fig. 11E, F). Front femur Type B_2 (Fig. 11B). Pulvilli absent, tarsal claws symmetrical.

***Male genitalia*.** Supra-anal plate asymmetrical, the left paraproct with dense spines on curly posterior margin; right paraproct with dense spines on curly apex (Fig. 11G). Subgenital plate sub-trapezoidal, the center of anterior slightly curved, interstylar margins straight. Styli medium, length about 1/5 of interstylar space (Fig. 11H). L1 subcircular, with a curved and long filamentary structure. L2v curved, bifurcated at the apex, with a sharp horn. L2vm broad. L3 robust, with extremely bent and sharp uncinate part (Fig. 11I). R1 highly sclerotized, the proximal part nearly dichotomous branching (Fig. 11J). R2 irregular, weakly sclerotized. R3 slightly curved, sheet-like (Fig. 11K).

***Female genitalia*.** Supra-anal plate nearly symmetrical. Paraprocts broad, not extending to the posterior margin of supra-anal plate. Intercalary sclerite short, nearly

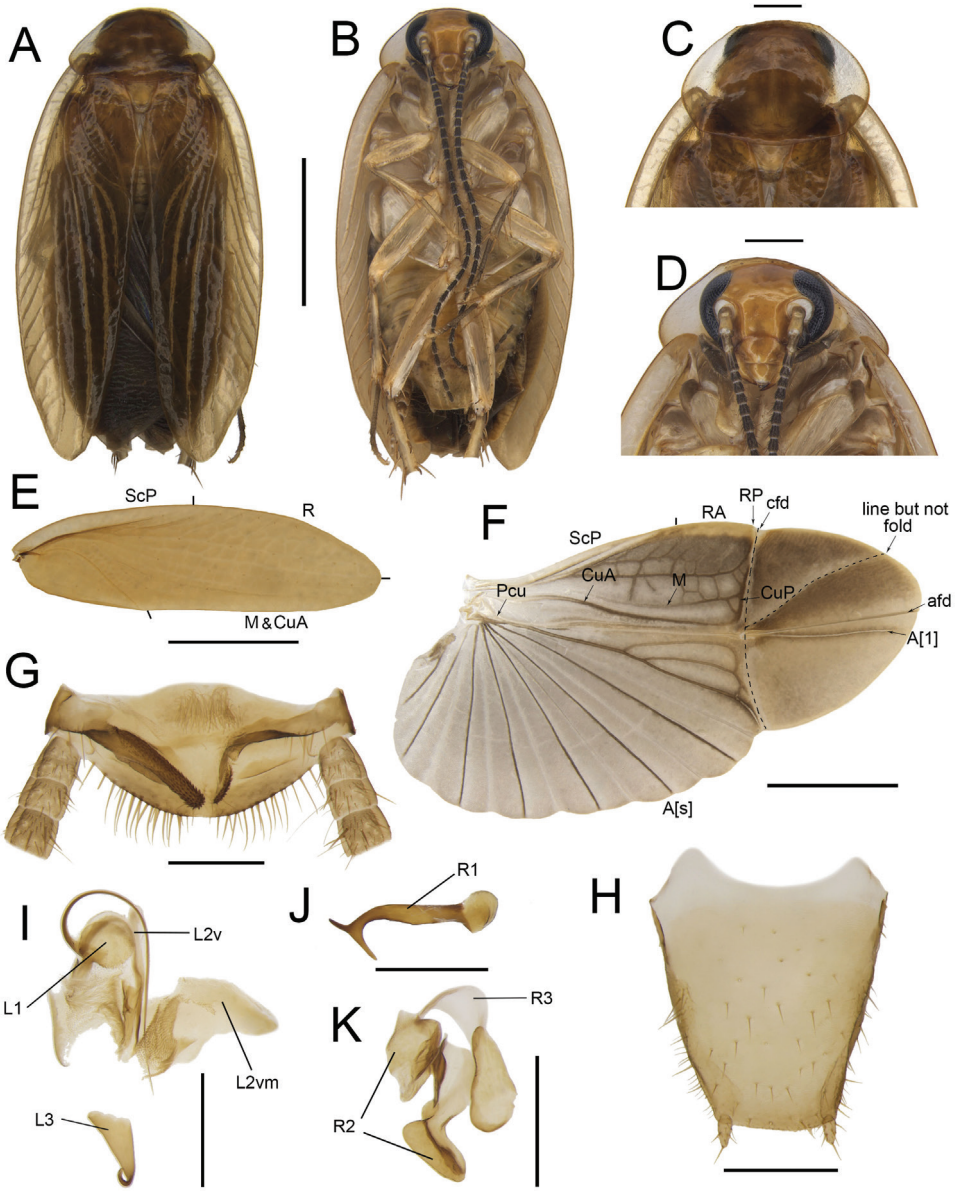

Figure 11. *Anaplecta paraomei* Zhu & Che, sp. nov. holotype (GZ2), male SWU-B-B-A060104 **A** habitus, dorsal view **B** habitus, ventral view **C** pronotum, dorsal view **D** head, ventral view **E** tegmina **F** wings **G** supra-anal plate, ventral view **H** subgenital plate, dorsal view **I** left phallomere, dorsal view **J, K** right phallomere **J** dorsal view **K** ventral view. Scale bars: 2 mm (**A–F**); 0.5 mm (**G–K**). Abbreviations: **afd** anal fold, **A[1]** the anterior one of the anal vein, **A[s]** the other element of vannal vein, **cfd** cubitus fold, **CuA** cubitus anterior, **CuP** cubitus posterior, **L1, L2, L3** sclerites of the left phallomere, **L2v** L2 ventral, **L2vm** median sclerite, **M** media, **Pcu** postcubitus, **R** radius, **RA** radius anterior, **RP** radius posterior, **R1, R2, R3** sclerites of the right phallomere, **ScP** subcostal posterior.

strip-shaped (Fig. 16D, E). Right first valvifer arm robust, curled (Fig. 16D). First valve robust. Second valve small, basally fused. Third valve broad. The anterior margin of anterior arch slightly curled, with a nearly transparent hook-shaped protrusion and the posterior margin hip-shaped. Basivalvula broad, with dense punctuations, the right lateral deeply concave (Fig. 16D). Vestibular sclerite broad, slightly curled, sheet-like. Laterosternal shelf slightly sclerotized, lateral margin nearly straight. (Fig. 16F).

Distribution. China (Guizhou).

Anaplecta condensa Zhu & Che, sp. nov.

http://zoobank.org/92D48955-FA05-41A2-8B3D-E51ABF2A102C
Figures 2C, D, 12, 16G–I

Type material. ***Holotype*:** China • male; Guizhou Prov., Libo County, Jiaou Village; 25°30.06'N, 107°67.02'E; 11 June 2019; Lu Qiu, Wen-Bo, Deng, leg.; SWU-B-B-A060121.

***Paratypes*:** China • 3 males and 1 female; same data as holotype; SWU-B-B-A060122 to 060125 • 2 males; Guangxi Prov., Guiping City; 31 May–2 June 2014; Shun-Hua Gui, Xin-Ran Li, Jian-Yue Qiu, leg.; SWU-B-B-A060126 and 060127.

Diagnosis. This species is very similar to *A. omei*, but can be distinguished as follows: 1) paraprocts both extending backward in *A. condensa* sp. nov., while only the left extending backward in *A. omei*; 2) R1 needle-shaped in *A. condensa* sp. nov., while bifurcated in *A. omei*; and 3) intercalary sclerite of *A. condensa* sp. nov. very small, filamentous, while that of *A. omei* is spindle-shaped.

Etymology. The specific epithet is derived from the Latin word *condensus*, referring to the paraprocts with dense spines on curly posterior margin.

Measurements (mm). Male: pronotum length × width: 1.36–1.39 × 1.78–1.84, tegmina length: 4.93–5.39, overall length: 5.92–6.59. Female: pronotum length × width: 1.29 × 1.73, tegmina length: 4.75, overall length: 5.82

Description. ***Coloration*.** Body brown (some individuals from Guiping yellowish brown) (Fig. 2C, D), face dark brown (Fig. 12A, B). Antennae and maxillary palpus brown (Fig. 12D). Pronotum dark brown, lateral edges nearly hyaline (Fig. 12C). Tegmina yellowish brown, anal field and base of mediocubital field slightly darker (Fig. 12E). Hind wings infuscate, costal field and appendicular field darker than remaining parts (Fig. 12F). Center of abdominal sterna yellow, gradually darkening to dark brown to edges, legs, and cerci dark yellowish brown (Fig. 12B).

***Head and thorax*.** The distance between antennal sockets slightly narrower than interocular space. Fifth maxillary palpus nearly oval, slightly thicker and wider than others (Fig. 12D). Pronotum semicircular, anterior margin arched, the center of posterior margin protrudes slightly (Fig. 12C). Tegmina with indistinct veins, radius posterior veins of hind wings slightly indistinct, without transverse veins between M and CuA (Fig. 12E, F). Front femur Type B_2 (Fig. 12B). Pulvilli absent, tarsal claws symmetrical.

***Male genitalia*.** Paraprocts both extend backwards and with dense spines on curly posterior margin (Fig. 12G). Subgenital plate sub-rectangular, the center of anterior

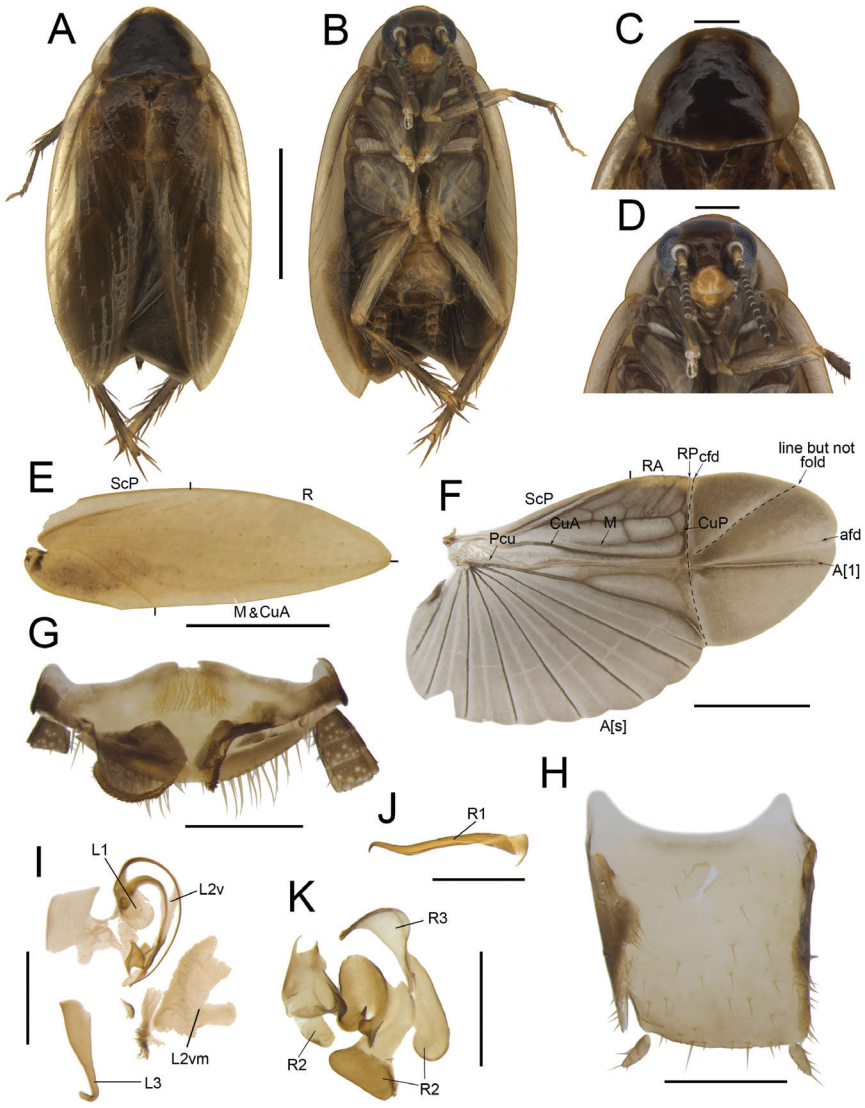

Figure 12. *Anaplecta condensa* Zhu & Che, sp. nov. holotype (GZ4), male SWU-B-B-A060121 **A** habitus, dorsal view **B** habitus, ventral view **C** pronotum, dorsal view **D** head, ventral view **E** tegmina **F** wings **G** supra-anal plate, ventral view **H** subgenital plate, dorsal view **I** left phallomere, dorsal view **J, K** right phallomere **J** dorsal view **K** ventral view. Scale bars: 2 mm (**A–F**); 0.5 mm (**G–K**). Abbreviations: **afd** anal fold, **A[1]** the anterior one of the anal vein, **A[s]** the other element of vannal vein, **cfd** cubitus fold, **CuA** cubitus anterior, **CuP** cubitus posterior, **L1, L2, L3** sclerites of the left phallomere, **L2v** L2 ventral, **L2vm** median sclerite, **M** media, **Pcu** postcubitus, **R** radius, **RA** radius anterior, **RP** radius posterior, **R1, R2, R3** sclerites of the right phallomere, **ScP** subcostal posterior.

and interstylar margins nearly straight. Styli long, so is the distance between them (Fig. 12H). L1 subcircular, with curved and long filamentary structure. L2v curved, bifurcated, with a sharp horn. L2vm broad. L3 extremely robust, uncinate part blunt

(Fig. 12I). R1 needle-shaped, the proximal part slightly curved (Fig. 12J). R2 irregular, weakly sclerotized. R3 slightly curved, sheet-like (Fig. 12K).

Female genitalia. Supra-anal plate nearly symmetrical, very blunt and round. Paraprocts broad, hind margin blunt, not extending to the posterior margin of supra-anal plate. Intercalary sclerite small, nearly filamentous. First valve robust. Second valve small, basally fused. Third valve broad. The anterior margin of anterior arch slightly curled, with a hook-shaped protrusion (Fig. 16G–H). Basivalvula broad, with dense punctuations, except for left lateral and anterior margin (Fig. 16G). Vestibular sclerite broad, slightly curled, sheet-like. Laterosternal shelf slightly sclerotized, lateral margin straight (Fig. 16I).

Distribution. China (Guizhou, Guangxi).

Anaplecta cruciata Deng & Che, 2020

Figure 13J–L

Anaplecta cruciata Deng & Che in Deng et al., 2020: 95–97.

Material examined. China • 8 males (paratypes) and 4 females (paratypes); Yunnan Prov., Xishuangbanna, Mengla County, Yaoqu Town; 21°14.60'N, 101°42.43'E; 820 m; 10 May 2015; Jian –Yue Qiu, leg.; SWU-B-B-A060128 to 060139 • 4 males; Yunnan Prov., Pu'er City, Mt. Wuliang; 24°38'N, 100°44'E; 1232 m; 21 July 2020; Li-Kang Niu, Rong Chen, leg.; SWU-B-B-A060140 to 060143 • 4 males and 3 females; Yunnan Prov., Pu'er City, Meizi Lake; 22°45.27'N, 100°59.60'E; 1365 m; 17 July 2020; Rong Chen, Yi-Shu Wang, leg.; SWU-B-B-A060144 to 060150.

Female genitalia. Supra-anal plate nearly symmetrical. Paraprocts broad, extending to the posterior margin of supra-anal plate. Intercalary sclerite nearly strip-shaped. First valve robust. Second valve small, basally fused. Third valve broad. The anterior margin of anterior arch slightly sclerotized, protruding forward in a Y-shape. Basivalvula nearly rectangular, with dense punctuations, anterior margin curled (Fig. 13J, K). Laterosternal shelf slightly sclerotized, lateral margin straight (Fig. 13L).

Distribution. China (Yunnan).

Anaplecta strigata Deng & Che, 2020

Figure 14J–L

Anaplecta strigata Deng & Che in Deng et al., 2020: 91–93.

Material examined. China • 11 males and 6 males, Yunnan Prov., Pu'er City, Meizi Lake; 22°45.27'N, 100°59.60'E; 1365 m; 17 July 2020; Rong Chen, Yi-Shu Wang, leg.; SWU-B-B-A060151 to 060167 • 3 females; Yunnan Prov., Xishuangbanna, Shangyong Town; 21°16.19'N, 101°30.42'E; 870 m; 7 July 2020; Du-Ting Jin, Rong

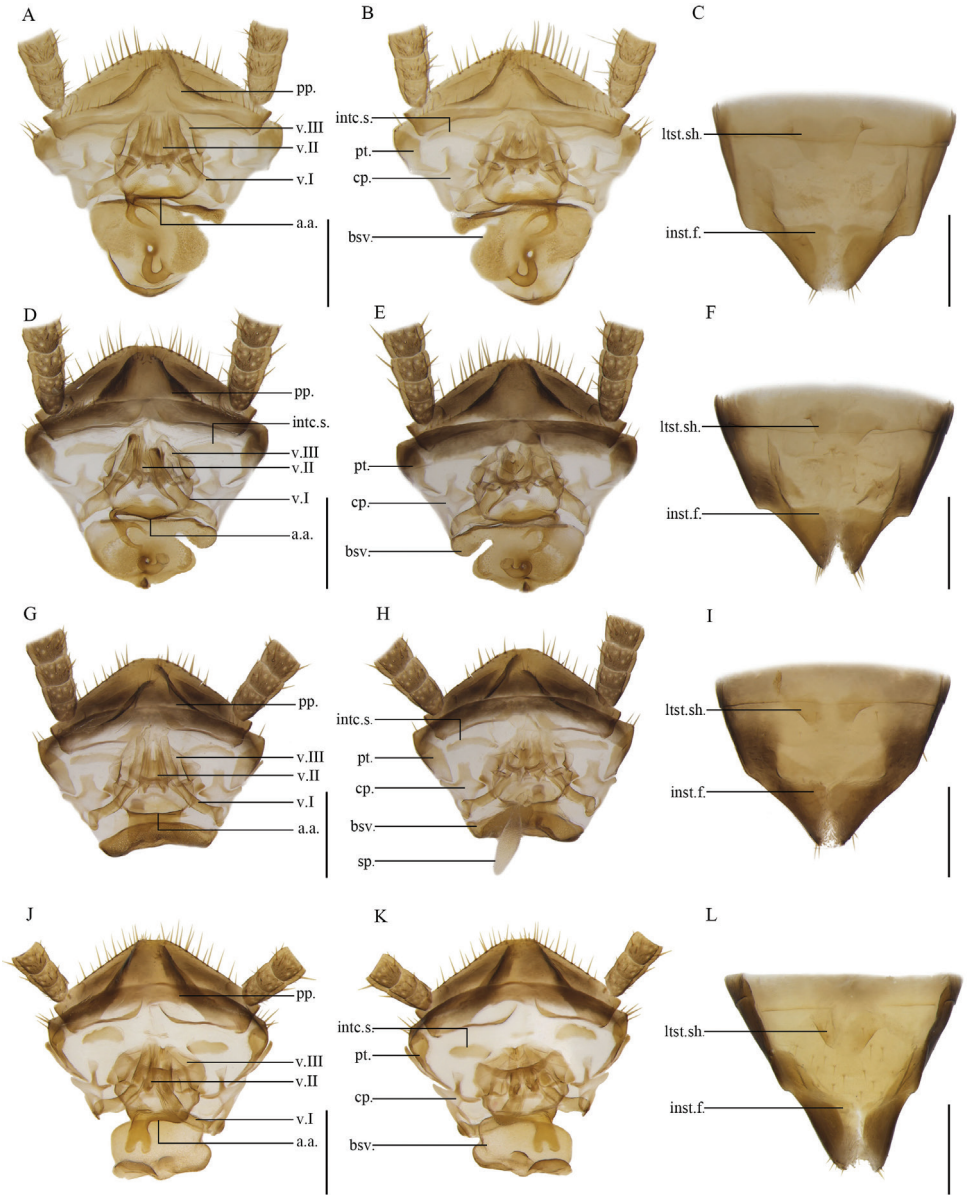

Figure 13. A–C *Anaplecta bicruris* Zhu & Che, sp. nov. paratype, female SWU-B-B-A060004 **D–F** *Anaplecta spinosa* Zhu & Che, sp. nov. paratype, female SWU-B-B-A060014 **G–I** *Anaplecta serrata* Zhu & Che, sp. nov. paratype, female SWU-B-B-A060020 **J–L** *Anaplecta cruciata* Deng & Che, 2020. Paratype, female SWU-B-B-A060136 **A, D, G, J** supra-anal plate, ventral view **B, E, H, K** supra-anal plate, dorsal view **C, F, I, L** subgenital plate, dorsal view. Scale bars: 2 mm. Abbreviations: **a.a**. anterior arch, **bsv.** basivalvula, **cp.** crosspiece, **intc.s.** intercalary sclerite, **inst.f.** intersternal fold, **ltst.sh.** laterosternal shelf, **pp.** paraprocts, **pt.** paratergites, **sp.** spermatheca, **v.I** first valve, **v.II** second valve, **v.III** third valve.

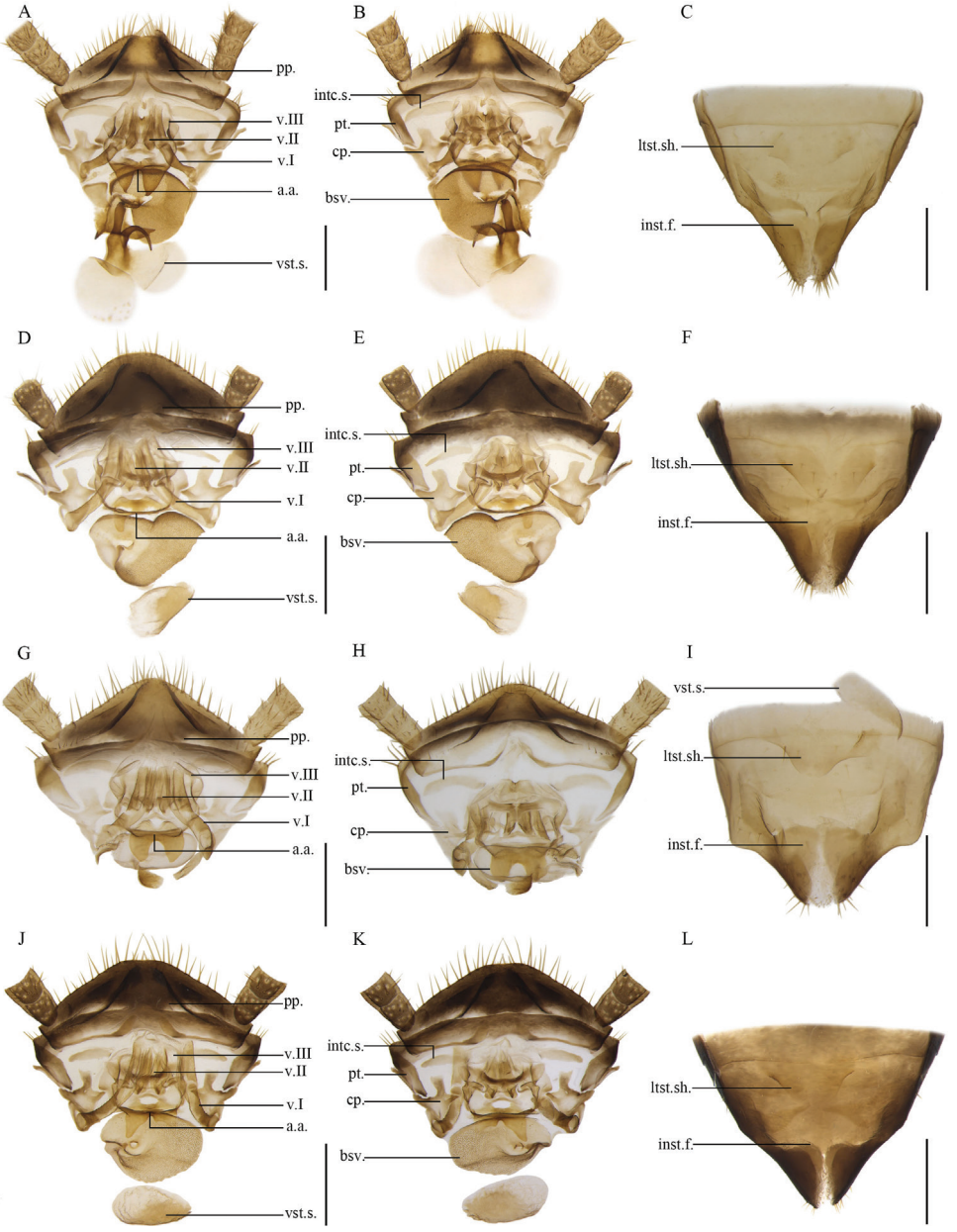

Figure 14. A–C *Anaplecta ungulata* Zhu & Che, sp. nov. paratype, female SWU-B-B-A060034 **D–F** *Anaplecta anomala* Zhu & Che, sp. nov. paratype, female SWU-B-B-A060068 **G-I** *Anaplecta bombycina* Zhu & Che, sp. nov. paratype, female SWU-B-B-A060078 **J-L** *Anaplecta strigata* Deng & Che, 2020. Female SWU-B-B-A060168 **A, D, G, J** supra-anal plate, ventral view **B, E, H, K** supra-anal plate, dorsal view **C, F, I, L** subgenital plate, dorsal view. Scale bars: 2 mm. Abbreviations: **a.a**. anterior arch, **bsv.** basivalvula, **cp.** crosspiece, **intc.s.** intercalary sclerite, **inst.f.** intersternal fold, **ltst. sh.** laterosternal shelf, **pp.** paraprocts, **pt.** paratergites, **v.I** first valve, **v.II** second valve, **v.III** third valve, **vst.s.** vestibular sclerite.

Chen leg.; SWU-B-B-A060168 to 060170 • 1 male; Hainan Prov., Linshui County, Mt. Diaoluo; 11 June 2020; Rong Chen, Li-Kang Liu, leg.; SWU-B-B-A060171.

Female genitalia. Supra-anal plate nearly symmetrical. Paraprocts broad, not extending to the posterior margin of supra-anal plate. Intercalary sclerite strip-shaped. First valve tubular, with scattered erect pubescence. Second valve small, basally fused. Third valve broad. The anterior margin of anterior arch slightly sclerotized, extending forward into two irregular protrusions. Basivalvula approximately triangular, most areas of the basivalvula with dense punctuations. Vestibular sclerite sheet-like, slightly curled (Fig. 14J, K). Laterosternal shelf broad, slightly sclerotized, lateral margin slightly curved (Fig. 14L).

Distribution. China (Hainan, Yunnan).

Anaplecta basalis Bey-Bienko, 1969

Figure 15D–F

Anaplecta basalis Bey-Bienko, 1969: 839; Deng et al., 2020: 101.

Material examined. China • 10 males and 7 females; Yunnan Prov., Mengla County, Menglun Town; 21°54.96'N, 101°14.53'E; 624 m; 27 April 2019; Zi-Long Bai, Zhi-Gang Chen leg.; SWU-B-B-A060172 to 060188 • 1 female, Yunnan Prov., Xishuangbanna, Ya'nuo Village; 21°59.70'N, 101°6.02'E; 1212 m; 14 July 2020; Du-Ting Jin, Yi-Shu Wang leg.; SWU-B-B-A060189 • 2 females; Yunnan Prov., Xishuangbanna, Guanping Village; 21°59.06'N, 101°64.40'E; 870 m; 14 July 2020; Rong Chen, Li-Kang Niu leg.; SWU-B-B-A060190 and 060191.

Female genitalia. Supra-anal plate nearly symmetrical. Paraprocts broad, extending to the posterior margin of supra-anal plate. Intercalary sclerite slender, long strip-shaped. First valve long. Second valve small, basally fused. Third valve broad. The anterior margin of anterior arch with two highly sclerotized strips (Fig. 15D, E). Basivalvula highly irregular, hind margin slightly curled, with sparse spines, both left and right sides with a brush-like structure (Fig. 15D), the area with punctuations nearly C-shaped (Fig. 15E). Vestibular sclerite irregular, hind margin with two long spines (Fig. 15D). Laterosternal shelf almost hyaline, lateral margin straight (Fig. 15F).

Distribution. China (Yunnan).

Anaplecta nigra Deng & Che, 2020

Figure 15G–I

Anaplecta nigra Deng & Che in Deng et al., 2020: 97–99.

Material examined. China • 1 male (holotype) and 1 female (paratype); Xizang Prov., Linzhi City, Motuo County; 29°12.98'N, 95°10.23'E; 1822 m; 16 July 2016; Jian-Yue Qiu, Hao Xu leg.; SWU-B-B-A060192 and 060193.

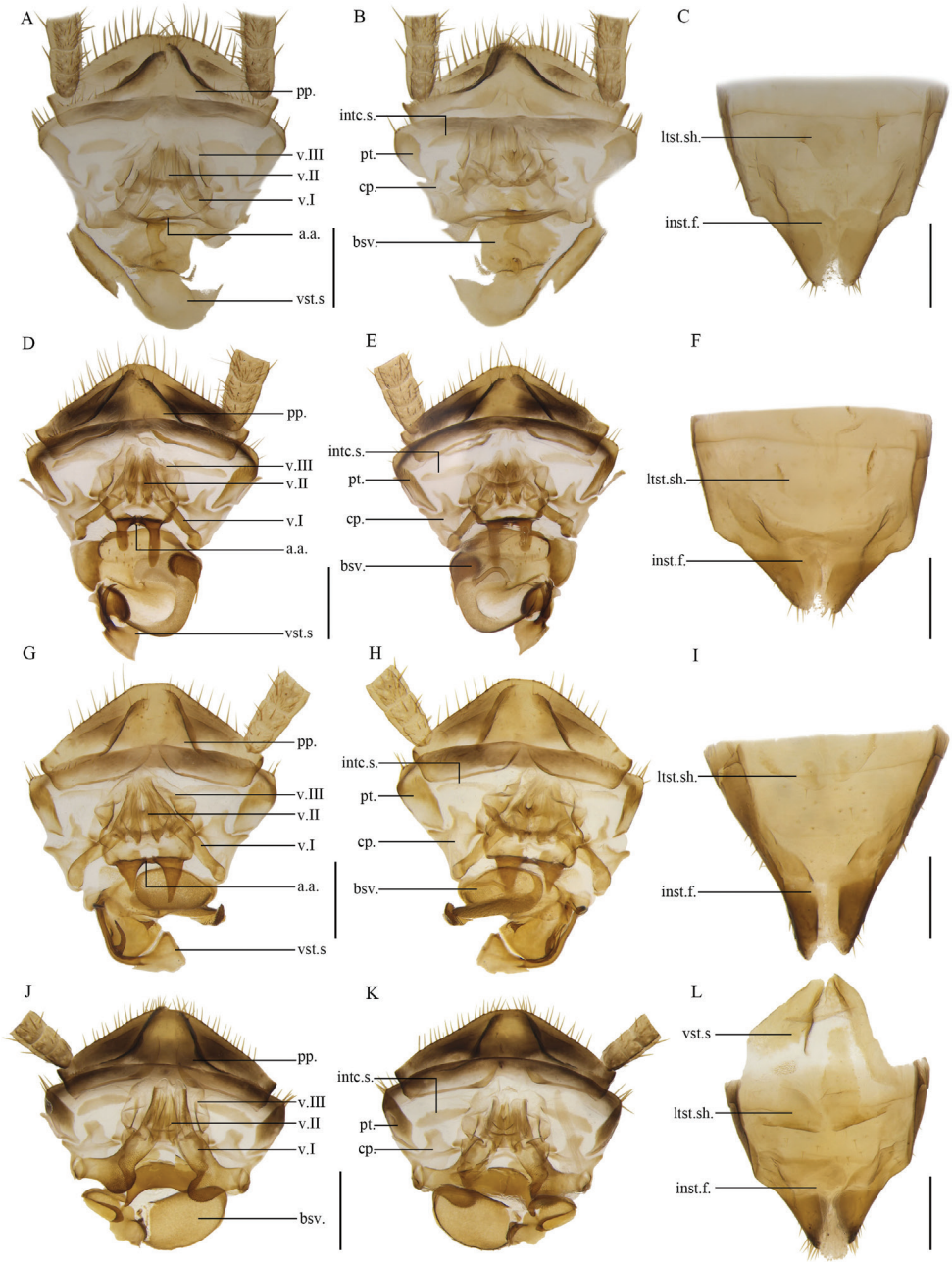

Figure 15. A–C *Anaplecta truncatula* Zhu & Che, sp. nov. paratype, female SWU-B-B-A060094 **D–F** *Anaplecta basalis* Bey-Bienko, 1969. Female SWU-B-B-A060182 **G–I** *Anaplecta nigra* Deng & Che, 2020. Paratype, female SWU-B-B-A060193 **J–L** *Anaplecta bicolor* Deng & Che, 2020. Paratype, female SWU-B-B-A060195 **A, D, G, J** supra-anal plate, ventral view **B, E, H, K** supra-anal plate, dorsal view **C, F, I, L** subgenital plate, dorsal view. Scale bars: 2 mm. Abbreviations: **a.a**. anterior arch, **bsv.** basivalvula, **cp.** crosspiece, **intc.s.** intercalary sclerite, **inst.f.** intersternal fold, **ltst.sh.** laterosternal shelf, **pp.** paraprocts, **pt.** paratergites, **v.I** first valve, **v.II** second valve, **v.III** third valve, **vst.s.** vestibular sclerite.

Female genitalia. Supra-anal plate nearly symmetrical. Paraprocts broad, not extending to the posterior margin of supra-anal plate. Intercalary sclerite slender. First valve long. Second valve small, basally fused. Third valve broad. The anterior margin of anterior arch slightly sclerotized, extending forward to form two elongated triangles protruding. Basivalvula irregular, curled, with dense punctuations. Vestibular sclerite irregular, hind margin with two long spines (Fig. 15G, H). Laterosternal shelf broad, slightly sclerotized, lateral margin straight (Fig. 15I).

Distribution. China (Xizang).

Anaplecta bicolor Deng & Che, 2020

Figure 15J–L

Anaplecta bicolor Deng & Che in Deng et al., 2020: 99–101.

Material examined. China • 1 male (holotype) and 1 female (paratype); Yunnan Prov., Xishuangbanna, Mengla County; 21°37.33'N, 101°35.28'E; 733 m; 23 May 2016, Lu Qiu, Zhi-Wei Qiu leg.; SWU-B-B-A060194 and 060195.

Female genitalia. Supra-anal plate nearly symmetrical. Paraprocts broad, extending to the posterior margin of supra-anal plate. Intercalary sclerite nearly strip-shaped, tapering to inside. First valve robust, finger-like protrusions on the inner edge with dense spines. Second valve small, basally fused. Third valve broad. The anterior margin of anterior arch protrudes forward in a flaky shape, slightly sclerotized, with an angular protrusion. Basivalvula highly irregular, most areas of the basivalvula with dense punctuations, the rest part curled (Fig. 15J, K). Vestibular sclerite sheet-like. Laterosternal shelf broad, slightly sclerotized, lateral margin straight (Fig. 15L).

Distribution. China (Yunnan).

Anaplecta omei Bey-Bienko, 1958

Figure 16J–L

Anaplecta omei Bey-Bienko, 1958: 591; Deng et al., 2020: 101.

Material examined. China • 2 males; Guangxi Prov., Guiping City; 31 May–2 June 2014; Shun-Hua Gui, Xin-Ran Li, Jian-Yue Qiu, leg.; SWU-B-B-A060196 and 060197 • 8 males and 12 females; Guizhou Prov., Tongren City, Mt. Fanjing; 27°70.28'N, 108°84.55'E; 13–14 June 2019; Shu-Ran Liao, Jia-Jun He leg.; SWU-B-B-A060198 to 060217 • 9 males and 3 females; Guizhou Prov., Guiyang City; 26°55.32'N, 106°76.47'E; 6 June 2019, Wen-Bo Deng, Lu-Qiu leg.; SWU-B-B-A060218 to 060229 • 11 males and 22 females; Sichuan Prov., Mt. Omei; 1–5 June 2013; Jin-Jin Wang, Yang Li leg.; SWU-B-B-A060230 to 060262 • 6 males; Guangdong Prov., Zhaoqing City, Mt. Qilin; 23°29.50'N, 109°59.56'E; 8 June 2019; Rong

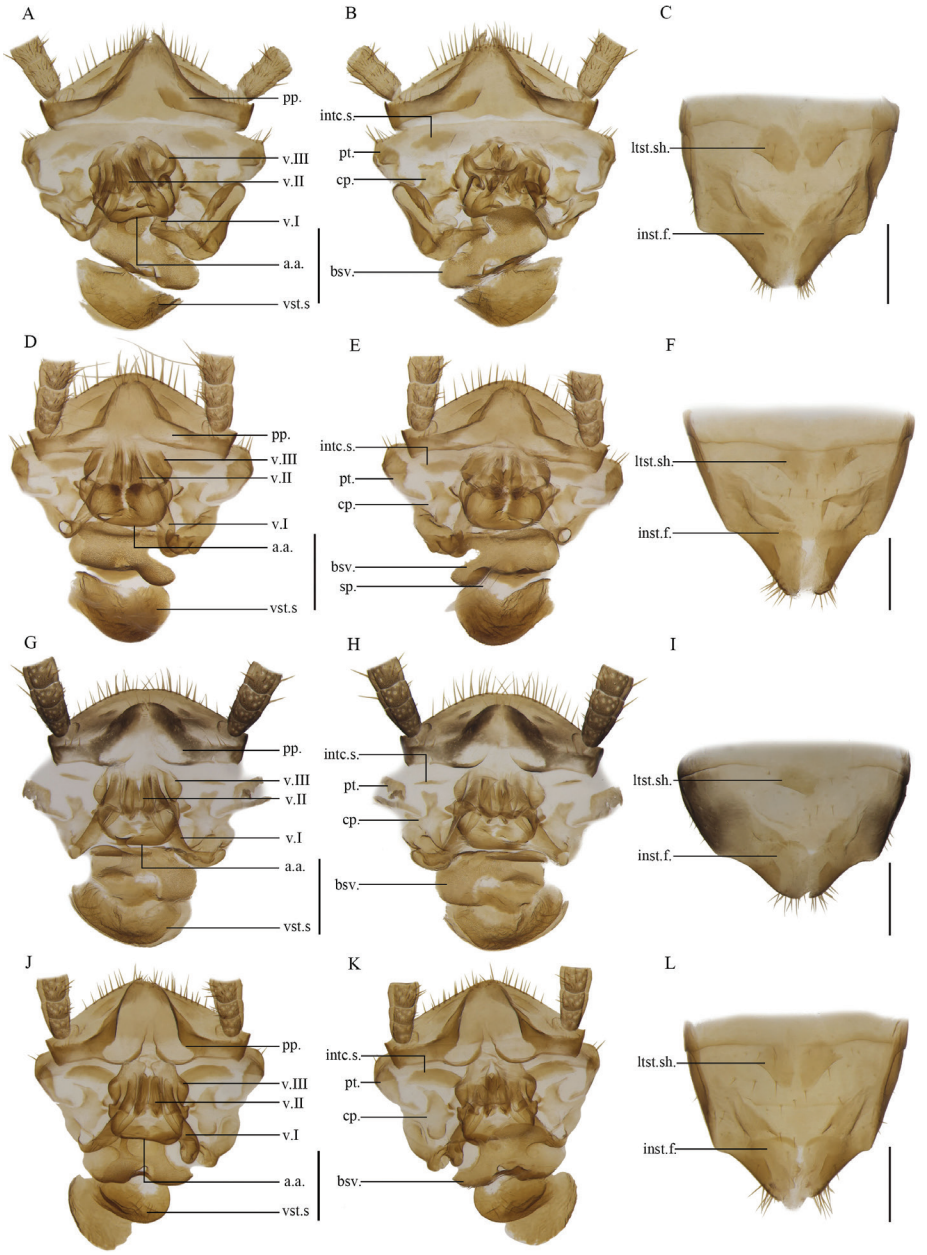

Figure 16. A–C *Anaplecta longihamata* Zhu & Che, sp. nov. paratype (ZWLS2), female SWU-B-B-A060099 **D–F** *Anaplecta paraomei* Zhu & Che, sp. nov. paratype (DS4_2), female SWU-B-B-A060117 **G–I** *Anaplecta condensa* Zhu & Che, sp. nov. paratype (GZ10), female SWU-B-B-A060125. **J–L** *Anaplecta omei* Bey-Bienko, 1958 (CQ5) female SWU-B-B-A060354 **A, D, G, J** supra-anal plate, ventral view **B, E, H, K** supra-anal plate, dorsal view **C, F, I, L** subgenital plate, dorsal view. Scale bars: 2 mm. Abbreviations: **a.a**. anterior arch, **bsv.** basivalvula, **cp.** crosspiece, **intc.s.** intercalary sclerite, **inst.f.** intersternal fold, **ltst.sh.** laterosternal shelf, **pp.** paraprocts, **pt.** paratergites, **v.I** first valve, **v.II** second valve, **v.III** third valve, **vlf.Ia** first valvifer arm, **vst.s.** vestibular sclerite.

Chen leg.; SWU-B-B-A060263 to 060268 • 3 males and 2 females; Hunan Prov., Mt. Mang; 11–12 July 2015; Zhi-Wei Qiu, Yong-Quan Zhao leg.; SWU-B-B-A060269 to 060273 • 31 males, 9 females; Chongqing City, Youyang County; 29°43.16'N, 109°28.37'E, 30 June 2019, Rong Chen, Hao Xu leg. SWU-B-B-A060274 to 060313 • 40 males, 31 females, Chongqing City, Beibei District; 2018–2019, laboratory staff, leg. SWU-B-B-A060314 to 060384 • 13 males and 1 female; Jiangxi Prov., Lushan City, Mt. Huanglong; 1–2 June 2017, Xin-Ran Li, Li-Li Wang, leg.; SWU-B-B-A060385 to 060398 • 1 male, Zhejiang Prov., Jiangshan City, Shuangxikou Village; 26–27 May 2017; Xin-Ran Li, Li-Li Wang, leg.; SWU-B-B-A060399.

Female genitalia. Supra-anal plate nearly symmetrical. Paraprocts broad, extending to the posterior margin of supra-anal plate. Intercalary sclerite short, nearly strip-shaped, slightly curved. One of first valvifer arm robust and curled. First valve robust. Second valve small, basally fused. Third valve broad. The anterior margin of anterior arch slightly curled, with a nearly transparent hook-shaped protrusion. Basivalvula broad, most areas with dense punctuations. Vestibular sclerite broad, slightly curled, sheet-like (Fig. 16J, K). Laterosternal shelf slightly sclerotized, lateral margin slightly curved (Fig. 16L).

Distribution. China (Anhui, Fujian, Jiangsu, Yunnan, Sichuan, Guizhou, Guangdong, Guangxi, Hunan, Chongqing, Zhejiang).

Anaplecta corneola Deng & Che, 2020

Figure 17A–C

Anaplecta corneola Deng & Che in Deng et al., 2020: 84–86.

Material examined. China • 20 males and 16 females; Hainan Prov., Ledong County, Mt. Jianfengling, Mingfeng Valley; 18°43.43'N, 108°48.45'E; 579 m; 21–28 May 2014; Shun-Hua Gui, Xin-Ran Li leg.; SWU-B-B-A060400 to 060435 • 14 males and 7 females; Hainan Prov., Ledong County, Mt. Jianfengling; 18°42.63'N, 108°52.75E; 940–960 m; 22–23 June 2020; Yong Li, Jing Zhu leg.; SWU-B-B-A060436 to 060456 • 1 male, Hainan Prov., Qiongzhong County, Mt. Limu; 19°110.59'N, 109°43.77'E; 650 m; 20 June 2020; Yong Li, Jing Zhu, leg.; SWU-B-B-A060457 • 1 female; Hainan Prov., Baisha County, Mt, Yinggeling; 19°04.79'N, 109°123.14'E; 352 m; 18 June 2020; Yong Li, Jing Zhu leg.; SWU-B-B-A060458.

Female genitalia. Supra-anal plate nearly symmetrical. Paraprocts broad, extending to the posterior margin of supra-anal plate. Intercalary sclerite nearly strip-shaped, tapering to sides. First valvifer arm short. First valve robust. Second valve small, basally fused. Third valve broad. The anterior margin of anterior arch slightly sclerotized, with a near cylindrical protrusion and dense tiny punctuations (Fig. 17A, B). Basivalvula irregular, the right part with dense punctuations, the left anterior margin extending posteriorly to crosspiece (Fig. 17A). Laterosternal shelf slightly sclerotized lateral margin straight (Fig. 17C).

Distribution. China (Fujian, Guangdong, Hainan, Hunan).

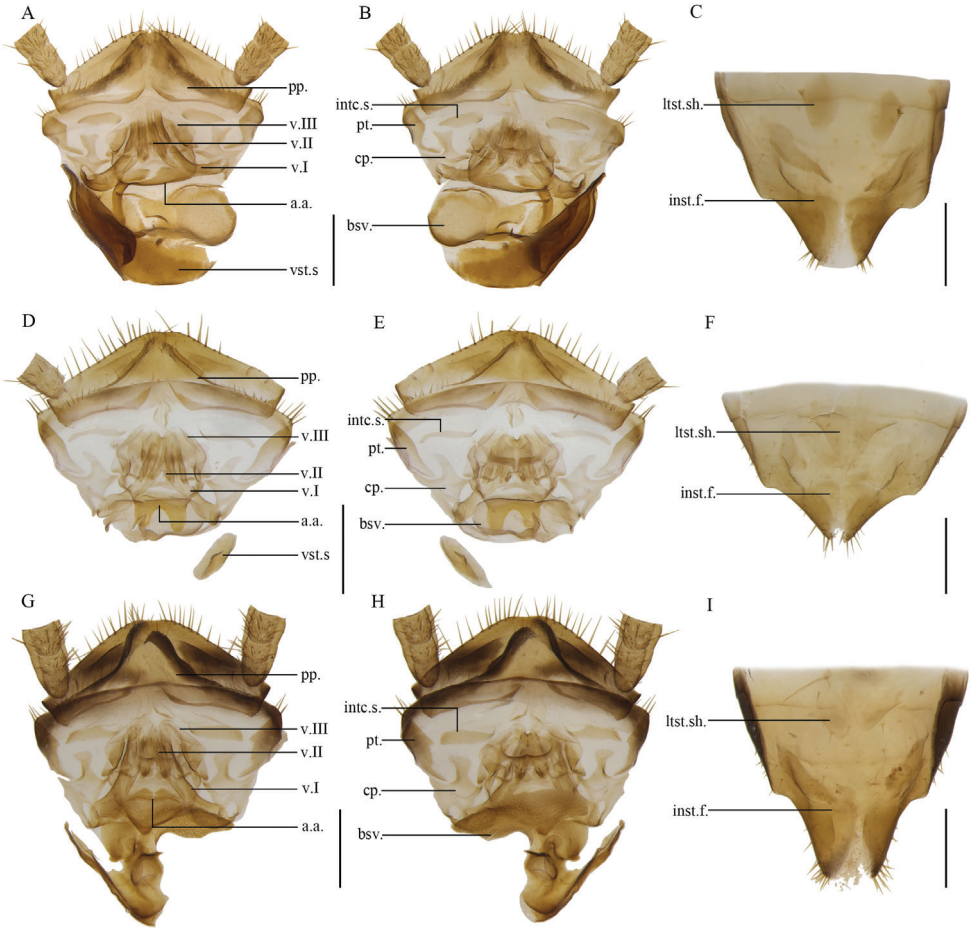

Figure 17. A–C *Anaplecta corneola* Deng & Che, 2020. Female SWU-B-B-A060450 **D–F** *Anaplecta arcuata* Deng & Che, 2020. Female SWU-B-B-A060460 **G–I** *Anaplecta staminiformis* Deng & Che, 2020. Paratype, female SWU-B-B-A060462 **A, D, G, J** supra-anal plate, ventral view **B, E, H, K** supra-anal plate, dorsal view **C, F, I, L** subgenital plate, dorsal view. Scale bars: 2 mm. Abbreviations: **a.a**. anterior arch, **bsv.** basivalvula, **cp.** crosspiece, **intc.s.** intercalary sclerite, **inst.f.** intersternal fold, **ltst.sh.** laterosternal shelf, **pp.** paraprocts, **pt.** paratergites, **v.I** first valve, **v.II** second valve, **v.III** third valve, **vst.s.** vestibular sclerite.

Anaplecta arcuata Deng & Che, 2020

Figure 17D–F

Anaplecta arcuata Deng & Che in Deng et al., 2020: 89–90.

Material examined. China • 1 male and 1 female; Hainan Prov.; Qiongzhong County, Mt. Limu; 19°110.59'N, 109°43.77'E; 650 m; 20 June 2020; Rong Chen, Li-Kang Niu, leg.; SWU-B-B-A060459 and 060460.

Male genitalia. On the basis of careful observation, we suspect that the L2d mentioned by Deng et al. (2020) may be the degraded right phallomere.

Female genitalia. Supra-anal plate nearly symmetrical. Paraprocts broad, not extending to the posterior margin of supra-anal plate. Intercalary sclerite slender. First valve robust. Second valve small, basally fused. Third valve broad. The anterior margin of anterior arch slightly sclerotized, extending forward in a flaky shape with a deep concave in the middle. Basivalvula nearly elliptic with dense punctuations. Vestibular sclerite sheet-like (Fig. 17D, E). Laterosternal shelf slightly sclerotized, lateral margin slightly curved (Fig. 17F).

Distribution. China (Hainan).

Anaplecta staminiformis Deng & Che, 2020

Figure 17G–I

Anaplecta staminiformis Deng & Che in Deng et al., 2020: 86–88.

Material examined. China • 1 male (holotype) and 1 female (paratype); Hainan Prov., Linshui County, Mt. Diaoluo; 18°28.50'N, 109°31.87'E; 423 m; 16 April 2015; Lu Qiu, Qi-Kun Bai leg.; SWU-B-B-A060461 and 060462 • 2 males (paratypes) and 4 females (paratypes); Hainan Prov., Ledong County, Mt. Jianfengling, Mingfeng Valley; 18°25.95'N, 108°28.96'E; 579 m; 18 May 2014; Shun-Hua Gui, Xin-Ran Li leg.; SWU-B-B-A060463 to 060468.

Female genitalia. Supra-anal plate nearly symmetrical. Paraprocts broad, not extending to the posterior margin of supra-anal plate. Intercalary sclerite nearly strip-shaped, tapering to insides. First valve robust. Second valve small, basally fused. Third valve broad. The anterior margin of anterior arch slightly sclerotized, extending forward in a heart shape, with a nodular protrusion at apex (Fig. 17G, H). Basivalvula irregular, the left anterior margin extending posteriorly to first valvifer arm, deep depression in the center, posterior margin broad with dense punctuations (Fig. 17G). Laterosternal shelf slightly sclerotized, lateral margin slightly curved (Fig. 17I).

Distribution. China (Hainan).

Anaplecta furcata Deng & Che, 2020

Anaplecta furcata Deng & Che in Deng et al., 2020: 93–95.

Material examined. China • 2 males (paratypes); Guangxi Prov., Jinxiu County, Mt Dayao; 24°8.43'N, 110°11.70'E; 944 m; 7 July 2015; Lu Qiu, Qi-Kun Bai leg.; SWU-B-B-A060469 and 060470

Distribution. China (Guangxi).

Discussion

In recent years, male genitalia were the main characteristics in the species delimitation of *Anaplecta* (Lucañas, 2016; Deng et al. 2020) but DNA barcodes can also help to delimit and distinguish species (Deng et al. 2020). During examination of samples of *Anaplecta omei*, we found some subtle morphological differences between samples collected in Libo, Dushan, Mt. Wuliang, and other regions. This included color, paraprocts, subgenital plates, and phallomeres. Although these specimens were recovered as four MOTUs in ABGD, these subtle differences in morphology were insufficient to determine whether they reflect intraspecific variation or interspecific differences. Therefore, we turned to the female genitalia for more evidence. Surprisingly, we found the shapes of first valvifer arm, intercalary sclerite, anterior arch, and basivalvula were stable within these four MOTUs and differed between MOTUs. Khalifa (1950) mentioned that when a pair of *Blattella germanica* mated, the hooked left phallomere (L3) extended and secured the first valve allowing the male to physically attach to the female during copulation. Therefore, we hypothesize that the long and robust hook of male genitalia of SP4 is to match the robust first valvifer arm of its female. Graves (1969) speculated that when transferring the spermatophore, the soft outer layer of the spermatophore hardens and would be against the female genital sclerites in order to ensure the openings of the sperm sacs aligned directly with the female spermathecal opening. Thus, we infer that the anterior arch and basivalvula might be related to this process of transferring the spermatophore. Taking all this evidence together, we can consider these MOTUs as different species: *A. longihamata* sp. nov., *A. paraomei* sp. nov., and *A. condensa* sp. nov. Similarly, we also found significant differences in other species in the anterior arch and basivalvula, indicating that the variation in female genitalia can be applied to identify the species of *Anaplecta*. However, this has often been neglected in the past study of *Anaplecta*, with the exception of McKittrick (1964), who described the female genitalia in detail. Only the valvular subgenital plate was involved in other studies (Roth, 1990; Deng et al. 2020). In our study, the characteristics of the female genitalia played an important role in detecting these three cryptic species; hence, researchers should pay more attention to female genitalia in future studies.

Acknowledgements

We thank all the collectors mentioned in this article for their efforts in specimen collection. We thank Prof. John Richard Schrock (Department of Biological Sciences, Emporia State University) for proofreading the final draft. We are also very grateful to Dr. Fred Legendre and Leonid Anisyutkin for their help in improving this manuscript. This study is supported by the National Natural Science Foundation of China (No. 31772506, 32070468, 32170458), the Program of the Ministry of Science and Technology of the People's Republic of China (2015FY210300) and GDAS Special Project of Science and Technology Development (No. 2020GDASYL-20200102021, 2020GDASYL-20200301003).

References

Aldrich BT, Zolnerowich G, Kambhampati S (2004) Interspecific morphological variation in the wood-feeding cockroach, *Cryptocercus* (Dictyoptera: Cryptocercidae). Arthropod Structure & Development 33(4): 443–451. https://doi.org/10.1016/j.asd.2004.06.005

Anisyutkin LN (2013) A description of a new species of the cockroach genus *Prosoplecta* saussure, 1864 (Dictyoptera, Ectobiidae) from South Vietnam. Entomological Review 93(2): 182–193. https://doi.org/10.1134/S0013873813020061

Anisyutkin LN (2014) On cockroaches of the subfamily Epilamprinae (Dictyoptera: Blaberidae) from South India and Sri Lanka, with descriptions of new taxa. Zootaxa 3847(3): e301. https://doi.org/10.11646/zootaxa.3847.3.1

Anisyutkin LN (2016) New data on the subfamily Epilamprinae (Dictyoptera, Blaberidae) of the New World, with description of a new genus and a new species from Ecuador. Entomological Review 96(2): 199–217. https://doi.org/10.1134/s001387381602001x

Asahina S (1977) Taxonomic notes on Japanese Blattaria VIII.The Anaplectidae of Japan and Taiwan. Japanese Journal of Sanitary Zoology 28(3): 272–280. https://doi.org/10.7601/mez.28.272

Bai QK, Wang LL, Wang ZQ, Lo N, Che YL (2018) Exploring the diversity of Asian *Cryptocercus* (Blattodea: Cryptocercidae): species delimitation based on chromosome numbers, morphology and molecular analysis. Invertebrate Systematics 32(1): 69–91. https://doi.org/10.1071/IS17003

Beccaloni GW (2014) Cockroach Species File Online. Version 5.0/5.0. http://cockroach.speciesfile.org/ [accessed 22 September 2021]

Bey-Bienko GY (1958) Results of the Chinese-Soviet Zoological-Botanical Expeditions of 1955–56 to southwestern China. Blattoidea of Szechuan and Yunnan II: 582–597.

Bey-Bienko GY (1969) New genera and species of cockroaches (Blattoptera) from tropical and subtropical Asia. Entomologica Obozrenie 48: 831–862.

Bohn H, Picker M, Klass KD, Colville JF (2010) A Jumping Cockroach from South Africa, *Saltoblattella montistabularis*, gen. nov. spec. nov (Blattodea: Blattellidae). Arthropod Systematics & Phylogeny 68(1): 53–69.

Bourguignon T, Tang Q, Ho SYW, Juna F, Wang ZQ, Arab DA, Cameron SL, Walker J, Rentz D, Evans TA, Lo N (2018) Transoceanic dispersal and plate tectonics shaped global cockroach distributions: Evidence from mitochondrial phylogenomics. Molecular Biology and Evolution 35(4): 970–983. https://doi.org/10.1093/molbev/msy013

Bruijning CFA (1948) Studies on Malayan Blattidae. Zoologische Mededelingen 29: 1–174.

Burmeister H (1838) Handbuch der Entomologie. Reimer II (2): 397–756.

Deng WB, Liu YC, Wang ZQ, Che YL (2020) Eight new species of the genus *Anaplecta* Burmeister, 1838 (Blattodea: Blattoidea: Anaplectidae) from China based on molecular and morphological data. European Journal of Taxonomy 720: 77–106. https://doi.org/10.5852/ejt.2020.720.1117

Deng WB (2020) Species Delimitation of Anaplectidae and Molecular Phylogeny of Blattoidea. Masters Dissertation. Southwest University, Chongqing, China.

Djernæs M (2018) Biodiversity of Blattodea-the cockroaches and termites. Insect Biodiversity: Science and Society: 359–378. https://doi.org/10.1002/9781118945582.ch14

Djernaes M, Klass KD, Eggleton P (2015) Identifying possible sister groups of Cryptocercidae+Isoptera: a combined molecular and morphological phylogeny of Dictyoptera. Molecular Phylogenetics and Evolution 84: 284–303. https://doi.org/10.1016/j.ympev.2014.08.019

Grandcolas P, Nattier R, Pellens R, Legendre F (2014) Diversity and distribution of the genus *Rothisilpha* (Dictyoptera, Blattidae) in New Caledonia: Evidence from new microendemic species. In: Guilbert É, Robillard T, Jourdan H, Grandcolas P (Eds), Zoologia Neocaledonica 8. Biodiversity studies in New Caledonia. Muséum national d'Histoire naturelle, Paris, 299–308. https://doi.org/10.1371/journal.pone.0080811

Graves PN (1969) Spermatophores of the Blattaria. Annals of the Entomological Society of America 62: 595–602. https://doi.org/10.1093/aesa/62.3.595

Hebard M (1924) Studies in the Dermaptera and Orthoptera of Ecuador. Proceedings of the Academy of Natural Sciences of Philadelphia 76: 109–248.

Khalifa A (1950) Spermatophore formation in *Blattella germanica*. Proceedings of the Royal Society of London A 25: 53–61. https://doi.org/10.1111/j.1365-3032.1950.tb00092.x

Kimura M (1980) A simple method for estimating evolutionary rates of base substitutions through comparative studies of nucleotide sequences. Journal of Molecular Evolution 16: 111–120.

Lanfear R, Frandsen PB, Wright AM, Senfeld T, Calcott B (2017) PartitionFinder 2: new methods for selecting partitioned models of evolution for molecular and morphological phylogenetic analyses. Molecular Biology and Evolution 34: 772–773. https://doi.org/10.1093/molbev/msw260

Li XR, Zheng YH, Wang CC, Wang ZQ (2018) Old method not old-fashioned: parallelism between wing venation and wing-pad tracheation of cockroaches and a revision of terminology. Zoomorphology 137(4): 519–533. https://doi.org/10.1007/s00435-018-0419-6

Lucañas CC (2016) First Philippine record of the cockroach genus *Anaplecta* Burmeister 1838 (Blattodea: Ectobiidae: Anaplectinae) with the description of a new species from Mt. Makiling. Laguna. Philipp Entremont 30(1): 11–16.

McKittrick FA (1964) Evolutionary studies of cockroaches. Cornell University Agricultural Experiment Station Memoir 389: 1–197.

Nguyen LT, Schmidt HA, von Haeseler A, Minh BQ (2015) IQ-TREE: a fast and effective stochastic algorithm for estimating maximum-likelihood phylogenies. Molecular Biology and Evolution 32(1): 268–274. https://doi.org/10.1093/molbev/msu300

Puillandre N, Lambert A, Brouillet S, Achaz G (2012) ABGD, Automatic Barcode Gap Discovery for primary species delimitation. Molecular Ecology 21(8): 1864–1877. https://doi.org/10.1111/j.1365-294X.2011.05239.x

Rehn, JAG (1916) Brazilian Orthoptera. Transactions of the American Entomological Society 42: 222–306.

Roth LM (1990) Revisionary studies on Blattellidae (Blattaria) from the Indo-Australian region. Memoirs of the Queensland Museum 28: 597–663.

Roth LM (1996) The cockroach genera *Anaplecta*, *Anaplectella*, *Anaplectoidea*, and *Malaccina* Blattaria, Blattellidae: Anaplectinae and Blattellinae). Oriental Insects 30(1): 301–372. https://doi.org/10.1080/00305316.1996.10434105

Shelford R (1906) Studies of the Blattidae. Remarks on the sub-families Ectobiinae and Phyllodromiinae. Transactions of the Entomological Society of London 54(2): 231–278. https://doi.org/10.1111/j.1365-2311.1906.tb02474.x

Wang CC, Wang ZQ, Che YL (2016) *Protagonista lugubris*, a cockroach species new to China and its contribution to the revision of genus *Protagonista*, with notes on the taxonomy of Archiblattinae (Blattodea, Blattidae). ZooKeys 574: 57–73. https://doi.org/10.3897/zookeys.574.7111

Wang ZQ, Li Y, Che YL, Wang JJ (2015) The wood-feeding genus *Cryptocercus* (Blattodea: Cryptocercidae), with description of two new species based on female genitalia. Florida Entomologist 98(1): 260–271. http://dx.doi.org/10.1653/024.098.0143

Wang ZQ, Shi Y, Qiu ZW, Che YL, Lo N (2017) Reconstructing the phylogeny of Blattodea: robust support for interfamilial relationships and major clades. Scientific Reports 7(1): 3903. https://doi.org/10.1038/s41598-017-04243-1

Supplementary material 1

Table S1. Pairwise genetic divergence of distances

Authors: Jing Zhu

Data type: genetic distances

Explanation note: Pairwise genetic divergence of distances calculated by K2P model method using cytochrome oxidase subunit I (COI) gene sequences in MEGA.

Link: https://doi.org/10.3897/zookeys.1080.74286.suppl1

ZooKeys 1080: 99–106 (2022)
doi: 10.3897/zookeys.1080.73194
https://zookeys.pensoft.net

SHORT COMMUNICATION

A peer-reviewed open-access journal
ZooKeys
Launched to accelerate biodiversity research

Genital anatomy, jaw and radula of *Guladentia subtussulcata* (Helicoidea, Cepolidae), endemic to western Cuba

Maike Hernández[1], Manuel A. Bauzá[1], Thierry Backeljau[2,3]

1 *Institute of Ecology and Systematics, Carretera Varona Km 3 1/5, Capdevila, Havana, Cuba* **2** *Royal Belgian Institute of Natural Sciences (RBINS), Vautierstraat 29, B-1000 Brussels, Belgium* **3** *Evolutionary Ecology Group, University of Antwerp, Universiteitsplein 1, B-2610 Antwerp, Belgium*

Corresponding author: Maike Hernández (maike.hernandez@gmail.com)

Academic editor: E. Gittenberger | Received 18 August 2021 | Accepted 3 November 2021 | Published 4 January 2022

http://zoobank.org/A14875D6-D9F9-4663-BD3F-40581D41A734

Citation: Hernández M, Bauzá MA, Backeljau T (2022) Genital anatomy, jaw and radula of *Guladentia subtussulcata* (Helicoidea, Cepolidae), endemic to western Cuba. ZooKeys 1080: 99–106. https://doi.org/10.3897/zookeys.1080.73194

Abstract

This study provides the first data on the genital anatomy, jaw and radula of *Guladentia subtussulcata* (L. Pfeiffer, 1863). The auxiliary copulatory organ of this species is very peculiar, similar to that of *Jeanneretia* L. Pfeiffer, 1877, and different from that of other cepolids. It consists of an elongate, pedunculate mucus gland inserted apically on a muscular papilla and an atrial sac, all covered by a sheath. A sheath-like accessory gland is inserted at the base of the atrial sac. Another similarity with *Jeanneretia* is the presence of a fertilization pouch-spermatheca complex with a single exposed spermatheca. Like *Jeanneretia*, *G. subtussulcata* has an oxygnath, highly arched jaw with slight striae over the entire surface and a broad, well-developed median projection. The radula has triangular and monocuspid central and lateral teeth (the central teeth are smaller than the rest). The marginal teeth are multicuspid with the mesocone and ectocones smaller than the endocones. The similar structures of the auxiliary copulatory organ (without dart sac) and spermatheca (simple) strongly suggest that *G. subtussulcata* and *Jeanneretia* spp. are closely related. As such, it remains to be decided whether *Guladentia* Clench & Aguayo, 1951 and *Jeanneretia* should continue to be treated as separate genera.

Keywords

Auxiliary copulatory organ, reproductive system, sheath-like accessory gland, Stylommatophora, West Indies

Introduction

Guladentia Clench & Aguayo, 1951, is a Cuban endemic terrestrial snail genus of the family Cepolidae. It was originally described as subgenus of *Jeanneretia* L. Pfeiffer, 1877 (Clench and Aguayo 1951) with *Helix subtussulcata* L. Pfeiffer, 1863 as type species and comprising three other species, viz. *Cepolis torrei* Clench & Aguayo, 1933, *Jeanneretia* (*Guladentia*) *modica* Clench & Aguayo, 1951 and *J.* (*G.*) *gundlachi* Clench & Aguayo, 1951. While *Guladentia* was explicitly maintained as a subgenus by Espinosa and Ortea (1999, 2009) and implicitly by Fontenla et al. (2013), it was considered as a separate genus by Zilch (1960), Schileyko (2004) and Hernández et al. (2017), though without providing a rationale. As such, *Guladentia* differs conchologically from *Jeanneretia* by (1) possessing a shell with a well-defined "gular" fold, which is an invagination of the shell on the base of the body whorl, curved and parallel with the whorl about midway between the whorl periphery and the columella, and by (2) having a long and curved tooth on the base of the shell within the aperture. Thus, according to Clench and Aguayo (1951) the shell structure of *Guladentia* would resemble that of the genus *Cepolis* Montfort, 1810 (Fig. 1).

Species of *Guladentia* occur in mountainous limestone areas in the central-western region of the Sierra de los Órganos, Cuba. They are quite rare (Clench and Aguayo 1951), yet, *G. subtussulcata* is the species with the widest distribution and that is the least difficult to collect. It is also the largest species in the genus (shell height: 16–31 mm; shell diameter: 21–31 mm).

Hernández et al. (2020) emphasized that the genital anatomy of a majority of Cepolidae taxa, including the genus *Guladentia*, is still unknown. The present contribution, therefore, aims to provide the very first data on the genital anatomy, jaw, and radula of the type species of this genus, viz. *G. subtussulcata*, and on the basis of these new data it also briefly reflects on the (sub)generic status of *Guladentia*.

Materials and methods

Nine live specimens of *G. subtussulcata* were collected from three localities in Viñales, Pinar del Río Province, Cuba. The material examined is deposited in the Malacological Collection of the Institute of Ecology and Systematics (CZACC; Colección Zoológica de la Academia de Ciencias de Cuba).

Material examined • 7 specimens; Mogote El Valle; 22°37'9.3"N, 83°41'33.09"W; 20 May 2014; M. Hernández Leg.; CZACC8. A.0300 to 0307 • 1 specimen; Mogote Dos Hermanas; 22°37'05"N, 83°44'38"W; 5 July 2014; M. Hernández Leg.; CZACC8. A.0308 • 1 specimen; Sierra de Viñales; 22°38'36"N, 83°44'46"W; 6 July 2014; M. Hernández Leg.; CZACC8. A.0309.

Specimens were drowned for 12 h in an airtight jar filled with water, after which they were removed from their shells and fixed in 70% ethanol. Specimens were dissected using a Carl Zeiss Stemi 2000 stereomicroscope. The reproductive tracts were

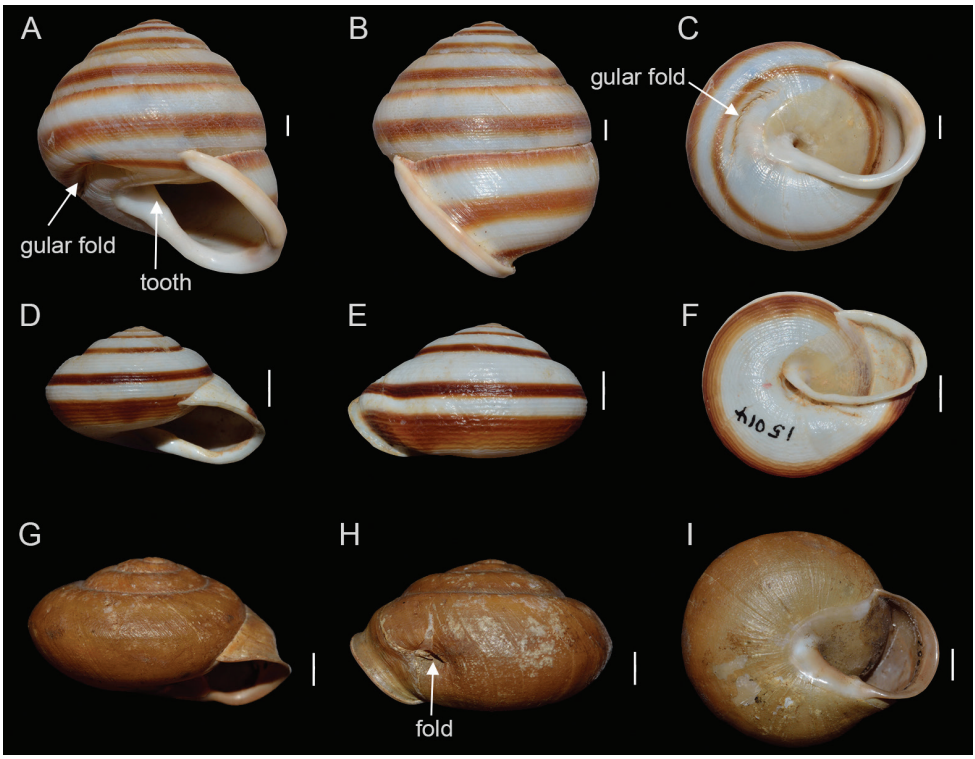

Figure 1. Shells of *Guladentia subtussulcata* **A–C** (**A** and **B** lateral views and **C** ventral view), *Jeanneretia parraiana* **D–F** (**D** and **E** lateral views and **F** ventral view), *Cepolis cepa* **G–I** (**G** and **H** lateral views and **I** ventral view). Scale bar = 5 mm.

photographed with a Nikon 5100 camera. Radula and jaw were extracted manually, cleaned by soaking in 10% KOH solution for about 6 h followed by rinsing in ethanol. They were mounted for scanning electron microscopy with a Thermo Fisher Quanta 200 scanning electron microscope.

The terminology of the reproductive apparatus follows Baur (2010) and Hernández et al. (2020). The length of seven genital structures was measured using scale paper (error 1 mm): flagellum, penis + distal epiphallus, proximal epiphallus, bursa-copulatrix duct, auxiliary copulatory organ, and length of the spermoviduct.

Results

Genital anatomy

The complete genitalia is shown in Fig 2A. The fertilization pouch–spermathecal complex comprises a fertilization pouch embedded in the albumen gland and a single, exposed spermatheca (Fig. 2D). Spermoviduct very long (mean length: 57 mm; range: 42–79 mm), in length followed by the bursa-copulatrix duct (mean length: 46 mm; range:

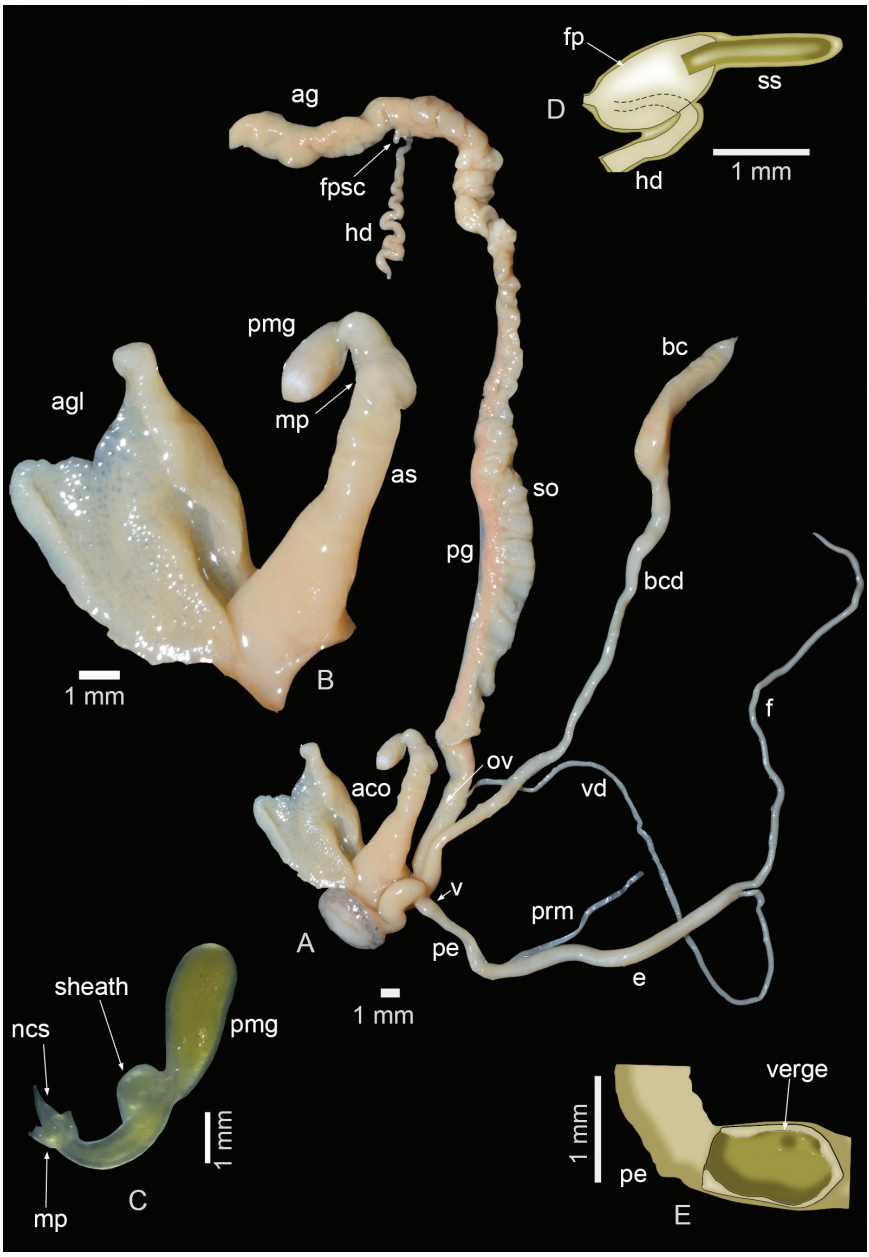

Figure 2. Genital anatomy of *Guladentia subtussulcata* **A** genitalia **B** auxiliary copulatory organ details) **C** details of the distal portion of the auxiliary copulatory organ **D** drawing of the fertilization pouch–spermathecal complex **E** drawing of the details of the verge. Abbreviations: aco = auxiliary copulatory organ, ag = albumen gland, agl = accessory gland, as = atrial sac, bc = bursa copulatrix, bcd = bursa-copulatrix duct, e = proximal epiphallus, fl = flagellum, fp = fertilization pouch, fpsc = fertilization pouch–spermathecal complex, hd = hermaphroditic duct, mp = muscular papilla, ncs = non-calcareous structure, pe = penis + distal epiphallus, ov = oviduct, pmg = pedunculated mucus gland, pg = prostatic gland, prm = penial retractor muscle, so = spermoviduct, ss = single spermatheca, v = verge, vd = vas deferens.

23–78 mm) and the flagellum (mean length: 39 mm; range: 23–65 mm). Vagina short. The penis + distal epiphallus of medium length (mean length: 8 mm; range: 5–14 mm), thin and cylindrical, internally with a verge located in the first third, which may be swollen and somewhat wrinkled (Fig. 2E). Proximal epiphallus (mean length; 15 mm; range: 7–26 mm) is longer than the penis + distal epiphallus. The auxiliary copulatory organ (mean length: 17 mm; range: 11–20 mm) (Fig. 2B, C) is soft and has no dart sac. It consists of an elongate, pedunculated mucus gland inserted apically on a muscular papilla (Fig. 2C) and an atrial sac (Fig. 2B), all covered by a sheath. One sheath-like accessory gland (consisting of alveoli) is inserted at the base of the atrial sac (Fig. 2B).

Jaw and radular morphology

The jaw is oxygnath (Fig. 3A), solid, high arched, almost smooth except for slight striae all over the surface, and with a wide, well-developed, median projection. The radula has a monocuspid, pointed and triangular central tooth, which is smaller than the other teeth and shorter than the base of the tooth (Fig. 3B). Lateral teeth monocuspid, pointed, triangular and as long as their base (Fig. 3B). Between the lateral and marginal teeth, there are transitional teeth with ectocones. Marginal teeth multicuspid with the mesocone and ectocones smaller than the endocones (Fig. 3C).

Discussion

The reproductive system of *Guladentia subtussulcata* is similar to that of other cepolid species by, amongst other features, the presence of an auxiliary copulatory organ. Yet, while in other cepolids this auxiliary copulatory organ contains a dart sac (on top of the muscular papilla), there is no dart sac in *G. subtussulcata* (Fig. 2B) and *Jeanneretia* ssp. (Hernández et al. 2021). Instead, these latter two taxa have a non-calcareous 'dart' (Fig. 2C), which is fused to a muscular papilla that opens directly into the atrial sac. More generally, the auxiliary copulatory organ of *G. subtussulcata* is similar in size and structure to that of *Jeanneretia* spp. as described by Hernández et al. (2021). In this sense it represents a unique feature within Cepolidae. Also, the simple spermatheca of *G. subtussulcata* is a unique feature within Cepolidae that links this species with *Jeanneretia* spp.

Conversely, *G. subtussulcata* and *Jeanneretia* ssp. differ markedly by their accessory glands: *G. subtussulcata* has a single sheath-like accessory gland (Fig. 2B), a unique feature within Cepolidae, whereas *Jeanneretia* ssp. have a pair of tubular accessory glands. Furthermore, compared to the data provided for *Jeanneretia* spp. by Hernández et al. (2021), *G. subtussulcata* has a much longer spermoviduct, but a much shorter flagellum, than *Jeanneretia* spp.

The jaw and radula of *G. subtussulcata* are extremely arched (Fig. 3A) like in *Jeanneretia* ssp. (Hernández et al. 2021), though the radular teeth of *G. subtussulcata* are a little more pointed than in *Jeanneretia* spp. In general, the radular morphology of *G. subtussulcata* complies with that of other cepolid genera, except *Polymita* Beck, 1937

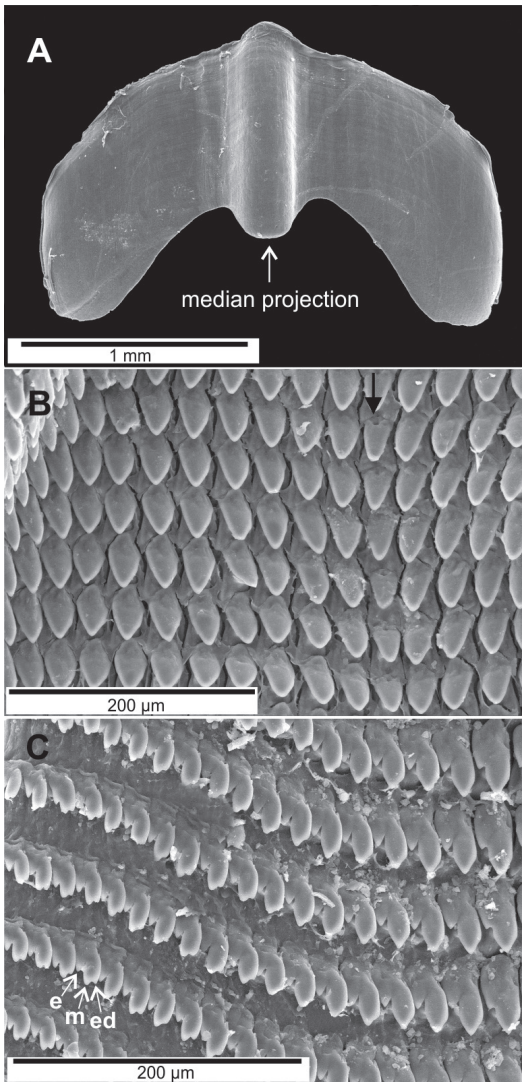

Figure 3. Scanning Electron Microscope photographs of the jaw and radula of *Guladentia subtussulcata*. **A** jaw **B** central and lateral teeth, central teeth marked with a black arrow **C** transitional and marginal teeth, the latter with their ectocones (e), mesocones (m), and endocones (ed).

(Moreno 1950), in which the radula is arranged in a "v" shape with all teeth equal in size (Hernández et al. 2021).

The structure of the auxiliary copulatory organ (without dart sac) and the spermatheca (simple) strongly suggests that *G. subtussulcata* and *Jeanneretia* spp. are closely related. Hence, the question arises whether *Guladentia* should be regarded as a separate genus or as a subgenus of *Jeanneretia*. The conchological differences between *G. subtussulcata* and *Jeanneretia* spp. may indicate a separation at the genus

level, with the gular shell fold (Fig. 1A) and the unique accessory gland structure (Fig. 2B) of *Guladentia* as the defining features of the genus. However, the genital anatomy of more *Guladentia* species should be studied and combined with DNA sequence data to infer the phylogenetic relationships of *Guladentia* and *Jeanneretia*. These additional data are not only necessary to verify whether these two taxa are monophyletic, but also to explore whether the conchological similarities between *Guladentia* and *Cepolis* suggested by Clench and Aguayo (1951) are synapomorphic or homoplasic character states.

Acknowledgements

We thank the Global Taxonomy Initiative of the CEBioS programme at RBINS, financed by the Belgian cooperation for development, for giving MHQ the opportunity to visit the malacology lab of RBINS. We thank the Oficina de Regulación y Seguridad Ambiental for access to protected areas and permission to collect. We are indebted to two anonymous reviewers for their constructive comments on the manuscript.

References

Baker HB (1943) Some Antillean Helicids. The Nautilus 56(3): 81–91.

Baur B (2010) Stylommatophoran Gastropods. In: Leonard JL, Córdoba-Aguilar A (Eds) The evolution of primary sexual characters in animals. Oxford: University Press, 197–217.

Clench WJ, Aguayo C (1951) The Cuban genus *Jeanneretia*. Revista de la Sociedad Malacológica "Carlos de la Torre" 7(3): 83–90.

Espinosa J, Ortea J (1999) Moluscos terrestres del archipiélago cubano. Avicennia, Supplemento 2: 1–137.

Espinosa J, Ortea J (2009) Moluscos terrestres de Cuba. UCP Print, Finland, 191 pp.

Fontenla JL, Espinosa J, Maceira D, Hernández M (2013) Biogeografía histórica de los géneros endémicos de moluscos terrestres de Cuba. Determinación y relaciones entre sistemas biogeográficos. Revista de la Academia Canaria de Ciencias 25: 141–162.

Hernández M, Backeljau T, Bauzá MA (2021) First data on the genital morphology, the jaw and the radula of the species of the genus *Jeanneretia* (Helicoidea: Cepolidae), endemic to western Cuba. Archiv für Molluskenkunde 150: 13–29. https://doi.org/10.1127/arch.moll/150/013-029

Hernández M, Bauzá MA, Franke S, Fernández-Velázquez A (2020) A new genus and species of cepolid from Cuba (Pulmonata, Helicoidea). Ruthenica 30: 155–164. https://doi.org/10.35885/ruthenica.2021.30(3).3

Hernández M, Alvarez-Lajonchere L, Martínez D, Maceira D, Fernández-Velázquez A, Espinosa J (2017) Moluscos terrestres y dulceacuícolas. In: Mancina CA, Cruz D (Eds) Diversidad biológica de Cuba: métodos de inventario, monitoreo y colecciones biológicas. Editorial AMA, La Habana, 164–191.

Ihering H von (1909) System und Verbreitung der Heliciden. Verhandlungen der kaiserlich-königlichen zoologisch-botanischen Gesellschaft in Wien 59: 420–455.

Moreno BMA (1950) Estudio anatómico del género *Polymita* Beck. Memorias de la Sociedad Cubana de Historia Natural 20(1): 21–35.

Nordsieck H (1987) Revision des Systems der Helicoidea (Gastropoda: Stylommatophora). Archiv für Molluskenkunde 118: 9–50.

Nordsieck H (2017) Pulmonata, Stylommatophora, Helicoidea: Systematics with comments. ConchBooks, Harxheim, Germany, 98 pp.

Pilsbry HA (1939) Land Mollusca of North America (North of Mexico). The Academy of Natural Sciences of Philadelphia, Monograph 1(3): 1–573.

Schileyko AA (2004) Treatise on recent terrestrial pulmonate molluscs. Part 12. Bradybaenidae, Monadeniidae, Xanthonychidae, Epiphragmophoridae, Helminthoglyptidae, Elonidae, Humboldtianidae, Sphincterochilidae, Cochlicellidae. Ruthenica, Supplement 2: 1627–1763.

Zilch A (1960) Handbuch der Paläozoologie. Band 6. Gastropoda. Teil 2. Euthyneura. Lieferung 4. Borntraeger, Berlin, Germany, 834 pp.

ZooKeys 1080: 107–133 (2022)
doi: 10.3897/zookeys.1080.71370
https://zookeys.pensoft.net

CHECKLIST

A peer-reviewed open-access journal
ZooKeys
Launched to accelerate biodiversity research

Diversity and distribution of the Isopoda (Crustacea, Peracarida) of Kuwait, with an updated checklist

Manal Abdulrahman Al-Kandari[1], Valiallah Khalaji-Pirbalouty[2], Hadeel Abdulkhaliq[1], Weizhong Chen[1]

1 *Ecosystem-Based Management of Marine Resources, Environment, and Life Sciences Research Center, Kuwait Institute for Scientific Research, Hamad Al-Mubarak Street, Building 900004, Area 1, Raas Salmiya, Kuwait*
2 *Department of Biology, Faculty of Basic Science, Shahrekord University, Shahrekord, Iran*

Corresponding author: Valiallah Khalaji-Pirbalouty (vkhalaji@sci.sku.ac.ir, khalajiv@yahoo.com)

Academic editor: Rachael Peart | Received 10 July 2021 | Accepted 8 December 2021 | Published 5 January 2022

http://zoobank.org/49DACA16-C82E-41D5-97D6-136127AD32F5

Citation: Al-Kandari MA, Khalaji-Pirbalouty V, Abdulkhaliq H, Chen W (2022) Diversity and distribution of the Isopoda (Crustacea, Peracarida) of Kuwait, with an updated checklist. ZooKeys 1080: 107–133. https://doi.org/10.3897/zookeys.1080.71370

Abstract

Thirty-eight species of Isopoda, belonging to 13 families and 29 genera, are listed from Kuwait based on previous literature records (of 17 species) and collections carried out along Kuwait's coastal and subtidal zones during the present study. The majority of species belongs to the suborder Cymothoida (23), followed by Sphaeromatidea (9), Oniscidea (3), Valvifera (2), and Asellota (1). In total, 25 species were collected and identified from 12 families and 22 genera from Kuwaiti coastal and subtidal areas. These include eight families, 15 genera, and 21 species recorded for the first time from Kuwait. Isopod diversity was highest in the sandy rock areas, including southern Kuwait, particularly in Al-Khiran and Al-Nuwaiseeb, and in mixed habitat (muddy, rocky, and sandy) intertidal transects such as in Failaka Island. The species number increased from the subtidal and lowest zones into the high tidal zone. Isopods were found in sandy substrata, among shells, cobbles, rocks, dead corals, and algae.

Keywords

Biodiversity, checklist, first records, geographical distribution, Isopoda, Kuwait

Introduction

The isopod fauna in Kuwait's intertidal and subtidal habitats have received little attention. The few significant accounts of Kuwait's marine isopods are those of Bowman and Tareen (1983), describing six new species of Cymothoidae. In addition, Abu-Hakima (1984) recorded a bopyrid, *Epipenaeon elegans* Chopra, 1923, and Jones (1986) in 'Field Guide to the Seashores of Kuwait' recorded six marine isopods from Kuwait. However, *Apanthura sandalensis* Stebbing, 1900, *Ligia exotica* Roux, 1828; and *Cymodoce richardsoniae* Nobili, 1906, were misidentified in his guide. They are reidentified as *Amakusanthura* sp., *L. persica* Khalaji-Pirbalouty & Wägele, 2010, and *C. delvarii* Khalaji-Pirbalouty, Bruce & Wägele, 2013, respectively, in this work.

Arcturinoides angulata Kensley, Schotte & Poore, 2007 and *Astacilla mccaini* Kensley, Schotte & Poore, 2007 have been reported by Kensley et al. (2007) from the coasts of Kuwait and Saudi Arabia and, most recently, Jones and Nithyanandan (2012) reported four species of the genus *Eurydice* Leach, 1815 from Kuwait and Saudi Arabia. In contrast, the isopod fauna along the Iranian coast of the Gulf has received more attention than adjacent regions (e.g., Khalaji-Pirbalouty and Wägele 2009, 2010a, b, c, 2011, 2012; Khalaji-Pirbalouty et al. 2013; Khalaji-Pirbalouty and Bruce 2014; Khalaji-Pirbalouty and Raupach 2014, 2016).

In 2013, a large-scale survey covering Kuwait's entire coastline and offshore islands was initiated to document biodiversity, species distribution, and species abundance of the intertidal fauna. This survey was completed in 2017 (Al-Kandari et al. 2017). A further complementary sampling of four sites was conducted from 2016 to 2018. Survey results for molluscs, decapods, and polychaetes have been published (Al-Kandari et al. 2019a, b, 2020a, b), and summaries on other taxa are in progress. Here we report the results for the crustacean order Isopoda.

Materials and methods

Intertidal and subtidal sampling

Thirty-eight intertidal transects and two subtidal sites were sampled quantitatively and qualitatively for macrofauna (Fig. 1, Table 1). Transects were located between Khor Al-Subiya in the north and the border with Saudi Arabia in the south. The surveys were conducted in daylight during the late autumn and winter seasons from December 2013 to December 2016. The sampling dates (see Table 1) and time for each site coincided with the lowest tides (as near to 0 chart datum as possible) using the Kuwait Port Authority's Tide Tables for 2013, 2014, 2015, and 2016. Kuwait's intertidal areas consist of coral, rocky, sandy, and/or muddy habitats or combinations thereof. At some transects, sandy mud or muddy sand covered a hard stratum throughout the intertidal range. Other transects consisted of combinations of sand and rocks, with some rocks

lose and resting on the surface and others being part of the bedrock. All sandy beaches, rocky beaches, underneath stones, rubble, algal turf, and/or seagrass beds were sampled at each transect. Samples were left in seawater for a day before the fauna was collected from the bottom of the containers. Additionally, fauna living within porous rocks was collected by breaking the rocks with a hammer, placing the resulting debris in isotonic magnesium chloride solution, and collecting the fauna after their relaxation. For soft substrates, a 25 × 25-cm square metal box corer, 15 cm deep, was placed randomly, and sediment was collected by spade from inside the corer. These samples were sieved with seawater using 0.3-mm mesh sieves 45- and 75-cm in diameter, and all sediment and organisms remaining were preserved with 5% buffered formalin for subsequent picking and identification. Isopod specimens were also collected qualitatively from under rocks and among intertidal vegetation. Sand was sieved further samples were collected from rocks broken by a hammer, washing algae, sponges and seagrass, turning over stones, as well as collecting directly in the habitat. Material was rinsed under seawater, and all the washings passed through a 0.3-mm mesh sieve to collect any isopod specimens. The collected isopods were fixed in a 75–95% ethanol solution for subsequent morphological and molecular analyses. All specimens were deposited in the Kuwait Institute for Scientific Research (**KISR**) reference collection.

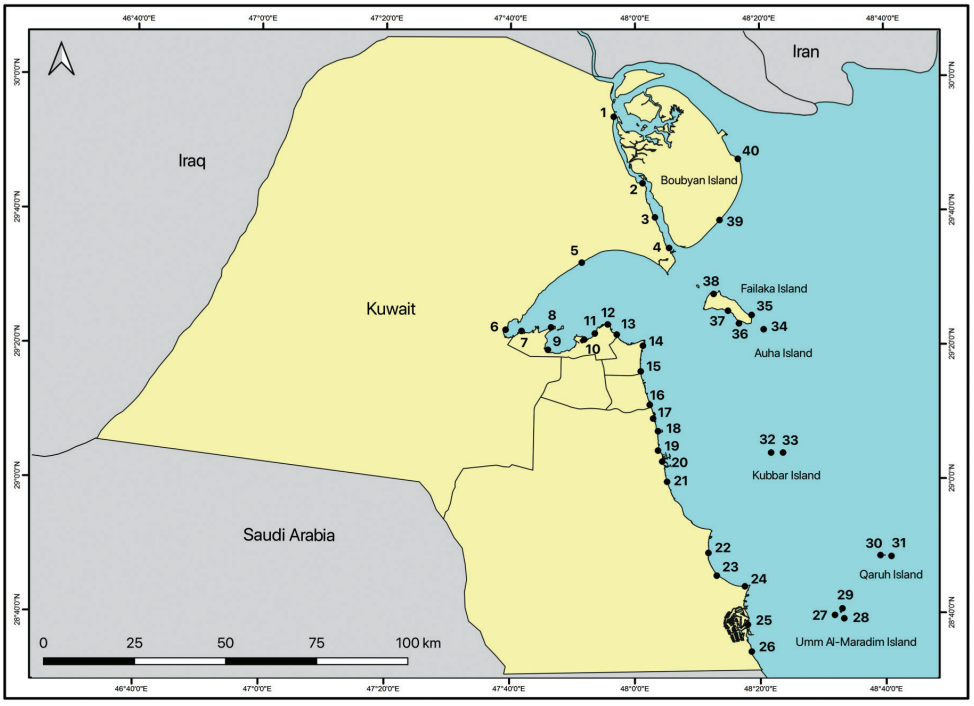

Figure 1. Map of the 40 sampling sites established in Kuwait's intertidal and subtidal zones; site numbers corresponding to Table 1.

Table 1. Sampling sites studied in the intertidal and subtidal zones of Kuwait with habitat details (*KPC = Kuwait Petroleum Corporation).

Site No.	Site Name (north to south)	Position			
		Sampling Dates	Coordinates	Area	Substrate
Khor Al-Subiya: north and west of Boubyan Island (BI)					
1	Umm Al-Shajar (north Khor Al-Subiya), (BI1)	29.12.2015	29°54.263'N, 48°01.475'E	BI	Mud
2	Khor Al-Subiya (Al-Magasel)	23.11.2014	29°44.476'N, 48°05.740'E	North	Mud-rock
3	Khor Al-Subiya (Al-Shumaima)	24.11.2014	29°39.403'N, 48°07.850'E	North	Mud-rock
4	Khor Subiyah (south)	25.11.2014	29°34.849'N, 48°10.248'E	North	Mud
Kuwait Bay					
5	Mudairah	30.12.2014	29°32.672'N, 47°55.394'E	Bay-mud	Mud
6	Al-Kuwaisat	17.11.2014	29°22.677'N, 47°42.480'E	Bay-mud	Mud
7	Al-Judailiat	02.02.2014	29°22.497'N, 47°45.183'E	Bay	Sand-rock
8	Aushairij	03.02.2014	29°23.047'N, 47°50.192'E	Bay	Sand-rock
9	Sulaibikhat Bay	06.11.2014	29°19.702'N, 47°49.670'E	Bay	Mud
10	Shuwaikh (KPC*), subtidal	22.02.2016	29°21.401'N, 47°56.390'E	Bay	Sand-rock
11	Kuwait Bay (Al-Salam Beach)	09.12.2013	29°21.631'N, 47°57.204'E	Bay	Sand-rock
12	Kuwait Bay (Ras Ajuza)	08.12.2013	29°23.481'N, 47°59.800'E	Bay	Sand-rock
East Kuwait Bay					
13	Al-Sha'Eab	19.01.2014	29°21.979'N, 48°01.344'E	Middle 1	Sand-rock
14	Al-Salmiya	19.12.2013	29°20.313'N, 48°05.775'E	Middle 1	Sand-rock
South Kuwait Bay					
15	Al-Messilah	18.12.2013	29°16.496'N, 48°05.407'E	Middle 1	Sand-rock
16	Al-Funaitees	19.12.2013	29°11.519'N, 48°06.938'E	Middle 1	Sand-rock
17	Abu Halifa	04.01.2014	29°08.154'N, 48°07.985'E	Middle 2	Sand-rock
18	Al-Mangaf	01.02.2014	29°06.041'N, 48°08.323'E	Middle 2	Sand-rock
19	Masfat Al-Ahmadi	10.12.2014	29°04.431'N, 48°08.676'E	Middle 2	Sand-rock
20	North Oil loading terminal, subtidal	28.09.2014	29°8.043'N, 48°09.139'E	Middle 2	Sand-rock
21	Mina Abdullah	16.02.2014	29°00.071'N, 48°09.853'E	Middle 2	Sand-rock
22	Al-Julaia'Ea	17.02.2014	28°49.480'N, 48°16.812'E	South	Sand-rock
23	Dohat Al-Zour	02.03.2014	28°46.100'N, 48°18.210'E	South	Sand-rock
24	Ras Al-Zour	08.01.2015	28°44.502'N, 48°22.950'E	South	Sand-rock
25	Al-Khiran	03.03.2014	28°38.813'N, 48°23.429'E	South	Sand-rock
26	Al-Nuwaiseeb	04.03.2014	28°34.794'N, 48°24.078'E	South	Sand-rock
Islands					
27	Umm Al-Maradim Island, east (UI1)	11.11.2014	28°40.778'N, 48°39.207'E	UI1	Sand-rock
28	Umm Al-Maradim Island, northeast (UI2)	11.11.2014	28°40.939'N, 48°39.196'E	UI2	Sand-rock
29	Umm Al-Maradim Island, northwest	11.11.2014	28°40.960'N, 48°39.173'E	UI3	Sand-rock
30	Qaruh Island (north), (QI1)	10.11.2014	28°49.105'N, 48°46.553'E	QI	Sand-rock
31	Qaruh Island (south), (Q2)	10.11.2014	28°49.022'N, 48°46.607'E	QI	Sand-rock
32	Kubbar Island (east), (Q3)	09.11.2014	29°04.278'N, 48°29.655'E	KI	Sand-rock
33	Kubbar Island (west)	09.11.2014	29°04.377'N, 48°29.472'E	KI	Sand-rock
34	Auha Island (northwest), (AI)	10.02.2016	29°22.726'N, 48°26.269'E	AI	Sand-rock
35	Failaka Island (east 2), (FI1)	25.12.2014	29°23.710'N, 48°24.136'E	FI	Sand-rock
36	Failaka Island (east 1), (F2)	24.12.2014	29°23.629'N, 48°23.958'E	FI	Sand-rock
37	Failaka Island (south), (FI3)	23.12.2014	29°25.625'N, 48°20.307'E	FI	Mud-rock
38	Failaka Island (northwest), (FI4)	22.12.2014	29°28.049'N, 48°17.838'E	FI	Mud-rock
39	Boubyan Island (south), (BI2)	24.01.2015	29°38.993'N, 48°18.830'E	BI	Mud
40	Boubyan Island (Ras Al-Gayed), (BI3)	25.01.2015	29°48.093'N, 48°21.975'E	BI	Mud

Species identification

For identification, morphological studies were conducted using a Leica DFC450 camera mounted on a Leica M125 Stereomicroscope equipped with an imaging system that was employed to obtain colour images of the specimens. For greater depth of field,

we merged 10–20 source images of a single specimen taken at different focus distances into one final image with the software LAS V4.5. The final image was edited using Adobe Photoshop. Isopods were identified to the lowest possible taxonomic level.

Results

In total, 25 species representing 12 families and 22 genera were identified from specimens collected in the present study. These species were collected from 31 intertidal transects, including 17 mainland and 14 island transects, and two subtidal sites (Table 2).

Sphaeromatidae Latreille, 1825 was the best-represented family with five genera and eight species, followed by the family Cirolanidae comprising five genera and five species. Two species were recorded in each of the families Gnathiidae and Arcturidae. The remaining seven families were represented by single species (Table 2). In descending order, the most widely distributed isopod species were *Amakusanthura* sp. from 20 transects, *Gnathia* sp., and *Sphaeromopsis sarii* Khalaji-Pirbalouty & Wägele, 2009, from 18 transects, *Astacilla mccaini* Kensley, Schotte & Poore, 2007, from 15 transects; *Heterodina mccaini* Schotte & Kensley, 2005, from 12 transects; *Cymodoce delvarii* Khalaji-Pirbalouty, Bruce & Wägele, 2013, occurred at 12 transects, and *Lanocira gardineri* Stebbing, 1904, was collected from ten transects. Interestingly, some species occurred in their 100s from single qualitative samples. Such high numbers for *S. sarii* and *C. delvarii* were obtained from randomly collected *Sargassum* at Al-Nuwaiseeb and Failaka Island. Similarly, high numbers of *S. sarii* occurred on algal turfs from Kubbar Island. Other species found in high numbers were found from rocks, dead coral, or dead shells and included *Gnathia* sp., *H. mccaini*, and *Sphaeroma walkeri* Stebbing, 1905.

Thirty-eight isopod species under five sub-orders, 13 families, and 29 genera are listed in taxonomic order, including Kuwait's previous records (17 species), type localities, and geographical distributions.

Table 2. List of isopod species recorded in Kuwait in the present survey (* indicates a new record to Kuwait) and from literature records.

Suborder	Family	Species	Reference
CYMOTHOIDA	Anthuridae	*Amakusanthura* sp. *	This study
CYMOTHOIDA	Expanathuridae	*Eisothistos* sp. *	This study
CYMOTHOIDA	Cirolanidae	*Atarbolana exoconta**	This study
CYMOTHOIDA	Cirolanidae	*Baharilana kiabii**	This study
CYMOTHOIDA	Cirolanidae	*Cirolana tarahomii**	This study
CYMOTHOIDA	Cirolanidae	*Eurydice arabica*	Jones and Nithyanandan (2012)
CYMOTHOIDA	Cirolanidae	*E. marzouqui*	Jones & Nithyanandan, 2012
CYMOTHOIDA	Cirolanidae	*E. peraticis*	Jones and Nithyanandan (2012); This study
CYMOTHOIDA	Cirolanidae	*Metacirolana* sp. *	This study
CYMOTHOIDA	Corallanidae	*Lanocira gardineri**	This study
CYMOTHOIDA	Cymothoidea	*Anilocra monoma*	Bowman & Tareen, 1983
CYMOTHOIDA	Cymothoidea	*Catoessa gruneri*	Bowman & Tareen, 1983
CYMOTHOIDA	Cymothoidea	*Cymothoa eremita*	Bowman & Tareen, 1983
CYMOTHOIDA	Cymothoidea	*Joryma sawayah*	Bowman & Tareen, 1983

Suborder	Family	Species	Reference
CYMOTHOIDA	Cymothoidea	*Mothocya* sp.	Bowman & Tareen, 1983
CYMOTHOIDA	Cymothoidea	*Nerocila arres*	Bowman & Tareen, 1983
CYMOTHOIDA	Cymothoidea	*N. kisra*	Bowman & Tareen, 1983
CYMOTHOIDA	Cymothoidea	*N. sigani*	Bowman & Tareen, 1983
CYMOTHOIDA	Cymothoidea	*N. phaiopleura*	Bowman & Tareen, 1983
CYMOTHOIDA	Gnathiidae	*Gnathia* sp.*	This study
CYMOTHOIDA	Gnathiidae	*Elaphognathia* sp.*	This study
CYMOTHOIDA	Bopyridae	*Epipenaeon elegans*	Abu-Hakima, 1984
CYMOTHOIDA	Bopyridae	*Parabopyrella* sp.*	This study
ONISCIDE	Ligiidae	*Ligia persica**	This study
ONISCIDE	Olibrinidae	*Olibrinus antennatus**	This study
ONISCIDE	Tylidae	*Tylos maindroni*	Taiti and Ferrara(1991); this study
SPHAEROMATIDEA	Sphaeromatidae	*Cymodoce delvarii**	This study
SPHAEROMATIDEA	Sphaeromatidae	*C. fuscina**	This study
SPHAEROMATIDEA	Sphaeromatidae	*C. waegelei**	This study
SPHAEROMATIDEA	Sphaeromatidae	*Dynamenella granulata**	This study
SPHAEROMATIDEA	Sphaeromatidae	*Heterodina mccaini**	This study
SPHAEROMATIDEA	Sphaeromatidae	*Sphaeroma khalijfarsi**	This study
SPHAEROMATIDEA	Sphaeromatidae	*S. walkeri**	This study
SPHAEROMATIDEA	Sphaeromatidae	*S. annandalaei*	This study
SPHAEROMATIDEA	Sphaeromatidae	*Sphaeromopsis sarii**	This study
VALVIFERA	Arcturidae	*Arcturinoides angulata*	Kensley et al. (2007); this study
VALVIFERA	Arcturidae	*Astacilla mccaini*	Kensley et al. (2007); this study
ASELLOTA	Paramunnidae	*Heterosignum* sp.*	This study

Taxonomy

Order Isopoda Latreille, 1817
Suborder Cymothoida Wägele, 1989
Superfamily Anthuroidea Leach, 1814
Family Anthuridae Leach, 1814
Genus *Amakusanthura* Nunomura, 1977

***Amakusanthura* sp.**
Figure 2A

Apanthura sandalensis — Jones, 1986: 148, pl. 40 [not *Apanthura sandalensis* Stebbing, 1900; misidentification].

Material examined. Kuwait. 3 specimens; St. 2; 29°44.476'N, 48°05.740'E; 23 Nov. 2014; ♀♀, 2 juveniles; St. 3; 29°39.403'N, 48°07.850'E; 24 Nov. 2014; (5 ♀♀); St. 4; 29°34.849' N, 48°10.248'E; 25 Nov. 2014, 2 ♂♂; St. 8; 29°23.047'N, 47°50.192'E; 3 Feb. 2014; 1 ♀; St. 11; 29°21.631'N, 47°57.204'E; 9 Dec. 2013; 2 ♀♀; St. 12; 29°23.481'N, 47°59.800'E; 8 Dec. 21013; (1 ♀), 1 juvenile; St. 18; 29°06.041'N, 48°08.323'E; 1 Feb. 2014; 3 ♀♀; St. 19; 29°04.431'N, 48°08.676'E; 10 Dec. 2014; 2 ♀♀; St. 22; 28°49.480'N, 48°16.812'E; 17 Feb 2014, 1 juvenile, 6 ♀♀; St. 24; 28°44.502'N, 48°22.950'E; 08 Jan. 2015; 1 ♀; St. 25; 28°38.813'N, 48°23.429'E; 3 Mar. 2014; 5 ♀♀, 2 juveniles; St. 26; 28°34.794'N, 48°24.078'E; 4 Mar. 2014; 5 ♀♀, 3 juveniles; St. 27; 28°40.778'N, 48°39.207'E;; 11 Nov. 2014; 3 ♀♀; St. 28; 28°40.939'N, 48°39.196'E; 11 Nov. 2014; 1 ♀; St. 29; 28°40.960'N, 48°39.173'E; 11 Nov. 2014; 2 ♀♀; St. 30; 28°49.105'N, 48°46.553'E; 10 Nov. 2014;

7 ♀♀; St. 32; 29°04.278'N, 48°29.655'E; 9 Nov. 2014; 12 ♀♀; St. 34; 29°22.726'N, 48°26.269'E; 10 Feb. 2014; 3 ♀♀; St. 36; 29°23.629'N, 48°23.958'E; 24 Dec. 2014; 2 ♀♀; St. 38; 29°28.049'N, 48°17.838'E; 22 Dec. 2014.

Remarks. *Amakusanthura motasi* (Negoescu, 1980) is the only species of this genus recorded from the nearest locality (Gulf of Aden). The specimens examined here differ from *A. motasi* in the shape of the pleon with different lengths of pleonites 1–5 (vs.

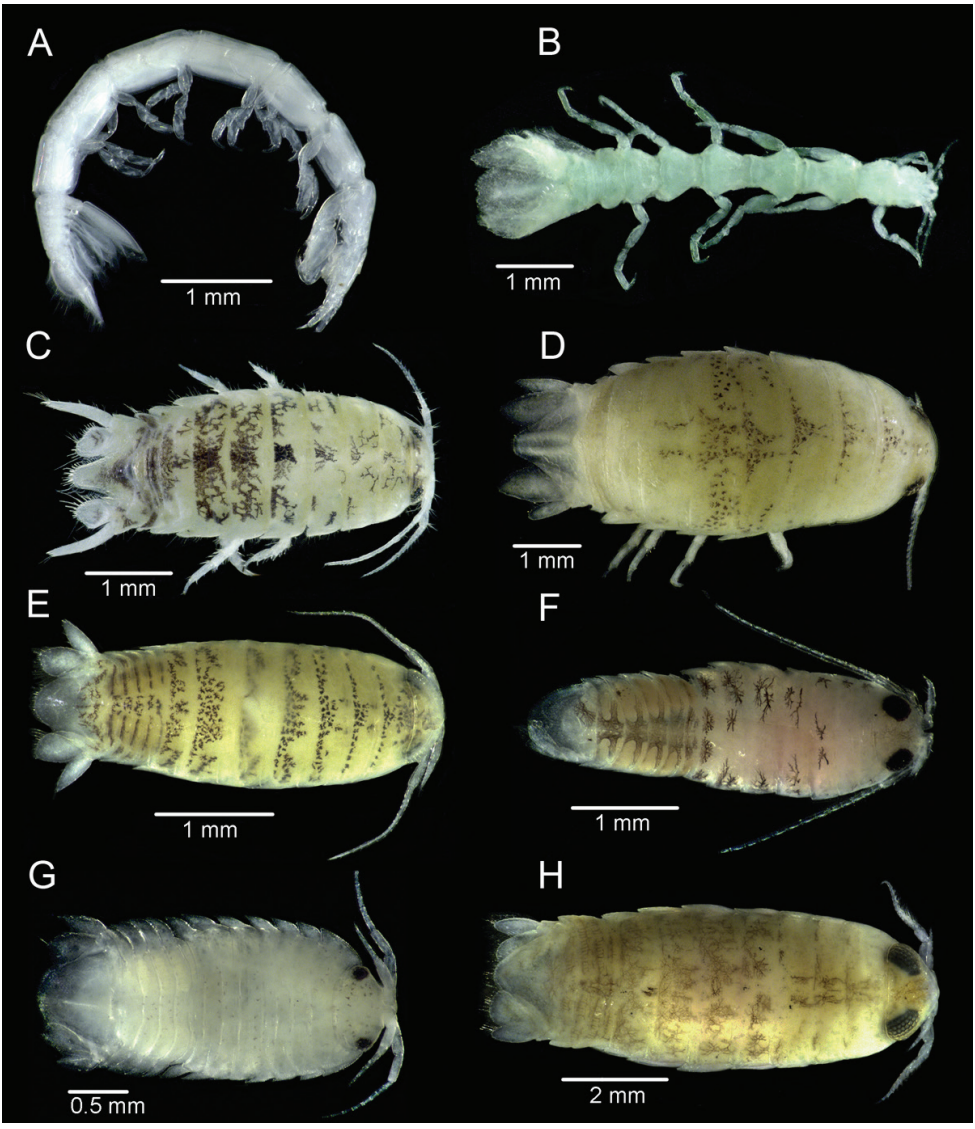

Figure 2. A *Amakusanthura* sp. from Kubbar Island **B** *Eisothistos* sp. from Failaka Island **C** *Atarbolana exoconta* Bruce & Javed, 1987 from Masfat Al-Ahmadi **D** *Baharilana kiabii* Khalaji- Pirbalouty & Wägele, 2011from Al-Nuwaiseeb **E** *Cirolana tarahomii* Khalaji-Pirbalouty & Wägele, 2011 from Quaruh Island **F** *Eurydice peraticis* Jones, 1974 from Alkhiran **G** *Metacirolana* sp. from Um-Almaradim **H** *Lanocira gardineri* Stebbing, 1904 from Al-Shamaimah.

pleonites 1–5 similar to each other in *A. motasi*), the setation of pereopods, uropods and pleotelson; antenna and antennular articles are narrower than in *A. motasi*.

Distribution. New record for Kuwait.

Family Expanathuridae Poore, 2001
Genus *Eisothistos* Haswell, 1884

***Eisothistos* sp.**
Figure 2B

Material examined. 1 ♂; St. 38; 29°28.049'N, 48°17.838'E; 22 Dec. 2014.

Distribution. New record for Kuwait

Family Cirolanidae Dana, 1852
Genus *Atarbolana* Bruce & Javed, 1987

***Atarbolana exoconta* Bruce & Javed, 1987**
Figure 2C

Atarbolana exoconta Bruce & Javed, 1987: 145, figs 1, 2, Manora Island, Pakistan (type locality); Khalaji-Pirbalouty & Raupach, 2016: 155–162, figs 2–6.

Material examined. 4 ♂♂, 5 ♀♀; St. 19; 29°04.431'N, 48°08.676'E; 10 Dec. 2014; 1 ♂, 8 ♀♀; St. 21; 29°00.071'N, 48°09.853'E; 16 Feb. 2014; 2 ♀♀: St. 27; 28°40.778'N, 48°39.207'E; 11 Nov. 2014.

Distribution. Pakistan, Oman Sea (Bruce and Javed 1987; Khalaji-Pirbalouty and Raupach 2016), new record for Kuwait.

Genus *Baharilana* Bruce & Svavarsson, 2003

***Baharilana kiabii* Khalaji-Pirbalouty & Wägele, 2011**
Figure 2D

Baharilana kiabii Khalaji-Pirbalouty & Wägele, 2011: 34–39, figs 1–4; Qeshm Island, Iran (type locality).

Material examined. 1 ♀, 1 juvenile; St. 19; 29°04.431'N, 48°08.676'E; 10 Dec. 2014; 2 ♀♀; St. 25; 28°38.813'N, 48°23.429'E; 3 Mar. 2014; 3 ♂♂, 5 ♀♀; St. 26; 28°34.794'N, 48°24.078'E; 4 Mar. 2014; 1 ♂, 1 juvenile; St. 27; 28°40.778'N, 48°39.207'E; 11 Nov. 2014; 1 ♀, 1 juvenile; St. 32; 29°04.278'N, 48°29.655'E; 9 Nov. 2014; 1 ♀; St. 35; 29°23.710'N, 48°24.136'E; 25 Dec. 2014.

Distribution. Qeshm Island, Hengam Island, Iran (Khalaji-Pirbalouty and Wägele 2011), new record for Kuwait.

Genus *Cirolana* Leach, 1818

***Cirolana tarahomii* Khalaji-Pirbalouty & Wägele, 2011**
Figure 2E

Cirolana tarahomii Khalaji-Pirbalouty & Wägele, 2011: 39–45, figs 5–8; Qeshm Island, Iran (type locality).

Material examined. 7 ♀♀, 3 juveniles; St. 30; 28°49.105'N, 48°46.553'E; 10 Nov. 2014; 1 ♀, St. 32; 29°04.278'N, 48°29.655'E; 9 Nov. 2014.

Distribution. Qeshm Island, Iran (Khalaji-Pirbalouty and Wägele 2011), new record for Kuwait.

Genus *Eurydice* Leach, 1815

***Eurydice arabica* Jones, 1974**

Eurydice arabica Jones, 1974: 202, fig. 2, Red Sea (type locality); Bruce, 1986: 221.

Distribution. Kuwait, Al-Ahmad Sea City waterways, Bahrain, Mashtan Island (Jones and Nithyanandan 2012).

***Eurydice marzouqui* Jones & Nithyanandan, 2012**

Eurydice marzouqui Jones & Nithyanandan, 2012: 47–48, figs 1–4; Tarut Bay, Saudi Arabia (type locality).

Distribution. Sabah Al-Ahmad Sea City Waterways, Kuwait; Manifa, Saudi Arabia (Jones and Nithyanandan 2012).

***Eurydice peraticis* Jones, 1974**
Figure 2F

Eurydice peraticis Jones, 1974: 204, fig. 3, Dammam, Saudi Arabia (type locality); Eleftheriou & Jones, 1976: 387; Bruce, 1986: 221; Kazmi et al. 2002: 91, fig. 66.

Material examined. 1 ♂; St. 8; 29°23.047'N, 47°50.192'E; 3. Feb. 2014; 2 ♀♀; St. 19; 29°04.431'N, 48°08.676'E; 10 Dec. 2014; 2 ♀♀; St. 21; 29°00.071'N, 48°09.853'E; 16 Feb. 2014; 2 ♂♂, 3 ♀♀; St. 25; 28°38.813'N, 48°23.429'E; 3 Mar. 2014; 1 ♀; St. 34; 29°22.726'N, 48°26.269'E; 10 Feb. 2016; 3 ♂♂, 7 ♀♀; St. 39; 29°38.993'N, 48°18.830'E; 24 Jan. 2015; 6 ♂♂, 9 ♀♀, 2 juveniles; St. 40; 25 Jan. 2015.

Distribution. Saudi Arabia, Bahrain, India, Pakistan, Kuwait (Eleftheriou and Jones 1976; Kazmi et al. 2002).

Genus *Metacirolana* Nierstrasz, 1931

***Metacirolana* sp.**
Figure 2G

Material examined. 1 ♂; St.2; 29°44.476'N, 48°05.740'E; 23 Nov. 2014; 4 ♀♀; St. 3; 29°39.403'N, 48°07.850'E; 24 Nov. 2014; 1 ♂; St.27; 28°40.778'N, 48°39.207'E; 11Nov. 2014; 1 ♂, 2 ♀♀; St.30; 28°49.105'N, 48°46.553'E; 10 Nov. 2014; 1 ♀; St. 34; 29°22.726'N, 48°26.269'E; 10 Feb. 2016; 2 ♂♂, 2 ♀♀; St. 36; 29°23.629'N, 48°23.958'E; 24 Dec. 2014.

Distribution. New record for Kuwait.

Family Corallanidae Hansen, 1890
Genus *Lanocira* Hansen, 1890

***Lanocira gardineri* Stebbing, 1904**
Figure 2H

Lanocira gardineri Stebbing, 1904: 706, pl. LI, A, Mahlosmadulu Atoll, Maldive Islands (type locality).

A comprehensive synonymy to the species can be found in Bruce and Sidabalok 2011: 25.

Material examined. 1 ♂, 4 ♀♀, 3 juveniles; St. 3; 29°39.403'N, 48°07.850'E; 24 Nov. 2014; 2 ♀♀; St. 12; 29°23.481'N, 47°59.800'E; 8 Dec. 2104; 1 ♀; St. 22; 28°49.480'N, 48°16.812'E; 17 Feb. 2014; 1 Juvenile; St. 30; 28°49.105'N, 48°46.553'E; 10 Nov. 2014; 2 ♂♂, 5 ♀♀; St. 3; 29°39.403'N, 48°07.850'E; 24 Nov. 2014; 3 ♂♂, 6 ♀♀; St. 35; 29°23.710'N, 48°24.136'E; 25 Dec. 2014; 2 ♂♂, 5♀♀, 2 ovigerous ♀♀, 5 juveniles; St. 36; 29°23.629'N, 48°23.958'E; 24 Dec. 2014; 1 ♀; St. 37; 29°25.625'N, 48°20.307'E; 23 Dec. 2014; 1 ♂; St. 38; 29°28.049'N, 48°17.838'E; 22 Dec. 2014; 2 ♂♂; St. 40; 29°48.093'N, 48°21.975'E; 20 Jan. 2015.

Distribution. Maldives, Kenya, Madagascar (Delaney 1989); Western Australia (Bruce and Sidabalok 2011); Iran (Khalaji-Pirbalouty, unpublished), new family for Kuwait.

Family Cymothoidae Leach, 1814

Of the cymothoid isopods (parasites of fishes), the following species have been reported by Bowman and Tareen (1983).

***Anilocra monoma* Bowman & Tareen, 1983**

Anilocra monoma Bowman & Tareen, 1983: 1, figs 3, 4, Kuwait (type locality).

Distribution. Kuwait (Bowman and Tareen 1983).

***Catoessa gruneri* Bowman & Tareen, 1983**

Catoessa gruneri Bowman & Tareen, 1983: 18, figs 14, 15, Kuwait (type locality).

Distribution. Kuwait (Bowman and Tareen 1983).

***Joryma sawayah* Bowman & Tareen, 1983**

Joryma sawayah Bowman & Tareen, 1983: 21, figs 16–18, Doha, Kuwait (type locality).
Livoneca sp., Mathews & Samuel, 1987: 144.

Distribution. Kuwait (Bowman and Tareen 1983).

***Nerocila arres* Bowman & Tareen, 1983**

Nerocila arres Bowman & Tareen, 1983: 12, figs 10–12; Kuwait (type locality).
Nerocila kisra Bowman & Tareen, 1983: 8, figs 6–8.

Distribution. Kuwait (Bowman and Tareen 1983).

***Nerocila sigani* Bowman & Tareen, 1983**

Nerocila sigani Bowman & Tareen, 1983: 12, fig. 9; Kuwait (type locality).

Distribution. Kuwait (Bowman and Tareen 1983).

***Nerocila phaiopleura* Bleeker, 1857**

Nerocila phaiopleura Bleeker, 1857: 25–26, fig. 3, Java (type locality); Bowman & Tareen, 1983: 5, fig. 5.

Distribution. A widespread species, recorded in the Indian Ocean from Hong Kong to South Africa (Bowman and Tareen 1983).

***Mothocya* sp.**

Mothocya sp., Bowman & Tareen, 1983: 25, fig. 19.
Cymothoa eremita ? (Brunnich, 1783), Bowman & Tareen, 1983: 25, fig. 20, India (type locality).

Distribution. India (Bowman and Tareen 1983)

Family Gnathiidae Leach, 1814
Genus *Gnathia* Leach, 1814

***Gnathia* sp.**
Figure 3A

Material examined. 1 ♂, 2 ♀♀; St. 7; 29°22.497'N, 47°45.183'E; 02 Feb. 2014; 1 ♀, 6 praniza larvae; St. 8; 29°23.047'N, 47°50.192'E; 3 Feb. 2014; 1 ♀, 6 praniza larvae; St. 10; 29°21.401'N, 47°56.390'E; 22 Feb. 2014; 1 ♂; St. 11; 29°21.631'N, 47°57.204'E; 9 Dec. 2013; 1 ♀; St. 12; 29°23.481'N, 47°59.800'E; 08 Dec. 2013; 3 ♀♀, 8 praniza larvae; St. 19; 29°04.431'N, 48°08.676'E; 10 Dec. 2014; 2 ♀♀, 1 praniza larva; St. 21; 29°00.071'N, 48°09.853'E; 16 Feb 2014; 1 ♀, 3 praniza larvae; St. 25; 28°38.813'N, 48°23.429'E; 3 Mar. 2014; 3 ♀♀, 1 ♂, 50 praniza larvae; St. 26; 28°34.794'N, 48°24.078'E; 4 Mar. 2014; 5 ♂♂, 9 ♀♀, 6 praniza larvae; St. 27; 28°40.778'N, 48°39.207'E; 11 Nov. 2014; 1 ♂, 3 praniza larvae; St. 28; 28°40.939'N, 48°39.196'E; 11Nov.2014; 8 ♂♂, 16 juveniles, 50 ♀♀, 3 praniza larvae; St. 30; 28°49.105'N, 48°46.553'E; 10 Nov. 2014; 3 ♀♀, 6 juveniles; St. 31; 28°49.022'N, 48°46.607'E; 10 Nov. 2014; 50 ♀♀ and praniza larvae; St. 32; 29°04.278'N, 48°29.655'E; 9 Nov. 2014; 3 ♀♀; St. 35; 29°23.710'N, 48°24.136'E; 25 Dec. 2014; 4 ♂♂, 2 sub adults ♂♂, 3 praniza larvae; St. 36; 29°23.629'N, 48°23.958'E; 24 Dec. 2014; 4 praniza larvae; St. 38; 29°28.049'N, 48°17.838'E; 22 Dec. 2014.

Remarks. The specimen is closely related to *Gnathia luxata* Kensley, Schotte & Poore, 2009 from Khawr Musharraba, Saudi Arabia, Persian Gulf. However, it differs from *G. luxata* by having a larger and conical mediofrontal process and bifid superior frontolateral process instead of a conical process. Also, the supraocular lobe is blunt and oblique rather than simply rounded.

Distribution. New record for Kuwait.

Genus *Elaphognathia* Monod, 1926

***Elaphognathia* sp.**
Figure 3B

Material examined. 1 ♂; St. 3; 24°11.2014'N, 48°07.850'E; 24 Nov. 2014.

Remarks. The specimen is similar to *E. gladia* Kensley, Schotte & Poore, 2009 in having the long, thin saber-like mandible from Somalia. However, it differs from

E. gladia in having a mandible with only one conical lobe at its base rather than two and having an acute mediofrontal process (vs. absent in *E. gladia*).

Distribution. New record for Kuwait.

Family Bopyridae Rafinesque, 1815
Genus *Epipenaeon* Nobili, 1906

***Epipenaeon elegans* Chopra, 1923**

Epipenaeon elegans Chopra, 1923: 454–456, figs 6–11, Ganges Delta, India (type locality); Dawson, 1958: 240; Tareen, 1982: 159–160; Abu-Hakima 1984: 51–58; Mathews et al. 1988: 53–62; Eslami & Mokhayer, 2002: 89–95; An et al. 2015: 2033.

Distribution. India; Kuwait; Abu Ali and Tarut (Saudi Arabia); Boushehr port (Iran).

Genus *Parabopyrella* Markham, 1985

***Parabopyrella* sp.**

Material examined. 1 ♂, 1 ♀; St.8; 29°23.047'N, 47°50.192'E; 3 Feb. 2014.

Remarks. Parasite, found on the gill of the common alpheid shrimp in Kuwait the *Alpheus lobidens* De Haan, 1849.

Distribution. New record for Kuwait.

Suborder Oniscidea Latreille, 1802
Family Ligiidae Brandt & Ratzeburg, 1831
Genus *Ligia* Fabricius, 1798

***Ligia persica* Khalaji-Pirbalouty & Wägele, 2010**
Figure 3C

Ligia persica Khalaji-Pirbalouty & Wägele, 2010b: 136–149, figs 2–7; Kish Island, Iran (type locality).
Ligia exotica Roux, 1828. – Jones, 1986: 148, pl. 40.

Material examined. 1 ♀; St. 7; 29°22.497'N, 47°45.183'E; 2 Feb. 2014; 4 ♂♂, 2 ♀♀; St. 8; 29°23.047'N, 47°50.192'E; 3 Feb. 2014; 3 ♂♂, 17 ♀♀; St. 12; 29°23.481'N, 47°59.800'E; 8 Dec. 2013 20 ♂♂ and ♀♀; St. 13; 29°21.979'N, 48°01.344'E; 19 Jan. 2014; 4 ♂♂, 6 ♀♀; St. 26; 28°34.794'N, 48°24.078'E; 4 Marc. 2014; 4 ♂♂, 4 ♀♀; St. 28; 28°40.939'N, 48°39.196'E; 11 Nov. 2014.

Distribution. Iran, Oman, and United Arab Emirates (Taiti and Checcucci 2011; Khalaji-Pirbalouty and Wägele 2010), new record for Kuwait.

Family Olibrinidae Budde-Lund, 1913
Genus *Olibrinus* Budde-Lund, 1913

***Olibrinus antennatus* Budde-Lund, 1902**

Olibrinus antennatus Budde-Lund, 1902: 379, Malaysia (type locality); Schmalfuss, 2003: 182; Taiti & Ferrara, 2004: 223, pl. 4.

Material examined. 1 ♀; St. 3; 29°39.403'N, 48°07.450'E; 24 Nov. 2014.

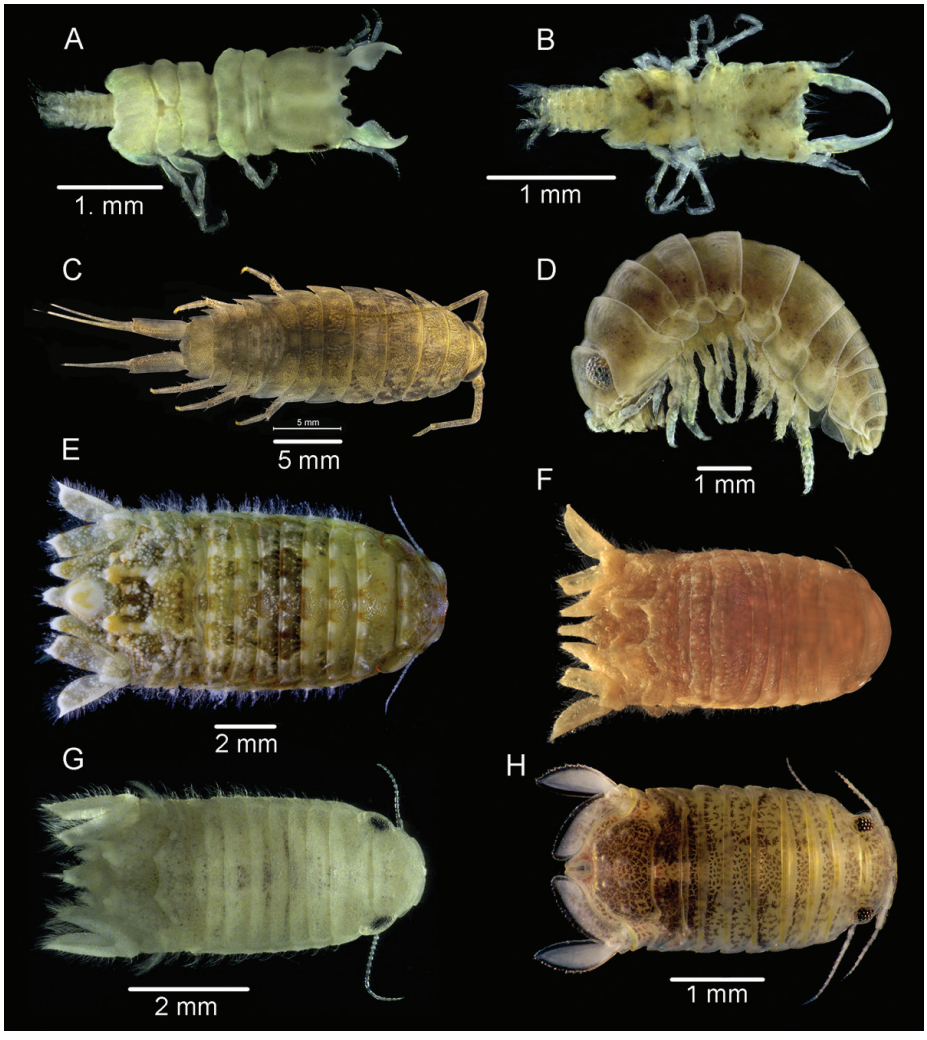

Figure 3. A *Gnathia* sp. from Al-Nuwaiseeb **B** *Elaphognathia* sp., from Al-Shamaimah **C** *Ligia persica* from Al-Nuwaiseeb **D** *Tylos maindroni* Giordani Soika, 1954 from Kubbar Island **E** *Cymodoce delvarii* Khalaji-Pirbalouty, Bruce & Wägele, 2013 from Al-Nuwaiseeb **F** *C. fuscina* Schotte & Kensley, 2005 from USNM **G** *C. waegelei* Khalaji-Pirbalouty & Raupach,, 2014 from Al-Nuwaseeb **H** *Dynamenella granulata* Javed & Ahmed, 1988 from Um-Almaradim.

Distribution. Indian Ocean (Taiti and Ferrara 2004), coastal waters of Iran (Khalaji-Pirbalouty, unpublished data), new record for Kuwait.

Family Tylidae Milne-Edwards, 1840
Genus *Tylos* Audouin, 1826

***Tylos maindroni* Giordani Soika, 1954**
Figure 3D

Tylos maindroni Giordani Soika, 1954: 76, figs 8, 9, pl. 10, Oman Sea, Muscat (type locality); Ferrara & Taiti, 1986: 94; Taiti & Ferrara, 1991: 213, fig. 3; Taiti et al. 2000: 148.
Tylos sp. Jones, 1986: 149, pl. 40.

Material examined. 2 juveniles; St. 4; (1 ♀); St. 28; 11 Nov. 2014; 2 ♂♂, 2 ♀♀; St. 33; 29°04.377'N, 48°29.472'E; (1 ♀, 3 juveniles); St. 35; 29°23.710'N, 48°24.136'E; 25 Dec. 2014; 1 ♀, 4 juveniles; St. 38; 29°22.726'N, 48°26.269'E; 22 Dec. 2014.

Distribution. Oman, Kuwait (Taiti and Ferrara 1991); Bandar-e-Charak, Bandar-e Bostanoo, Iran (Khalaji-Pirbalouty, unpublished data).

Suborder Sphaeromatidea Wägele, 1989
Family Sphaeromatidae Latreille, 1825
Genus *Cymodoce* Leach, 1814

***Cymodoce delvarii* Khalaji-Pirbalouty, Bruce & Wägele, 2013**
Figure 3E

Cymodoce delvarii Khalaji-Pirbalouty et al.,, 2013: 523–528, figs 16–19; Boushehr Province, Iran (type locality).
Cymodoce richardsoniae Jones, 1986: 149, pl. 40 [not *C. richardsoniae* Nobili, 1906; misidentification].

Material examined. 1 ♂, 1 ♀, 1 subadult ♂, 1 juvenile; St. 3; 29°39.403'N, 48°07.850'E; 24 Nov. 2014; 6 ♂♂ 25 ♀♀, 6 sub adult ♂♂; St. 12; 29°23.481'N, 47°59.800'E; 8 Dec. 2013; 1 juvenile St.15; 29°16.496'N, 48°05.407'E; 18 Dec. 2013; 1 ♀, 1 sub-adult ♂, 1 juvenile; St.18; 29°06.041'N, 48°08.323'E; 1 Feb. 2014; 1 ♀; St.19; 29°04.431'N, 48°08.676'E; 10 Dec. 2014; 2 juveniles; St. 25; 28°38.813'N, 48°23.429'E; 3 Mar. 2014; 4 ♀♀, many juveniles; St. 26; 28°34.794'N, 48°24.078'E; 4 Mar. 2014; 1 ♀; St. 28; 28°40.939'N, 48°39.196'E; 11 Nov. 2014; 1 ♀; St. 32; 29°04.278'N, 48°29.655'E; 9 Nov. 2014; 1 ♂, 15 ♀♀; St. 34; 29°22.726'N, 48°26.269'E; 10 Feb. 2016; 1 ♀; St. 35; 29°23.710'N, 48°24.136'E; 25 Dec. 2014; 2 ♂♂, 26 ♀♀, many juveniles; St. 36; 29°23.629'N, 48°23.958'E; 24 Dec. 2014.

Distribution. Bousher Province, Iran (Khalaji-Pirbalouty, Bruce and Wägele 2013), new record for Kuwait.

Cymodoce fuscina Schotte & Kensley, 2005

Figure 3F

Cymodoce fuscina Schotte & Kensley, 2005: 1245–1248, figs 19–20, Safaniya and Manifa, Saudi Arabia (type locality); Ulman et al. 2017: 27.
Cymodoce sp. Jones, 1986: 149, pl. 40.

Material examined. 2 ♂♂ and 3 ♀♀; Kuwait Fishery Station (from Smithsonian Natural History Museum collection, USNM 1145230).

Distribution. Saudi Arabia, United Arab Emirates, the Mediterranean basin, Greece (Schotte and Kensley 2005; Ulman et al. 2017), new record for Kuwait.

Cymodoce waegelei Khalaji-Pirbalouty & Raupach, 2014

Figure 3G

Cymodoce waegelei Khalaji-Pirbalouty & Raupach, 2014: 242–249, figs 7–12, Boushehr Province, Iran (type locality); Khalaji-Pirbalouty et al. 2015: 34, fig. 2.

Material examined. 2 ♂♂, 3 ♀♀; St. 25; 28°38.813'N, 48°23.429'E; 3 Mar. 2014; 4 ♂♂, 9 ♀♀; St. 26; 28°34.794'N, 48°24.078'E; 4 Mar. 2014; 1 ♂, 1 ♀ St. 27; 28°40.778'N, 48°39.207'E; 11 Nov. 2014.

Distribution. Bousher Province and Hengam Island, Iran (Khalaji-Pirbalouty and Raupach 2014; Khalaji-Pirbalouty et al. 2015), new record for Kuwait.

Genus *Dynamenella* Hansen, 1905

Dynamenella granulata Javed & Ahmed, 1988

Figure 3H

Dynamenella granulata Javed & Ahmed, 1988: 234–236, figs 1–3, Karachi coast, Pakistan (type locality).

Materials examined. 1 juvenile; St. 25; 28°38.813'N, 48°23.429'E; 3 Mar. 2014; 1 sub-adult ♂, 2 ♀♀, 1 juvenile; St. 28; 28°40.939'N, 48°39.196'E; 11 Nov. 2014; 4 sub-adults ♂♂, 5 ♀♀, 5 juveniles; St. 33; 29°04.377'N, 48°29.472'E; 9 Nov. 2014.

Distribution. Pakistan and Iran coasts (Javed & Ahmed, 1988; Khalaji-Pirbalouty unpublished data), new record for Kuwait.

Genus *Heterodina* Schotte & Kensley, 2005

***Heterodina mccaini* Schotte & Kensley, 2005**
Figure 4A

Heterodina mccaini Schotte & Kensley, 2005: 1259–1261, figs 27, 28, Manifa, Saudi Arabia (type locality).

Material examined. > 100 ♂♂ and ♀♀; St. 7; 29°22.497'N, 47°45.183'E; 2 Feb. 2014; 1 ♀; St. 8; 29°23.047'N, 47°50.192'E; 7 ♀♀; St. 12; 29°23.481'N, 47°59.800'E; 8 Dec. 2013; 8 ♂♂, > 100 ♀♀ and Juveniles; St. 19; 47°59.800'N, 48°08.676'E; 10 Dec. 2014; 1 ♀; St. 21; 29°00.071'N, 48°09.853'E; 16 Feb. 2014; 5 ♂♂, 23 ♀♀; St. 25; 28°38.813'N, 48°23.429'E; 3 Mar. 2014; > 100 ♂♂ and ♀♀; St. 26; 28°34.794'N, 48°24.078'E; 4 Mar. 2014; 2 ♀♀, 1 juvenile; St. 32; 29°04.278'N, 48°29.655'E; 9 Nov. 2014; 2 ♀♀; St. 34; 29°22.726'N, 48°26.269'E; 10 Feb. 2016; 1 ♂, 1 ♀; St. 37; 29°25.625'N, 48°20.307'E; 23 Dec. 2014; 3 ♀♀; St. 38; 29°28.049'N, 48°17.838'E; 22 Dec. 2014.

Distribution. Manifa and Ras Tanajib, Saudi Arabia (Schotte and Kensley 2005), new record for Kuwait.

Genus *Sphaeroma* Bosc, 1802

***Sphaeroma walkeri* Stebbing, 1905**
Figure 4B

Sphaeroma walkeri Stebbing, 1905: 31–33, pl. VII, Jokkenpiddi Paar, Sri Lanka (type locality). Latest synonymies to the species can be found in Martínez-Laiz et al., (2018: 13).

Material examined. 8 ♂♂, 5 ♀♀, 10 juveniles; St. 24; 28°44.502'N, 48°22.950'E; 8 Jan. 2015; 9 ♀♀; St. 25; 28°38.813'N, 48°23.429'E; 3 Mar. 2014.

Distribution. *Sphaeroma walkeri* is one the most widespread species of the marine isopods, reported along the Indian, Atlantic, and Pacific oceans coastal zones (Khalaji-Pirbalouty and Wägele 2010c; Martínez-Laiz et al. 2018).

***Sphaeroma khalijfarsi* Khalaji-Pirbalouty & Wägele, 2010**
Figure 4C

Sphaeroma khalijfarsi Khalaji-Pirbalouty & Wägele, 2010c: 3–9, figs 1–5, Qeshm Island, Iran (type locality).

Material examined. 3 ♀♀, 25 juveniles; St. 4; 29°34.849'N, 48°10.248'E; 25 Nov. 2014; 1 juvenile; St. 17; 29°08.154'N, 48°07.985'E; 4 Jan. 2014; 2 ♀♀; St.

26; 28°34.794'N, 48°24.078'E; 4 Mar. 2014; 2 ♂♂, 6 ♀♀, 6 juveniles; St. 39; 29°38.993'N, 48°18.830'E; 24 Jan. 2015; 4 ♂♂, 25 ♀♀, 21 juveniles; St. 40; 29°48.093'N, 48°21.975'E; 25 Jan. 2015.

Distribution. Qeshm Island, Bandare Abbas, Bandare Kolahi, Iran (Khalaji-Pirbalouty and Wägele 2010c), new record for Kuwait.

Sphaeroma annandalei Stebbing, 1911

Sphaeroma annandalei Stebbing, 1911: 181, pl. X, West Bengal, India (type locality); Barnard, 1936: 174; Barnard, 1940: 405; Pillai, 1955: 134, figs 23–35, pl. VII; Joshi & Bal, 1959: 62; Kensley, 1978: 113; Jones, 1986: 149, pl. 40; Khalaji-Pirbalouty & Wägele, 2010: 31–37, figs 1–5.
Sphaeroma irakiensis irakiensis Ahmed, 1971: 77–79, fig. 1.

Distribution. India, Habbanyyah Lake, and Shat Al- Arab River (Iraq); Arvand Kenar (Iran); Kuwait.

Genus *Sphaeromopsis* Holdich & Jones, 1973

Sphaeromopsis sarii Khalaji-Pirbalouty & Wägele, 2009

Figure 4D

Sphaeromopsis sarii Khalaji-Pirbalouty & Wägele, 2009: 34–42, figs 1–5, Kish Island, Iran (type locality).

Material examined. 1 ♀; St. 4; 29°34.849'N, 48°10.248'E l; 25 Nov. 2014; 3 ♀♀l; St. 12; 29°23.481'N, 47°59.800'E; 8 Dec. 2013; 100 ♂♂ and ♀♀; St. 15; 29°16.496'N, 48°05.407'E; 2 ♂♂, 15 ♀♀; St. 18; 29°06.041'N, 48°08.323'E; 1 Feb. 2014; 1 ♂, 10 ♀♀; St. 21; 29°00.071'N, 48°09.853'E; 16 Feb. 2014; 2 ♂♂, 12 ♀♀, 2 Juveniles; St. 24; 28°44.502'N, 48°22.950'E; 8 Jan. 2015; 3 ♂♂, 8 ♀♀; St. 25; 28°38.813'N, 48°23.429'E; 3 Mar. 2014; 1 ♀; St. 26; 28°34.794'N, 48°24.078'E; 4 Mar. 2014; 22 ♂♂, 9 ♀♀, 2 juveniles; St. 27; 28°40.778'N, 48°39.207'E; 11 Nov. 2014; 28 ♂♂, 31 ♀; St. 28; 28°40.939'N, 48°39.196'E; 11 Nov, 2014; 35 ♂♂ and ♀♀; St. 29; 28°40.960'N, 48°39.173'E; 11 Nov. 2014; > 100 ♂♂ and ♀♀; St. 30; 28°49.105'N, 48°46.553'E; 10 Nov. 2014; 3 ♂♂, 43 ♀♀; St. 31; 28°49.022'N, 48°46.607'E; 10 Nov. 2014; > 100 ♂♂ and ♀♀; St. 32; 29°04.278'N, 48°29.655'E; 9 Nov. 2014; 9 ♂♂, 12 ♀♀, 3 juveniles; St. 33; 29°04.377'N, 48°29.472'E; 9 Nov. 2014 13 ♂♂, 14 ♀♀; St. 34; 29°22.726'N, 48°26.269'E; 10 Feb. 2016; > 100 ♂♂ and ♀♀, St. 36; 29°23.629'N, 48°23.958'E; 10 Feb. 2016; > 100 ♂♂ and ♀♀; St. 37; 29°25.625'N, 48°20.307'E; 23 Dec. 2014.

Distribution. Kish, Qeshm, Hengam Islands, Iran (Khalaji-Pirbalouty and Wägele 2009; Khalaji- Pirbalouty et al. 2015), new record for Kuwait.

Suborder Valvifera Sars, 1882
Family Arcturidae Sars, 1897
Genus *Arcturinoides* Kensley, 1977

***Arcturinoides angulata* Kensley, Schotte & Poore, 2007**
Figures 4E, 7F

Arcturinoides angulata Kensley et al., 2007: 433–436, figs 3, 4, Kuwait Bay (type locality).

Material examined. 1 ♀; St. 7; 29°22.497'N, 47°45.183'E; 2 Feb. 2014; 1 ♀; St. 8; 29°23.047'N, 47°50.192'E; 3 Feb. 2014; 2 ♂♂; St. 34; 29°22.726'N; 48°26.269'E; 10 Feb. 2016; 1 ♂; St. 35; 29°23.710'N, 48°24.136'E; 25 Dec. 2014.

Distribution. United Arab Emirates, Kuwait Bay, Kuwait (Kensley et al. 2007).

Genus *Astacilla* Cordiner, 1793

***Astacilla mccaini* Kensley, Schotte & Poore, 2007**
Figure 4G, H

Astacilla mccaini Kensley et al., 2007: 437–440, figs 5, 6, Manifa Bay, Saudi Arabia (type locality).

Material examined. 10 ♂♂; St. 20; 29°8.043'N, 48°9.139'E; 28 Sep. 2014; 1 ♀; St. 21; 29°00.071'N, 48°09.853'E; 16 Feb. 2014; 1 ♂; St. 34; 29°22.726'N, 48°26.269"E; 10 Feb. 2016; 1 ♂; St. 35; 29°23.710'N, 48°24.136'E; 25 Dec. 2014; 6 ♂♂, 2 ovigerous ♀♀, 2 juveniles; St. 36; 29°23.629'N, 48°23.958'E; 25 Dec. 2014.

Distribution. Manifa Bay, Saudi Arabia; Kuwait Bay, Kuwait (Kensley et al. 2007).

Suborder Asellota Latreille, 1802
Family Paramunnidae Vanhöffen, 1914
***Heterosignum* Gamô, 1976**

Type species. *Heterosignum mutsuensis* Gamô, 1976

***Heterosignum* sp.**

Material examined. 3 ♀; St. 28; 28°40.939'N, 48°39.196'E; 11 Nov, 2014; 1 ♀; St. 25; 28°38.813'N, 48°23.429'E; 3 Mar. 2014.

Distribution. New record for Kuwait.

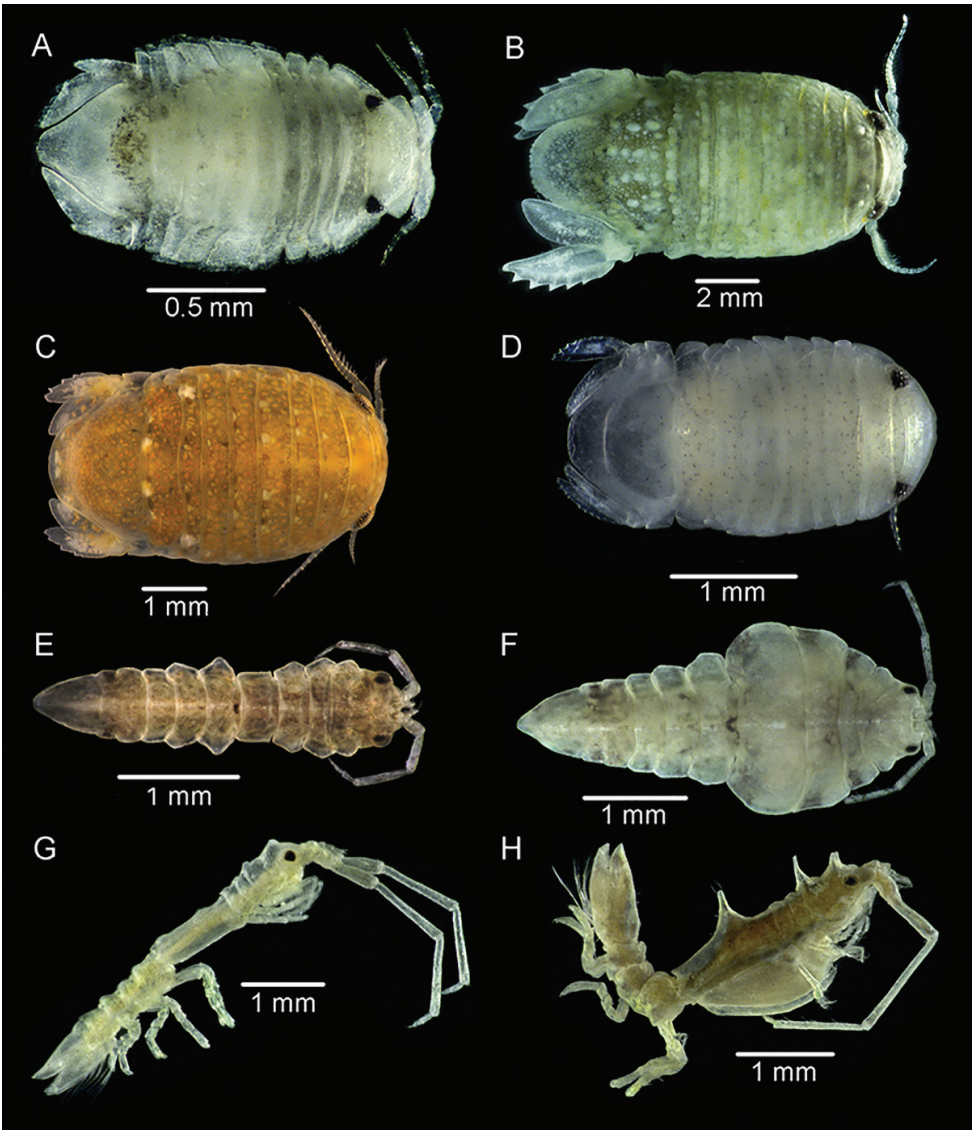

Figure 4. A *Heterodina mccaini* Schotte & Kensley, 2005 from Al-Nuwaiseeb **B** *Sphaeroma walker* Stebbing, 1905 from Al-Zhor **C** *S. khalijfarsi* Khalaji-Pirbalouty & Wägele, 2010 from Boubyan Island **D** *Sphaeromopsis sarii* Khalaji-Pirbalouty & Wägele, 2009 from Kubbar Island **E** *Arcturinoides angulata* Kensley, Schotte & Poore, 2007 ♂, from Al-Doha **F** *A. angulata* ♀ from Al-Doha **G** *Astacilla mccaini* Kensley, Schotte & Poore, 2007 ♂, from Failaka Island **H** *A. mccaini* ♀, from Failaka Island.

Discussion

Bowmen and Tareen (1983) were the first to study Kuwait's isopod fauna, recording nine species of Cymothoidae, all ectoparasitic on marine fishes (Table 6). Jones (1986) included six isopod species in his 'Field Guide to the Seashores of Kuwait': *Apanthura sandalensis*, *Ligia exotica*, and *Cymodoce richardsoniae* are reidentified as

Amakusanthura sp., *L. persica*, and *C. delvarii*, respectively. Moreover, *Cymodoce* sp. of Jones (1986) is reidentified as *Cymodoce fuscina* and *Tylos* sp. is identified as *Tylos maindroni*. The widespread supratidal isopod *Tylos maindroni* was previously reported from Kuwait by Taiti and Ferrara (1991). However, *Sphaeroma annandalei* Stebbing, 1911 was not found in the current study: the known distribution of *S. annandalei* is from the West Bengal estuaries in India to the Arvandroud (Shatt-Al-Arab) riverbanks between Iran and Iraq (Khalaji-Pirbalouty and Wägele 2010).

Two additional species, *Arcturinoides angulata* and *Astacilla mccaini*, were collected from Kuwait Bay by Kensley et al. (2007). In monitoring the fauna of recently dredged canals in the Al-Khiran area of Kuwait, Jones and Nithyanandan (2012) discovered and described two new isopod species from Kuwait and mentioned the occurrence of a third, increasing the valid species of Isopoda recorded from Kuwait to 17. With the present survey, we now count 38 species of Isopoda, more than doubling Kuwait's known isopod fauna. Twenty-one of the 25 species collected for this study represent first records for Kuwait (Table 2). Only four of these 25 species were reported previously: *Eurydice peraticis*, *Tylos maindroni*, *Arcturinoides angulata*, and *Astacilla mccaini*.

The geographical distribution of isopod species in Kuwait waters show very different patterns. The burrowing isopod *Sphaeroma walkeri* was found living in soft rocks in the high intertidal area of the Al-Zour coast. The type locality of this species is Sri Lanka, and it has been considered restricted to the northern Indian Ocean. This thermophilic species is also tolerant to a range of salinities, and its distribution is worldwide in the tropics (Ríos-Touma et al. 2017). The ranges of other species are also limited to the Indian Ocean. For example, *Lanocira gardineri*, is widely distributed from western Australia (Bruce and Sidabalok 2011) and the Maldives, Kenya, and Madagascar (Delaney 1989). Delaney (1989) recorded it from the Khor Abdullah estuary, Iraq, in the northwestern Gulf. Tolerance of salinity fluctuations is believed to be a primary reason for the wide distribution of this species throughout the Indian Ocean. Other species, such as *Dynamenella granulata*, and *Atarbolana exoconta*, are widely distributed along the northeastern coast of the Gulf and along the Pakistani coast. Their distribution pattern is similar to some brachyuran decapods as suggested by Apel and Türkay (1999) and Naderloo et al. (2011). According to this distribution pattern, the fiddler crab fauna of the southern and western Gulf is similar in East Africa, the Gulf of Aden, and the Red Sea. At the same time, the fauna of the northeastern parts of the Persian Gulf is also somewhat similar to that of the northeastern Arabian Sea coasts of Pakistan and India. Finally, some of the known species of isopoda (e.g., *Heterodina mccaini* ; *Sphaeroma khalijfarsi*, and *Sphaeromopsis sarii*) are indigenous to the Gulf.

The new results reveal a low species richness of Isopoda in Kuwait waters compared to the adjacent regions of the Indian Ocean. Based on Kensley's (2001) isopod checklist, the Indian Ocean exhibits a high species diversity of more than 1000 species. Of these, 268 species inhabit the Indian coastal region, and fewer than half that number, 121 species, has been recorded from Pakistan's coast by Kazmi et al. (2002). The apparently low species richness of Isopoda in the Kuwait region compared to that of other areas of the Indian Ocean is due to Kuwait's limited coastline, less than 200 km, but also to the Gulf's young age, less than 6,000 years BP (Sheppard et al. 2010), and the harsh

environmental conditions. The age of the environment is an essential factor for the evolution of diversity (Gaston and Chown 1999). The seabed regions of the Gulf presently at depths of 4–6 m have only been submerged for 3,000–4,000 years (Sheppard et al. 2010). Therefore, the current coastal habitat development is comparatively young.

The harsh environmental conditions in Kuwait coastal zone arise from high temperatures and high salinity. Salinities exceed 40 PSU, and summer temperatures often exceed 35 °C. For instance, from 2000 to 2013, the mean seawater temperature in Kuwait Bay was 23.6 °C with a range of 9.7–36.0 °C, and salinity ranged from 30–46 PSU (Al-Yamani et al. 2004). Furthermore, extreme air temperatures with highs up to 55°C in the summer months and winter lows around freezing are known from Kuwait (Jones 1986).

However, a comparison between this study and restricted localities of similar size suggested no lower diversity in Kuwait. Brusca (1987) reported 36 species of marine isopods from the Galapagos. Seventeen species of these were shallow-water species from the littoral to a depth of 100 m. Furthermore, Kensley (1984) identified only 24 species of isopods from the Belizean reef crest. The low species composition of these studies may arise from limited sampling. This study focuses on the Kuwaiti shoreline; therefore, many species living in sub-tidal depths were not collected.

Some isopod species appear to be introduced into Kuwait Bay from outside of the Gulf. For example, *Cymodoce fuscina* and *C. waegelei* were found in the subtidal zone of the Iranian and Arabian coasts of the Gulf, but were also recently reported from the Mediterranean basin, Greece (Ulman et al. 2017) and Egypt (pers. obs.). This distribution supports the hypothesis of a human- assisted introduction, such as through ballast water discharge. According to the Public Relations Department of Hormozgan Ports, Iran, ca. 53,000 tanker and cargo ships enter the Gulf annually and ca. 40% of the world's total oil transportation passes through the Strait of Hormuz (Al-Yamani et al. 2015). In this context, ships transport a billion tonnes of ballast water annually, so although this intertidal study was comprehensive, it was only limited to sampling in the intertidal zone. Repeated sampling during different seasons as well as subtidal investigations would certainly increase Kuwait's known isopod fauna.

The present study provides a baseline account of Kuwait's coastal zone isopod fauna. The next step will be evaluating their ecology and conservation status. As Kuwait is one of the major oil exporters, invasive species are a significant issue, mainly due to the discharge of ballast water from oil tankers and cargo ships. Therefore, prevention is crucial for decision-making and implementation of invasion control and detection of new exotics. The results of this study highlight the need for further morphological as well as molecular studies to clarify the taxonomic status of some specimens, and a larger sampling effort in deeper waters of this area.

Acknowledgements

Gratitude to the Kuwait Petroleum Company (KPC) and the Kuwait Institute for Scientific Research (KISR) for providing financial support for this project. Special thanks to Miss Zainab Sattari for her support during the project with fieldwork and data

entry, and Miss Muneera Aljeri for preparing the GIS map. We thank especially Dr. James Bishop for his helpful suggestions on the first draft of the manuscript. Dr. Wolfgang Wägele (Zoological Research Museum Alexander Koenig, Bonn), Dr. Gary Poore (Museums Victoria), Dr. Niel Bruce (Queensland Museum), Dr. Lena Hartebrodt (University of Auckland), Dr. Brenda Doti (Universidad de Buenos Aires, Argentina), and Dr. Rachael Peart (National Institute of Water and Atmospheric Research, New Zealand) are thanked for their constructive suggestions and comments that improved the manuscript. Extended thanks to all KISR staff in project FM075C for helping in macrofauna sampling in the field and sample processing in the laboratory.

References

Abu-Hakima R (1984) Preliminary observations on the effects of *Epipenaeon elegans* Chopra (Isopoda: Bopyridae) on reproduction of *Penaeus semisulcatus* de Haan (Decapoda; Penaeidae). International Journal of Invertebrate Reproduction and Development 7: 51–62. https://doi.org/10.1080/01688170.1984.10510071

Al-Kandari M, Sattari Z, Hussain S, Radashevsky VI, Zhadan A (2019a) Checklist of intertidal polychaetes (Annelida) of Kuwait, Northern part of the Arabian Gulf. Regional Studies in Marine Science 32: e100872. https://doi.org/10.1016/j.rsma.2019.100872

Al-Kandari M, Oliver G, Chen W, Taqi A, Skryabin V, Yousif A, Raghu M, Al-Jazzaf S, Al-Hamad A (2019b) Diversity and distribution of the intertidal Mollusca of the State of Kuwait, Arabian Gulf. Regional Studies in Marine Science 33: e100905. https://doi.org/10.1016/j.rsma.2019.100905

Al-Kandari M, De Grave S, Hussain S, Anker A (2020a) Five New Records of Mantis Shrimps (Stomatopoda) From Kuwait. Crustaceana 93: 671–675. https://doi.org/10.1163/15685403-642bja10011

Al-Kandari M, Anker A, Hussain S, AL-Yassen Sh, Sattari Z, De Grave S (2020b) New records of decapod crustaceans from Kuwait (Malacostraca: Decapoda). Zootaxa 4803: 251–280. https://doi.org/10.11646/zootaxa.4803.2.2

Al-Kandari M, Bishop J, Chen W, Skryabin V, Polikarpov I, Sattari Z, Taqi A, Hussain S (2017) Biodiversity, Distribution and Abundance of Intertidal Macrofauna in Kuwait. Final Report FM075C, KISR 14461, Kuwait Institute for Scientific Research.

Al-Yamani F, Skryabin V, Durvasula SRV (2015) Suspected ballast water introductions in the Arabian Gulf. Aquatic Ecosystem Health and Management 18: 282–289. https://doi.org/10.1080/14634988.2015.1027135

Al-Yamani FY, Skryabin V, Boltachova N, Revkov N, Makarov M, Grinstov V, Kolesnikova E (2012) Illustrated Atlas on the Zoobenthos of Kuwait. Kuwait Institute for Scientific Research, 383 pp.

An J, Boyko CB, Li X (2015) A Review of Bopyrids (Crustacea: Isopoda: Bopyridae) Parasitic on caridean Shrimps (Crustacea: Decapoda: Caridea) from China. Bulletin of the American Museum of Natural History 399: 1–85. https://doi.org/10.1206/amnb-921-00-01.1

Apel M, Türkay M (1999) Taxonomic composition, distribution and zoogeographic of the grapsid and ocypodid crab fauna of intertidal soft bottoms in the Arabian Gulf. Estuarine, Coastal and Shelf Science 49: 131–142. https://doi.org/10.1016/S0272-7714(99)80018-3

Barnard KH (1914) Contributions to the crustacean fauna of South Africa, 3. Additions to the marine Isopoda, with notes on some previously incompletely known species. Annals of the South African Museum 10: 325–442. https://doi.org/10.5962/bhl.part.9319

Bowman TE, Tareen IU (1983) Cymothoidae from Fishes of Kuwait (Arabian Gulf) (Crustacea: Isopoda). Smithsonian Contributions to Zoology, 30 pp. https://doi.org/10.5479/si.00810282.382

Bruce NL (1980) The systematics of some Japanese marine isopod Crustacea (Fam. Sphaeromatidae) of the genera *Dynoides* Barnard, 1914 and *Cymodocella* Pfeffer, 1887, with description of two new species. Crustaceana 38: 199–211. https://doi.org/10.1163/156854080X00643

Bruce NL (1986) Cirolanidae (Crustacea: Isopoda) of Australia. Records of the Australian Museum 6: 1–239. https://doi.org/10.3853/j.0812-7387.6.1986.98

Brusca RC (1987) Biogeographic relationships of Galapagos marine isopod crustaceans. Bulletin of Marine Science 41: 268–281.

Bruce NL, Javed W (1987) A new genus and species of cirolanid isopod Crustacea from the northern Indian Ocean. Journal of Natural History 21: 1451–1460. https://doi.org/10.1080/00222938700770911

Bruce NL, Sidabalok C (2011) The genus *Lanocira* Hansen, 1890 (Corallanidae: Isopoda: Crustacea) in tropical Australian waters. Zootaxa 2793: 23–34. https://doi.org/10.11646/zootaxa.2793.1.2

Brusca RC, Brusca GJ (2003) Invertebrates. Sinauer Associates, Sunderland, 936 pp.

Brusca RC, Coelho V, Taiti S (2001) A guide to the Costal Isopods of California. http://tolweb.org/notes/?note_id=3004

Budde-Lund G (1902) A list of terrestrial isopods. In: Lanchester W (Ed.) On the Crustacea collected during the Skeat Expedition to the Malay Peninsula. Proceedings of the Zoological Society of London 1902: 379–381.

Chopra B (1923) Bopyrid isopods parasitic on Indian Decapoda Macrura. Records of the Indian Museum 25: 411–550. [pls 11–21]

Dawson CE1 (1958) Observations on the infection of the shrimp, *Penaeus semisulcatus*, by *Epipenaeon elegans* in the Persian Gulf. Journal of Parasitology 44: 240–241. https://doi:10.2307/3274711

Delaney PM (1989) Phylogeny and biogeography of the marine isopod family Corallanidae (Crustacea, Isopoda, Flabellifera). Contributions to Science, Natural Museum of Los Angeles County 409: 1–75. https://doi.org/10.5962/p.226815

Eleftheriou A, Jones DA (1976) The genus *Eurydice* on the west coast of India. Journal Zoological Society London 178: 385–394. https://doi.org/10.1111/j.1469-7998.1976.tb02276.x

Eslami F, Mokhayer B (2002) Occurrence of Bopyridae parasite (*Epipenaeon elegans*) in green tiger shrimp in the Persian Gulf (Bushehr Waters). Iranian Scientific Fisheries Journal 10: 89–96.

Gamô S (1976) *Heterosignum mutsuensis* gen. nov., sp. nov., a new isopod crustacea from Mutsu Bay, northern Japan (Paraselloidea, Munnidae). Proceedings of the Japanese Society of Systematic Zoology 12: 39–45.

Gaston KJ, Chown SL (1999) Elevation and climatic tolerance: a test using dung beetles. Oikos 86: 584–590. https://doi.org/10.2307/3546663

Giordani Soika A (1954) Ecologia, sistematica, biogeografia ed evoluzione del *Tylos latreillei* 703 auct. (Isop. Tylidae). Bollettino del Museo civico di Storia naturale di Venezia 7: 63–83.

Javed W, Ahmed R (1988) Two new species of the genus *Dynamenella* from the northern Arabian Sea (Isopoda). Crustaceana 55: 234–241. https://doi.org/10.1163/156854088X00320

Jones DA (1974) The systematics and ecology of some sand beach isopods (Family Cirolanidae) from the coasts of Saudi Arabia. Crustaceana 26: 201–211. https://doi.org/10.1163/156854074X00569

Jones DA (1982) New isopods of the genus *Lanocira* (Corallanidae) from the Indian Ocean region. Crustaceana 42: 65–75. https://doi.org/10.1163/156854082X00704

Jones DA (1986) A field guide to the sea shores of Kuwait and the Arabian Gulf. University of Kuwait, Distributed by Blandford Press, Dorset, 192 pp.

Jones DA, Nithyanandan M (2012) Taxonomy and distribution of the genus *Eurydice* Leach, 1815 (Crustacea, Isopoda, Cirolanidae) from the Arabian region, including three new species. Zootaxa 716(3314): 45–57. https://doi.org/10.11646/zootaxa.3314.1.4

Kazmi QBM, Schotte M, Yousof F (2002) An illustrated key to the Malacostraca (Crustacea) of the Northern Arabian Sea, Part V: Isopoda. Pakistan Journal of Marine Sciences 11: 47–116.

Kensley B (1978) Guide to the Marine Isopods of Southern Africa. South African Museum & The Rustica Press, Wynberg, Cape Town, 173 pp.

Kensley B (1984) The role of isopod crustaceans in the reef crest community at Carrie Bow Cay, Belize. Marine Ecology 5: 29–44. https://doi.org/10.1111/j.1439-0485.1984.tb00305.x

Kensley B (2001) Biogeography of the marine Isopoda of the Indian Ocean, with a checklist of species and records. In: Brusca RC, Kensley B (Eds) Isopod Systematics and Evolution. Crustaceana 13: 205–264.

Kensley B, Schotte M, Poore GCB (2007) New species and records of valviferan isopods (Crustacea: Isopoda: Valvifera) from the Indian Ocean. Proceedings of the Biological Society of Washington 120: 429–445. https://doi.org/10.2988/0006-324X(2007)120[429:NSAROV]2.0.CO;2

Kensley B, Schotte M, Poore GCB (2009) Gnathiid isopods (Crustacea: Isopoda: Gnathiidae), mostly new, from the Indian Ocean. Proceedings of the Biological Society of Washington 122(1): 32–51. https://doi.org/10.2988/07-16.1

Khalaji-Pirbalouty V, Bruce, NL (2014) A review of the genus *Heterodina* Kensley & Schotte, 2005 (Crustacea: Isopoda: Sphaeromatidae) with description of a new species from Iran. Zootaxa 3887: 494–500. https://doi.org/10.11646/zootaxa.3887.4.7

Khalaji-Pirbalouty V, Bruce NL, Wägele JW (2013) The genus *Cymodoce* Leach, 1814 (Crustacea: Isopoda: Sphaeromatidae) in the Persian Gulf with description of a new species. Zootaxa 3686: 501–533. https://doi.org/10.11646/zootaxa.3686.5.1

Khalaji-Pirbalouty V, Hajializadeh P, Sourinejad I (2015) A Report on the Isopods of the Coastal Waters of the Persian Gulf: the Hengam Island. Journal of the Persian Gulf 6: 33–38.

Khalaji-Pirbalouty V, Raupach MJ (2014) A new species of *Cymodoce* Leach, 1814 (Crustacea: Isopoda: Sphaeromatidae) based on morphological and molecular data, with a key to the Northern Indian Ocean species. Zootaxa 3826(1): 230–254 https://doi.org/10.11646/zootaxa.3826.1.7

Khalaji-Pirbalouty V, Raupach MJ (2016) DNA barcoding and morphological studies confirm the occurrence of three *Atarbolana* (Crustacea: Isopoda: Cirolanidae) species along the coastal zone of the Persian Gulf and Gulf of Oman. Zootaxa 4200: 153–173. https://doi.org/10.11646/zootaxa.4200.1.7

Khalaji-Pirbalouty V, Wägele JW (2009) Two new species of *Sphaerompsis* (Crustacea: Isopoda: Sphaeromatidae) from Persian Gulf. Zootaxa 2305: 33–50. https://doi.org/10.11646/zootaxa.2305.1.3

Khalaji-Pirbalouty V, Wägele JW (2010a) A new record of *Sphaeroma annandalei* Stebbing, 1911 (Crustacea: Isopoda: Sphaeromatidae) from the Persian Gulf, and description of a new related species (*Sphaeroma silvai* nov. sp.) from the South Atlantic Ocean. Zootaxa 2508: 30–752. https://doi.org/10.11646/zootaxa.2508.1.2

Khalaji-Pirbalouty V, Wägele JW (2010b) Two new species of *Ligia* Fabricius, 1798 (Crustacea: Isopoda: Ligiidae) from coasts of the Persian and Aden gulfs. Organisms Diversity and Evolution 10: 135–145. https://doi.org/10.1007/s13127-010-0003-5

Khalaji-Pirbalouty V, Wägele JW (2010c) A new species and a new record of *Sphaeroma* Bosc, 802 (Sphaeromatidae: Isopoda: Crustacea) from intertidal marine habitats of the Persian Gulf. Zootaxa 2631: 1–18. https://doi.org/10.1007/s13127-010-0003-5

Khalaji-Pirbalouty V, Wägele JW (2011) Two new species of cirolanid isopods (Crustacea: Isopoda: Cirolanidae) from Qeshm and Kish Islands in the Persian Gulf). Zootaxa 2930: 33–46. https://doi.org/10.11646/zootaxa.2930.1.3

Martínez-Laiz G, Ros M, Guerra-García JM (2018) Marine exotic isopods from the Iberian Peninsula and nearby waters. PeerJ 6: e4408. https://doi.org/10.7717/peerj.4408

Mathews CP, Samuel M (1987) The incidence of *Livoneca* sp. (Isopoda) on *Helotes sexlineatus* (Pisces) in Kuwait waters. Journal of Applied Ichthyology 3: 142–144. https://doi.org/10.1111/j.1439-0426.1987.tb00467.x

Monod T (1933) Mission Robert-Ph. Dollfus en Egypte, Tanaidacea et Isopoda. Memoires de l'Institut d'Egypte 21: 161–264.

Santucci R (1937) La *Ligia exotica* Roux sulle coste del Mar Rosso. Bollettino dei Musei e Laboratorii di Zoologia e Anatomia Comparata della R. Università di Genova 17: 1–10.

Naderloo R, Türkay M, Apel M (2011) Brachyuran crabs of the family Macrophthalmidae Dana, 1851 (Decapoda: Brachyura: Macrophthalmidae) of the Persian Gulf. Zootaxa 2911: 1–4. https://doi.org/10.11646/zootaxa.2911.1.1

Nierstrasz HF (1917) Die isopoden-sammlung im Naturhistorishen reichs-museum zu Leiden II. Cymothoidae, Sphaeromidae, Serolidae, Anthuridae, Idotheidae, Asellidae, Janiridae, Munnopsidae. Zoologische Mededelingen 3: 87–119.

Perry DM, Brusca RC (1989) Effects of the root-boring isopod *Sphaeroma peruvianum* on red mangrove forests. Marine Ecology Progress Series 57: 287–292. https://doi.org/10.3354/meps057287

Pillai NK (1967) Littoral and parasitic isopods from Kerala: Families Eurydicidae, Corallanidae and Aegidae. Journal of the Bombay Natural History Society 64: 267–283.

Poore GCB (2001) Families and genera of Isopoda Anthuridea. Crustacean Issues 13: 63–173.

Ríos-Touma B, Holzenthal RW, Huisman J, Thomson R, Rázuri-Gonzales E (2017) Diversity and distribution of the Caddisflies (Insecta: Trichoptera) of Ecuador. PeerJ 5: e2851. https://doi.org/10.7717/peerj.2851

Schotte M, Kensley B (2005) New species and records of Flabellifera from the Indian Ocean (Crustacea: Peracarida: Isopoda) Journal of Natural History 39: 1211–1282. https://doi.org/10.1080/00222930400005757

Sheppard C, Al-Husiani M, Al-Jamali F, Al-Yamani F, Baldwin R, Bishop J, Benzoni F, Dutrieux E, Dulvy NK, Durvasula SRV, Jones DA, Loughland R, Medio D, Nithyanandan M, Pilling GM, Polikarpov I, Price ARG, Purkis S, Riegl B, Saburova M, Samimi Namin K, Taylor O, Wilson S, Zainal K (2010) The Gulf: A young sea in decline. Marine Pollution Bulletin 60: 13–38. https://doi.org/10.1016/j.marpolbul.2009.10.017

Stebbing TRR (1904) Marine Crustaceans. XII. Isopoda, with description of a new genus. In: Gardiner JS (Ed.) Fauna and Geography of the Maldive and Laccadive Archipelagoes. University Press, Cambridge, 699–721.

Taiti S, Checcucci I (2011) Order Isopoda, suborder Oniscidea. In: Van Harten A (Ed.) Arthropod Fauna of the UAE 4: 33–58.

Taiti S, Ferrara F (1991) Terrestrial Isopods (Crustacea) from the Hawaiian Islands. Bishop Museum Occasional Papers 31: 202–227.

Taiti S, Ferrara F (2004) The terrestrial Isopoda (Crustacea: Oniscidea) of the Socotra Archipelago. Fauna of Arabia 20: 211–325.

Taiti S, Ferrara F, Davolos D (2000) The terrestrial Isopoda (Crustacea: Oniscidea) of Oman. Fauna of Arabia 18: 145–163.

Tareen IU (1985) First record of two bopyrid parasites of *Penaeus semisulcatus* from the Arabian Gulf. Kuwait Institute for Scientific Research, Technical Report 1845: 1–15.

Ulman A, Ferrario J, Occhpinti-Ambrogi A, Arvanitidis Ch, Bandi A, Bertolino M, Bogi C, Chatzigeorgiou G, Çiçek BA, Deidun A, Ramos-Esplà A, Koçak C, Lorenti M, Martinez- Laiz G, Merlo G, Princisgh E, Scribano G, Marchini A (2017) A massive update of non- indigenous species records in Mediterranean marinas. PeerJ 5: e3954. https://doi.org/10.7717/peerj.3954

ZooKeys 1080: 1356–163 (2022)
doi: 10.3897/zookeys.1080.69060
https://zookeys.pensoft.net

RESEARCH ARTICLE

A peer-reviewed open-access journal
ZooKeys
Launched to accelerate biodiversity research

Wing interference patterns are consistent and sexually dimorphic in the four families of crane flies (Diptera, Tipuloidea)

Robert T. Conrow[1], Jon K. Gelhaus[2]

1 *Department of Biodiversity, Earth & Environmental Sciences, Drexel University, 2024 MacAlister Hall Philadelphia, PA, 19104, USA* **2** *Department of Entomology, Academy of Natural Sciences of Drexel University, 1900 Benjamin Franklin Parkway, Philadelphia, PA, 19103, USA*

Corresponding author: Robert T. Conrow (rtconrow@gmail.com)

Academic editor: Netta Dorchin | Received 9 July 2021 | Accepted 26 August 2021 | Published 5 January 2022

http://zoobank.org/4B52C927-DCD0-43C4-8153-94A3DC02643B

Citation: Conrow RT, Gelhaus JK (2022) Wing interference patterns are consistent and sexually dimorphic in the four families of crane flies (Diptera, Tipuloidea). ZooKeys 1080: 1356–163. https://doi.org/10.3897/zookeys.1080.69060

Abstract

Wing interference patterns (WIP) are stable structural colors in insect wings caused by thin-film interference. This study seeks to establish WIP as a stable, sexually dimorphic, species-level character across the four families of Tipuloidea and investigate generic level WIP. Thirteen species of Tipuloidea were selected from museum specimens in the Academy of Natural Sciences of Drexel University collection. One wing from a male and female of each representative species was excised and mounted to a slide with coverslip, placed against a black background, and imaged using an integrated microscope camera. Images were minimally retouched but otherwise unchanged. Descriptions of the WIP for each sex of each species are provided. Twelve of thirteen species imaged had WIP, which were stable and species specific while eight of those twelve had sexually dimorphic WIP. Comparisons of three species of *Nephrotoma* were inconclusive regarding a generic level WIP. *Gnophomyia tristissima* had higher intraspecific variation than other species examined. This study confirms stable, species specific WIP in all four families of crane flies for the first time. More research must be done regarding generic-level stability of WIP in crane flies as well as the role sexual and natural selection play in the evolution of wing interference patterns in insects.

Keywords

Cryptic, Cylindrotomidae, dimorphism, Limoniidae, morphology, Pediciidae, Tipulidae, WIP

Introduction

Wing interference patterns (WIP) were historically known but only recently revealed to be a cryptic physical character of insect wings first reported by Shevtsova et al. (2011). WIP colors and patterns are stable regardless of the angle viewed, so are not iridescent (Shevtsova et al. 2011), but they exist thanks to the same physical property of light that generates iridescence in soap bubbles and oil slicks: thin film interference (Sun et al. 2013). Thin film interference occurs when light enters one of two parallel, thin, non-absorbing (i.e., light) layers, or films, and then bounces between the upper and lower films until exiting through one film (Sun et al. 2013). Thin film interference is most common in the clear wings of insects, with the two thin, chitinous layers forming the parallel thin films (Sun et al. 2013) and 20% of light passing into the wing being reflected between the planes, and exiting through the upper layer (Shevtsova et al. 2011). When the light exits the upper plane of the wing, the thickness of the chitin, as well as the microtopography of the wing at the point of exit will dictate the color observed (Shevtsova 2012). These patterns are created from stable structural properties of the wing, but our ability to observe them may be obscured against white or light-colored backgrounds or enhanced with a black background and bright light perpendicular to the plane of the wing (Shevtsova et al. 2011).

Research suggests that WIP are a novel morphological character that may be sexually selected for in some groups. Cryptic species have been discovered using WIP in two genera of wasps in the family Eulophidae (Shevtsova and Hansson 2011; Hansson and Hambäck 2013). Several works have used WIP as a character in describing a novel species (Buffington 2012; Mitroiu 2013) and as a character in a dichotomous key (Mitroiu 2013; Zhang et al. 2014). Sexual dimorphism of WIP has been documented in many groups of wasps and flies (Shevtsova et al. 2011; Shevtsova and Hansson 2011; Shevtsova 2012) and sexual selection of male WIP by female *Drosophila melanogaster* Meigen, 1830 has been observed (Katayama et al. 2014; Hawkes et al. 2019).

Most research on WIP in insects has focused on small Hymenoptera and Diptera with clear wings and reduced venation; the result is a continuous pattern across the wing. The existence of WIP in these groups has been well documented in the Cynipoidea (Buffington and Sandler 2011), Eulophidae (Hansson and Shevtsova 2010, 2012) and Drosophilidae (Shevtsova et al. 2011; Katayama et al. 2014; Hawkes et al. 2019). A few studies have looked at larger wasps (Shevtsova et al. 2011; Kangasniemi 2012) or larger flies (Shevtsova et al. 2011; Zhang et al. 2014) or other orders of insects like Odonata (Brydegaard et al. 2018) and Hemiptera (Simon 2013).

Crane flies (Tipuloidea) are one of the largest groups in Diptera with 15,632 recognized species and a global distribution (Oosterbroek 2021). Crane flies vary in wing length from 3 to 36 mm and occupy a diverse set of habitats (Gelhaus and Podenine 2019) and act as a major food source in aquatic and riparian ecosystems (Baxter et al.

2005; Gelhaus and Podeniene 2019). Furthermore, there is evidence of cryptic species within the superfamily (Ujvárosi et al. 2010; Salmela et al. 2014) and a lack of monophyly within the families (Petersen et al. 2010). Tipuloidea is represented in the WIP literature from a single male specimen of *Tipula* (*Savtshenkia*) *confusa* van der Wulp, 1883 presented in Shevtsova et al. (2011). Before that, though, the patterns were mentioned without additional emphasis in at least a few species descriptions of crane flies as early as a century ago (Enderlein 1912). Given the size, diversity, and unresolved phylogeny below the family level, establishment of a novel character such as WIP is essential to our understanding of the group.

Crane flies have relatively large wings with multiple branches of major veins that form upwards of fifteen cells. Additionally, crane flies can have pigment, setae, folds, and reinforcements of the wing surface and veins; all of which play a role in the overall visibility of the WIP (Shevtsova 2012). Crane flies are poorly represented in the current WIP literature; many of the other taxa examined have wings that are small, clear, and with reduced venation. The largest known species of crane fly in North America is *Holorusia hespera* Arnaud & Byers, 1990 (Alexander, 1920, as *rubiginosa*) which has a wing length of 40 mm while the smallest species has a wing length of 2.0 mm (de Jong et al. 2007). We suspect given this wide range of wing lengths that WIP will be vastly different among the species of Tipuloidea. Additionally, Shevtsova et al. (2011) showed that in Hymenoptera and Diptera, WIP follow the Newton series: a repeating stable series of color bands known to occur in thin films of between 50 and 1500 nm thickness (Shevtsova et al. 2011). We did not measure wing thickness or map the Newton sequence on our WIP images, but we suspect some of the largest species of the group will have wings too thick to transmit a WIP. If so, we expected to observe opaque, gray wings as described in Shevtsova et al. (2011).

We aim to establish the existence of Wing Interference Patterns across the four families of Tipuloidea using male/female representative pairs and to provide descriptions of the color and pattern of WIP for both sexes for each species. We also seek to establish the stability of WIP within a species and confirm sexual dimorphism in each representative species.

Materials and methods

All specimens were selected from the entomology collection at the Academy of Natural Sciences of Drexel University (**ANSP**) in Philadelphia, Pennsylvania. We examined 45 species (2373 individuals) (Table 1) and selected representative species for each family, with additional species sampled to evaluate generic level WIP relationships (*Nephrotoma spp.*) and to investigate intraspecific variation (*Gnophomyia tristissima* Osten Sacken, 1860) (Table 2). In each representative species both a male and female specimen were selected for comparison. Additionally, both pinned specimens

Table 1. Linked data table of a list of all species of Tipuloidea examined for WIP in this study. The family and valid nomenclature for each species is listed in addition to the presence or absence of a WIP and the number of specimens examined for each species.

Family	Species	WIP present	Number of specimens examined
Cylindrotomidae	*Cylindrotoma distinctissima* (Meigen, 1818)	yes	69
Cylindrotomidae	*Diogma glabrata* (Meigen, 1818)	yes	7
Cylindrotomidae	*Liogma nodicornis* (Osten Sacken, 1865)	yes	44
Limoniidae	*Eugnophomyia luctuosa* (Osten Sacken, 1860)	yes	3
Limoniidae	*Gnophomyia tristissima* Osten Sacken, 1860	yes	67
Limoniidae	*Gnophomyia cockerelli* Alexander, 1919	yes	29
Limoniidae	*Molophilus pubipennis* Osten Sacken, 1860	yes	32
Limoniidae	*Ormosia romanovichiana* Alexander, 1953	yes	60
Limoniidae	*Dactylolabis cubitalis* (Osten Sacken, 1869)	yes	18
Limoniidae	*Epiphragma fasciapenne* Say, 1823	yes	123
Limoniidae	*Limnophila macrocera* (Say, 1823)	yes	78
Limoniidae	*Dicranomyia liberta* Osten Sacken, 1860	yes	113
Limoniidae	*Dicranoptycha sobrina* Osten Sacken, 1860	yes	82
Limoniidae	*Elephantomyia westwoodi westwoodi* Osten Sacken, 1869	yes	107
Pediciidae	*Pedicia albivitta* Walker, 1848	yes	26
Pediciidae	*Tricyphona calcar* (Osten Sacken 1860)	yes	12
Pediciidae	*Tricyphona degenerata* Alexander, 1917	yes	3
Pediciidae	*Tricyphona immaculata* (Meigen, 1804)	yes	18
Pediciidae	*Tricyphona inconstans* (Osten Sacken 1860)	yes	92
Pediciidae	*Ula elegans* Osten Sacken, 1869	yes	24
Tipulidae	*Phoroctenia vittata angustipennis* (Loew, 1872)	yes	3
Tipulidae	*Tanyptera dorsalis* (Walker, 1848)	yes	20
Tipulidae	*Dolichopeza carolus* Alexander, 1940	yes	61
Tipulidae	*Dolichopeza dorsalis* (Johnson, 1909)	yes	7
Tipulidae	*Dolichopeza johnsonella* (Alexander, 1931)	yes	8
Tipulidae	*Dolichopeza obscura* (Johnson, 1909)	yes	48
Tipulidae	*Dolichopeza polita polita* (Johnson, 1909)	yes	4
Tipulidae	*Dolichopeza tridenticulata* Alexander, 1931	yes	47
Tipulidae	*Brachypremna dispellens* (Walker, 1861)	yes	87
Tipulidae	*Holorusia hespera* Arnaud & Byers, 1990	no	41
Tipulidae	*Nephrotoma ferruginea* (Fabricius, 1805)	yes	70
Tipulidae	*Nephrotoma macrocera* (Say, 1823)	yes	106
Tipulidae	*Nephrotoma eucera* (Loew, 1863)	yes	97
Tipulidae	*Nephrotoma virescens* (Loew, 1864)	yes	89
Tipulidae	*Tipula* (*Arctotipula*) *williamsiana* Alexander, 1940	no	55
Tipulidae	*Tipula* (*Beringotipula*) *borealis* Walker, 1848	yes	43
Tipulidae	*Tipula* (*Beringotipula*) *coloradensis* Doane, 1911	yes	75
Tipulidae	*Tipula* (*Lunatipula*) *atrisumma* Doane, 1912	yes	51
Tipulidae	*Tipula* (*Lunatipula*) *duplex* Walker, 1848	yes	101
Tipulidae	*Tipula* (*Lunatipula*) *valida valida* Loew, 1863	yes	47
Tipulidae	*Tipula* (*Pterelachisus*) *trivittata* Say, 1823	yes	106
Tipulidae	*Tipula* (*Trichotipula*) *oropezoides* Johnson, 1909	yes	78
Tipulidae	*Tipula* (*Vestiplex*) *longiventris* Loew, 1863	yes	21
Tipulidae	*Tipula* (*Yamatotipula*) *sayi* Alexander, 1911	yes	52
Tipulidae	*Tipula* (*Yamatotipula*) *tricolor* Fabricius, 1775	yes	49
Total number of specimens examined:			2373

and ethanol-preserved specimens of the same sex and species were compared to determine if preservation had an effect on the stability of WIP. No deviations were seen in WIP color or pattern between same sex specimens of the same species and as such specimens from both preservation methods were used in this study. Preservation type of each specimen used in this study is provided (Table 2). Herein we follow the four-

Table 2. Linked data table of each specimen image included in this study. The taxonomy and valid nomenclature for each species is listed in addition to the collection location, date, figure reference(s), and preservation type for each specimen.

Specimen code	Species	Sex (M/F)	Location data	Date collected	Figure reference(s)	Preservation type
ANSP-ENT-128038	*Gnophomyia tristissima* Osten Sacken, 1860	F	West Fairmount Park, Philadelphia, PA, USA	1998–06–08	Fig. 1A	Ethanol
ANSP-ENT-128039	*Gnophomyia tristissima* Osten Sacken, 1860	F	West Fairmount Park, Philadelphia, PA, USA	1998–06–08	Figs 1B, 3C	Ethanol
ANSP-ENT-128040	*Gnophomyia tristissima* Osten Sacken, 1860	F	Black Mountains, NC, USA	1912–05–26	Fig. 1C	Pinned
ANSP-ENT-128044	*Gnophomyia tristissima* Osten Sacken, 1860	M	West Fairmount Park, Philadelphia, PA, USA	1998–06–08	Fig. 1D	Ethanol
ANSP-ENT-128043	*Gnophomyia tristissima* Osten Sacken, 1860	M	Tarrytown, NY, USA	1913–06–20	Fig. 1E	Pinned
ANSP-ENT-128041	*Gnophomyia tristissima* Osten Sacken, 1860	M	West Fairmount Park, Philadelphia, PA, USA	1998–06–08	Figs 1F, 3D	Pinned
no code	*Gnophomyia tristissima* Osten Sacken, 1860	F	Montgomery County, MD, USA	2020–06–21	Fig. 9C	none
no code	*Gnophomyia tristissima* Osten Sacken, 1860	M	Montgomery County, MD, USA	2020–06–22	Fig. 9C	none
ANSP-ENT-128045	*Dolichopeza obscura* (Johnson, 1909)	F	South Wales, NY, USA	1911–07–09	Fig. 5C	Pinned
ANSP-ENT-128046	*Dolichopeza obscura* (Johnson, 1909)	M	Black Mountains, NC, USA	1912–06–10	Figs 2, 5D	Pinned
ANSP-ENT-128047	*Cylindrotoma distinctissima* (Meigen, 1818)	F	West Fairmount Park, Philadelphia, PA, USA	1998–07–03	Fig. 3A	Ethanol
ANSP-ENT-128048	*Cylindrotoma distinctissima* (Meigen, 1818)	M	West Fairmount Park, Philadelphia, PA, USA	1998–07–03	Fig. 3B	Ethanol
ANSP-ENT-128049	*Dactylolabis cubitalis* (Osten Sacken, 1869)	F	Black Mountains, NC, USA	1912–05–28	Fig. 4A	Pinned
ANSP-ENT-128050	*Dactylolabis cubitalis* (Osten Sacken, 1869)	M	Black Mountains, NC, USA	1912–05–29	Fig. 4B	Pinned
ANSP-ENT-128051	*Dicranomyia liberta* Osten Sacken, 1860	F	West Fairmount Park, Philadelphia, PA, USA	1998–07–22	Fig. 4C	Ethanol
ANSP-ENT-128052	*Dicranomyia liberta* Osten Sacken, 1860	M	West Fairmount Park, Philadelphia, PA, USA	1998–07–22	Fig. 4D	Ethanol
ANSP-ENT-128053	*Tricyphona inconstans* (Osten Sacken, 1860)	F	West Fairmount Park, Philadelphia, PA, USA	1998–07–22 to 08–16	Fig. 5A	Ethanol
ANSP-ENT-128054	*Tricyphona inconstans* (Osten Sacken, 1860)	M	West Fairmount Park, Philadelphia, PA, USA	1998–07–22 to 08–16	Fig. 5B	Ethanol
ANSP-ENT-128055	*Brachypremna dispellens* (Walker, 1861)	F	West Fairmount Park, Philadelphia, PA, USA	1998–06–20	Fig. 6A	Ethanol
ANSP-ENT-128056	*Brachypremna dispellens* (Walker, 1861)	M	West Fairmount Park, Philadelphia, PA, USA	1998–06–20	Fig. 6B	Ethanol
ANSP-ENT-128057	*Holorusia hespera* Arnaud & Byers, 1990	F	Trout Creek, Juab Co., UT, USA	1922–07–22	Fig. 6C	Pinned
ANSP-ENT-128058	*Holorusia hespera* Arnaud & Byers, 1990	M	Los Padres N.F., San Luis Obispo Co., CA, USA	2019–07–01	Fig. 6D	Pinned
ANSP-ENT-128059	*Nephrotoma ferruginea* (Fabricius, 1805)	F	West Fairmount Park, Philadelphia, PA, USA	1998–06–13 to 07–03	Fig. 7A	Pinned
ANSP-ENT-128060	*Nephrotoma ferruginea* (Fabricius, 1805)	M	West Fairmount Park, Philadelphia, PA, USA	1998–06–13 to 07–03	Fig. 7B	Pinned
ANSP-ENT-128061	*Nephrotoma macrocera* (Say, 1823)	F	Black Mountains, NC, USA	1912–06–05	Fig. 7C	Ethanol
ANSP-ENT-128062	*Nephrotoma macrocera* (Say, 1823)	M	West Fairmount Park, Philadelphia, PA, USA	1998–06–13 to 07–03	Fig. 7D	Ethanol
ANSP-ENT-128063	*Nephrotoma virescens* (Loew, 1864)	F	West Fairmount Park, Philadelphia, PA, USA	1998–06–13 to 07–03	Fig. 7E	Ethanol
ANSP-ENT-128064	*Nephrotoma virescens* (Loew, 1864)	M	West Fairmount Park, Philadelphia, PA, USA	1998–06–13 to 07–03	Fig. 7F	Ethanol
ANSP-ENT-128065	*Tipula* (*Beringotipula*) *borealis* Walker, 1848	F	Swarthmore, PA	1904–08–27	Fig. 8A	Pinned
ANSP-ENT-128066	*Tipula* (*Beringotipula*) *borealis* Walker, 1848	M	Stony Run Trail, York Co., PA, USA	1998–09–12	Fig. 8B	Pinned
ANSP-ENT-128067	*Tipula* (*Yamatotipula*) *sayi* Alexander, 1911	F	West Fairmount Park, Philadelphia, PA, USA	1998–09–22	Fig. 8C	Ethanol
ANSP-ENT-128068	*Tipula* (*Yamatotipula*) *sayi* Alexander, 1911	M	West Fairmount Park, Philadelphia, PA, USA	1998–09–22	Fig. 8D	Ethanol
no code	*Tipula* (*Yamatotipula*) *aprilina* Alexander, 1918	M	Lindenwold, Camden Co., NJ, USA	2021–04–20	Fig. 9A	none
no code	*Tipula* (*Yamatotipula*) *aprilina* Alexander, 1918	F	Lindenwold, Camden Co., NJ, USA	2021–04–20	Fig. 9B	none
no code	*Elliptera clausa* Osten Sacken, 1877	unknown	Pioneer, Amador Co., CA, USA	2016–05–27	Fig. 9D	none

family taxonomy of Oosterbroek (2021). We selected taxa based on availability in the collection and the condition of the wings, as the wings of many pinned specimens were exceedingly brittle and often curled or folded, rendering them unusable for imaging. We specifically chose one species, *Holorusia hespera*, based on size, as we expected this species to have wings too thick to display a WIP. Within each sex for each species, we observed wings across age (1904–2019), geography, and preservation type to confirm stability of the WIP within a species. We found no evidence that any of these metrics had an effect on the stability of WIP. Through this investigation we discovered higher intraspecific variation in *G. tristissima* and chose to image additional specimens for this species (Fig. 1).

Specimens were prepared as in Shevtsova et al. (2011) with certain exceptions. We excised one wing from each specimen, and placed each wing on a slide. Next a drop of 70% ethanol was added to help flatten and orient the wing on the slide and while still wet from the ethanol, a cover slip was carefully placed on top of the wing and slide. We applied gentle pressure to the cover slip to remove air bubbles. Once the ethanol had evaporated the cover slip was adhered to the slide by placing a small drop of Euparal at each corner, making sure that none of the Euparal had seeped onto the wing. Initially we had tested adhesives and fixatives placed over the entire cover slip, but this blocked transmission of WIP.

A black background was created using light-absorbing black-out fabric with adhesive backing from Edmund Optics (Item #54–585). This fabric was placed beneath each wing slide prior to imaging. Imaging for all but three species was performed using a Leica S9i stereomicroscope (Model AF6000). Images for three species (*Tipula* (*Yamatotipula*) *sayi* Alexander, 1911, *Dolichopeza* (*Oropeza*) *obscura* (Johnson, 1909), and *Nephrotoma macrocera* (Say, 1823)) were too distorted to be used and were reshot using a Leica (Model EZ4 D) stereomicroscope with an integrated 3mp camera. Each specimen was imaged using LEICA APPLICATION SUITE X (version 3.0.11.20652). Files were saved in .tiff format and edited in ADOBE PHOTOSHOP (version CS6). Alterations in Photoshop were restricted to increasing the saturation by no more than 10%, reducing brightness by up to 20%, increasing the contrast by up to 20%, cropping the wing from the background, darkening the background, and using the spot-healing tool to remove dust and debris as needed. We follow the four-pattern concept of WIP put forth in Buffington and Sandler (2011): campiform (WIP of mostly one color, usually blue), galactiform (mottled patches and swirls of color like the spirals of galaxies), radiform (radial bands emerging from the medial sector and expanding in concentric bands to the margin), and striatiform (longitudinal bands of color that often follow anal veins). Wing definitions follow those of Saigusa (2006) (Fig. 2).

Descriptions of WIP herein are an attempt to provide a written account of the WIP across the entire wing. This was difficult to capture in a single image, mostly due to the size of many wings as well as the folds and textured surfaces of the wings of many crane flies examined. In the larger species, the veins themselves were thick enough to keep the wing from lying flat on the slide. Rather than making composite images we attempted to provide as complete a WIP as possible in a single image. As such, cells

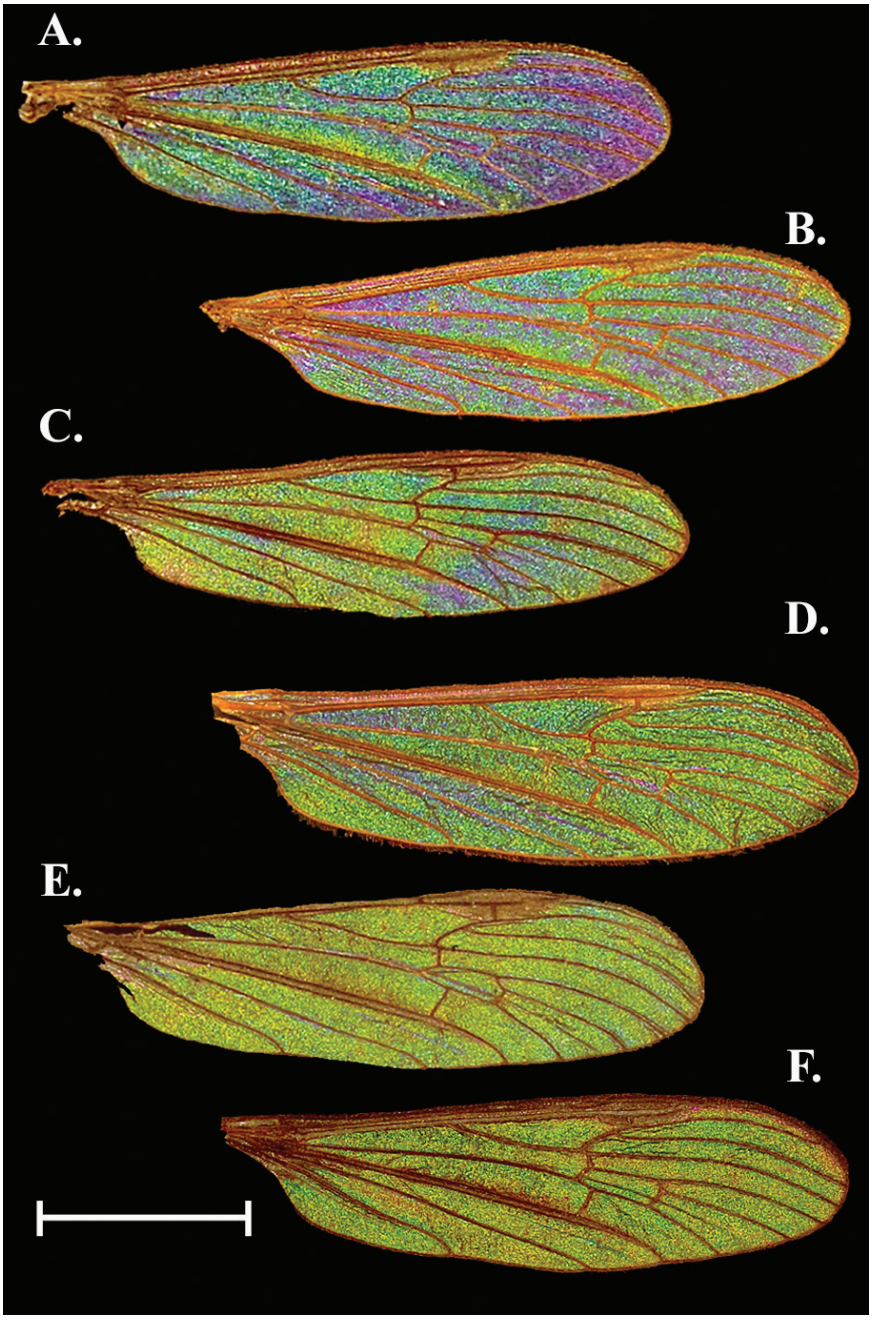

Figure 1. Comparison of the variation in WIP of three female and three male specimens of *Gnophomyia tristissima*. Females examined in this study were found to have a range of WIP from **A** dark blue/ purple **B** blue with mottled yellow **C** green/yellow with hints of blue which appeared most like the male WIP. Males examined also had a range of WIP from **D** green with mottled blue which appeared most like the female WIP **E** solidly green **F** green with mottled magenta. Patterns B and E were the most encountered patterns for females and males, respectively. Scale bars: 1.0 mm.

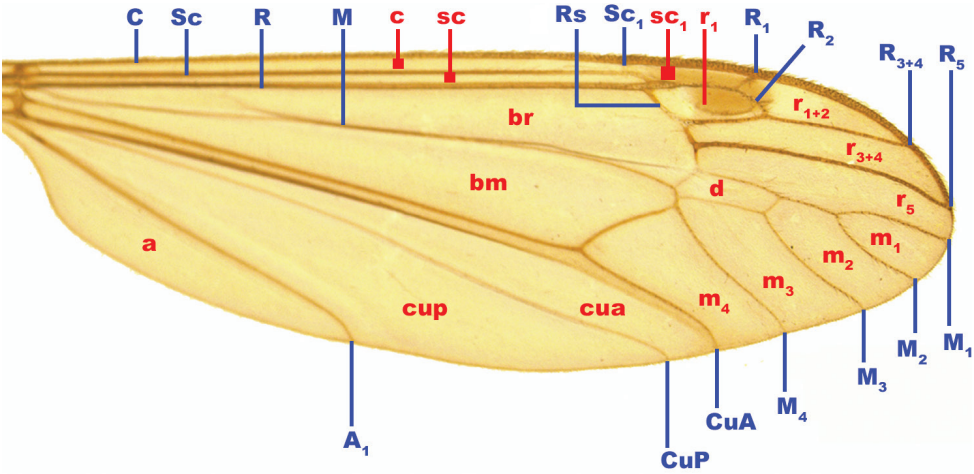

Figure 2. Excised wing of a male specimen of *Dolichopeza obscura* against a white background with notations of wing veins and cells used in this study. Veins are noted in blue with uppercase letters while cells are noted in red with lowercase letters; naming and notations follow those of Saigusa (2006). Abbreviations: **A/a**: anal vein/cell, **bm**: basal medial cell, **br**: basal radial cell, **C/c**: costal vein/cell, **CuA/cua**: anterior cubitus vein/cell, **CuP/cup**: posterior cubitus vein/cell, **d**: discal cell**, M/m**: Medial vein/cell, **R/r**: radial vein/cell, **Rs**: radial sector vein, **Sc/sc**: subcostal vein/cell. Image not to scale.

adjacent to the costal margin (especially c, sc_1, and sc_2 that in many taxa are exceedingly narrow) often have WIP that are distorted by corrugation, folds, and pigment. We have still attempted to provide those details in the descriptions and have noted in parentheses behind the given characters when they are not visible in the corresponding figure though WIP should be visible when observed in person.

Abbreviations

A/a	anal vein/cell;
ANSP	Academy of Natural Sciences of Drexel University;
bm	basal medial cell;
br	basal radial cell;
C/c	costal vein/cell;
CuA/cua	anterior cubitus vein/cell;
CuP/cup	posterior cubitus vein/cell;
d	discal cell;
M/m	Medial vein/cell;
R/r	radial vein/cell;
Rs	radial sector vein;
Sc/sc	subcostal vein/cell;
WIP	Wing Interference pattern(s).

Results

WIP descriptions

Family Cylindrotomidae

***Cylindrotoma distinctissima* (Meigen, 1818)**
Fig. 3

General appearance. In both sexes, the basal half of the wing green to green-yellow (with males being greener and females brighter and more yellow) with swirling magenta striations and beyond the cord a mostly magenta apical half forming a patch or spot. Males with magenta bands reduced before the cord and expanded beyond. Generally, males appear more magenta at a distance while the females appear more banded red/green. The pattern is striatiform before the cord and galactiform after.

Female description (Fig. 3A). Cells c, sc_1, and sc_2 with WIP obscured by wing topography but can appear as a mottled green/ magenta (not visible in Fig. 3); cell r_1 green with a magenta band through the center, and distal edge of cell obscured by pterostigma pigment, which may bleed into nearby cells. All other cells r and m, as well as d, show strong magenta in the center with various-sized patches of green edging the margins. Cells cua, cup, bm, and br with large striations of green and magenta with many stretching over more than one cell; the green is generally kept to the center of the cell. The anterior edge of cup has a small strip of indigo edging vein CuA and green coloration in cells a_1, cup, and cua appearing to bleed into yellow. Apical edge of cell A_1 with magenta where vein A meets the wing margin, in center of cell three magenta spots surrounded by green, magenta may also edge the margin.

Male description (Fig. 3B). Similar to female in color and pattern but magenta bands reduced before the cord and expanded after.

Notes. There can be some subtle pattern differences in males of this species but they do not appear to be sexually dimorphic as this variation is inconsistent.

Family Limoniidae

***Gnophomyia tristissima* Osten Sacken, 1860**
Figs 1, 3

General appearance. Sexually dimorphic. Female with galactiform dark blue patches over a green background with some yellow-green patches. Male a bright yellow green galactiform, occasionally with faint magenta patches/bands. This species had higher intraspecific variation and variation within the sexes than any other species examined.

Female description (Figs 1A–C, 3C). Cell c and sc with WIP obscured by wing topography but often with mottled magenta overall (1A, D, not visible in Fig. 3). A thin band of yellow green can be seen lining the pterostigma pigmentation posteriorly;

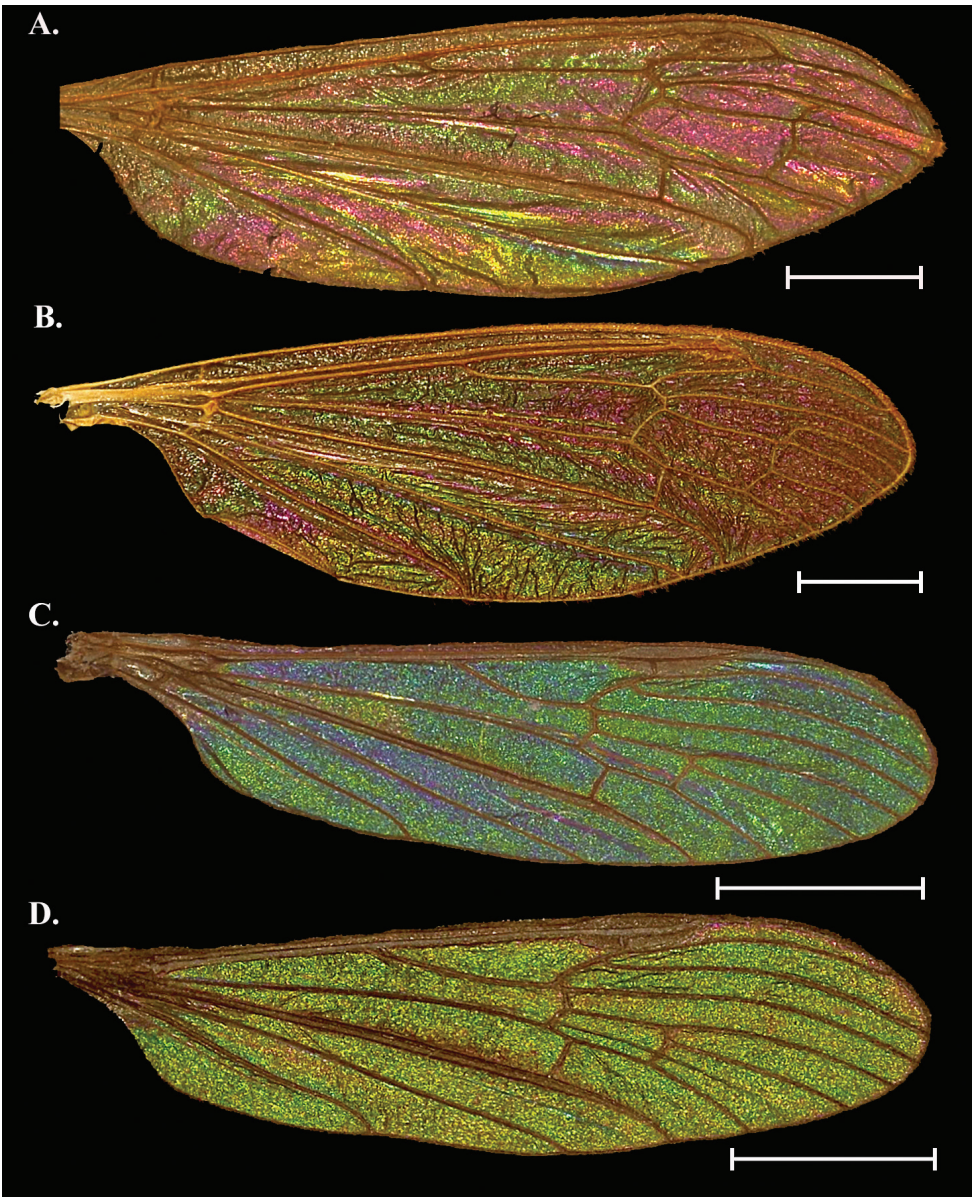

Figure 3. Wing Interference Pattern on excised wings of male/ female pair of two species of Tipuloidea. Excised wings of a male/ female pair of two species of crane flies. Wings were excised, flattened between a glass slide and cover slip, and photographed under a microscope using transmitted light **A** *Cylindrotoma distinctissima* female **B** *Cylindrotoma distinctissima* male **C** *Gnophomyia tristissima* female **D** *Gnophomyia tristissima* male. Scale bars: 1.0 mm.

the band usually originates at the proximal edge of the pterostigma, staying rather regular in width following R through the r_1, widening as it reaches R_2 and passing into cells r_3 and r_2, then looping around and ending where R_1 meets the margin. This color is highly variable and can exist as nothing more than a hint of yellow or expanded

wider; it may follow the wing margin at least through r_2 if not further to the posterior wing margin. All r and m cells, as well as cell d uniform blue green, with purple lining the margins (the width of these purple bands is highly variable). Cells cua, cup, a_1, bm, and br with a similar pattern to the apical cells but with less purple overall. Cell cua with a large fold that is usually purple (occasionally yellow). A second fold originates in br, follows into d and ends in cell m_{2+3}.

Male description (Figs 1D–F, 3D). Male WIP generally yellow green campiform with some degree of blue and yellow but patterns as in female, band originating at pterostigma magenta, folds in basal cells blue.

Notes. Variations in the WIP of *G. tristissima* were greater than the intraspecific variation seen in other species examined in this study. Females and males both appeared to have a gradient. The darkest females (Fig. 1A) appear almost indigo near the margin and basal cells a mottled green blue while the lightest wings (Fig. 1C) have blue reduced throughout and only prominent near the cord and generally appearing more like a male wing. The most common female WIP configuration (Fig. 1B) is a solid blue to blue green with only hints of yellow around the cord. Males have a similar gradient and the darkest male WIP have flares of blue as in light females (Fig. 1C). The most common males are solidly green (Fig. 1E) but may have some hints of magenta tracing veins. A third type of male WIP are similar to the common pattern but with magenta regions expanded (Fig. 1F). Occasionally small striations like those around the pterostigma can be inverted so females have a magenta band and males with a yellow-green band.

Dactylolabis cubitalis (Osten Sacken, 1869)

Fig. 4

General appearance. Sexually dimorphic. Wing galactiform with large green splotches and thin magenta striations originating from the base of the wing moving outward. Both sexes have a magenta band near the center of the wing but the magenta occupies different cells in males and females.

Female description (Fig. 4A). Cell r_1 and r_{1+2} both with a band of magenta following the posterior edge with the rest of the cell a mottled magenta and green where visible. Cell r_3 mostly green, cell r_4 mostly green with an oblong spot of magenta in the center of the cell. Cells r_5, m_1 to m_4, and d forming a multi-cell pattern featuring a green splotch centered on m_3 and reaching into m_1 and m_5 to either side. Each cell also has magenta lining the margin. Cells cua, cup, and a_1 with magenta striations originating from the wing origin and ending at the anal margin and generally paralleling veins. Cell bm with a green center, br like bm but with green center faint.

Male description (Fig. 4B). Pattern similar overall to female with these exceptions: cells r_3 and r_4 with magenta expanded while r_5 has greener than in female. It is as though the magenta patterning in the female has been shifted anteriorly by one cell in the radial cells. The multi-cell pattern across median cells is inverse of female with a magenta spot situated in cells m_3 and m_4 centered on M_4. All basal cells as in female.

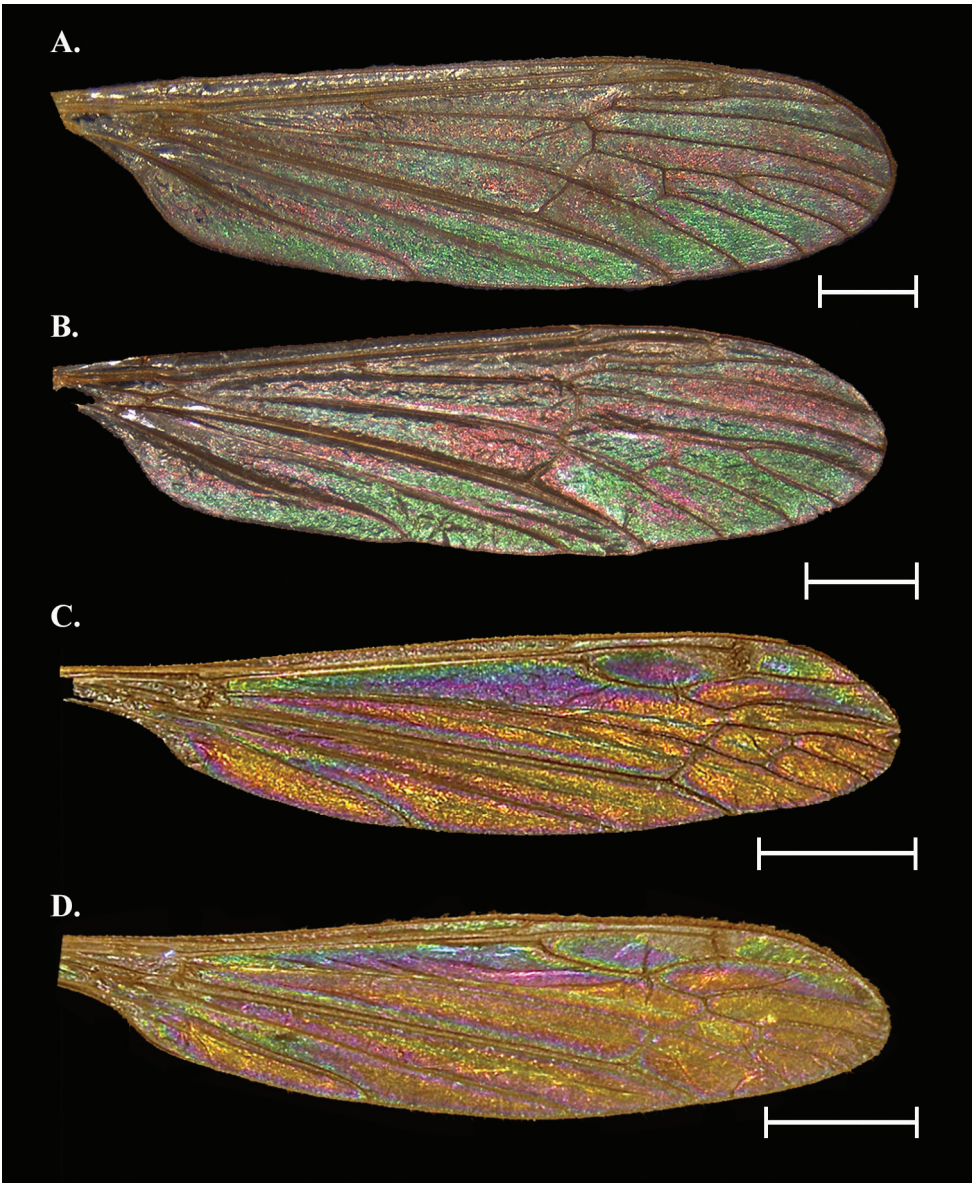

Figure 4. Wing Interference Pattern on excised wings of male/ female pair of two species of Tipuloidea **A** *Dactylolabis cubitalis* female **B** *Dactylolabis cubitalis* male **C** *Dicranomyia liberta* female **D** *Dicranomyia liberta* male. Scale bars: 1.0 mm.

Notes. Both sexes have a "spot" near the apex of the wing that originates on either edge of r_4 about halfway between the basal edge and the wing margin. In the female this is a barely visible magenta spot, but in the male this spot expands to fill most of r_4 as well as part of r_3 and r_5. All cells basal to the cord are similar between the sexes. Pattern galactiform with striatiform portions present.

***Dicranomyia liberta* Osten Sacken, 1860**
Fig. 4

General appearance. Pattern is a bold galactiform containing almost the entire spectrum of colors found in WIP. Anterior cells with large bold blue to purple centers encircled by green, yellow, and magenta in that order.

Female description (Fig. 4C). Cell c, sc, and sc_1 obscured by wing topography but can appear as mottled green/ magenta (not visible in Fig. 4C). Pterostigma obscures distal half of cell r_1 and the proximal edge of cell r_{1+2}. Cell r_1 otherwise with magenta splotch at center surrounded by a narrow blue band (the combination of which appears purple) then a green oval surrounding that becoming yellow at the margin of the cell. Cell r_{1+2} with pattern similar to r1 but with hints of magenta at the margin. Cell r_{3+4} with bright yellow oval at proximal end, encircled by a magenta band, followed by blue, green, yellow, and magenta bands. Cells r_5, m_1 to m_3, and d campiform yellow with small green striations through the center of cells or magenta directly adjacent to the veins. Cells cua, cup, a_1, and bm also campiform yellow but with bright striations of green, magenta, and blue tracing the veins and following to the wing margin. Cell br with a large magenta spot in the center of the cell and tapering to the proximal and distal ends. On the proximal half the magenta is surrounded by blue, green, and yellow bands while on the distal edge the blue band gives way to a magenta band followed by a golden yellow band.

Male description (Fig. 4D). Almost identical to female, but may be a bit dull as compared to female WIP.

Notes. The WIP of this species is one of the most colorful we encountered in this study, and one of the few containing yellow as a dominant color. The WIP in *D. liberta* does not appear to be sexually dimorphic and differences between the sexes are not consistent.

Family Pediciidae

***Tricyphona inconstans inconstans* (Osten Sacken 1860)**
Fig. 5

General appearance. Sexually dimorphic. Pattern striatiform in basal cells and galactiform in apical cells. Both sexes have basal half of the wing green with magenta striations including one that extends to the margin. Two spots occur on the posterior half of the wing. In females these spots are yellow to yellow-green but in males the spots are blue to purple-magenta.

Female description (Fig. 5A). Cells c, sc, sc_1, r_1, and r_{1+2} obscured by topography/ pigmentation though r_1 and r_{1+2} with mottled magenta and green, though this may or may not be visible. Cells r_3 and r_4 mostly magenta with a ribbon of light green on apical edge of r_3. A magenta band starts in r_3 and following the posterior wing margin to at least cell cua. Cells r_5 to m_4 and d forming a large, light green circle with the outer

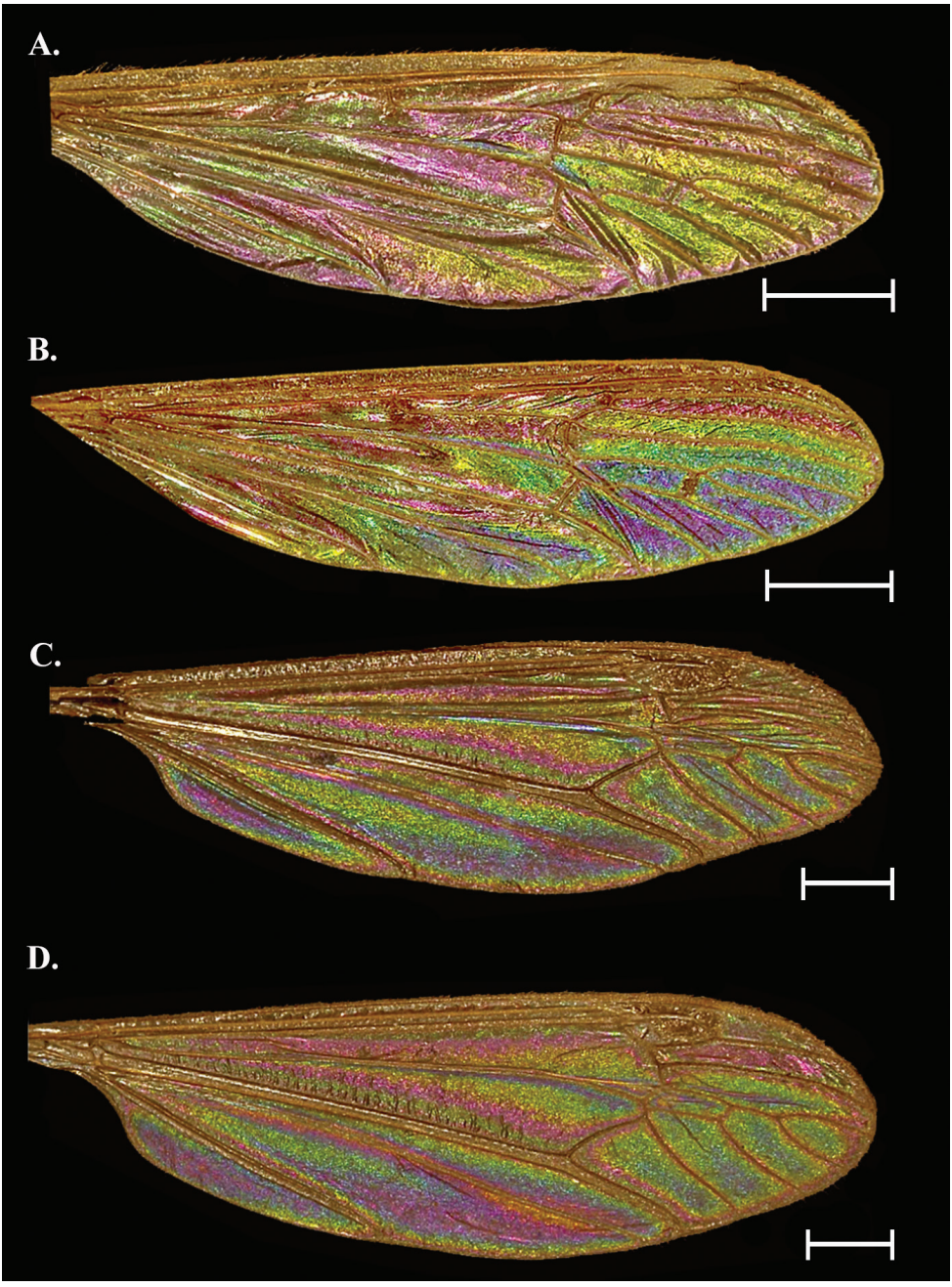

Figure 5. Wing Interference Pattern on excised wings of male/ female pair of two species of Tipuloidea **A** *Tricyphona inconstans inconstans* female **B** *Tricyphona inconstans inconstans* male **C** *Dolichopeza obscura* female **D** *Dolichopeza obscura* male. Scale bars: 1.0 mm.

margins of the outer cells continuing the magenta strip at the margins. Cell cua and cup with a light green oval centered over CuP and surrounded by magenta. Cells bm and br mostly magenta with the basal sections green.

Male description (Fig. 5B). Similar to female with the following exceptions: Cell r_4 green/yellow, all m and d cells a deep magenta/purple at center, followed by a thin ring of blue, green, and yellow at the margins. The band following the posterior margin yellow, spot centered on CuA with magenta center encircled by concentric blue, green, yellow, and magenta bands. Cell a_1 as in female but magenta reduced. Cell bm as in female but color inverted.

Notes. Color but not pattern is dimorphic, and males are distinct in having a bright blue spot centered in the m cells while females lack almost any blue coloration, instead having the spot green. The same is the case with the spots on cua and cup. In males, these blue patches are in stark relief to the magenta/green of the wing.

Family Tipulidae

***Dolichopeza obscura* (Johnson, 1909)**
Fig. 5

General appearance. Sexually dimorphic. Bright and colorful galactiform patterns with striatiform near the base. Three large magenta striations starting near wing origin, two of which terminate at the cord, the anterior-most band continues to the margin. Two large blue to purple-magenta spots near posterior margin, otherwise wing cells green with faint blue centers and sometimes magenta lining the margins.

Female description (Fig. 5C). Cells c and sc with deep ridges/baffles but with spots of magenta and green (not visible in Fig. 5C). Cells r_3 and r_{4+5} mostly green with a magenta striation through the middle of each cell. All m cells as well as cell d with large blue/purple spots in the center that transition to green, followed by concentric rings of yellow and magenta to the margins that gives the effect of a rusty brown WIP. Cells cua and cup with a magenta spot that forms on either side of vein CuP, close to where the vein reaches the margin. The magenta bleeds into both cells, transitioning to blue/purple, then green, and finally yellow near the basal edge of the cell. This "spot" occupies most of the distal portion of the cells. Cell a_1 with a large magenta spot in the center, surrounded by concentric rings of blue/purple, green, yellow, and magenta touching the margins. Cells bm and br with three striations running parallel to M and CuA, respectively. The striations from posterior to anterior are green, magenta, and yellow. A blue streak parallels M in bm,

Male description (Fig. 5D). As in the female with the following exceptions: Cells r_5 and m_1 to m_4 with magenta and blue/ purple centers reduced to small spots. Magenta spot between cua and cup expanded, filling more than half the distal halves of the cells. The magenta spot in cell a_1 is similarly expanded, with only a small band of green/yellow at the margins. The blue streak in br is expanded to a large blue/purple striation situated apically from the yellow band.

Notes. Much like *C. distinctissima*, it is unclear if the differences in *D. obscura* are due to plasticity or true sexual dimorphism. The pattern and most colors are identical, though the differences in the male (noted above) do appear more substantial, we still consider this species to lack sexually dimorphic WIP.

Brachypremna dispellens (Walker, 1861)

Fig. 6

General appearance. Sexually dimorphic. Females with green and magenta striations before the cord and cells with green centers and magenta edges beyond the cord. Males have nearly identical patterns, but all instances of magenta and green are inverted. Cells beyond the cord galactiform.

Female description (Fig. 6A). Cells c and sc obscured by ridging/thickness of wing, though small patches of magenta or green may show through (not visible in Fig. 6A). Cells sc_1, sc_2, and distal half of r_1 with WIP obscured by pterostigma; proximal half of r_1 with green center ridged by magenta. Cell r_{1+2} with magenta center surrounded by green. Cell r_3 with a similar pattern as r_{1+2}, though pattern is more striated in r_3. Cells r_{4+5}, m_1 to m_4, cua, br, and d with center green and magenta lining the margin of each cell, though magenta can be broken or uneven and invade the green region. Cells a_1, cup, cua, and bm with magenta center and green edging the margin, can also be broken or invading the magenta region.

Male description (Fig. 6B). As in the female wing with the following differences: All r cells with green center and magenta edging the margin; patterns as in female. All m cells, cua, and a_1 with center magenta and green invading the magenta region; patterns as in female. Cells cup, bm, and br with green centers and magenta edging margins; patterns as in female.

Notes. This is the clearest example in the taxa studied where the WIP patterns are identical between males and females but with the magenta and green regions inverted almost exactly.

Holorusia hespera Arnaud & Byers, 1990

Fig. 6

General appearance. WIP absent. Appearance is a glossy opaque amber color.

Female description (Fig. 6C). Wing lacks any WIP. All cells are a uniform tan-amber in pigment, but no interference pattern is transmitted. Wing surface is heavily textured and ridging and folds are visible across the surface of the wing.

Male description (Fig. 6D). Wing is similar to female and lacks any WIP.

Notes. As noted in Shevtsova et al. (2011) WIPs become obscured as wing thickness approaches 1500 nm. While we did not measure the thickness of wings for this study, the size of *H. hespera* suggests the thickness of the wing is a likely reason for the absence of WIP.

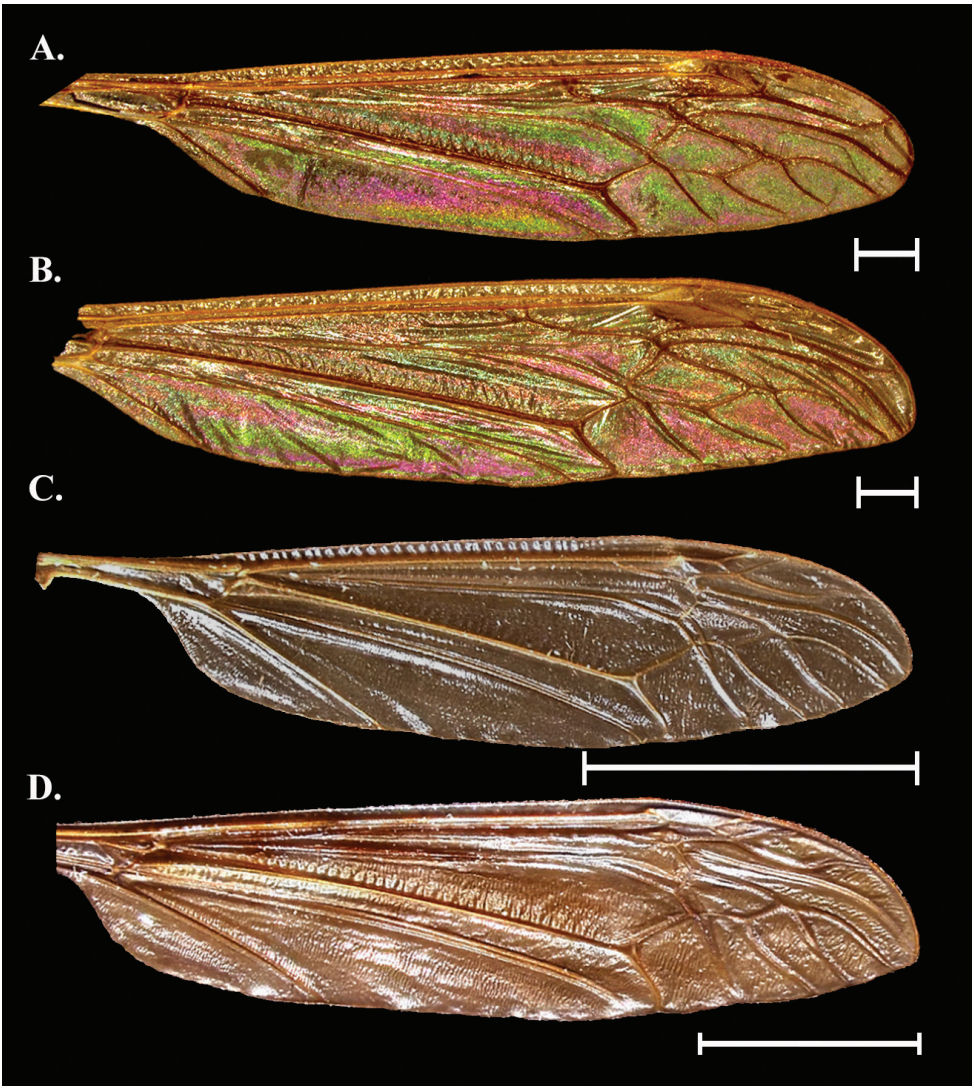

Figure 6. Wing Interference Pattern on excised wings of male/ female pair of two species of Tipuloidea **A** *Brachypremna dispellens* female **B** *Brachypremna dispellens* male **C** *Holorusia hespera* female **D** *Holorusia hespera* male. Scale bars: 1.0 mm (**A, B**), 1.0 cm (**C, D**).

Nephrotoma ferruginea (Fabricius, 1805)

Fig. 7

General appearance. Sexually dimorphic. Pattern is striatiform but cells beyond the cord campiform green with magenta spots and striations. Both sexes with four large magenta striations starting near the origin and terminating at the cord; the anterior-most striations continue past the cord to near the margin; magenta striations are larger

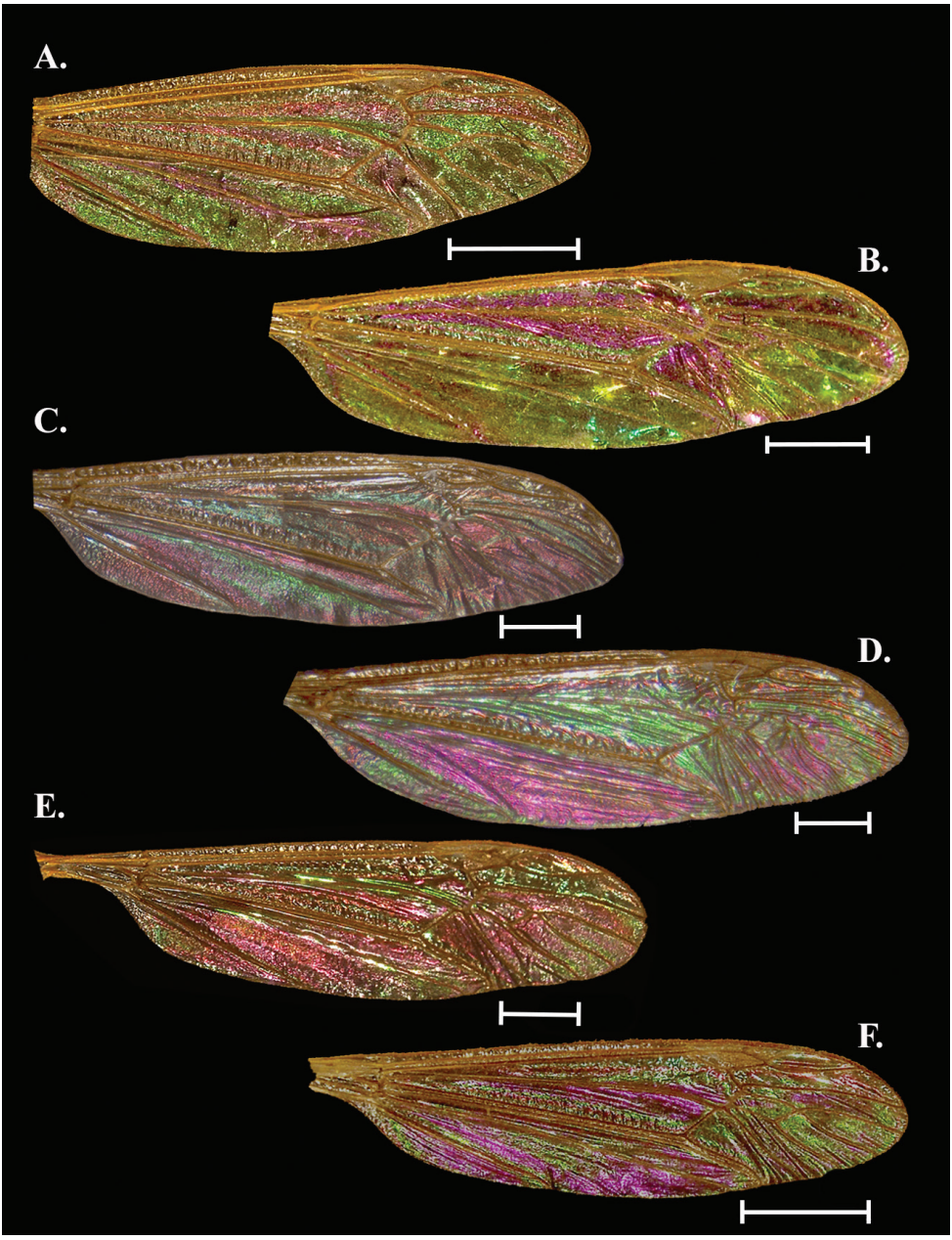

Figure 7. Wing Interference Pattern on excised wings of male/ female pair of two species of Tipuloidea **A** *Nephrotoma ferruginа* female **B** *Nephrotoma ferruginа* male **C** *Nephrotoma macrocera* female **D** *Nephrotoma macrocera* male **E** *Nephrotoma virscens* female **F** *Nephrotoma virscens* male. Scale bars: 1.0 mm.

and brighter in males. Wings have a glossy sheen to them that causes the WIP to seem slightly washed out or glass-like.

Female description (Fig. 7A). Cells c, sc, r_1, and r_{1+2} obscured by topography and pigment. Cell r_3 green-magenta band near the center. Cell r_4 with most of the

center magenta and green to the margins; a small striation breaks vein R_5 and enters r_5, ending at the wing margin near the end of vein M_1. Cells r_5, m_1 to m_3, and d solidly green, with small flares of magenta at the margins; cell m_4 with a magenta spot in the center and green to the margins. All basal cells green with magenta striations following veins.

Male description (Fig. 7B). As in female but with magenta expanded anteriorly and reduced posteriorly.

Notes. *Nephrotoma ferruginea* appeared to have less intraspecific variation in WIP than others based on the large number of specimens examined. Patterns are similar but colors sexually dimorphic. The WIP in this species is difficult to capture as a full pattern due to natural folds in the wing and males especially can look glassy or washed-out.

Nephrotoma macrocera (Say, 1823)

Fig. 7

General appearance. Sexually dimorphic. Female wing mottled green and magenta striatiform before the cord while magenta predominates beyond. Male wing mostly green overall with a clear magenta spot centered around m cells and most of cua and cup magenta. Striatiform pattern with galactiform portions beyond the cord.

Female description (Fig. 7C). Cells c, sc, r_1, and r_{1+2} obscured by topography and pigment. Proximal r cells mainly green with small magenta striations. Cells m_1 to m_3 and d solidly magenta, with small flares of green at the margins; cell m_4 green with an indistinct magenta striation stretching diagonally from the end of M_4 to the origin of the M-Cu cross vein. Basal cells with almost alternating magenta and green striations.

Male description (Fig. 7D). Cells r_5, m_1 to m_4, and d green but with a large generally oval magenta spot centered around m_2 and m_3. Cells cua and cup a bold magenta with only a faint trace of green at the exterior margins of each cell. Cell a_1, bm, and br much greener than female.

Notes. Males and females are similar in that the color is predominantly green and magenta but there is some inversion of a pattern. Some cells look similar, others with color inverted, and some cells completely different between the sexes. The result is a very showy male wing with big blocks of color while the female has a more subdued, mottled look.

Nephrotoma virescens (Loew, 1864)

Fig. 7

General appearance. Sexually dimorphic. Prior to the cord, wings with wide magenta bands in both sexes. Females are mostly magenta beyond the cord with green in the anterior most cells. Males mostly green beyond cord with a magenta spot near the

anterior distal margin. Patterns are galactiform beyond the cord and striatiform before it, though striations are seen after the cord as well.

Female description (Fig. 7E). Cells c, sc, r_1, and r_{1+2}obscured by topography and pigment. Cells r_3 and r_4 mostly green, cells r_5, m_1 to m_4, and d magenta, but with green striations and a green spot centered in m_3. Basal cells with large magenta striations filling most of the cells and small green striations between them. A green spot sits on CuP and crosses into cua and cup.

Male description (Fig. 7F). Similar to female pattern but some colors different or inverted. Proximal r cells, all m cells, and cell d opposite to female, with more magenta anteriorly and mostly green posteriorly. Most cells prior to the cord as in female but some colors inverted. Also, green spot centered on CuP expanded and magenta in males.

Notes. As in *Nephrotoma macrocera*, this species shows male and female wings with similar WIP patterns but inverted colors. Male wings are distinctly green with small striations and spots of magenta while female wings have a magenta base with green striations and spots.

Tipula (*Beringotipula*) *borealis* Walker, 1848

Fig. 8

General appearance. WIP similar in both sexes but with variously sized and spaced pigment clouds of grey and brown. Otherwise WIP dull, mostly green with clouds of magenta. Pattern mostly galactiform with some striations on the basal half of the wing.

Female description (Fig. 8A). Cells c, sc, r_1, and r_{1+2} obscured by pigment and texture. A large brown cloud of pigment centered in the middle of r_3 obscuring WIP in cells r_2, r_3, and cell r_{4+5} but generally both cells green near the base and magenta near the margin. Cell r_{4+5} green with magenta lining the margins and a magenta band through the center of the cell. All m cells with a magenta band that traces the margin and a larger band near the apical third of the cell that cuts across each cell and joins the center magenta band in r_{4+5}; cell d green with magenta center. Cell cua partially obscured with pigment but generally green with magenta at margins, cup and a_1 green with large magenta centers and magenta lining the margins. Both bm and br with pigment partially blocking WIP but appear to follow patterns of other cells with large green patches and smaller magenta bands near margins.

Male description (Fig. 8B). WIP as in female, with some magenta regions more pronounced than the female pattern.

Notes. WIP patterns are stable in this species, but the placement of the wing pigment is variable. This means the pigment can obscure portions of the WIP which may superficially appear like the WIP is unstable. Like other species in this study, *T. borealis* males have the same pattern as females but with expanded magenta regions. This does not seem to be dimorphic, but more study is needed.

***Tipula* (*Yamatotipula*) *sayi* Alexander, 1911**
Fig. 8

General appearance. Sexually dimorphic. Patterns similar but with male magenta regions expanded or reduced compared to females. Overall wings appear green with magenta striations, but lower halves of wing tip in both sexes solidly green.

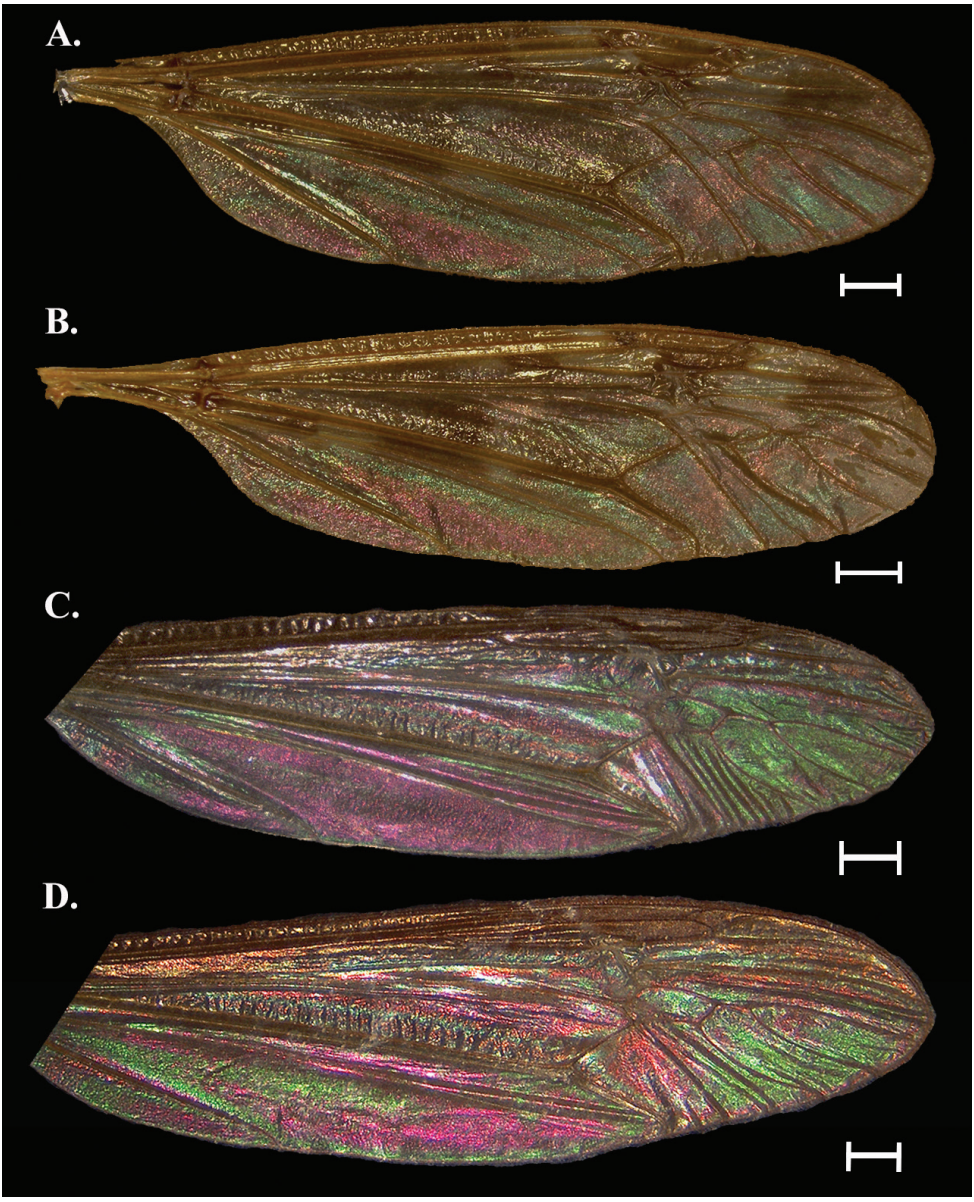

Figure 8. Wing Interference Pattern on excised wings of male/ female pair of two species of Tipuloidea **A** *Tipula* (*Beringotipula*) *borealis* female **B** *Tipula* (*Beringotipula*) *borealis* male **C** *Tipula* (*Yamatotipula*) *sayi* female **D** *Tipula* (*Yamatotipula*) *sayi* male. Scale bars: 1.0 mm.

Female description (Fig. 8C). Cells c, sc, r_1, r_{1+2}, and the anterior half of r_2 obscured by a dark pigmentation band that runs parallel to the apical wing margin. The basal portion of r_1 with magenta anteriorly and green posteriorly. All proximal r cells, m_{1-3}, and cell d forming a solid green field with two magenta striations anteriorly and small red spots posteriorly. Basal cells all mostly magenta with narrow green striations.

Male description (Fig. 8D). WIP as in female with following exceptions: all r cells with more magenta than female, all m cells with more magenta than female, cua and cup greener than in female, br and bm with more magenta than female.

Notes. This species has a subtle dimorphism. Like others, the pattern between the sexes is similar, but with pattern deviations and color inversions. Wings have deep folds and as such WIP can be obscured, especially in dried specimens.

Discussion

We confirm stable, structural Wing Interference Patterns (WIP) in the four families of Tipuloidea. Despite small deviations the overall patterns were stable within each sex and/ or species and were not affected by age of specimen, location collected, or method of preservation. Twelve of the thirteen species sampled had a distinct WIP across the entire wing surface. The sole exception was *Holorusia hespera*, which lacked a WIP, likely due to the size and thickness of the wing as we predicted (Fig. 6C, D). This agrees with the findings of Shevtsova et al. (2011) who noted that the WIP of flies follow the Newton sequence, and wings thicker than 1500 nm will lack a WIP and appear opaque gray. We found eight of the twelve species with a WIP were sexually dimorphic in color if not pattern; *Cylindrotoma distinctissima* (Fig. 3A, B), *Dicranomyia liberta* (Fig. 4C, D), *Dolichopeza obscura* (Fig. 5C, D), and *Tipula borealis* (Fig. 8A, B) lacked sexually dimorphic WIP.

We have demonstrated that WIP are stable within each sex and each species. In ten of twelve species there were minimal variations in WIP consistent with phenotypic variation. Because WIP color is determined by the nanometer-level thickness of the chiton layer, one could expect that among individuals of the same sex there would be some degree of variation in wing thickness. Indeed, these results support the findings of Shevtsova et al. (2011) and Shevtsova and Hansson (2011) who both noted patterns are more stable than color or hue of WIP. We also provide the first cell-by cell descriptions of WIP as a diagnostic character. One species, *Gnophomyia tristissima*, showed increased variation in color and pattern relative to the other species we examined. Both males and females showed this variation and there appeared to be a gradient of WIP color. Additionally, some males and females showed an almost inverted WIP. More work is needed to understand if this is simply a gradient of wing thickness or if there is a selection force acting on the WIP in this species.

Sexual dimorphism of WIP in crane flies is clear and common in the species we examined. While there is no documented evidence of sexual selection of WIP in Tipuloidea, female choice of WIP has been demonstrated in various species of *Drosophila*

(Ala-Honkola and Manier 2016; Hawkes et al. 2019) including evidence that females use visual cues in choosing mates and prefer winged males (Watanabe et al. 2018). Further, Katayama et al. (2014) found that females of *D. melanogaster* preferred wings of mates with a high degree of saturation and a centrally stable hue. Even with our limited sampling of species, many of the sexually dimorphic species in our study had males with bolder, more contrasted colors than females. *G. tristissima* is a widespread species (Alexander 1920) and as such we may be seeing the results of female choice of WIP or a geographic effect. A larger study of this species should be done to try and gauge the level of variation as well as the existence of sexual selection for WIP in *G. tristissima*. Butterworth et al. (2021) performed quantitative, viewer independent methods to evaluate WIP in Calliphoridae, a method that is well suited for examining the variation in *G. tristissima* as well as further WIP studies in Tipuloidea.

Our work suggests that WIP are a stable, reliable species level trait in Tipuloidea and this agrees with the recent WIP literature (Shevtsova et al. 2011; Shevtsova and Hansson 2011; Zhang et al. 2014; and Butterworth et al. 2021). In Tipuloidea, traditional identification of species is often based on male genitalic features, with females in some groups being difficult to identify to species, and even identification keys to the species level are not available for the female stage for many genera. The WIP may provide a useful set of features for separating very similar species in the female stage, e.g., in *Tipula* (*Beringotipula*) separation of the over 20 species in North America at present is based on male genitalic features only.

Additionally, we did not see evidence of a generic level pattern among the three species of *Nephrotoma* examined, although all three species generally had green/magenta striated wings. We are aware of two studies to examine generic level WIP (Buffington and Sandler 2011; Shevtsova and Hansson 2011) both of which found some suggestion of a generic level WIP in certain taxa. We sampled only three of 484 species in the genus *Nephrotoma*. Given the size of the genus, a more focused study examining a larger number of species within the genus, examining the WIP of *Nephrotoma* in a phylogenetic context, and use of viewer independent testing would help increase our understanding of WIP at the generic level.

We note that pigmented patterning on the wing appears to reduce the extent of WIP, at least based on our limited survey here. Species with either costal darkening (*Tipula sayi*, *Tricyphona inconstans*) or more extensive marmorated pattern (*Tipula borealis*, *Dactylolabis cubitalis*), had reduced WIP, at least in the region of the pigment and the pterostigma. Freeman (1968) suggested that marmorated and spotted wing patterns in crane flies are associated with woodland habitats, while clear or striped wings with open habitats; these two different light exposures might impact WIP visibility. Within these broad wing pattern categories, though, there can be a range of wing orientation when at rest which can also impact WIP visibility. For example, *Tipula borealis* holds the wings outstretched and at a slight angle (Fig. 9A, B), while patterned wing *Dactylolabis* (*Dactylolabis*) *montana* (Osten Sacken, 1860) and *Dicranomyia* (*Dicranomyia*) *simulans simulans* (Walker, 1848) (similar to *Dactylolabis cubitalis*) rest with the wings closed over the abdomen (Fig. 9C, D; Adler and Adler 1991).

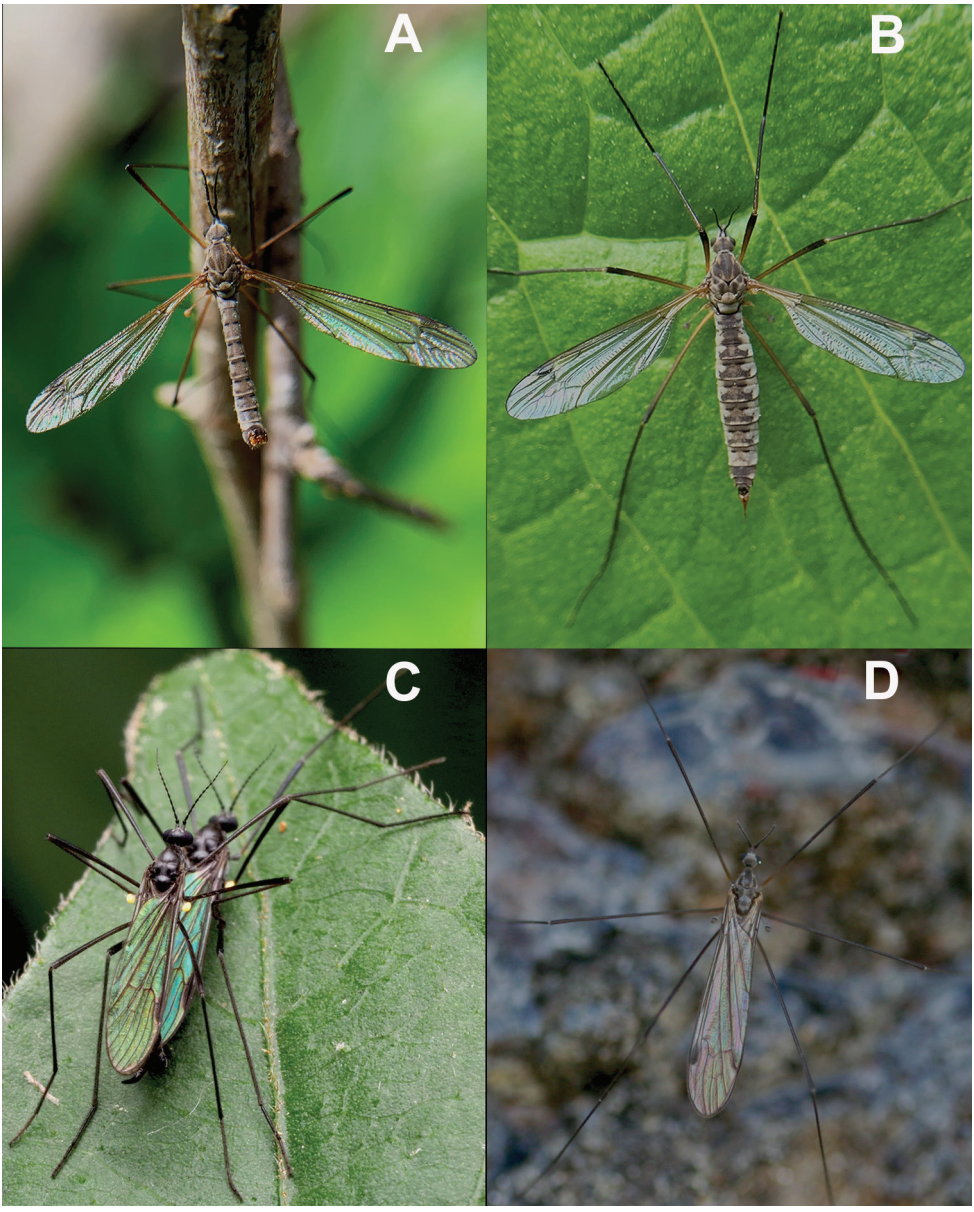

Figure 9. Images showing WIP on several species of crane fly in nature **A** male *Tipula* (*Yamatotipula*) *aprilina* Alexander, 1918 displaying WIP in nature **B** female *Tipula* (*Yamatotipula*) *aprilina* displaying WIP in nature **C** pair of *Gnophomyia tristissima* perched on a leaf in copula. Both flies are displaying their sexually dimorphic WIP. The female (bottom) has a blue WIP while the male (top) displays a green WIP **D** an individual of *Elliptera clausa* Osten Sacken, 1877 displaying a WIP with wings folded. Sex unknown. Copyright (**A, B**) 2021, photograph JK Gelhaus; (**C**) 2020, photograph Katja Schulz, used with permission by the artist and under a creative commons license (https://creativecommons.org/licenses/by/4.0/) with alterations limited to cropping and resizing of this image; (**D**) 2016, photograph JK Gelhaus. Images are not to scale.

Wing interference patterns are stable and they are readily visible in nature (Fig. 9A–D), but their visibility depends on the angle at which light hits the wing as well as the angle it is viewed (Shevtsova 2012). A good example is the male wing of *Dolichopeza obscura* used in this study. When the wing of the male specimen of *D. obscura* is displayed on a white background with light from many different angles it appears clear or slightly stained (Fig. 2) while the same wing, when placed on a dark background with light parallel to the wing displays a bold and intricate WIP (Fig. 5D). Using a pinned museum specimen, we have demonstrated how quickly the WIP transmission can change with a change in background color (see Suppl. material 1: Movie S1). Given this, it is possible that crane flies are using WIP as a type of dynamic flash coloration (Murali 2018) to avoid predation. Additionally, erratic flight patterns have been found to increase the effectiveness of dynamic flash coloration to avoid predation (Murali and Kodandaramaiah 2020) and Pritchard (1983) notes both the wing pattern and the flight pattern of crane flies act to obfuscate the flies from predators. This is merely an observation, and we recommend a true behavioral study to understand what role, if any, WIP plays in predator avoidance strategies in Tipuloidea.

We do remain curious if the WIP in one individual is recognized by other conspecific crane flies. Although WIP were selected for in *Drosophila* (Katayama et al. 2014), in most cases crane flies do not exhibit complicated male-female pre-copulatory behavior (Pritchard 1983), and in many crane flies males seem to find females by touching legs during male search of vegetation (some Limoniidae, Tipulidae Stich 1963; Pritchard 1983) or in mating swarms (some Limoniidae, Pediciidae, Alexander 1920; Pritchard 1983). Also, crane flies males search for females or swarm usually during crepuscular periods (Sullivan 1981) or at least early morning and late afternoon (Gelhaus, pers. obs.) when lighting would not be expected to highlight WIPs. Males could potentially recognize a species-specific WIP at close range after initial leg contact, though.

Conclusions

The scope of this study was to establish the existence of WIP in the four families of Tipuloidea and confirm that WIP could exhibit sexual dimorphism. We have confirmed stable, structural WIP in male/female pairs of twelve species of crane fly across the four families of Tipuloidea. Of these, eight species displayed sexually dimorphic WIP between male and female specimens. One species showed high intraspecific variation that may be a result of sexual selection, though more research is required. Our work supports the consensus in the literature that WIP are species-specific. This work provides the basis for further research and documentation of WIP in crane flies. We did not compare subspecies in this study and comparisons at the generic level were inconclusive, though we cannot discount a generic level WIP relationship. We believe WIP could be a useful tool to discern cryptic species in crane flies or as a novel character to identify females that cannot be separated based on the current morphology. Additionally, WIP may be used for predator avoidance by crane flies.

Acknowledgements

We would like the thank the Malacology Department and Entomology Department of The Academy of Natural Sciences of Philadelphia at Drexel University (ANSP) for use of their imaging equipment and especially Paul Calomon, Dr. Daniel Otte, Isabelle Betancourt, and Joseph Sweeney for training on imaging equipment and software. We would like to also thank Dr. Sigitas Podenas, Vilnius University, Lithuania for early help on imaging of the wings. Thank you to the Richard Engle and Gelhaus lab members (Bolortsetseg Erdenee, Larry Henderson, Steve Mason, Joseph Sweeney) at Drexel University for suggesting edits to an earlier version of this manuscript. Finally, many thanks to Dr. Greg Setliff of Kutztown University of Pennsylvania for first putting the WIP bug in our ears many years ago.

The Department of Biodiversity, Earth & Environmental Sciences of Drexel University and its travel grant, the Teck-Kah Lim travel award, and The William L. McLean III Fellowship for the study of environmental sciences and ornithology all contributed funds used to complete and/or present this research.

References

Adler PH, Adler CRL (1991) Mating behaviour and the evolutionary significance of mate guarding in three species of crane flies (Diptera: Tipulidae). Journal of Insect Behaviour 4: 619–632. https://doi.org/10.1007/BF01048074

Ala-Honkola O, Manier MK (2016) Multiple mechanisms of cryptic female choice act on intraspecific male variation in *Drosophila simulans*. Behavior and Ecological Sociobiology, 70: 519–532. https://doi.org/10.1007/s00265-016-2069-3

Alexander CP (1920) The crane-flies of New York. Pt. 2. Biology and phylogeny. Cornell University Agricultural Experimental Station Memoir 38: 691–1133. https://doi.org/10.5962/bhl.title.33641

Baxter CV, Fausch KD, Saunders CW (2005) Tangled webs: Reciprocal flows of invertebrate prey link streams and riparian zones. Freshwater Biology 50: 201–220. https://doi.org/10.1111/j.1365-2427.2004.01328.x

Brydegaard M, Jansson S, Schulz M, Runemark A (2018) Can the narrow red bands of dragonflies be used to perceive wing interference patterns? Ecology and Evolution 8: 5369–5384. https://doi.org/10.1002/ece3.4054

Buffington ML (2012) Description of *Nanocthulhu lovecrafti*, a preternatural new genus and species of Trichoplastini (Figitidae: Eucoilinae). Proceedings of the Entomological Society of Washington 114(1): 5–15. https://doi.org/10.4289/0013-8797.114.1.5

Buffington ML, Condon M (2013) The description and bionomics of *Tropideucoila blepharoneurae* Buffington and Condon, new species (Hymenoptera: Figitidae: Zaeucoilini), parasitoid of *Blepharoneura* Loew fruit flies (Tephritidae). Proceedings of The Entomological Society of Washington 115(4): 349–357. https://doi.org/10.4289/0013-8797.115.4.349

Buffington ML, Sandler RJ (2011) The occurrence and phylogenetic implications of wing interference patterns in Cynipoidea (Insecta: Hymenoptera). Invertebrate Systematics 25: 586–597. https://doi.org/10.1071/IS11038

Butterworth NJ, White TE, Byrne PG, Wallman JF (2021) Love at first flight: wing interference patterns are species-specific and sexually dimorphic in blowflies (Diptera: Calliphoridae). Journal of Evolutionary Biology 34(3): 558–570. https://doi.org/10.1111/jeb.13759

de Jong H, Oosterbroek P, Gelhaus J, Reusch H, Young C (2007) Global diversity of craneflies (Insecta, Diptera: Tipuloidea or Tipulidae sensu lato) in freshwater. In: Balian EV, Lévêque C, Segers H, Martens K (Eds) Freshwater Animal Diversity Assessment. Developments in Hydrobiology, vol. 198. Springer, Dordrecht, 457–467. https://doi.org/10.1007/978-1-4020-8259-7_46

Enderlein G (1912) Studien uber die Tipuliden, Limoniiden, Cylindrotomiden und Ptychopteriden. Zoologische Jahrbucher, Abteilung fur Systematik, Geographie und Biologie der Tiere 32: 1–88. https://www.biodiversitylibrary.org/part/37822

Freeman BE (1968) Studies on the ecology of adult Tipulidae (Diptera) in southern England. Animal Ecology 37: 339–362. https://doi.org/10.2307/2952

Gelhaus JK, Podeniene V (2019) Chapter 24: Tipuloidea. In: Merritt R, Cummins K, Berg MB (Eds.) An introduction to the aquatic insects of North America, Kendall Hunt Dubuque, IA, USA, 1023–1070. https://he.kendallhunt.com/product/introduction-aquatic-insects-north-america

Hansson C, Hambäck PA (2013) Three cryptic species in *Asecodes* (Förster) (Hymenoptera, Eulophidae) parasitizing larvae of *Galerucella* spp. (Coleoptera, Chrysomelidae), including a new species. Journal of Hymenoptera Research 30: 51–64. https://doi.org/10.3897/jhr.30.4279

Hansson C, Shevtsova E (2010) Three new species of *Achrysocharoides* Girault (Hymenoptera: Eulophidae) parasitoids of *Phyllonorycter spp.* (Lepidoptera: Gracillariidae) on *Acer platanoides* and *Robinia pseudoacacia*. Zootaxa 2388: 23–43. https://doi.org/10.11646/zootaxa.2388.1.2

Hansson C, Shevtsova E (2012) Revision of the European species of Omphale Haliday (Hymenoptera: Chalcidoidea: Eulophidae). ZooKeys 232: 1–157. https://doi.org/10.3897/zookeys.232.3625

Hawkes MF, Duffy E, Joag R, Skeats A, Radwan J, Wedell N, Sharma MD, Hosken DJ, Troscianko J (2019) Sexual selection drives the evolution of male wing interference patterns. Proceedings of the Royal Society B, 286: 20182850–20182850. https://doi.org/10.1098/rspb.2018.2850

Kangasniemi S (2012) Constructing phylogenetic trees using wing interference patterns in the tribe Meteorini (Braconidae, Hymenoptera). Master's Thesis, Uppsala University, Stockholm. http://files.webb.uu.se/uploader/271/BIOMSc-13-008-Kangasniemi-Sanna-report.pdf

Katayama N, Abbott JK, Kjærandsen J, Takahashi Y, Svensson EI (2014) Sexual selection on wing interference patterns in *Drosophila melanogaster*. Proceedings of the Academy of Sciences of the United States of America 111(42): 15144–15148. https://doi.org/10.1073/pnas.1407595111

Mitroiu M-D (2013) Afrotropical Watshamia. Entomological Science 16: 191–195. https://doi.org/10.1111/j.1479-8298.2012.00554.x

Murali G (2018) Now you see me, now you don't: dynamic flash coloration as an antipredator strategy in motion. Animal Behaviour 142: 207–220. https://doi.org/10.1016/j.anbehav.2018.06.017

Murali G, Kodandaramaiah U (2020) Size and unpredictable movement together affect the effectiveness of dynamic flash coloration. Animal Behaviour 62: 87–93. https://doi.org/10.1016/j.anbehav.2020.02.002

Oosterbroek P (2021) Catalogue of the Craneflies of the World. www.ccw.naturalis.nl [accessed 22 June 2021]

Petersen MJ, Bertone MA, Wiegmann BM, Courtney GW (2010) Phylogenetic synthesis of morphological and molecular data reveals new insights into the higher-level classification of Tipuloidea (Diptera). Systematic Entomology 35(3): 526–545. https://doi.org/10.1111/j.1365-3113.2010.00524.x

Pritchard G (1983) Biology of Tipulidae. Annual Review of Entomology 28: 1–22. https://doi.org/10.1146/annurev.en.28.010183.000245

Robinson WH (2005) Handbook of urban insects and arachnids. Cambridge University Press: Cambridge, viii + 472 pp. https://doi.org/10.1017/CBO9780511542718

Saigusa T (2006) A new interpretation of the wing venation of the order Diptera and its influence on the theory of the origin of the Diptera (Insecta: Holometabola). Presented at the 6th International Congress of Dipterology, Fukuoka, Japan, 26 pp. http://www.online-keys.net/sciaroidea/2000_/Saigusa_2006_wing_venation.pdf

Salmela J, Kaunisto KM, Vahtera V (2014) Unveiling of a cryptic Dicranomyia (Idiopyga) from northern Finland using integrative approach (Diptera, Limoniidae). Biodiversity Data Journa 2014(2): e4238. https://doi.org/10.3897/BDJ.2.e4238

Shevtsova E (2012) Seeing the invisible: Evolution of wing interference patterns in Hymenoptera, and their application in taxonomy. Doctoral Thesis, Lund University, Lund. https://portal.research.lu.se/portal/en/publications/seeing-the-invisible-evolution-of-wing-interference-patterns-in-hymenoptera-and-their-application-in-taxonomy(6fcceb5d-e41b-455c-b3d9-52d7ba6562f2).html

Shevtsova E, Hansson C (2011) Species recognition through wing interference patterns (WIPs) in *Achrysocharoides* Girault (Hymenoptera, Eulophidae) including two new species. ZooKeys 154: 9–30. https://doi.org/10.3897/zookeys.154.2158

Shevtsova E, Hansson C, Janzen DH, Jostein K (2011) Stable structural patterns displayed on transparent insect wings. Proceedings of the National Academy of Sciences of the United States of America 108(2): 668–673. https://doi.org/10.1073/pnas.1017393108

Simon E (2013) Preliminary study of wing interference patterns (WIPs) in some species of soft scale (Hemiptera, Sternorrhyncha, Coccoidea, Coccidae). ZooKeys 319: 269–281. https://doi.org/10.3897/zookeys.319.4219

Stich HF (1963) An experimental analysis of the courtship pattern of *Tipula oleracea* (Diptera). Canadian Journal of Zoology 41: 99–109. https://doi.org/10.1139/z63-011

Sullivan RT (1981) Insect swarming and mating. Florida Entomologist 64: 44–65. https://doi.org/10.2307/3494600

Sun J, Bhushan B, Tong J (2013) Structural coloration in nature. RSC Advances 3: 14862–14889. https://doi.org/10.1039/c3ra41096j

Ujvárosi L, Bálint M, Schmitt T, Mészáros N, Ujvárosi T, Popescu O (2010) Divergence and speciation in the Carpathians area: patterns of morphological and genetic diversity of the crane fly *Pedicia occulta* (Diptera: Pediciidae). Freshwater Science 29(3): 1075–1088. https://doi.org/10.1899/09-099.1

Watanabe K, Suzuki Y, Inami S, Ohashi H, Sakai T (2018) Light is required for proper female mate choice between winged and wingless males in Drosophila. Genes & Genetic Systems 93(3): 119–123. https://doi.org/10.1266/ggs.18-00004

Zhang M, Chu W-W, Pape T, Zhang D (2014) Taxonomic review of the *Sphecapatodes ornata* group (Diptera: Sarcophagidae: Miltogramminae), with description of one new species. Zoological Studies 2014: 53–48. https://doi.org/10.1186/s40555-014-0048-9

Supplementary material 1

Movie S1

Authors: Robert T. Conrow, Jon K. Gelhaus

Data type: video (mpeg) file

Explanation note: Movie of pinned male specimen of *Gnophomyia tristissima* with shifting background color to display how WIP can change based on background alone. We created this video in the lab to demonstrate how visual transmission of WIP changes with changes to the background. When the background is white, the wing appears clear but as we move the black background under the wing the WIP is instantly visible. Given this rapid change, we question if this rapid change in WIP could be utilized as an anti-predator defense. Movie created using the rear-facing camera of a LG-G7 cell phone (Model LM-G710TM, Android version 10, software version G710TM30b).

Link: https://doi.org/10.3897/zookeys.1080.69060.suppl1

ZooKeys 1080: 165–208 (2022)
doi: 10.3897/zookeys.1080.71192
https://zookeys.pensoft.net

RESEARCH ARTICLE

A peer-reviewed open-access journal
ZooKeys
Launched to accelerate biodiversity research

The genus *Cletocamptus* (Harpacticoida, Canthocamptidae): a reappraisal, with proposal of a new subfamily, a new genus, and a new species

Samuel Gómez[1], Beatriz Yáñez-Rivera[2]

1 *Universidad Nacional Autónoma de México, Instituto de Ciencias del Mar y Limnología, Unidad Académica Mazatlán; Joel Montes Camarena s/n, Mazatlán, 82040, Sinaloa, Mexico* **2** *Consejo Nacional de Ciencia y Tecnología-Centro de Investigación en Alimentación y Desarrollo, Unidad Mazatlán en Acuicultura y Manejo Ambiental; Av. Sábalo Cerritos s/n, Estero del Yugo, Mazatlán, 82112, Sinaloa, Mexico*

Corresponding author: Samuel Gómez (samuelgomez@ola.icmyl.unam.mx)

Academic editor: Kai Horst George | Received 6 July 2021 | Accepted 1 October 2021 | Published 7 January 2022

http://zoobank.org/966E76BB-3209-4D2A-A014-6AADE07A9823

Citation: Gómez S, Yáñez-Rivera B (2022) The genus *Cletocamptus* (Harpacticoida, Canthocamptidae): a reappraisal, with proposal of a new subfamily, a new genus, and a new species. ZooKeys 1080: 165–208. https://doi.org/10.3897/zookeys.1080.71192

Abstract

A new species of *Cletocamptus* closely related to *C. helobius* was found in sediment samples taken from a polluted estuarine system in north-western Mexico. The genus *Cletocamptus* was relegated to *species incertae sedis* in 1986, and this finding prompted us to evaluate the current taxonomic position of the genus within the Canthocamptidae. The latter has been subdivided in several, seemingly unnatural subfamilies in the past to better understand the relationships between its constituent taxa. In this study we propose a new subfamily, the Cletocamptinae **subfam. nov.** for *Amphibiperita*, *Cletocamptus*, and *Cletocamptoides* gen. nov., defined by the synapomorphic subdistal ventral spinules on the rostrum. The genus *Cletocamptoides* **gen. nov.** is proposed for *C. helobius*, *C. merbokensis*, and *C. biushelo* **sp. nov.**, and is supported by the 'cletodid' shape of the body and the reduced one-segmented endopod of the fourth swimming leg. *Cletocamptus* includes all the other species with long slender spinules on the posterior margin of prosomites and with the sexually modified inner spine on the second endopodal segment of the second swimming leg in the males. *Amphibiperita* retained the primitive female fifth leg with exopod and baseoendopod separated, and the primitive prehensile endopod of the first leg, but is defined by the loss of the antennary exopod. Other (syn)apomorphies are given, and the evolution of the mandibular palp is briefly discussed. Additionally, a diagnosis for the new subfamily, *Cletocamptinae* **subfam. nov.**, an amended narrower diagnosis for *Cletocamptus*, the diagnosis for *Cletocamptoides* **gen. nov.**, and a phylogenetic analysis supporting the proposal of these new taxa, are given.

Keywords
Copepoda, Crustacea, diversity, meiofauna, phylogeny, systematics

Introduction

Several canthocamptid species were found in meiofauna samples taken during a short-term study on the effects of organic pollution on the diversity and abundance of harpacticoids. *Cletocamptus sinaloensis* Gómez, Fleeger, Rocha-Olivares & Foltz, 2004 was by far the most abundant canthocamptid, followed by *Mesochra* cf. *pygmaea* (Claus, 1863), but the most intriguing was a form of *Cletocamptus* Schmankevitsch, 1875 closely related to *C. helobius* Fleeger, 1980, the latter known from salt marshes in Louisiana (Fleeger 1980). The genus *Cletocamptus* was erected by Schmankevitsch (1875) for *C. retrogressus* Schmankevitsch, 1875 and the species was allocated in the Cletodidae Scott T., 1904, but Por (1986) removed the genus from the Cletodidae and reallocated it into the Canthocamptidae *incertae sedis* where it stays until today. The find of this material prompted us to analyze and reconsider the taxonomic position of the genus. The taxonomic history of the Canthocamptidae is very complex, and the main approach to understand the relationships amongst its constituent genera has been the proposal of several subfamilies and species groups, e.g., the Rhyncoceratinae Labbé, 1926, the Biarticulata and the Uniarticulata (Chappuis 1929a), the Canthocamptinae Brady, 1880, the Halocanthocamptinae Pesta, 1932, the six species groups of Gurney (1932), the Morariinae Borutzky, 1952, the Epactophaninae Borutzky, 1952, and more recently the *Mesochra* group *sensu* Karaytuğ and Huys (2004), but it seems none of these subfamilies/groups are natural units. In this study, we propose a new subfamily, the Cletocamptinae subfam. nov. for three genera, *Cletocamptus*, *Amphibiperita* Fiers & Rutledge, 1990, and *Cletocamptoides* gen. nov., the latter for *C. helobius*, *C. merbokensis* Gee, 1999, and *Cletocamptoides biushelo* sp. nov. The new subfamily is justified by the synapomorphic subdistal ventral spinules of the rostrum. The relationships amongst the new genera are discussed and apomorphies for them and for some species are given.

Material and methods

Field and laboratory work

Sediment samples were taken at several sampling stations along Urías system (northwestern Mexico) (see Gómez 2020: 43, fig. 1) with an Eckman grab (sampling area of 625 cm^2). Triplicate sediment cores were taken at each sampling site with acrylic corers (sampling area of 24.6 cm^2) and the upper 3 cm layer of each sample was retrieved

and fixed in pure ethanol. Macro- and meiofauna were separated with 500 and 38 µm sieves and meiofauna was extracted through centrifugation with Ludox HS-40 following Burgess (2001) and Rohal et al. (2016) and preserved in pure ethanol. The biological material was sorted at a magnification of 40× using an Olympus SZX12 stereomicroscope equipped with DF PLAPO 1× objective and WHS10× eyepieces, and harpacticoid copepods were stored separately in 1 ml vials with pure ethanol. Illustrations and figures were made from the whole individual and its dissected parts using a Leica DMLB microscope equipped with L PLAN 10× eyepieces, N PLAN 100× oil immersion objective, and drawing tube. The dissected parts were mounted on separate slides using lactophenol as mounting medium. Huys and Boxshall (1991) was followed for general terminology.

Abbreviations used in the text

BENP	baseoendopod;
ENP	endopod;
EXP	exopod;
EXP (ENP)1 (2, 3)	first (second, third) exopodal (endopodal) segment;
P1–P6	first to sixth legs.

Phylogenetics

A phylogenetic analysis was performed with 39 characters and 36 taxa (Tables 1, 2). The taxa considered in this analysis were: the genus *Cletocamptus* as defined below (species with poor descriptions were excluded), the genus *Cletocamptoides* gen. nov. as defined below, *Amphibiperita neotropica* Fiers & Rutledge, 1990, and some of the best described species of the subfamilies Canthocamptinae, Hemimesochrinae, and Epactophaninae (see Table 2). We used the Podogennonta as defined by Seifried (2003) as outgroup. Our phylogenetic analysis does not aim at the complete understanding of the relationships amongst all the canthocamptid subfamilies, or amongst the genera and species of Cletocamptinae subfam. nov., and is not to be regarded as definitive, but only as illustrative to support the proposal of Cletocamptinae subfam. nov. and *Cletocamptoides* gen. nov.

The maximum parsimony analysis was performed using Phylip ver. 3.697 (Felsenstein 2005) and Bayesian inference with MrBayes ver. 3.2.7a (Huelsenbeck and Ronquist 2001). A Wagner parsimony method with unordered multistates, randomize input order species and weights option was carried out. Missing data were coded as '?', inapplicable states were coded as '-'. A consensus tree was obtained from the majority rule and support values were performed from 10,000 bootstrap replicates. For the Bayesian inference, all characters were of equal weights. The default prior distribution of parameters was used for MCMCMC analyses, with one cold chain and three heated chains for 1,000,000 generations and sampled every 100th

Table 1. List of characters used for the phylogenetic analysis.

Character	Description
1	Body shape: cletodid, with somitic constrictions between somites (1), non-cletodid, without somitic constrictions between somites (0)
2	Posterior ornament of the cephalothorax: unornamented (0), finely serrated/crenulated (1), coarsely serrated (2), short spinules (3), long spinules (4)
3	Posterior ornament of free prosomites: unornamented (0), finely serrated/crenulated (1), coarsely crenulated (2), coarsely serrated (3), short spinules (4), long spinules (5)
4	Sensilla-bearing socles: absence (0), presence (1)
5	Rostrum: not fused to cephalothorax (0), fused to cephalothorax (1)
6	Rostrum ventral ornament: unornamented (0), spinules or setules (1)
7	Number of segments of the female antennule 1: nine (0), eight (1), seven (2), six (3), five (4), four (5)
8	Number of abexopodal setae on the allobasis of the antenna: two (0), one (1) none (2)
9	Number of segments of the antennary exopod: three (0), two (1), one (2), one- seta (3), absent (4)
10	Number of segments of the mandibular palp: one (0), two or more (1)
11	Ramification of the mandibular palp: biramous (exopod and endopod discernible even if rami fused to basis) (0), monoramous (only endopod discernible even if fused to basis) (1)
12	Number of setae on the mandibular palp: four (0), three (1), two (2), one (3), unarmed (4)
13	Number of setae on the syncoxa of the maxilliped: four (0), one (1), unarmed (2)
14	Shape of P1 ENP: prehensile (0), not prehensile (1)
15	Number of segments of P1 ENP: three (0), two (1), one (2), represented by spine or seta (3), absent (4)
16	Inner setae on P1 ENP1 when two or three-segmented: present (0), absent (1)
17	Number of segments of P2 ENP when present: three (0), two (1), one (2)
18	Inner seta of P2 ENP1 when ENP two- or three-segmented: present (0), absent (1)
19	Inner seta of P2 ENP2 when ENP three-segmented: present (0), absent (1)
20	Number of setae of P2 ENP2 when ENP two-segmented: five (0), four (1), three (2), two (3), one (4), unarmed (5)
21	Number of setae of P2 ENP3 when ENP three-segmented: five (0), four (1), three (2), two (3)
22	Number of setae of P3 EXP3 when EXP three-segmented: eight (0), seven (1), six (2), five (3), four (4)
23	Number of segments of the female P3 ENP when present: three (0), two (1), one (2)
24	Inner seta of P3 ENP1 when ENP two- or three-segmented: present (0), absent (1)
25	Number of setae of P3 ENP1 when ENP one-segmented: three (0), two (1)
26	Number of setae of the female P3 ENP2 when ENP two-segmented: six (0), five (1), four (2), three (3), two (4)
27	Number of setae of P4 EXP3 when EXP three-segmented: eight (0), seven (1), six (2), five (3), four (4)
28	Number of segments of P4 ENP when present: three (0), two (1), one (2), represented by spine or seta (3)
29	Inner seta of P4 ENP1 when ENP two-segmented: present (0), absent (1)
30	Number of setae of P4 ENP1 when ENP one-segmented: four (0), three (1), two (2), one (3)
31	Number of setae of P4 ENP2 when ENP two-segmented: five (0), four (1), three (2), two (3), one (4)
32	Subdistal spine of P2 ENP: present (0), absent (1)
33	Subdistal spine of P3 ENP: present (0), absent (1)
34	Female P5 BENP/EXP fusion: not fused (0), fused (1)
35	Male rostrum dimorphism: present (1), absent (0)
36	Male P5 BENP/EXP fusion: not fused (0), fused (1)
37	Number of setae of male P5 ENP lobe: six (0), three (1), two (2), one (3), unarmed (4)
38	Number of segments of male P3: three (0), two (1)
39	Shape of inner apophysis of male P3: arrow-head tip (0), simple (1)

generation, discarding the first 20% of the burning. Finally, ITOL v5 was used for visualization and editing trees. We used the bioinformatics server Chihuil at Instituto de Ciencias del Mar y Limnología-Universidad Nacional Autómoma de México (**ICML-UNAM**).

In addition to the limited number of canthocamptid taxa used for our phylogenetic analysis, we consulted the available descriptions of 102 species distributed in 45 genera of the different canthocamptid subfamilies for our comparative analysis.

Table 2. Character matrix and weights used for the maximum parsimony analysis.

Subfamily	Species	Characters																																				
		1–10										11–20										21–30										31–39								
		1	2	3	4	5	6	7	8	9	0	1	2	3	4	5	6	7	8	9	0	1	2	3	4	5	6	7	8	9	0	1	2	3	4	5	6	7	8	9
Cletocamptinae	*Amphibiperita neotropica*	0	3	4	0	0	1	3	1	4	1	1	4	1	0	1	0	1	0	-	2	-	2	1	1	-	2	2	1	1	-	2	1	1	0	1	1	1	1	1
subfam. nov.	*Cletocamptoides biushelo* sp. nov.	1	1	1	0	0	1	3	0	3	0	1	3	1	1	1	1	1	0	-	2	-	3	1	1	-	3	4	2	-	2	-	0	0	1	?	?	?	?	?
	Cletocamptoides helobius comb. nov.	1	?	?	0	0	1	3	1	3	0	1	3	2	1	1	1	1	0	-	2	-	3	1	1	-	3	4	2	-	3	-	0	0	1	?	1	1	1	1
	Cletocamptoides merbokensis comb. nov.	1	1	1	1	0	1	3	1	2	0	0	2	2	1	1	1	1	0	-	3	-	3	1	1	-	4	4	2	-	2	-	1	1	1	0	1	1	0	1
	Cletocamptus albuquerquensis	0	4	5	0	0	1	3	0	2	0	1	4	1	1	1	0	1	1	-	2	-	3	1	1	-	1	4	1	1	-	3	0	0	1	1	1	1	1	1
	Cletocamptus assimilis	0	4	5	0	0	1	3	0	2	0	1	4	1	1	1	0	1	1	-	2	-	3	1	1	-	3	4	1	1	-	3	0	0	1	?	?	?	?	?
	Cletocamptus axi	0	4	5	0	0	1	3	0	2	0	1	4	1	1	1	0	1	1	-	2	-	3	1	1	-	3	4	1	1	-	3	0	0	1	1	1	1	0	1
	Cletocamptus cecsurirensis	0	4	5	0	0	1	3	0	2	0	1	4	1	1	1	0	1	1	-	2	-	3	1	1	-	3	4	1	1	-	3	0	0	1	1	1	1	0	1
	Cletocamptus confluens	0	4	5	0	0	1	3	0	2	0	1	3	1	1	1	0	1	1	-	2	-	3	1	1	-	1	4	1	1	-	3	0	0	1	?	1	1	1	1
	Cletocamptus deborahdexterae	0	4	5	0	0	1	3	0	2	0	1	4	1	1	1	0	1	1	-	2	-	3	1	1	-	3	4	1	1	-	3	0	0	1	1	1	1	0	1
	Cletocamptus dominicanus	0	1	1	0	0	1	3	0	2	0	1	4	1	1	1	0	1	1	-	2	-	3	1	1	-	1	4	2	-	2	-	0	0	1	1	1	1	1	1
	Cletocamptus fourchensis	0	4	5	0	0	1	3	0	2	0	1	4	1	1	1	1	1	1	-	2	-	3	1	1	-	3	4	1	1	-	3	0	0	1	1	1	1	0	1
	Cletocamptus goenchim	0	4	5	0	0	1	3	0	2	0	1	4	1	1	1	0	1	1	-	2	-	2	1	1	-	1	3	1	1	-	3	0	0	1	1	1	1	0	1
	Cletocamptus gomezi	0	4	5	0	1	1	3	1	2	0	1	4	1	1	1	0	1	1	-	1	-	3	1	1	-	1	4	1	1	-	3	0	0	1	?	1	1	0	1
	Cletocamptus levis	0	4	5	0	0	1	3	0	2	0	1	4	1	1	1	0	1	1	-	2	-	3	1	1	-	3	4	1	1	-	3	0	0	1	1	1	1	0	1
	Cletocamptus nudus	0	4	5	0	0	1	3	0	2	0	1	4	1	1	1	0	1	1	-	2	-	2	1	1	-	3	3	1	1	-	3	0	0	1	1	1	1	0	1
	Cletocamptus pilosus	0	4	5	0	0	1	3	0	2	0	1	4	1	1	1	0	1	1	-	1	-	2	1	1	-	1	3	1	1	-	3	0	0	1	1	1	1	0	1
	Cletocamptus retrogressus	0	4	5	0	0	1	3	1	2	1	1	3	1	1	1	1	1	1	-	1	-	2	1	1	-	1	3	1	1	-	3	0	0	1	1	1	1	0	1
	Cletocamptus samariensis	0	?	?	0	0	1	3	0	2	0	1	4	1	1	1	0	1	1	-	2	-	2	1	1	-	3	3	1	1	-	3	0	0	1	1	1	1	0	1
	Cletocamptus schmidti	0	4	5	0	0	1	3	0	2	0	1	4	1	1	1	0	1	1	-	2	-	2	1	1	-	3	3	1	1	-	3	0	0	1	1	1	1	0	1
	Cletocamptus sinaloensis	0	4	5	0	0	1	3	0	2	0	1	4	1	1	1	0	1	1	-	2	-	3	1	1	-	3	4	1	1	-	3	0	0	1	1	1	1	0	1
	Cletocamptus spinulosus	0	0	5	0	0	1	3	0	2	0	1	4	1	1	1	0	1	1	-	2	-	3	1	1	-	3	4	1	1	-	3	0	0	1	1	1	1	0	1
	Cletocamptus stimpsoni	0	4	4	0	0	1	3	0	2	0	1	4	1	1	1	0	1	1	-	2	-	2	1	1	-	1	3	1	1	-	3	0	0	1	1	1	1	0	1
	Cletocamptus tainoi	0	4	4	0	0	1	3	0	2	0	1	4	1	1	1	0	1	1	-	2	-	3	1	1	-	1	4	1	1	-	3	0	0	1	1	1	1	1	1
	Cletocamptus tertius	0	4	5	0	0	1	3	0	2	0	1	4	1	1	1	0	1	1	-	2	-	3	1	1	-	3	4	1	1	-	3	0	0	1	1	1	1	0	1
Canthocamptinae	*Canthocamptus incurvisetosus*	0	0	0	0	1	0	1	?	1	?	?	4	1	0	0	0	0	0	0	-	0	1	1	0	-	1	1	1	0	-	0	0	0	0	0	0	2	0	0
	Canthocamptus odaeensis	0	0	0	0	1	0	1	?	1	1	0	4	1	0	0	0	0	0	0	-	0	1	1	0	-	1	1	1	0	-	0	0	0	0	0	0	2	0	0
	Elaphoidella bulgarica	0	0	0	0	?	?	1	1	2	?	?	?	?	1	0	0	1	0	0	-	-	2	1	0	1	-	2	2	-	1	-	0	0	0	0	0	4	0	1
	Elaphoidella_formosanus	0	0	0	0	1	0	1	?	2	?	?	?	?	1	0	0	1	1	0	-	-	2	1	1	1	-	3	1	0	-	1	0	0	0	0	0	4	0	1
	Elaphoidella hirsutus	0	2	3	0	1	0	1	?	2	?	?	?	?	1	0	0	1	0	0	-	-	2	1	1	0	-	2	1	1	-	1	0	0	0	?	?	?	?	?
Hemimesochrinae	*Isthmiocaris laurae*	0	0	0	0	0	0	3	1	2	0	0	3	1	1	1	1	2	-	-	-	-	4	2	-	1	-	4	2	-	3	-	0	0	1	0	0	2	0	0
	Isthmiocaris longitelson	0	0	0	0	0	0	3	1	2	1	1	4	1	1	2	-	-	-	-	-	-	5	-	-	-	-	-	-	-	-	-	-	1	0	1	3	0	0
	Itunella arenaria	0	0	2	0	0	0	2	1	2	0	0	4	1	1	1	1	2	-	-	-	-	3	2	-	0	-	3	2	-	1	-	0	0	0	0	0	2	1	-
Hepactophaninae	*Stygepactophanes_occitanus*	0	0	0	0	1	0	2	0	2	0	1	4	2	1	1	1	1	1	-	2	-	4	1	1	-	3	3	2	-	2	-	0	0	0	?	?	?	?	?
	Epactophanes philippinus	0	0	0	0	1	0	2	1	2	0	1	4	2	1	1	1	1	1	-	4	-	3	1	1	-	4	3	2	-	3	-	1	1	0	0	1	4	0	1
Outgroup	Podogennonta	0	0	0	0	?	?	0	?	0	1	0	0	0	0	0	0	0	0	0	-	0	0	0	0	-	-	0	0	0	-	-	?	?	0	?	0	1	0	?
Weights		5	1	3	1	1	A	1	1	1	1	1	1	1	5	1	1	1	5	1	1	1	1	1	1	1	1	1	3	1	1	1	1	1	5	1	1	1	1

Results

Taxonomy

Family Canthocamptidae Brady, 1880

Subfamily Cletocamptinae subfam. nov.
http://zoobank.org/E20214E6-38CB-4E00-8082-490FA7FA50A8

Type genus. *Cletocamptus* Schmankevitsch, 1875.

Other genera. *Amphibiperita* Fiers & Rutledge, 1990, *Cletocamptoides* gen. nov.

Diagnosis. Canthocamptidae. Body fusiform, without clear distinction between prosome and urosome. Without nuchal organs on cephalothorax or body somites. Female rostrum distinct, rarely fused to cephalothorax, large and triangular with broad proximal margin; ornamented with ventral (sub)distal spinules or (occasionally) setules and with rounded or (rarely) bilobed tip in both sexes. Cephalothorax and/or prosomites with posterior margins serrated or ornamented with short or long slender spinules; posterior margin of urosomites except for anal somite serrated or with short spinules; posterior margin of cephalothorax and body somites without or (rarely) with cuticular sensillum-bearing socles. Anal operculum without dorsal ornamentation or with transverse row of strong large or short, small spinules; posterior margin unornamented, serrated, or with small or large spinules. Female genital somite and third urosomite separated dorsolaterally, completely fused ventrally forming genital double-somite. Female antennule six-, rarely seven-segmented. Antenna with allobasis, with one or two abexopodal setae (proximal element basal, distal seta endopodal); exopod one-segmented, longer than wide or minute, or absent. Mandibular palp one-segmented, very small and wider than long, or longer than wide; basis and endopod incorporated to basis or (rarely) with basis and endopod distinct (uniramous); exopod absent or (rarely) represented by single seta; when palp uniramous, then basis unarmed or with one seta, endopod with three setae at most; when palp one-segmented and longer than wide, then with two basal and two endopodal setae at most, and exopod (when present) represented by single seta; when palp one-segmented very small and wider than long, then basis and endopod not discernible, with one or two (most probably endopodal) setae, with or without surface (most probably exopodal) seta on coxa. Maxillule with endopod and exopod incorporated to basis; praecoxal arthrite with ventral seta thick and strongly spinulose, or slender and pinnate or smooth. Maxilla with two syncoxal endites; endopod completely incorporated to allobasis. Maxilliped subchelate; syncoxa with one seta; basis unarmed; claw with accessory seta. P1 not prehensile, rarely prehensile; P1–P4 EXP three-segmented; female P1–P3 ENP two-segmented, P4 ENP two- or one-segmented; inner exopodal and endopodal setae with or without comb tip. Female P5 EXP and BENP fused, occasionally separated; both baseoendopods of P5 separated. Armature formulae as follows:

	P1	P2	P3	P4	P5
EXP	0;1;0,1-2,2	0;1;1,2,2	0;1;1-2,2,2	0;0-1;0-2,2,2	♀3-5 ♂3-4
ENP	0-1;1,1-2,1	0-1;0-2,1-2,0-1	♀0;0-2,1-2,0-1 ♂dimorphic: 0-1;iap;0,2,0 or 0-1;iap,2,0 or 0;iap,1,oap	0;0,2,0 or 0,2,0	♀5-6 (7*) ♂3

iap, inner apophysis; oap, outer apophysis.
*The seven-segmented antennule of *C. gravihiatus* (Shen & Sung, 1963) requires confirmation.

Female P6 with one or two setae. Caudal rami with six or seven setae; setae IV and V fused basally or separated.

Sexual dimorphism can be expressed in a) rostrum slenderer in the male, b) the male antennule (chirocer or subchirocer), c) basis of P1 (with or without inner distal process), d) outer spine on P2 ENP2 (thicker and/or shorter than in the female), e) P2 EXP and/or P3 and P4 EXP (segments longer than in the female, outer spines stronger than in the female, rami curved inwards,), f) shape of P2-P4 ENP (segments thicker than in female), g) P3 ENP (two- or three-segmented; when three-segmented then inner apophysis on second segment; when two-segmented then inner apophysis medially or subdistally on second segment, occasionally with additional outer apophysis; inner apophysis simple, without arrow-head tip, variable in length; with or without asprothekes on second segment), h) P5 (both legs fused medially or separated; EXP and BENP fused; both legs separated or fused to somite), i) P6 (composed of two lappets articulated to somite or asymmetrical in which case only one leg functional, the other fused to somite; unarmed or (occasionally) with one or two setae), j) caudal rami (longer than in the female).

Genus *Cletocamptus* Schmankevitsch, 1875

Type species. *Cletocamptus retrogressus* Schmankevitsch, 1875 (type by original designation).

Other species. *Cletocamptus affinis* Kiefer, 1957, *C. albuquerquensis* (Herrick, 1894), *C. assimilis* Gomez & Gee, 2009, *C. axi* Mielke, 2000, *C. cecsurirensis* Gómez, Scheihing & Labarca, 2007, *C. chappuisi* Gómez, Gerber & Fuentes-Reinés, 2017, *Cletocamptus confluens* (Schmeil, 1894), *C. deborahdexterae* Gómez, Fleeger, Rocha-Olivares & Foltz, 2004, *C. dominicanus* Kiefer, 1934, *C. feei* (Shen, 1956), *C. fourchensis* Gómez, Fleeger, Rocha-Olivares & Foltz, 2004, *C. goenchim* Gómez, Ingole, Sawant & Singh, 2013, *C. gomezi* Suárez-Morales, Barrera-Moreno & Ciros-Pérez, 2013, *C. gravihiatus* (Shen & Sung, 1963), *C. koreanus* Chang, 2013, *C. levis* Gómez, 2005, *C. mongolicus* Stěrba, 1968, *C. nudus* Gómez, 2005, *C. pilosus* Gomez & Gee, 2009, *C. samariensis* Fuentes-Reinés, Zoppi de Roa & Torres, 2015, *C. schmidti* Mielke, 2000, *C. sinaloensis*

Gómez, Fleeger, Rocha-Olivares & Foltz, 2004, *C. spinulosus* Gomez & Gee, 2009, *C. stimpsoni* Gómez, Fleeger, Rocha-Olivares & Foltz, 2004, *C. tainoi* Gómez, Gerber & Fuentes-Reinés, 2017, *C. tertius* Gomez & Gee, 2009, *C. trichotus* Kiefer, 1929.

Species *incertae sedis*. *Marshia brevicaudata* Herrick, 1894.

Species inquirendae. *Cletocamptus bermudae* Willey, 1930, *C.* cfr. *bicolor sensu* Herbst (1960), *C. brehmi* Kiefer, 1933, *Cletocamptus deitersi* (Richard, 1897), *C. deitersi sensu* Chappuis (1934), *C. deitersi sensu* Daday (1902), *C. deitersi sensu* Dussart (1974), *C. deitersi sensu* Hamond (1973), *C. deitersi sensu* Herbst (1960), *C. deitersi sensu* Kiefer (1936), *C. deitersi sensu* Suárez-Morales et al. (1996), *C. deitersi sensu* Tai and Song (1979), *C. ecuadorianus* Löffler, 1963, *C. gabrieli* Löffler, 1961, *C. kummleri* (Delachaux, 1917), *Godotella dadayi* Delachaux, 1917.

Doubtful records. *C. deitersi*: in Apostolov (1984), Brehm (1936, 1965), Chappuis (1936), Dussart and Frutos (1986), Loftus and Reid (2000), Oliveira et al. (1971), Ranga Reddy and Radhakrishna (1979), Ringuelet (1958a, 1958b, 1960, 1962), Ringuelet et al. (1967), Ruber et al. (1994), Sitjar (1988), Zamudio-Valdéz (1991).

Diagnosis. Canthocamptidae: Cletocamptinae. Body fusiform, without clear distinction between prosome and urosome. Without nuchal organs on cephalothorax or body somites. Female rostrum distinct, rarely fused to cephalothorax, large and triangular with broad proximal margin; ornamented with ventral (sub)distal spinules and with rounded tip in both sexes. Posterior margin of cephalothorax and/or prosomites with long and slender, or short spinules, or serrated; posterior margin of urosomites except for anal somite with short spinules or serrated; body somites without cuticular sensillum-bearing socles; anal operculum without dorsal ornamentation or with transverse row of strong, large, or short, small spinules; posterior margin unornamented, or with small or large spinules. Female genital somite and third urosomite separated dorsolaterally, completely fused ventrally forming genital double-somite. Female antennule six-, rarely seven-segmented (the latter reported for *C. gravihiatus* requires confirmation). Antenna with allobasis, with one or two abexopodal setae (proximal element basal, distal seta endopodal); exopod one-segmented and longer than wide, or minute, rarely represented by single seta (the latter reported for *C. chappuisi* requires confirmation). Mandibular palp one-segmented, rarely two-segmented (basis and endopod distinct as in *C. retrogressus*); when one-segmented, then very small and wider than long, or as long as wide (*C. dominicanus*), or longer than wide (*C. confluens*, *C. gomezi*); when palp one-segmented, then basis and endopod not discernible, rarely discernible (represented by single seta as in *C. confluens* and *C. dominicanus*); endopod with two setae, rarely with one single element (*C. pilosus*); exopod absent; with or without surface (most probably exopodal) seta on coxa, the latter present only in some species with a one-segmented palp wider than long, absent in species with palp as long as wide or longer than wide. Maxillule with endopod and exopod incorporated to basis; praecoxal arthrite with ventral seta thick and strongly spinulose, or slender and pinnate or smooth. Maxilla with two syncoxal endites; endopod completely incorporated to allobasis. Maxilliped subchelate; syncoxa with one seta; basis unarmed; claw with accessory seta. P1 ENP not prehensile; P1–P4 EXP three-segmented; female P1–P3

ENP two-segmented, P4 ENP two- or one-segmented; inner exopodal and endopodal setae with or without comb tip (see Gómez et al. 2017). Female P5 EXP and BENP fused; both baseoendopods of P5 separated. Armature formulae as follows:

	P1	P2	P3	P4	P5
EXP	0;1;0,1-2,2	0;1;1,2,2	0;1;1-2,2,2	0;0-1;0-1,2,2	♀4-5 ♂3-4
ENP	0-1;1,1,1	0;1-2,1-2,1	♀0;1-2,1-2,1 ♂dimorphic 0;iap;0,2,0 or 0;iap,2,0* or 0;iap,1,oap**	0;0,2,0 or 0,2,0***	♀5-6 (7+) ♂3

iap, inner apophysis; oap, outer apophysis; * two-segmented with one inner apophysis on second segment in *C. albuquerquensis*, *C. chappuisi*, *C. dominicanus*, *C. tainoi*; ** two segmented, with one inner and one outer apophysis on second segment in *C. confluens*; *** one-segmented in *C. dominicanus*; + the seven setae observed in *C. gravihiatus* requires confirmation

Female P6 with one or two setae. Caudal rami with six or seven setae; setae IV and V fused basally or separated.

Sexual dimorphism expressed in a) rostrum (slenderer than in female), b) the male antennule (subchirocer), c) basis of P1 (with inner distal process), d) outer spine on P2 ENP2 (thicker and/or shorter than in the female), e) P3 ENP (three-segmented as in most species, or two-segmented as in *C. albuquerquensis*, *C. chappuisi*, *C. confluens*, *C. dominicanus*, and *C. tainoi*; when three-segmented then inner apophysis on second segment; when two-segmented then inner apophysis medially as in *C. dominicanus*, or subdistally on second segment as in *C. albuquerquensis*, *C. chappuisi*, *C. confluens*, and *C. tainoi*, but occasionally with additional outer apophysis as in *C. confluens*), f) P5 (both legs fused medially as in most species, or separated as in *C. axi*, *C. cecsurirensis*, *C. retrogressus*, and *C. schmidti*; EXP and BENP fused, and both legs articulating with somite, g) P6 (composed of two lappets articulated to somite and unarmed as in most species or, occasionally, with one seta attributable to intraspecific variability as in *C. axi*, *C. schmidti*, *C. sinaloensis*). Additionally, sexual dimorphism can be expressed also (depending on the species) in a) P2 EXP and/or P3 and P4 EXP (segments longer than in the female, outer spines stronger than in the female, and/or rami curved inwards as in *C. retrogressus*, *C. confluens*, *C. albuquerquensis*, *C. samariensis*, *C. spinulosus*, *C. tainoi*, *C. trichotus*), b) shape of P2–P4 ENP (segments thicker than in female as in *C. confluens*), c) caudal rami (longer than in the female).

Genus *Amphibiperita* Fiers & Rutledge, 1990

Type species. *Amphibiperita neotropica* Fiers & Rutledge, 1990 (type by original designation).

Diagnosis. As in Fiers and Rutledge (1990: 114).

Genus *Cletocamptoides* gen. nov.
http://zoobank.org/21C7CBBC-D8D9-49F5-8A10-DA83FC30E2A1

Type species. *Cletocamptoides merbokensis* (Gee, 1999) comb. nov. (= *Cletocamptus merbokensis* Gee, 1999)

Other species. *Cletocamptoides helobius* (Fleeger, 1980) comb. nov. (= *Cletocamptus helobius* Fleeger, 1980), *Cletocamptoides biushelo* sp. nov.

Diagnosis. Canthocamptidae. Body fusiform, without clear distinction between prosome and urosome; body with somitic constrictions between somites. Without nuchal organs on cephalothorax or body somites. Female rostrum distinct, large, and triangular with broad proximal margin; ornamented with ventral (sub)distal spinules or setules; with rounded or bilobed tip. Cephalothorax and/or prosomites with posterior margins serrated; posterior margin of urosomites except for anal somite serrated; posterior margin of cephalothorax and body somites without or with cuticular sensillum-bearing socles. Anal operculum without dorsal ornamentation or with transverse row of mall spinules; posterior margin unornamented or serrated. Female genital somite and third urosomite separated dorsolaterally, completely fused ventrally forming genital double-somite. Female antennule six-segmented. Antenna with allobasis, with one or two abexopodal setae (proximal element basal, distal seta endopodal); exopod one-segmented and minute, or absent. Mandibular palp one-segmented, longer than wide; endopod incorporated to basis, with two basal and two endopodal setae at most; exopod absent or represented by single seta. Maxillule with endopod and exopod incorporated to basis; praecoxal arthrite with ventral seta thick and strongly spinulose, or slender and pinnate. Maxilla with two syncoxal endites; endopod completely incorporated to allobasis. Maxilliped subchelate; syncoxa unarmed or with one seta; basis unarmed; claw with accessory seta. P1 ENP not prehensile; P1–P4 EXP three-segmented; female P1–P3 ENP two-segmented, P4 ENP one-segmented; inner exopodal and endopodal setae with or without comb tip. Female P5 EXP and BENP fused, separated by shallow or deep notch; both baseoendopods of P5 separated. Armature formulae as follows:

	P1	P2	P3	P4	P5
EXP	0;1;0,2,2	0;1;1,2,2	0;1;1,2,2	0;0-1;0,2,2	♀3–4 ♂3–4
ENP	0;1,1,1	0;0-1,1-2,0-1	♀0;0-1,1-2,0-1 ♂dimorphic: 0;iap;0,2,0 or 0;iap,2,0	0,2,0	♀5–6 ♂3

iap, inner apophysis; oap, outer apophysis.

Female P6 with two setae. Caudal rami slightly convergent; with six setae; setae IV and V separated; seta IV normal, whip-like, slightly tapering posteriad, or with bulbous base.

Sexual dimorphism can be expressed in a) the male antennule (subchirocer), b) setae on P2 ENP2 (spiniform as in *C. merbokensis* comb. nov.), c) P3 ENP (two- or three-segmented; when three-segmented then inner apophysis on second segment

(*C. merbokensis* comb. nov.); when two-segmented then inner apophysis subdistally on second segment (*C. helobius* comb. nov.); inner apophysis simple, without arrow-head tip, variable in length), d) P5 (both legs fused medially (*C. merbokensis* comb. nov.) or separated (*C. helobius* comb. nov.); EXP and BENP fused; both legs separated (*C. helobius* comb. nov.) or fused to somite (*C. merbokensis* comb. nov.)), e) P6.

Etymology. The Ancient Greek sufix εἶδος, eîdos, meaning likeness and refers to the resemblance of the new genus with *Cletocamptus*.

***Cletocamptoides biushelo* sp. nov.**

http://zoobank.org/658B2BB2-1122-454E-B63B-ACC05A76B601

Figs 1–7

Type locality. Urías estuary, Mazatlán, Sinaloa State, stn. 5 (23.2056°N, 106.3715°W; 0.6 m depth; organic carbon content 0.99%; organic matter content 1.71%; sand 78.61%; clay 6.72%; silt 14.67%) (see also Gómez 2020: 43, fig. 1).

Other localities. Urías estuary, Mazatlán, Sinaloa State, stn. 7 (23.2174°N, 106.3917°W; 3.7 m depth; organic carbon content 5.59%; organic matter content 9.62%; sand 10.78%; clay 37.54%; silt 51.68%) (see also Gómez 2020: 43, fig. 1).

Material examined. Female holotype dissected (ICML-EMUCOP-180119-179); 18 Jan. 2019; S. Gómez leg. One additional female from stn 7 (see above) was used for molecular analyses.

Description. Female. Total body length of holotype 411 μm measured from anterior tip of rostrum to posterior margin of caudal rami. Habitus (Fig. 1A, D) semi-cylindrical, progressively tapering posteriad, without clear demarcation between prosome and urosome; body with somitic constrictions between somites; without cuticular sensilla-bearing socles. Prosome (Fig. 1A, D) consisting of cephalothorax, P1-bearing somite fully incorporated to the latter, and three free-pedigerous somites bearing P2–P4. Rostrum (Figs 1A, D, 3A) well-developed, not fused to cephalothorax, triangular, with wide base and rounded tip, with two subdistal sensilla, with row of subdistal spinules ventrally. Cephalothorax with depressions and with sensilla as shown; posterodorsal margin serrated, lateral margin with short slender spinules. P2–P4-bearing somites with posterior sensilla as depicted; posterior margin serrated; lateral margin with short slender spinules. Urosome (Figs 1A, D, 2A) comprising fifth pedigerous somite, genital double-somite, two free abdominal somites, and anal somite. P5-bearing somite largely as in previous somite but with fewer sensilla. Second (genital somite) and third urosomites separated dorsolaterally, fused ventrally forming genital double-somite; first half with posterior margin serrated, posterior half with posterior slender short spinules; both halves with sensilla as shown; anterior half with P6 (see below); posterior half with ventrolateral small slender spinules as depicted. Fourth urosomite largely as preceding somite (second half of genital double-somite), but with more spinules lateroventrally. Fifth somite as previous one dorsolaterally, ventrally with fewer spinular rows. Anal somite slightly wider than long; with small triangular operculum

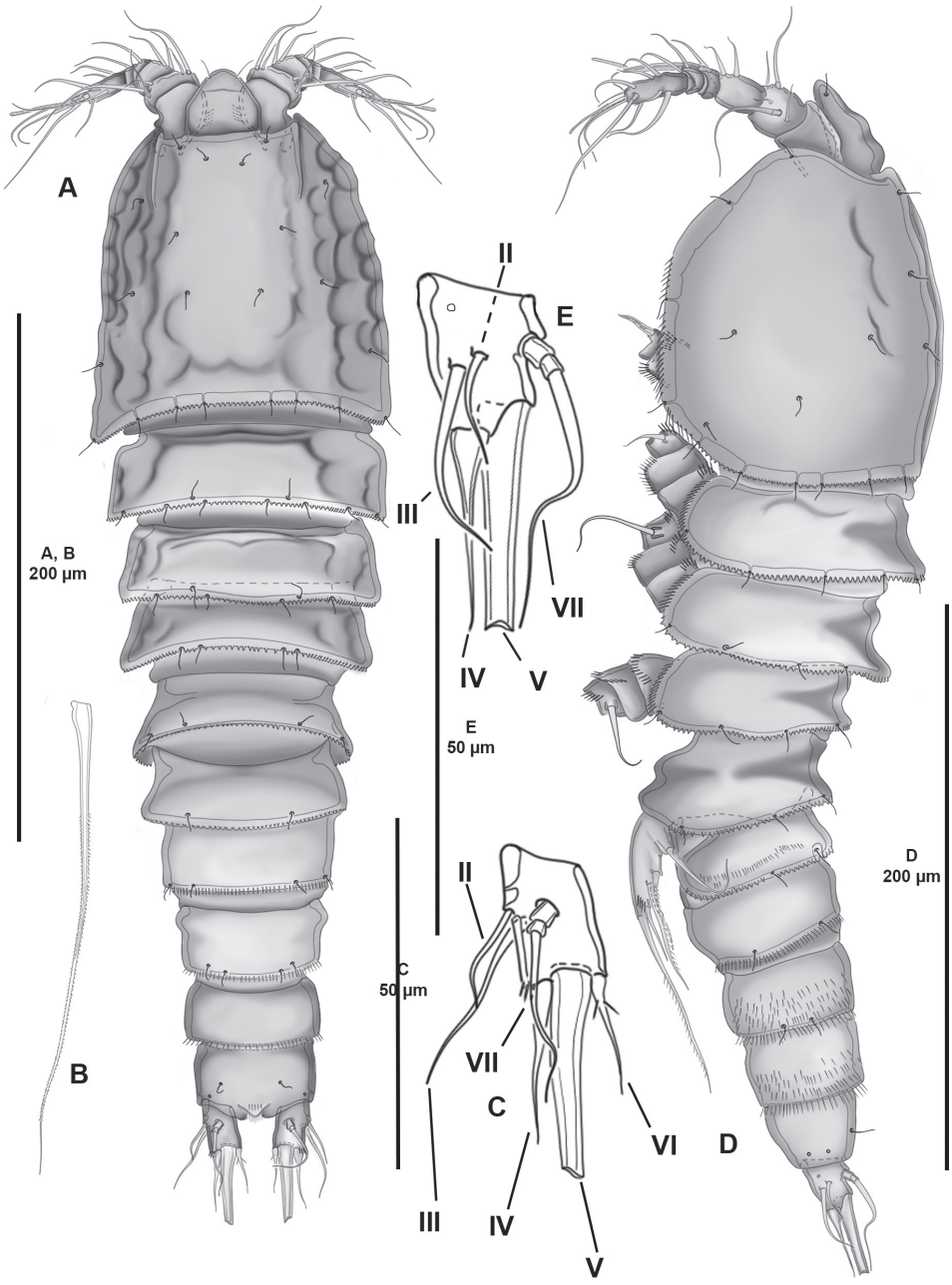

Figure 1. *Cletocamptoides biushelo* sp. nov., female holotype **A** habitus, dorsal **B** caudal seta V **C** left caudal ramus, dorsal **D** habitus, lateral **E** left caudal ramus, lateral.

ornamented with small dorsal spinules, flanked by pair of sensilla; ventrally cleft medially, with pair of medial pores, with inner small spinules along inner margin of medial cleft. Caudal rami 1.5 × as long as wide; with inner long slender spinules; with six setae as follows: seta I missing; seta II and III lateral, issuing midway outer margin of ramus,

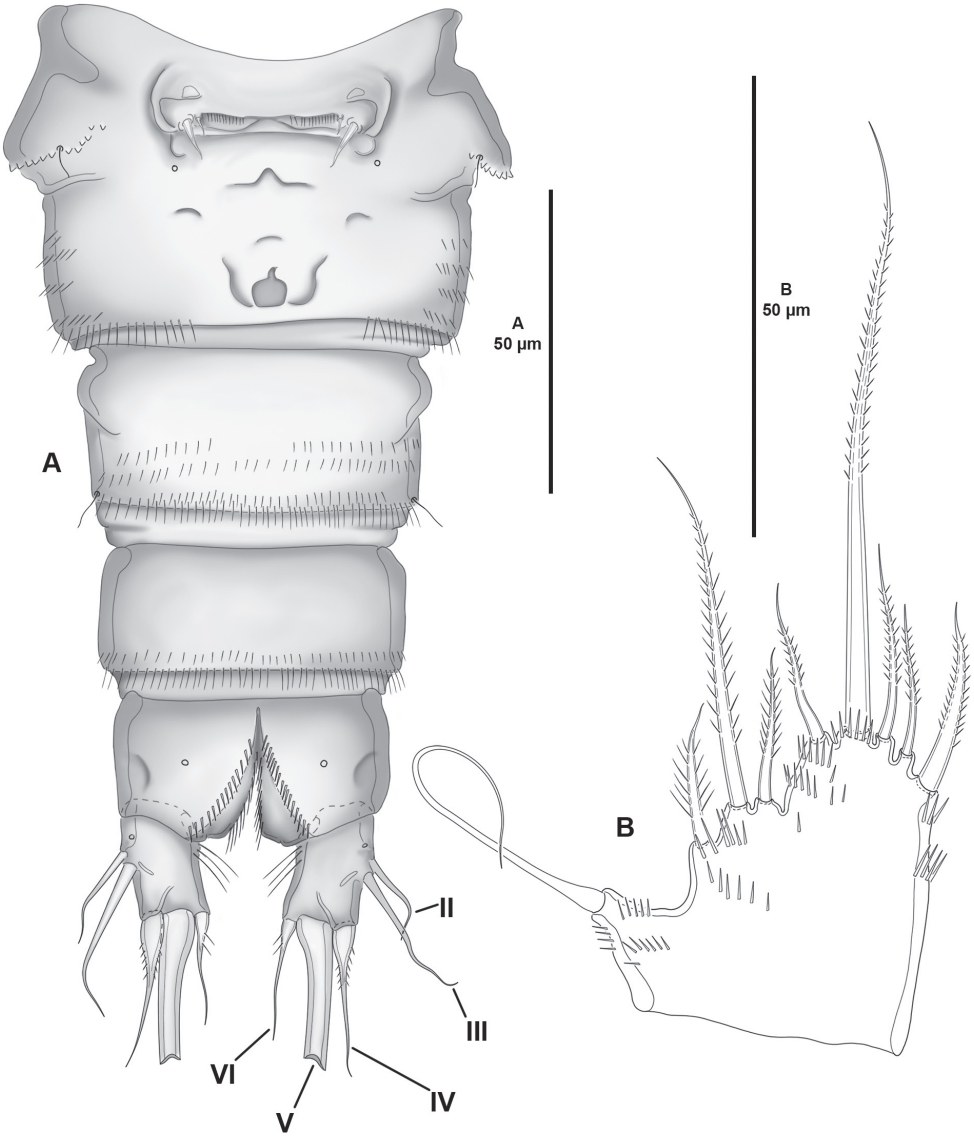

Figure 2. *Cletocamptoides biushelo* sp. nov., female holotype **A** urosome, ventral (P5-bearing somite omitted) **B** P5, anterior.

the former proximal to and slightly as long as half the length of the later; seta IV arising at outer distal corner, as long as seta III, with bulbous base; seta V longest, without breaking plane, minutely bipinnate; seta VI issuing at inner distal corner, slightly shorter than seta IV, with two proximal spinules as shown, with bulbous base; dorsal seta VII located at the center of ramus, as long as seta III, tri-articulated at its base.

Antennule (Fig. 3A) six-segmented; first segment with two inner spinular rows, remaining segments with outer spinular row as depicted; all setae smooth. Armature formula as follows: 1[1], 2[7], 3[4], 4[1+(1+ae)], 5[1], 6[8+(2+ae)].

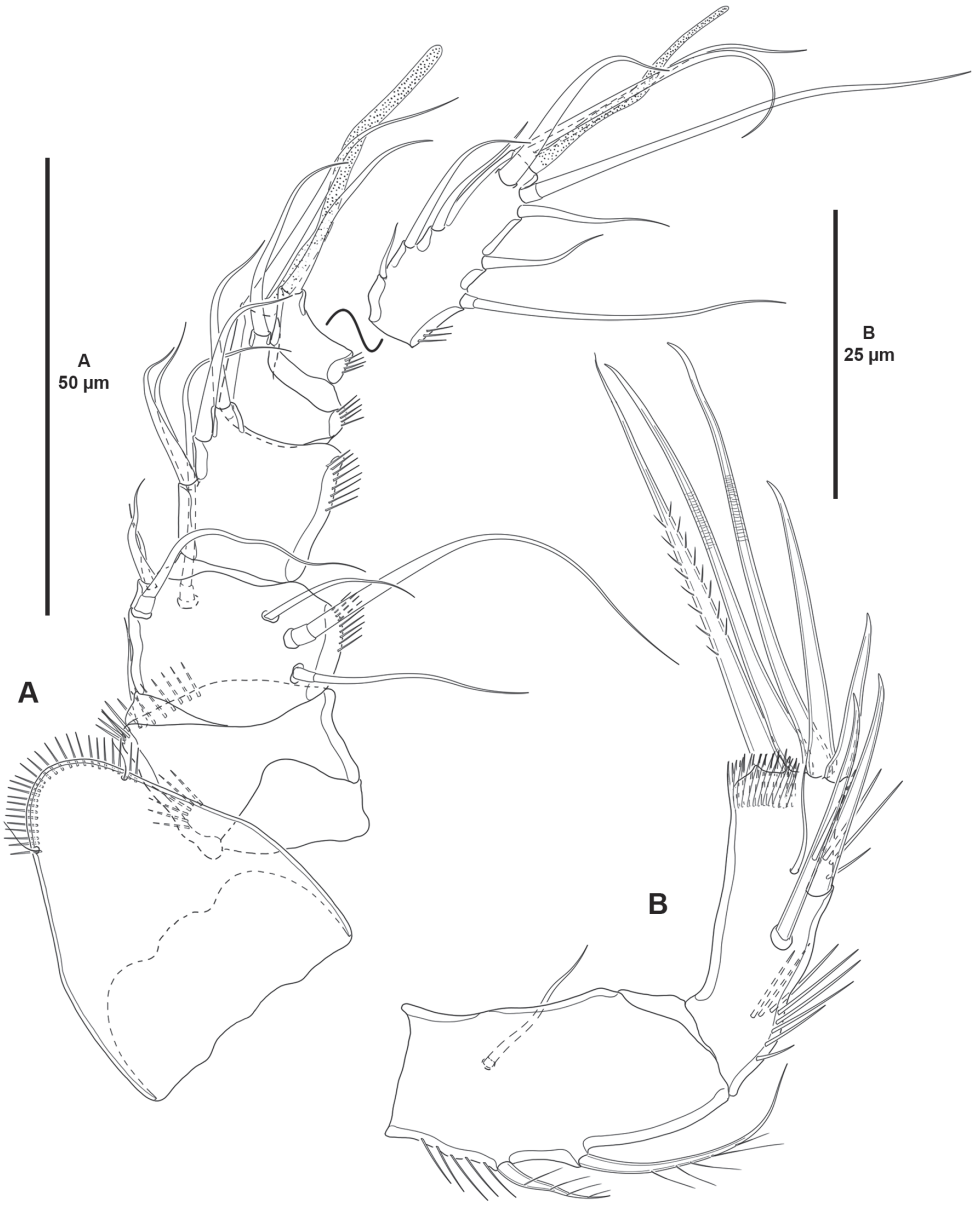

Figure 3. *Cletocamptoides biushelo* sp. nov., female holotype **A** rostrum and antennule **B** antenna.

Antenna (Fig. 3B) with allobasis ornamented with short longitudinal row of spinules proximally, armed with two abexopodal setae (one basal, one endopodal). Exopod one-segmented, minute, with one seta. Free endopodal segment as long as allobasis, with inner spinules proximally and subdistally, and with outer subdistal frill; with two inner spines and one slender seta medially, distally with two inner spines, two medial geniculate setae, and one outer spinulose element.

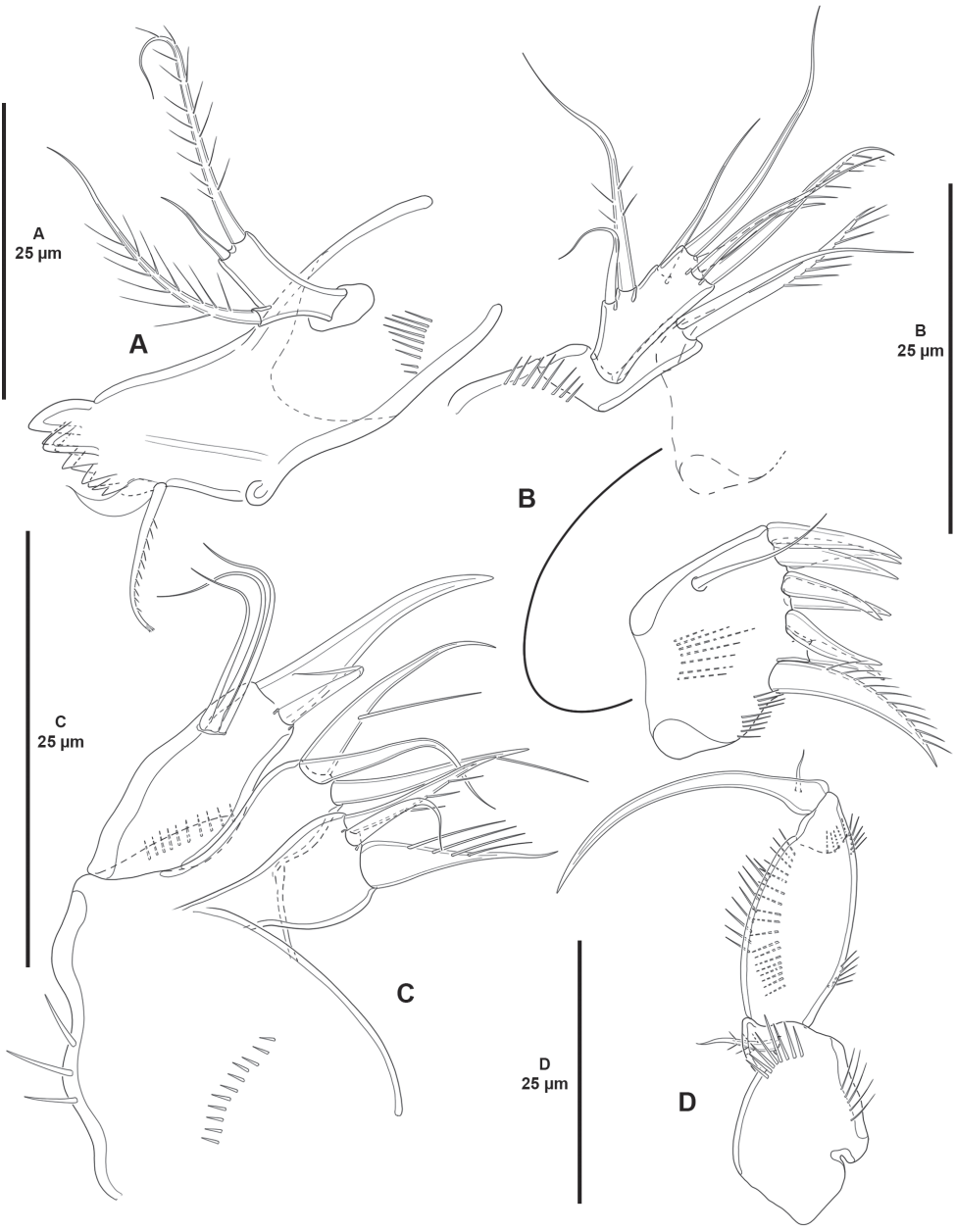

Figure 4. *Cletocamptoides biushelo* sp. nov., female holotype **A** mandible **B** maxillule **C** maxilla **D** maxilliped.

Mandible (Fig. 4A) with well-developed coxa ornamented with short spinular row as shown; gnathobase well-developed, with bi- and unicuspid teeth distally, and one thick bulbous element, and one ventral pinnate seta. Palp one-segmented, with three setae (one basal, two endopodal).

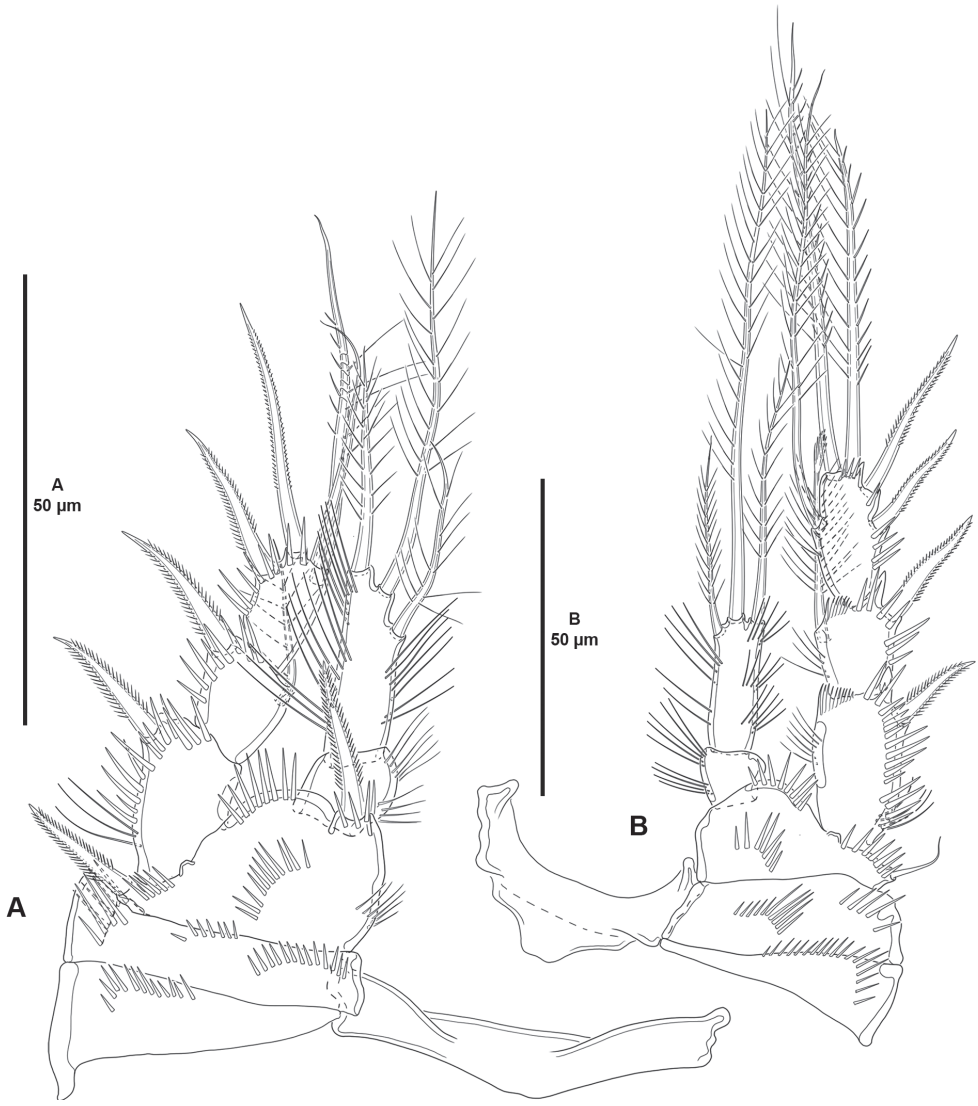

Figure 5. *Cletocamptoides biushelo* sp. nov., female holotype **A** P1, anterior **B** P2, anterior.

Maxillule (Fig. 4B) with robust praecoxa ornamented with spinules at base of coxal endite, and medially and ventrally on arthrite, the latter with one surface seta, seven distal spines and one ventral strong unipinnate seta. Coxal endite with two setae. Endopod and exopod incorporated to basis, the latter with four, endopod with one, exopod with two setae.

Maxilla (Fig. 4C) with syncoxa ornamented with medial and distal rows of small spinules, and with few larger outer spinules; with two endites bearing three setae each. Allobasis drawn out into claw accompanied by one seta. Endopod completely incorporated to basis, represented by three setae.

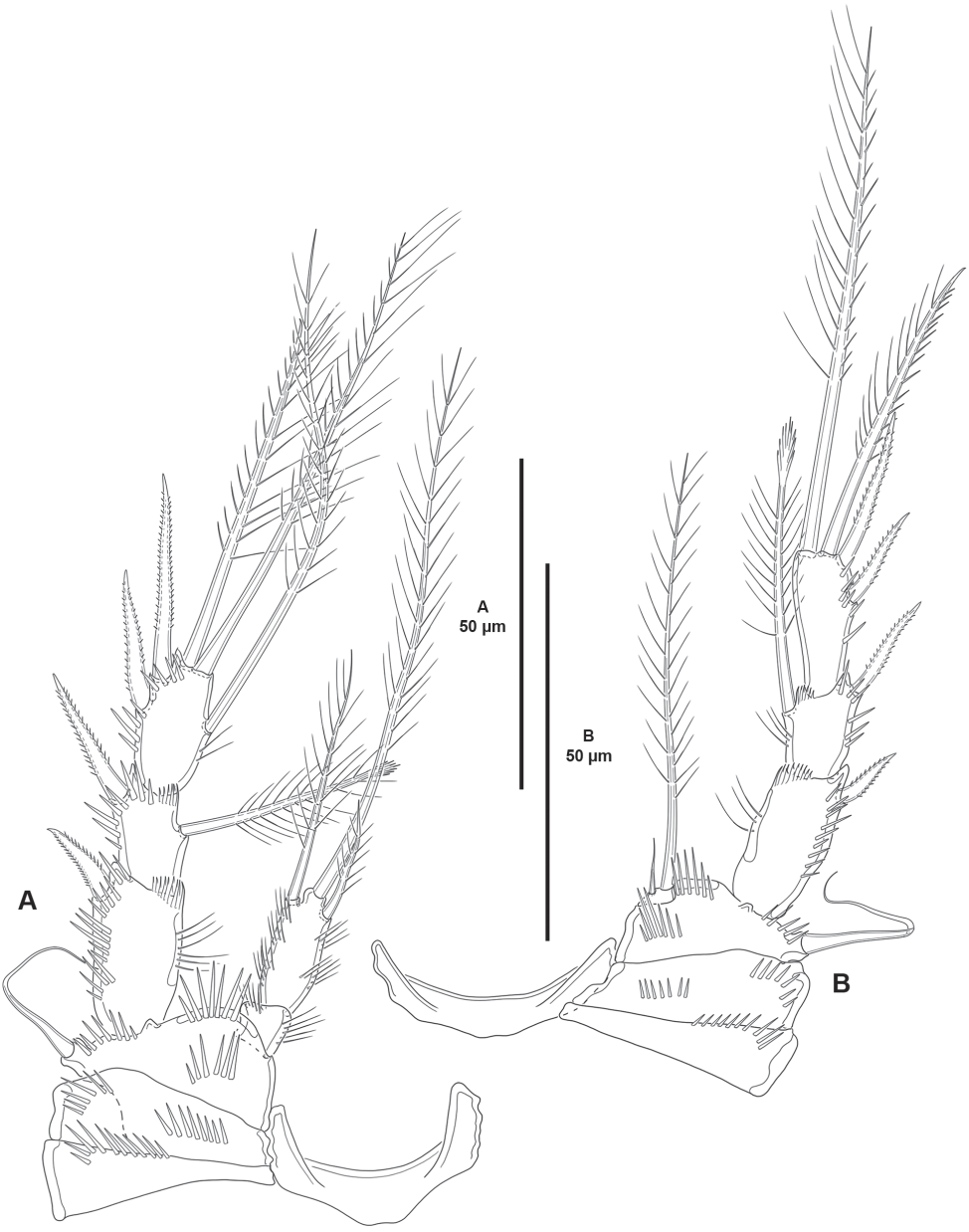

Figure 6. *Cletocamptoides biushelo* sp. nov., female holotype **A** P3, anterior **B** P4, anterior.

Maxilliped (Fig. 4D) subchelate. Syncoxa with spinules as shown, with one subdistal seta. Basis with one anterior and one posterior spinular row, with outer spinules proximally and subdistally. Endopod drawn out into curved claw with minute accessory seta.

P1 (Fig. 5A) with elongate bare intercoxal sclerite. Praecoxa triangular, with medial subdistal row of spinules. Coxa rectangular, wider than long, with two medial

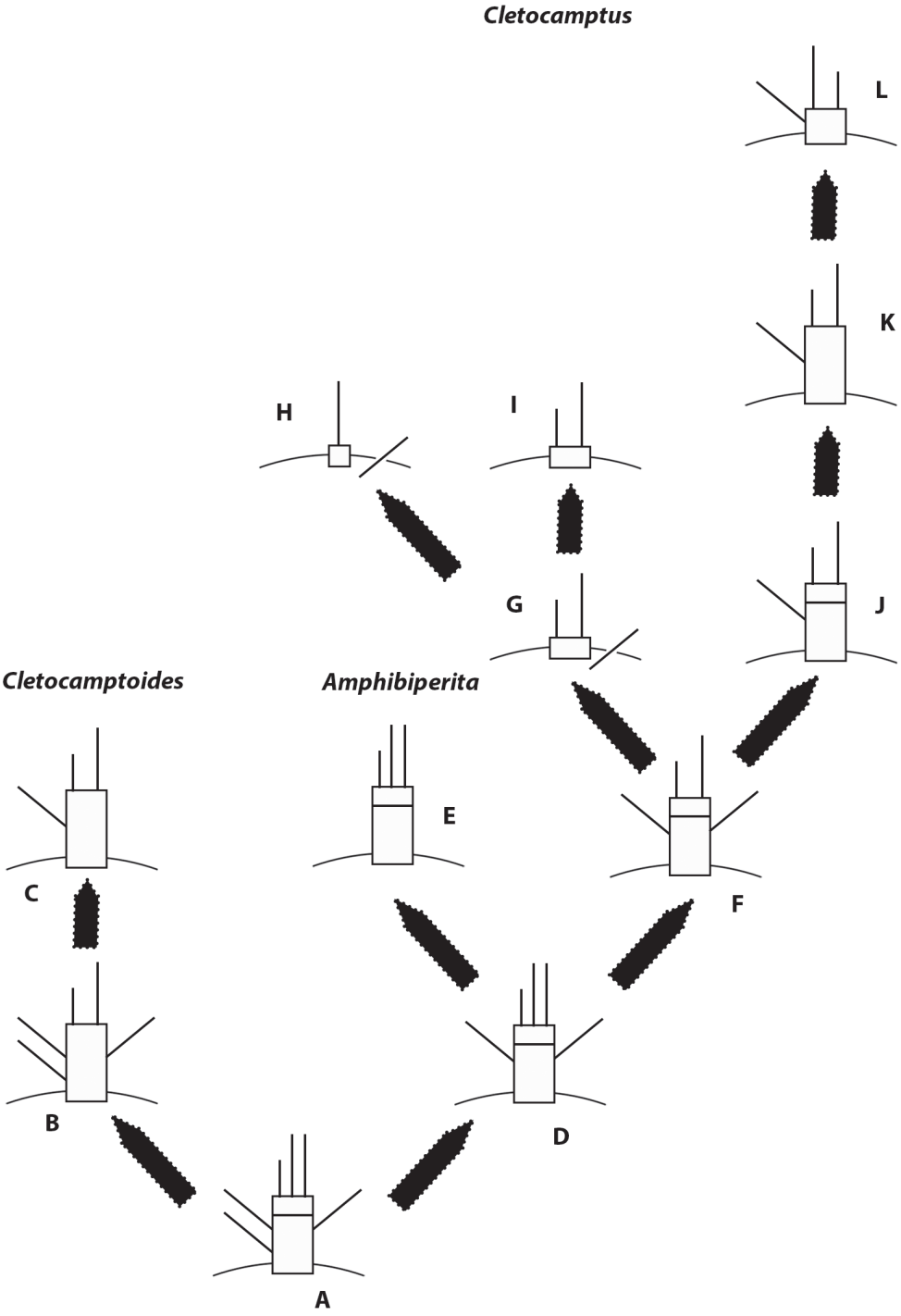

Figure 7. Schematic representation of the evolution of the mandibular palp in Cletocamptinae subfam. nov.

transverse rows of spinules as shown, and one posterior and one anterior short row of larger spinules close to outer margin. Basis with anterior spinules medially, on outer margin, at base of inner and outer spines, and between rami. Exopod three-segmented, situated at a lower level than the endopod, reaching tip of ENP2; segments with outer and subdistal spinules as shown; EXP1 without, EXP2 with inner seta; EXP3 with two outer spines and two distal setae of which innermost geniculate. Endopod two segmented, not prehensile; segments with inner and outer long slender spinules as depicted; ENP1 unarmed; ENP2 with three setae.

P2–P3 (Figs 5B, 6A) with elongate bare intercoxal sclerite. Praecoxa triangular, with transverse row of spinules as shown. Coxa rectangular, wider than long; with one medial and one outer spinular row. Basis with spinules medially, at base of endopod, and between rami; with outer seta (of P2 visibly shorter than in P3). Exopod three-segmented, situated at a lower level than endopod; spinular ornamentation of segments as shown; EXP1 and EXP2 with, EXP3 without inner distal frill; EXP1 without, EXP2 with inner seta with comb tip; EXP3 with one inner element without comb tip, two distal setae, and two outer spines. Endopod two-segmented; segments with spinular ornamentation as shown; ENP1 small, as long as wide, unarmed; ENP2 elongated, with three setae.

P4 (Fig. 6B) with intercoxal sclerite, praecoxa, coxa and basis as in P3. Exopod largely as in P3 except for two apical setae, and two outer spines on EXP3. Endopod one-segmented, minute, wider than long; with two setae of which innermost reduced.

P1–P5 armature formulae as follows:

	P1	P2	P3	P4	P5
Exopod	0,1,022	0,1,122	0,1,122	0,1,022	3
Endopod	0,210	0,111	0,111	020	5

P5 (Fig. 2B) with baseoendopod and exopod fused, rami separated by shallow notch; spinular ornamentation as shown. Baseoendopod with outer seta arising from short setophore; endopodal lobe with five setae. Exopod with three setae.

Genital field (Fig. 2A) with median copulatory pore on second half of genital double-somite; each P6 represented by two setae.

Male. Unknown.

Etymology. The specific epithet is an anagram for "helobius" and refers to the close relationship between the Mexican new species and *C. helobius* comb. nov.

Phylogenetics

The selected characters (Table 1) in the matrix (Table 2) integrate the main attributes of canthocamptids regarding the body shape (character 1), posterior ornament of the cephalothorax and prosomites (characters 2 and 3), presence of cuticular sensillum-bearing socles (character 4), shape and ornamentations of the rostrum (characters 5 and 6), segmentation of the female antennule (character 7), armature complement of the antennary allobasis and segmentation of the antennary exopod (characters 8 and

9), segmentation, shape, and armature complement of the mandibular palp (characters 10–12), armature complement of the syncoxa of the maxilliped (character 13), several features of P1–P5 (characters 14–34), and male dimorphism (characters 35–39).

The heuristic search yielded nine equally most parsimonious trees of 220 steps, and consistency index of 0.39. The extended majority rule consensus tree is shown in Figure 8. The results show the monophyly of Cletocamptinae subfam. nov. and *Cletocamptoides* gen. nov. which are well supported clades with high bootstrap values. The Bayesian inference analysis recognized and supported the monophyly of Cletocamptinae subfam. nov. and *Cletocamptoides* gen. nov. Our Bayesian results indicate that *Amphibiperita* is nested within *Cletocamptus*, rendering the relationships between the genus *Cletocamptus* and *Amphibiperita* unresolved. However, we maintained the genus *Amphibiperita* separated from *Cletocamptus* due the maximum parsimony support as well as their unique characteristics (see below).

Discussion

Historical background and identification of the problem

The family Canthocamptidae was created and diagnosed by Brady (1880: 47) for *Canthocamptus* Westwood, 1836, *Mesochra* Boeck, 1865, *Attheyella* Brady, 1880, *Tetragoniceps* Brady & Robertson, 1876, *Diosaccus* Boeck, 1872, *Laophonte* Philippi, 1840, *Normanella* Brady, 1880, *Cletodes* Brady, 1872, and *Enhydrosoma* Boeck, 1872. The subfamily was subsequently raised to family level by Sars (1906: 193). Sars (1911: 418) foresaw the separation of *Pteropsyllus* Scott T., 1906a, *Evansula* Scott T., 1906b, *Tetragoniceps*, and *Leptastacus* Scott T., 1906a from the Canthocamptidae to a different family. Several groups/subfamilies have been proposed in the past as an effort to disentangle the complicated phylogenetic relationships amongst the canthocamptid genera.

Labbé (1926) proposed a new subfamily of Canthocamptidae, the Rhyncoceratinae, and one year later, Labbé (1927) gave a more detailed description of the species within that subfamily with additional figures. Labbé's (1926; 1927) works were plagued with taxonomical errors, wrong identifications, and descriptions, and were harshly criticized by Gurney (1927) and Lang (1948) who finally disposed of the Rhyncoceratinae. As far as we are aware, the subfamily Rhyncoceratinae was never mentioned afterwards.

In a preliminary note on the revision of the freshwater genus *Canthocamptus*, Chappuis (1929a) subdivided the genus into several new genera distributed in two groups based on the one- or two-segmented condition of the antennary exopod, the Biarticulata for *Canthocamptus*, *Bryocamptus* Chappuis, 1929a and *Echinocamptus* Chappuis, 1929a (= *Bryocamptus* (*Echinocamptus*) Chappuis, 1929a), and the Uniarticulata for *Attheyella* and *Elaphoidella* Chappuis, 1929a. That same year, Chappuis (1929b) abandoned that system. Sixteen marine, one brackish, and nine freshwater genera were known at the time of Chappuis' (1929b) paper, but he could not inspect but freshwater

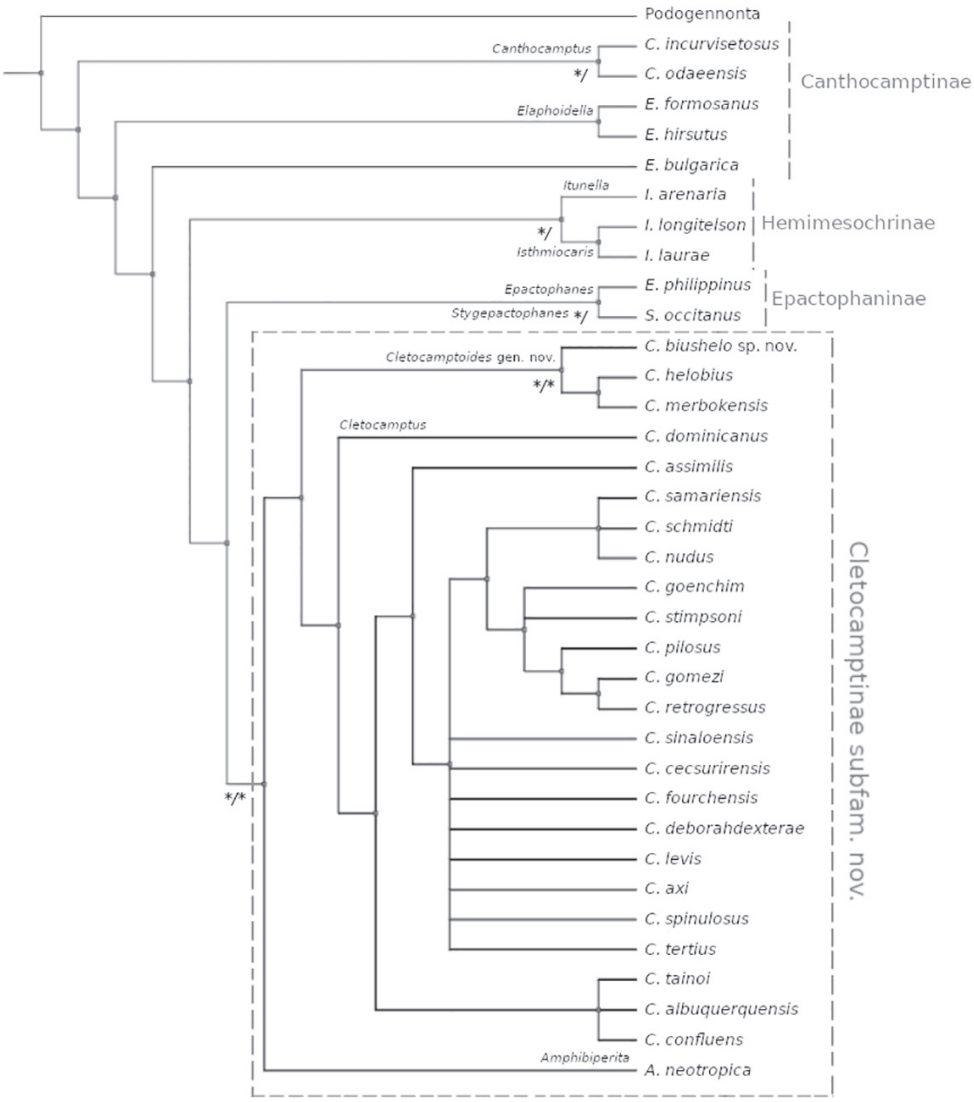

Figure 8. Phylogenetic hypothesis showing the relative position of Cletocamptinae subfam. nov. and *Cletocamptoides* gen. nov. Bootstrap (boot) and BI posterior probabilities (pp) represented as boot/pp. * Nodes of high support, boot > 90%; pp > 0.95.

material (Chappuis 1929b). However, based on the available literature, he noted that the marine and brackish genera were far different (for a list of marine and freshwater genera allocated into the Canthocamptidae by that time, see Monard 1927) and proposed and diagnosed the subfamily Canthocamptinae for freshwater canthocamptids: *Canthocamptus*, *Paracamptus* Chappuis, 1929b (= *Pesceus* Özdikmen, 2008), *Bryocamptus*, *Maraenobiotus* Mrázek, 1893, *Hypocamptus* Chappuis, 1929b, *Echinocamptus* (= *Bryocamptus* (*Echinocamptus*)), *Ceuthonectes* Chappuis, 1924, *Moraria* Scott T. & Scott

A., 1893, *Attheyella*, *Elaphoidella*, *Epactophanes* Mrázek, 1893, and several species incertae sedis (Chappuis 1929b: 495–496). Pesta (1932) believed that the morphological variability of the Canthocamptidae could be better understood by grouping its genera into two subfamilies. For this, he (Pesta 1932) proposed and diagnosed the subfamily Halocanthocamptinae for those genera inhabiting coastal marine and brackish waters, as well as continental saline habitats: *Mesochra* Boeck, 1865, *Paramesochra* Scott T., 1892, *Remanea* Klie, 1929, *Leptomesochra* Sars, 1911, *Evansula*, and *Leptastacus* (Pesta 1932: 79), and the subfamily Canthocamptinae Brady, 1880 for freshwater forms: *Nitocrella* Chappuis, 1924, *Canthocamptus*, *Hypocamptus*, *Maraenobiotus*, *Moraria*, *Epactophanes*, *Elaphoidella*, *Attheyella*, *Paracamptus*, *Echinocamptus*, and *Bryocamptus* (Pesta 1932: 91–92). Monard (1935) expressed some doubts about the naturalness of Pesta's (1932) scheme but believed that it was, at least, practical. Gurney (1932) did not accept the concept of the Ameiridae and subdivided the Canthocamptidae into six groups, two of which (the first and the third) were included by Lang (1936) in his list of ameirid genera. The other groups of Gurney (1932) are a) *Tetragoniceps* for *Tetragoniceps*, *Phyllopodopsyllus* Scott T., 1906a, *Pteropsyllus*, *Paramesochra*, *Leptopsyllus* Scott T., 1894, and *Diagoniceps* Willey, 1930, b) *Evansula* for *Evansula*, *Leptastacus*, and *Leptopontia* Scott T., 1902, c) *Cletomesochra* for *Cletomesochra* Sars, 1920 (= *Heteropsyllus* Scott T., 1894), *Hemimesochra* Sars, 1920, *Nannomesochra* Gurney, 1932, *Leptomesochra*, *Pseudomesochra* Scott T., 1902, and *Paramesochra*, and d) *Canthocamptus* for the freshwater canthocamptids and *Mesochra*.

In a preliminary note, Lang (1944) removed *Paramesochra* from the Canthocamptidae to his newly created family Paramesochridae Lang, 1944, and proposed a new family, Tetragonicepsidae Lang, 1944 (whose spelling was subsequently corrected to Tetragonicipitidae) for *Tetragoniceps*, *Pteropsyllus*, *Diagoniceps*, *Phyllopodopsyllus* and *Paraphyllopodopsyllus* Lang, 1944 (= *Phyllopodopsyllus*). Lang (1948) believed that the Canthocamptidae and the Cletodidae bear a sister group relationship and that the difficulties for the separation of both families are the result of poor descriptions of freshwater canthocamptids. He (Lang 1948) rejected all the subdivisions of the Canthocamptidae pending a thorough review of the family, and included into this family the following genera: *Hypocamptus*, *Maraenobiotus*, *Morariopsis* Borutzky, 1931, *Itunella* Brady, 1896, *Orthopsyllus* Brady & Robertson, 1873, *Ceuthonectes*, *Spelaeocamptus* Chappuis, 1933, *Attheyella*, *Canthocamptus*, *Bryocamptus*, *Nannomesochra*, *Mesochra*, *Echinocamptus*, *Moraria*, *Paracamptus*, *Antarctobiotus* Chappuis, 1930, *Afrocamptus* Chappuis, 1932, *Epactophanes*, and *Elaphoidella*.

By the early 1950's, Borutzky (1952) re-diagnosed the Canthocamptidae and the subfamilies Halocanthocamptinae, with *Mesochra* and "the genera most closely related to it " (Borutzky 1952: 124), and Canthocamptinae with *Canthocamptus*, *Paracamptus*, *Bryocamptus*, *Arcticocamptus* Chappuis, 1929b (= *Bryocamptus* (*Arcticocamptus*) Chappuis, 1929b), *Echinocamptus* (= *Bryocamptus* (*Echinocamptus*)), *Maraenobiotus*, *Hypocamptus*, *Attheyella*, *Elaphoidella*, and *Spelaeocamptus*, and added the Morariinae for *Ceuthonectes*, *Moraria*, *Morariopsis* and some species incertae sedis, and the Epactophaninae for *Epactophanes*. He (Borutzky 1952) diagnosed these four subfamilies

based on the structure of the female genital field and on the structure of the male P3 ENP. Later on, Por (1986: 423) proposed and (re)diagnosed the subfamily Hemimesochrinae Por, 1986 for those genera which, despite having a non-prehensile P1 ENP, were left into the Canthocamptidae in Lang (1948); these genera are: *Nannomesochra*, *Hemimesochra*, *Heteropsyllus*, *Mesopsyllus* Por, 1960, *Poria* Lang, 1965 (= *Hanikraia* Huys, 2009), and *Dahlakia* Por, 1986 (= *Dahlakocamptus* Huys, 2009). Additionally, Por (1986) relegated to incertae sedis the genera *Cletocamptus* and *Parepactophanes* Kunz, 1935, as well as *Hemimesochra rapiens* Becker, 1979 (= *Perucamptus rapiens* (Becker, 1979)), and *Heteropsyllus serratus* Schriever, 1983. One year later, Hamond (1987) suggested to consider no less than 18 taxa as subgenera of *Canthocamptus* s. lat. "until all their respective type species, and as many others as possible from all over the world, can be studied again by modern standards "… "as part of a world revision" (Hamond 1987: 1027; but see also Wells 2007).

With 864 species distributed in 58 valid genera (WoRMS 2021), the Canthocamptidae is currently one of the most species-rich families within Harpacticoida. The Canthocamptidae is not a natural assemblage and could be divided into several families (Huys et al. 1996; Gómez Noguera and Fiers 1997; Boxshall and Halsey 2004; Huys and Conroy-Dalton 2006). The taxonomy and the phylogenetic relationships are immersed in chaos, and the different canthocamptid subfamilies are seldom mentioned in the recent literature probably because the genera described more recently are difficult to attribute to any of the existing subfamilies, and if forced, the subfamilial diagnoses have often to be widened more to include, probably unrelated taxa, exacerbating the already complicated systematics of the group. This problem is also common at the genus level, and is evident in *Hemimesochra*, which is a heterogeneous grouping of distantly related taxa (see Huys and Thistle 1989). The complexity of the Canthocamptidae is also fuelled by the weak boundaries between the Canthocamptidae and the Cletodidae and their respective genera. Huys and Thistle (1989) agreed with Por (1986) in that the dismantling of the Cletodidae *sensu* Lang (1944, 1948) was a necessary step, but did not accept Por's (1968) view of taking the "variability within the Cletodidae, and the notion of genus itself "… "in a much wider sense than in any other harpacticoid family" (Por 1968: 46). Huys and Thistle's (1989) reasoning is adopted here. Huys and Thistle (1989) succeeded in narrowing the generic diagnosis of *Hemimesochra* by distributing its species in *Boreolimella* Huys & Thistle, 1989, *Perucamptus* Huys & Thistle, 1989, *Carolinicola* Huys & Thistle, 1989, *Mesopsyllus*, and *Pusillargillus* Huys & Thistle, 1989, leaving *H. clavularis* Sars, 1920 as the type and only species of *Hemimesochra*. They (Huys and Thistle 1989) concluded that *Bathycamptus* Huys & Thistle, 1989, *Psammocamptus* Mielke, 1975 and *Boreolimella* are phylogenetically related, being *Bathycamptus* the sister taxon of *Psammocamptus*, that *Boreolimella* is probably the sister taxon of the *Bathycamptus-Psammocamptus* lineage, and that *Mesopsyllus* could be a potential relative of this genus group.

George and Schminke (2003) noted that *Isthmiocaris* George & Schminke, 2003 could well be related to *Bathycamptus* and *Itunella*. Later on, Huys and Kihara (2010) removed *Metahuntemannia* Smirnov, 1946 and *Pottekia* Huys, 2009 from the

Nannopodidae Brady, 1880 and found that these two genera are probably related to *Psammocamptus*, *Bathycamptus*, *Perucamptus*, and *Isthmiocaris*. However, as far as we are aware, no apomorphies have been found so far for the Hemimesochrinae. The same applies for the other canthocamptid subfamilies.

Karaytuğ and Huys (2004) proposed a practical, not necessarily phylogenetic, group of marine and brackish canthocamptids, the *Mesochra* group, in which the male P6 is represented by unarmed membranous flaps, and the female P6 is represented by one to three setae. Following Karaytuğ and Huys (2004), this species group includes species currently allocated into the Canthocamptinae and Hemimesochrinae, and two species incertae sedis; these are: *Mesochra* and *Amphibiperita* (Canthocamptinae), and *Psammocamptus*, *Bathycamptus*, *Mesopsyllus*, *Isthmiocaris*, *Hemimesochra*, *Poria*, *Perucamptus*, *Pusillargillus* (Hemimesochrinae), and *Taurocletodes* Kunz, 1975, and *Parepactophanes* (Canthocamptidae incertae sedis). The genus *Mesochra* is not a natural unit and is most probably polyphyletic (Gómez Noguera and Fiers 1997; Karaytuğ and Huys 2004), but if Karaytuğ and Huys' (2004) assumption is correct, this might reflect the artificial nature of the canthocamptid subfamilies.

More recently, George (2020) contributed with important changes to the family Cletodidae *sensu* Por (1986), which has been regarded in the past as the sister taxon of the Canthocamptidae. He (George 2020) proposed the Cletodoidea Bowman and Abele (1982) for some Ancorabolidae Sars, 1909 *sensu* George (2020) and Cletodidae for which he detected 19 autapomorphies (George 2020). George (2020) also gave an amended diagnosis for the Cletodidae, which he extended to include several genera that belonged to the Ancorabolidae, and proposed a new subfamily, the Cletodinae Scott T., 1904 for the ancorabolid *Ceratonotus* group *sensu* Conroy-Dalton (2001) and *Cletodes*, defined by seven autapomorphies (George 2020). For the Cletodidae, he (George 2020) detected a set of five autapomorphies: a) P1 ENP not prehensile, P1 ENP1 dwarfed; b) P1 ENP2 elongate, at least as long as ENP1; c) the medial apical geniculate seta of the Cletodoidea (seta 5-en in George 2020: 470, fig. 3C) reverted into a bipinnate or plumose seta (5-en in George 2020: 470, fig. 3D) in Cletodidae; d) the outer distal claw-like element on the P1 ENP2 in the Cletodoidea (1-en in George 2020: 470, fig. 3C) reverted into a spine (1-en in George 2020: 470, fig. 3D) in Cletodidae; and e) loss of the accompanying seta on the maxillipedal claw.

The complexity of the Canthocamptidae is evident and it is due to bad and incomplete descriptions (Hamond 1987). Hamond (1987) proposed the revision of 18 taxa as part of a world revision using modern standards. Wells (2007) commented positively on Hamond's (1987) proposal but at the same time he foresaw that this would not find ready support due to the massive effort that this would imply. Some authors have contributed to our understanding of the intergeneric relationships within isolated subfamilies. Huys and Thistle (1989), George and Schminke (2003), and Huys and Kihara (2010) have proved, at least partially, that the subfamily Hemimesochrinae is a compact unit, not so the other canthocamptid subfamilies. In our opinion, the establishment of well-defined taxonomic taxa (subfamilies, genera, species groups, etc.) is an obligate step towards a world revision of the family. The relationships between the

Canthocamptinae and other genera outside that subfamily are still uncertain, and the proposal of a new subfamily, Cletocamptinae subfam. nov., for a well-defined, seemingly monophyletic group of genera (*Cletocamptus*, *Amphibiperita*, and *Cletocamptoides* gen. nov.) as well as the narrowing of the diagnosis for *Cletocamptus*, are justified and follow the same reasoning as explained below.

Reconstruction of the common ancestor of the Cletocamptinae subfam. nov.

The high morphological diversity of the Canthocamptidae makes difficult the detection of (aut)apomorphies to substantiate the establishment and proposal of monophyletic taxa. In this sense, the role of weighted characters for the maximum parsimony approach was essential and allowed high support. The genus *Cletocamptus* as known before the present study, seems to be composed of two different lineages, the *merbokensis-helobius-biushelo*-lineage (mhb-lineage; for *C. merbokensis*, *C. helobius*, and *C. biushelo* sp. nov.) and the *retrogressus*-lineage (for the rest of the species of *Cletocamptus*). The split of *Cletocamptus* into two genera is proposed in this study: *Cletocamptoides* gen. nov. for the mhb-lineage, and *Cletocamptus* for the *retrogressus*-lineage.

The reconstruction of the hypothetical ancestor of the Cletocamptinae subfam. nov. is necessary to justify the (aut)(syn)apomorphies for the three genera within the new subfamily. The hypothetical ancestor was reconstructed based on plesiomorphic and (aut)apomorphic states of a selected set of characters, as essential to explain our hypotheses and phylogenetic reasoning.

Most canthocamptids possess a body without somitic constrictions between somites, and few species, e.g., *C. merbokensis* comb. nov., *C. helobius* comb. nov., *C. biushelo* sp. nov., possess a body with somitic constrictions between somites conferring the body a cletodid appearance. The latter is regarded here as the derived (synapomorphic) condition for the mhb-lineage. The ancestral Cletocamptinae subfam. nov. is hypothesized to lack somitic constrictions between somites, tapering gradually posteriad. The latter is considered as the primitive condition and is present in the *retrogressus*-lineage.

The posterior margin of body somites of most genera of the Canthocamptidae is plain, without any ornamentation, including one species of Cletocamptinae subfam. nov., *C. chappuisi*, but its condition requires confirmation; it is finely or deeply serrated in some genera, e.g., *Antrocamptus* Chappuis, 1957, *Attheyella*, *Canthocamptus*, *Elaphoidella*, *Moraria*, *Paramoriaropsis* Brancelj, 1991, *Spelaeocamptus*, and *C. dominicanus*; it is ornamented with short spinules, e.g., *Attheyella*, and *C. albuquerquensis* and *C. tainoi*, or with long slender spinules, e.g., *Cletocamptus* as defined here. It is assumed that the plain condition of the posterior margin of body somites is the most primitive within the Canthocamptidae. Species of some genera developed serrate posterior margins that eventually developed into short spinules. The ancestral Cletocamptinae subfam. nov. is hypothesized to have retained the finely serrate posterior margins present in *Cletocamptoides* gen. nov., and displayed by other canthocamptids (see above) The presence of long slender spinules in the posterior margin of body somites of *Cletocamptus* as defined here, is assumed to be the derived condition.

Posterior cuticular sensillum-bearing socles have been observed only in *C. merbokensis* comb. nov., for which this condition is regarded as apomorphic. All other canthocamptids lack cuticular sensillum-bearing socles and is regarded here as a clear plesiomorphy and is the hypothesized condition in the ancestral Cletocamptinae subfam. nov.

The rostrum is separated from the cephalothorax in species of *Bryocamptus*, *Gulcamptus* Miura, 1969, *Itunella*, *Mesochra*, *Moraria*, *Pordfus* Özdikmen, 2008, *Boreolimella*, *Carolinicola*, *Dahlakocamptus*, *Heteropsyllus*, *Perucamptus*, *Isthmiocaris*, and *Psammocamptus*. It is fused and sometimes reduced in the remaining genera. The well-developed rostrum separated from the cephalothorax is regarded here as the primitive condition for the family, and is assumed to have been retained in the ancestral Cletocamptinae subfam. nov. The condition of the rostrum of *C. gomezi*, which has been described as fused to the cephalothorax (Suárez-Morales et al. 2013) requires confirmation.

The rostrum lacks any spinular ornamentation in the Canthocamptidae; as far as we know, ventral subdistal spinular ornamentation is present only in the Cletocamptinae subfam. nov. for which is a clear autapomorphy and justifies the new subfamily.

As far as we are aware (we could not review all the descriptions for all the species of Canthocamptidae though), the male rostrum is non-dimorphic in most canthocamptids (e.g., Canthocamptinae, Hemimesochrinae and Epactophaninae), and is regarded here as the primitive condition, which was retained in the ancestral Cletocamptinae subfam. nov. The male rostrum is sexually dimorphic in *Cletocamptus* and *Amphibiperita* for which is regarded here as synapomorphic.(it is also sexually dimorphic in *Taurocletodes tumenae* Karaytuğ & Huys, 2004 (the male of *T. dubius* (Noodt, 1958) remains unknown), but the significance of its presence in *Cletocamptus* and *T. tumenae* is uncertain). *Cletocamptoides* gen. nov. retained the primitive non-dimorphic male rostrum.

The canthocamptid female antennule can be eight- to five-segmented. Following Huys and Boxshall (1991) oligomerization is the main evolutionary trend in Copepoda, and the eight-segmented female antennule is the most plesiomorphic condition within the Canthocamptidae. The female antennule is six-segmented in the new subfamily, and is regarded here as the condition for the ancestral Cletocamptinae subfam. nov. *Cletocamptus gravihiatus* was described possessing seven-segmented female antennules, but this requires confirmation.

The canthocamptid antenna has undergone fusion of the basis and the first endopodal segment to form an allobasis. The allobasis of canthocamptids is unarmed or equipped with one or two (one basal, one endopodal) abexopodal setae. The latter is regarded here as the most primitive condition of the allobasis. Two abexopodal setae are retained in most species of Cletocamptinae subfam. nov., but some species (*C. gomezi*, *C. feei*, *C. retrogressus*, *C. merbokensis* comb. nov., *C. helobius* comb. nov., *A. neotropica*) underwent loss of one seta, most probably the endopodal element. The antennary exopod of canthocamptids is mostly one-segmented, but the two-segmented condition is present in species of *Bryocamptus*, *Canthocamptus*, *Gulcamptus*, *Maraenobiotus*, *Mesochra*, and *Heteropsyllus*; it is represented by one seta in species of *Stenocaris* and is absent in *Dahmsopottekina* Özdikmen, 2009. The antennary exopod of the Cletocamptinae

subfam. nov. is elongate and one-segmented except for *C. feei* for which the exopod was reported as two-segmented (the latter requires confirmation though), *C. chappuisi* whose antennary exopod was reported as represented by one seta as in *C. helobius* comb. nov. and *C. biushelo* sp. nov., and *Amphibiperita* in which the antennary exopod is lost. The antennary exopod of *C. dominicanus* is a minute segment with a single seta. The ancestral antenna of Cletocamptinae subfam. nov. is assumed to possess an allobasis with two abexopodal setae, and a one-segmented exopod; the free endopodal lobe possessed two spines and a slender seta laterally, and three spines and two geniculate setae distally.

The mandibular palp of Podogennonta is composed of a basis with four setae; a one-segmented endopod with three proximal lateral, three subdistal lateral, and three sets of setae fused basally with three, two, and two setae, respectively; and a four-segmented exopod with armature formula 2, 1, 1, 2 (Seifried 2003). Within the Canthocamptidae, *Carolinicola* (Hemimesochrinae) possesses a primitive biramous palp with the basis possessing three setae, the endopod being armed with six elements, and the one-segmented exopod with four setae (Huys and Thistle 1989). The reconstruction of the mandibular palp of the ancestor of the Cletocamptinae subfam. nov. (Fig. 7A) is based on the most plesiomorphic states observed in the different taxa included in the new subfamily. The ancestral mandibular palp (Fig. 7A) of the Cletocamptinae subfam. nov. is assumed to be two-segmented; basis with two setae; endopod one-segmented, separated from the basis, and equipped with three setae, of which innermost shortest; exopod incorporated into the basis but represented by one seta. The ancestral mandibular palp underwent several changes in different lineages. The ancestral palp (Fig. 7A) lost one of the apical setae, and the basis and endopod became fused (Fig. 7B) like in *C. merbokensis* comb. nov. Further losses include one of the basal setae and the exopodal seta (Fig. 7C) like in *C. helobius* comb. nov. and *C. biushelo* sp. nov. On the other hand, the mandibular palp might have lost one basal seta leading the precursor of *Amphibiperita-Cletocamptus* (Fig. 7D). In one lineage, the mandibular palp lost the remaining basal seta and the exopodal element (Fig. 7E) resulting in an unarmed basis and a trisetose endopod like in *Amphibiperita*. In another lineage, the mandibular palp of the precursor of *Amphibiperita-Cletocamptus* underwent loss of one of the endopodal setae (Fig. 7F) leading the ancestor of *Cletocamptus*. In one lineage, the basis fused into the coxa with the resulting loss of the basal seta, and the exopodal seta became incorporated into the coxa (Fig. 7G) as in *C. assimilis*, *C. axi*, *C. cecsurirensis*, *C. deborahdexterae*, *C. fourchensis*, *C. goenchim*, *C. koreanus*, *C. levis*, *C. nudus*, *C. pilosus*, *C. schmidti*, *C. sinaloensis*, *C. spinulosus*, and *C. tertius*. The inner endopodal seta looks longer than the outer element in *C. nudus*, and this requires confirmation. One of the endopodal setae, most probably the inner short element, became lost leading a minute endopodal segment with one seta only accompanied by the accessory exopodal seta issuing from the coxa like in *C. pilosus* (Fig. 7H). Further loss includes the disappearance of the exopodal seta (Fig. 7I) like in *C. albuquerquensis*, *C. gomezi*, *C. samariensis*, *C. stimpsoni*, and *C. tainoi*. The palp of *C. gomezi* looks somewhat elongate in Suárez-Morales et al. (2013: 213, fig. 3D) and requires confirmation. In another lineage, the exopodal seta

became lost (Fig. 7J) like in *C. retrogressus*. Further modifications involve the fusion of the endopod and basis (Fig. 7K) like in *C. confluens*, and reduction of the palp (Fig. 7L) like in *C. dominicanus*. A transposition of the apical short and long setae was observed in the latter species but the significance of this is uncertain.

The maxillulary basis, exopod and endopod are fused into a single unit, making difficult the homologation and correct counting of their setae. A careful and more detailed study of this appendage is pending, but it seems that the coxal endite bears two setae, and the basis, exopod and endopod are represented by three setae each, and this is considered as the ancestral state for the maxillule. On the other hand, a very strong and spinulose ventral element is present in several species of *Cletocamptus*, e.g., *C. assimilis*, *C. axi*, *C. cecsurirensis*, *C. deborahdexterae*, *C. fourchensis*, *C. levis*, *C nudus*, *C. samariensis*, *C. schmidti*, *C.*, and *C. sinaloensis*, but also in *C. helobius* comb. nov., and *C. biushelo* sp. nov., and seems to have appeared independently in different lineages; the ventral seta on the praecoxal arthrite in the other species is visibly slenderer and is regarded here as the plesiomorphic condition found in the ancestral Cletocamptinae subfam. nov. The condition of *C. gomezi* is not conclusive and requires confirmation.

The architecture of the maxilla and maxilliped is rather constant within the new subfamily. The ancestral maxilla is assumed to bear two syncoxal endites; the endopod is assumed to be completely absorbed into the allobasis and represented by three setae. The ancestral maxilliped is subchelate; the syncoxa bears one seta; the basis is unarmed; the endopod is drawn out into a claw with one accompanying seta.

The hypothetical ancestral segmentation and armature formulae of P1–P5 is:

	P1	P2	P3	P4	P5
EXP	0;1;0,2,2	0;1;1,2,2	0;1;2,2,2	0;1;2,2,2	♀5 ♂4
ENP	0-1;1,2,1	0-1;2,2,1	♀0;2,2,1 ♂dimorphic: 0-1;iap;0,2,0	0;0,2,0	♀6 ♂3

iap, inner apophysis

The inner setae of P1–P4 EXP are assumed to be whip-like in the ancestral Cletocamptinae subfam. nov., i.e., devoid of a comb tip. See Gómez et al. (2017: 350, table 5) for the species of *Cletocamptus* with setae with comb tip. *Cletocamptoides biushelo* sp. nov. bears a seta with comb tip on P2–P4 EXP2; the condition of *C. helobius* comb. nov. is assumed to be the same. The inner setae of P2 and P3 EXP (P4 EXP lack inner setae) of *Cletocamptoides merbokensis* comb. nov., and the inner setae of *A. neotropica* are all whip-like. The ancestral P1 ENP is assumed to be two-segmented and prehensile. For the justification of the prehensile P1 ENP as the plesiomorphic state see George (2020). The ancestral sexual dimorphism of P3 ENP is assumed to be expressed in a three-segmented ramus, with inner sinuous slender long apophysis devoid of an arrow-like tip, as seen in all the members of the Cletocamptinae subfam. nov.

The pair of P5 in the females are separated (baseoendopods not fused medially) in all species of Cletocamptinae subfam. nov. The female P5 EXP and BENP are fused in all species of Cletocamptinae subfam. nov. except for *A. neotropica* in which the female P5 EXP and BENP are separated. The ancestral pair of the female P5 are

assumed to be separated; the exopod and the baseoendopod of each leg are assumed to be separated; the exopod is assumed to bear five setae as in most species of the new subfamily (four setae are present only in *A. neotropica*, *C. samariensis*, *C. confluens*, and *C. merbokensis* comb. nov.; three setae are present only in the new species described herein and in *C. helobius* comb. nov.), and the endopodal lobe is equipped with six setae as in most species of the new subfamily (seven setae have been reported for *C. feei* but this requires confirmation; five setae are present in *C. biushelo* sp. nov. and *C. helobius* comb. nov.). The ancestral pair of the male P5 of Cletocamptinae subfam. nov., are assumed to be fused medially as in most species of the new subfamily (the condition of *C. axi*, *C. cecsurirensis*, *C. retrogressus*, and *C. schmidti* is not conclusive), and the exopod and baseoendopod are assumed to be fused but separated by a deep notch as in most species for which the males are known (e.g., *C. deborahdexterae*, *C. stimpsoni*, and *C. sinaloensis*); the endopodal lobe is hypothesized to be armed with three setae as in the males of all the species of Cletocamptinae subfam. nov. for which the males are known; the ancestral exopod is assumed to bear four elements (three elements have been reported only for *A. neotropica*, *C. confluens*, *C. koreanus*, *C. samariensis*, and *C. helobius* comb. nov.).

The female P6 of the ancestral Cletocamptinae subfam. nov. is assumed to bear two setae; the male P6 is assumed to be represented by two articulate unarmed flaps.

The ancestral caudal rami are assumed here to be longer than broad as in some species of *Cletocamptus*, and equipped with seven setae.

The genus *Cletocamptus*

The genus *Cletocamptus* was erected by Schmankevitsch (1875) for *C. retrogressus*. The status of several species of the genus can be found in Gómez et al. (2004), Gómez (2005), Gómez et al. (2007), Gómez and Gee (2009), Gómez et al. (2013), and Gómez et al. (2017), and the complete list of species of the genus as redefined here can be found in the generic diagnosis above.

The ancestral Cletocamptinae subfam. nov. is hypothesized to lack somitic constrictions between somites, tapering gradually posteriad. *Cletocamptus* retained the plesiomorphic lack of such somitic constrictions.

Cletocamptoides gen. nov. displays the ancestral shape of somites with finely serrated posterior margins (see below), and the long slender spinules displayed by most species of *Cletocamptus* are assumed here to be the apomorphic condition for the posterior margin of body somites. Also, *Cletocamptus* retained the plesiomorphic lack of posterior cuticular sensillum-bearing socles on body somites.

Amongst the species of *Cletocamptus*, only *C. gomezi* has been described with the rostrum fused to the cephalothorax (Suárez-Morales et al. 2013), but this requires further confirmation. In general, the rostrum of *Cletocamptus* retained its plesiomorphic condition, i.e., well-developed and separated from the cephalothorax. However, the rostrum of *Cletocamptus*, as in the other two genera of Cletocamptinae, *Cletocamptoides* gen. nov. and *Amphibiperita*, display the synapomorphic subdistal ventral spinules that

are of diagnostic value for the new subfamily. As said above, and as far as we are aware, the male rostrum is sexually dimorphic in *Cletocamptus* and *Amphibiperita* and seems to be non-dimorphic in *Cletocamptoides* gen. nov. The sexually dimorphic rostrum of *Cletocamptus* is deemed to be derived and constitutes a synapomorphy for that genus and *Amphibiperita*. The significance of the dimorphic male rostrum in *Cletocamptus* and *Taurocletodes tumenae* is uncertain, but this is probably the result of convergence. The relatively low consistency index of the tree of maximum parsimony confirms homoplasy events that could be related to this convergence process.

Cletocamptus retained the six-segmented female antennule hypothesized for the ancestral Cletocamptinae subfam. nov. The seven-segmented female antennule of *Cletocamptus gravihiatus* awaits verification.

Cletocamptus retained the ancestral allobasis of the antenna as well as the two abexopodal setae, and only *C. gomezi*, *C. feei*, and *C. retrogressus* lost one of these setae (one seta only is present also in *C. merbokensis* comb. nov., *C. helobius* comb. nov., and *A. neotropica*). *Cletocamptus* also retained the plesiomorphic one-segmented elongate antennary exopod (the two-segmented condition of the antennary exopod of *C. feei* requires to be confirmed) and the architecture of the free endopodal segment as described above for the ancestral Cletocamptinae subfam. nov.

The architecture of the mandibular palp of *Cletocamptus* is variable and underwent considerable reduction as has been detailed above. Briefly, the mandibular palp of the ancestral *Cletocamptus* might have been two-segmented, i.e., basis and endopod separated, being the basis and endopod equipped with one and two setae respectively, and the exopod represented by one seta (Fig. 7F). The ancestral mandibular palp underwent several changes (Fig. 7G–L) across two main lineages, the *retrogressus-confluens-dominicanus*-lineage (rcd-lineage; Fig. 7J, K, L), and the *assimilis-pilosus-albuquerquensis*-lineage (apa-lineage; Fig. 7G–I) (see also above). The rcd-lineage is defined upon the synapomorphic loss of the exopodal seta; *C. confluens* and *C. dominicanus* underwent secondary fusion of the basis and endopod which is regarded as synapomorphic for them, and *C. dominicanus* underwent secondary apomorphic reduction of the palp. The apa-lineage is defined here upon the synapomorphic absorption of the basis into the coxa and incorporation of the exopodal seta into the latter. *Cletocamptus pilosus* (Fig. 7H) underwent further loss of one of the endopodal setae which is considered here apomorphic for the species. *Cletocamptus albuquerquensis*, *C. gomezi*, *C. samariensis*, *C. stimpsoni*, and *C. tainoi* (Fig. 7I) underwent secondary loss of the exopodal seta which is regarded here as synapomorphic for them.

The maxillule is probably the most complicated buccal appendage in Harpacticoida due to the fusion of the basis, endopod and exopod in many taxa, which makes difficult the homologation and correct counting of the setal elements. Pending a more detailed and precise study of this appendage in *Cletocamptus*, the coxal endite possesses two setae, and the basis, the endopod and exopod are fused into one single unit, with three setae representing each of them. On the other hand, a core of species, C. *assimilis*, *C. axi*, *C. cecsurirensis*, *C. deborahdexterae*, *C. fourchensis*, *C. levis*, *C. nudus*, *C. samariensis*, *C. schmidti*, *C.*, and *C. sinaloensis*, share the presence of a very strong

spinulose ventral seta on the praecoxal arthrite, which is regarded here as derived within the genus (the condition in *C. gomezi* is inconclusive; a similar seta is present in some species of *Cletocamptoides* gen. nov.). On the contrary, a visibly slenderer seta in the other species of the genus is regarded here as the plesiomorphic condition (a similar seta is present in *C. merbokensis* comb. nov.).

The maxilla and maxilliped retained the plesiomorphic architecture of the Cletocamptinae subfam. nov. as described above.

The P1 ENP of *Cletocamptus* is two-segmented and non-prehensile. As said above, this is the derived condition within Canthocamptidae as opposed to the plesiomorphic prehensile endopod (see George 2020). Gómez et al. (2017) gave a list of species of *Cletocamptus* armed with setae with comb tips on P2–P4 EXP2. The presence of such setae is deemed to be derived as opposed to the whip-like setae, but this condition seems to occur widely in the Canthocamptidae.

Sexual dimorphism in *Cletocamptus* is expressed in a variety of modifications. These have been outlined above. The most common modifications in the appendages of the males include the subchirocer antennule, the basis of P1 with one inner distal process, the inner spine on P2 ENP2 with several degrees of modifications, the three-segmented P3 ENP with an inner apophysis on second segment and two apical setae on the distal segment, and the fused exopod and baseoendopod of P5. Deviations occur in some species though. The shape of the outer spine on P2 ENP2 varies from slightly modified as in *C. albuquerquensis*, *C. cecsurirensis*, *C. confluens*, *C. dominicanus*, *C. retrogressus*, *C. samariensis*, and *C. tainoi*, to moderately modified as in *C. axi*, *C. deborahdexterae*, *C. fourchensis*, *C. goenchim*, *C. gomezi*, *C. levis*, *C. schmidti*, *C. spinulosus*, *C. stimpsoni*, and *C. tertius*, and strongly modified into a recurved spine as in *C. pilosus*, and *C. sinaloensis*. The inner spine on the male P2 ENP2 is not dimorphic in *A. neotropica* and *Cletocamptoides* gen. nov., and the sexually modified inner spine on P2 ENP2 is regarded here as an apomorphy for *Cletocamptus*. The male P3 ENP in most species retained the three-segmented condition with an inner apophysis on second segment which is regarded here as plesiomorphic, but the second and third segments underwent fusion leading a two-segmented ramus with the inner apophysis well-developed and situated medially on second segment as in *C. dominicanus*, or very short and recurved, and situated subdistally on second segment as in *C. albuquerquensis*, *C. chappuisi*, *C. confluens*, and *C. tainoi*. The former division between the second and third segments of the P3 ENP is still visible in *C. dominicanus*, which also possesses very long asprothekes (see Gómez et al. 2017). A similar condition of the male P3 ENP, two-segmented with inner apophysis medially on second segment, is present also in *A. neotropica*. The P3 ENP2 and ENP3 of *C. albuquerquensis*, *C. chappuisi*, and *C. tainoi* are also fused, but the inner apophysis migrated to a subapical position and underwent extreme reduction, and became recurved. A similar condition is present in *C. helobius* comb. nov. The condition of the male P3 ENP of *C. confluens* is unique in that the second segment possesses and additional outer apophysis whose female homologue is uncertain. The pair of male P5 are fused medially in most species, but the exopod and endopod are separated in *C. axi*, *C. cecsurirensis*, *C. retrogressus*, and

C. schmidti. The significance of this is not clear, but this could be due to character reversal. The male P6 of *Cletocamptus* is an unarmed articulated plate. A small seta has been observed issuing from P6 in some species, but the presence of this seta is most probably due to intraspecific variability. Several sexual modifications are present also in the relative length and shape of P2 EXP and/or P3–P4 EXP as in *C. retrogressus*, *C. confluens*; *C. albuquerquensis*, *C. samariensis*, *C. spinulosus*, *C. tainoi*, and *C. trichotus*. Similar sexual dimorphism in P4 EXP in which the first segment is visibly more robust has been documented for *Amphibiperita* (see Fiers and Rutledge 1990).

The genus *Amphibiperita*

The genus *Amphibiperita* has been diagnosed by Fiers and Rutledge (1990). They (Fiers and Rutledge 1990) gave a lengthy discussion on the relationships between *Mesochra* and *Amphibiperita* and justified the creation of the latter for *M. neotropica* Jakobi, 1956. Briefly, Fiers and Rutledge (1990) removed *M. neotropica* from *Mesochra* based on the sexual dimorphism of P4 EXP, lack of antennal exopod, reduced mandibular palp, number of setae on the endopods of swimming legs (lack of the outer element on ENP2), and shape of the female genital field. Fiers and Rutledge (1990) commented on the uniqueness of the shape of the sexually dimorphic male P4 EXP1, but similar dimorphism is present in some species of *Cletocamptus*, pointing to a probable sister-group relationship between these two genera, which can be reinforced by the synapomorphic sexually dimorphic rostrum in both genera. Fiers and Rutledge (1990) also commented on the unique lack of the outer subdistal element of P1–P4 ENP2 (Fiers and Rutledge (1990) explicitly included here the P1 ENP, but this ramus is prehensile in *Amphibiperita*, with ENP2 being armed with a distal outer claw, a distal inner bipinnate seta, and an inner small slender seta, and in our opinion, the inclusion of P1 ENP in Fiers and Rutledge's (1990) comment is not correct and is most probably a slip of the pen). On the other hand, the subdistal outer element on P2–P4 ENP2 is also missing in *C. merbokensis* comb. nov., being the supernumerary setae in *A. neotropica* the main difference between both species (three, four, and three elements in total in P2–P4 ENP2 in *A. neotropica*, but two, two, and two setae in P2–P4 ENP2 in *M. merbokensis* comb. nov.). Also, the complement armature of P4 ENP2 or only segment in the Cletocamptinae subfam. nov. as defined here is consistently composed of two apical elements only in all but in *A. neotropica*, which possesses one inner additional seta. As noted above, sexual dimorphism in *Amphibiperita* is expressed in the antennule, rostrum, segmentation of the urosome, P5, P6, and more importantly in the shape of the P4 EXP1 and modification of the P3 ENP. Some comments on the dimorphic P4 EXP1 and P3 ENP, and rostrum were given above. The male P5 of *Amphibiperita* follows the general pattern of *Cletocamptinae* subfam. nov., i.e., exopod and endopod fused and both legs fused medially into an elongate plate with three endopodal and three exopodal setae. On the contrary, the baseoendopod and exopod are separated in the female P5 and is regarded here as primitive within the new subfamily.

Karaytuğ and Huys' (2004) *Mesochra* group (see above) was proposed for marine and brackish canthocamptids in which the male P6 is represented by unarmed membranous flaps, and the female P6 is represented by one to three setae (*Mesochra*, *Amphibiperita*, *Psammocamptus*, *Bathycamptus*, *Mesopsyllus*, *Isthmiocaris*, *Hemimesochra*, *Poria*, *Perucamptus*, *Pusillargillus*, *Taurocletodes*, and *Parepactophanes*) as opposed to most freshwater canthocamptids in which the male sixth legs bear two or three well-developed setae (Karaytuğ and Huys 2004, and references therein). *Cletocamptus* and *Cletocamptoides* gen. nov. should be added to this list. The significance of the occasional presence of one seta in some species of *Cletocamptus* is still controversial (see above).

The genus *Cletocamptoides* gen. nov.

The ancestral Cletocamptinae subfam. nov. lack somitic constrictions between somites (see above). The body shape of *Cletocamptoides* gen. nov. is cletodid-like, i.e., body somites clearly separated by somitic constrictions, and is a probable apomorphy for the new genus. On the other hand, *C. merbokensis* comb. nov. is the only species with integumental sensillum-bearing socles along the posterior margin of pro- and urosomites (except anal somite). However, the presence of integumental sensillum-bearing socles are deemed to be apomorphic for *C. merbokensis* comb. nov., and do not seem to indicate a close relationship with the Cletodidae.

The posterior margin of body somites of most canthocamptid genera can be plain, finely or deeply serrate, or with long slender spinules (see above). The posterior margin of the body somites of *Cletocamptoides* gen. nov. is finely serrate and is regarded here as plesiomorphic within the Cletocamptinae subfam. nov.

The condition of the antennary exopod and the mandibular palp of *C. merbokensis* comb. nov. are the most primitive within *Cletocamptoides* gen. nov. The antennary exopod of *C. merbokensis* comb. nov. is one-segmented and elongate, and bears three setae (one lateral, two distal); the antennary exopod of *C. helobius* comb. nov. and *C. biushelo* sp. nov. is reduced to one minute segment bearing only one seta. Similar antennary exopods are also found in Cletodidae.

The condition of the mandibular palp is more primitive in *C. merbokensis* comb. nov. than in the other two species of the genus. The mandibular palp of *C. merbokensis* comb. nov. possesses five setae; three setae are present in *C. helobius* comb. nov., and *C. biushelo* sp. nov. Besides the supernumerary setal complement in *C. merbokensis* comb. nov. relative to the other two species of the new genus, the basis and exopod are still discernible in the former species, being the inner – basal – extension armed with two setae; the basis of the mandibular palp of *C. helobius* comb. nov. and *C. biushelo* sp. nov. is completely absorbed into the palp but is still discernible by the presence of one inner seta. The exopod of the mandibular palp of *C. merbokensis* comb. nov. is indicated by a small outer protuberance with one seta; the exopod in *C. helobius* comb. nov. and *C. biushelo* sp. nov. underwent complete reduction and is not discernible. The two apical setae on the mandibular palp of these three species are regarded here as endopodal, and judging by their relative lengths, being the inner seta visibly shorter than the outer, both

setae are homologous in these three species and in those species with similar armature (see above). The one-segmented condition of the mandibular palp is the most common in the Cletodidae, but the basal, endopodal and/or exopodal setae are still discernible in some species (e.g., *Paracrenhydrosoma normani* Gee, 1999b); the basis and endopod are separated, and the exopod is absorbed into the basis and is represented by a seta in *Pyrocletodes* Coull, 1973 (e.g., *P. coulli* Dinet, 1976); uniramous mandibular palps (basis and endopod separated) without any trace of the exopod are present also in some species of *Paracrenhydrosoma* (e.g., *P. cornuta* Kornev & Chertoprud, 2008, *P. kiai* Song, Dahms, Lee, Ryu & Khim, 2014), and in the monotypic genus *Nannopodella* Monard, 1928.

The unisetose condition of the maxillipedal syncoxa is present in most Cletocamptinae subfam. nov., and it is unarmed only in *C. merbokensis* comb. nov. and *C. helobius* comb. nov. for which is regarded here as apomorphic. Unarmed maxillipedal syncoxae are also present in species of some other canthocamptids e.g., *Attheyella*, *Lessinocamptus*, *Paramoriaropsis* Brancelj, 1991, *Pordfus* Özdikmen, 2008, and *Termomesochra* Itô & Burton, 1980 (Canthocamptinae), and *Stygepactophanes* and *Epactophanes* (Epactophaninae); the maxillipedal syncoxa is unisetose in the Cletodidae (George 2020).

The P1 ENP of *Cletocamptoides* gen. nov. displays the derived two-segmented condition (see also George (2020) for a detailed explanation on the plesiomorphic prehensile versus the derived non-prehensile P1 ENP in Podogennonta), but the armature complements of P2 and P3 of *C. helobius* comb. nov. and *C. biushelo* sp. nov. display a more primitive trisetose condition of P2–P3 ENP2, relative to the bisetose more derived condition of P2–P3 ENP2 of *C. merbokensis* comb. nov. Fiers and Rutledge (1990) noticed the lack of a subdistal outer element on P3–P4 ENP2 and used that character to differentiate *Amphibiperita* from *Mesochra*. The same condition is present in *C. merbokensis* comb. nov.

One-segmented P4 endopods are present in species of some other canthocamptids, e.g., *Antrocamptus* Chappuis, 1957, *Australocamptus* Karanovic, 2004, *Gulcamptus* Miura, 1969, *Hypocamptus*, *Lessinocamptus* Stoch, 1997, *Morariopsis*, and *Elaphoidella* (Canthocamptinae), *Itunella* and *Isthmiocaris* (Hemimesochrinae), and *Stygepactophanes* Moeschler & Rouch, 1984 and *Epactophanes* (Epactophaninae), but as far as we know from the literature available, it is an elongate and well-developed ramus. Within the new subfamily, a one-segmented P4 ENP is present also in *C. dominicanus*, but it is elongated. The P4 ENP of *Cletocamptoides* gen. nov. is one-segmented but it has undergone extreme reduction and is an apomorphy, and probable autapomorphy, detected for the new genus.

Both rami of P5 are fused and separated from the supporting somite in the females and males of the genera attributed to the Cletocamptinae subfam. nov., except for the female P5 of *Amphibiperita* whose female P5 EXP is separated from the baseoendopod. Both P5 are fused in the males, except for some species of *Cletocamptus* (e.g., *C. axi*, *C. cecsurirensis*, *C. retrogressus* and *C. schmidti*), and *C. helobius* comb. nov. The male of *C. merbokensis* comb. nov. displays the more derived condition of P5, being completely absorbed into the somite, and is considered a potential apomorphy for the species. The male and female P5 of *C. helobius* comb. nov. and *C. biushelo* sp. nov. resembles

those of *C. dominicanus*, *C. albuquerquensis*, *C. confluens*, *C. tainoi*, and most probably *C. chappuisi*, in that both rami are hardly discernible and are separated only by a superficial shallow notch. A similar P5 is present also in *Carolinicola* Huys & Thistle, 1989 (Hemimesochrinae). The structure of the cletodid P5 is variable; the endopodal lobe and the basis can be fused or separated, and the exopod can be fused to or separated from the baseoendopod (George 2020).

The *Mesochra* group as defined by Karaytuğ and Huys (2004) (see above) is characterized by the male and the female P6 being represented by unarmed membranous flaps, and by one to three setae, respectively. Besides the twelve genera attributed to this species group by Karaytuğ and Huys (2004) (see above), *C. merbokensis* comb. nov. also belongs to this group. The presence of such male P6 in different lineages could be the result of the artificial nature of the canthocamptid subfamilies, but it is most probably due to convergent evolution. The uni-, bi-, or trisetose condition of the female P6 is widely distributed in the family.

Acknowledgements

Thanks go to Abraham Guerrero Ruíz (Centro de Investigación en Alimentación y Desarrollo, Unidad Mazatlán) and Sergio Rendón Rodríguez (Instituto de Ciencias del Mar y Limnología, Unidad Académica Mazatlán) for their help during the sampling campaigns, and to Nataly Ortíz Gálvez and Ángel A. Valenzuela Cruz for their help during the sampling campaigns and for processing the sediment samples. We are grateful to Paulo H. C. Corgosinho, Süphan Karaytuğ for their constructive criticism and comments to the first draft of the manuscript. This is a contribution to project IN202019 Biodiversidad de la meiofauna en un ecosistema costero contaminado del sur de Sinaloa: un enfoque integrativo de técnicas taxonómicas clásicas y moleculares financed by the Programa de Apoyo a Proyectos de Investigación e Innovación Tecnológica (DGAPA-PAPIIT) of the Universidad Nacional Autónoma de México.

References

Apostolov A (1984) Sur la présence de *Cletocamptus deitersi* (Richard, 1897) (Copepoda, Harpacticoida) à Cuba. Travaux du Museum d'Histoire Naturelle "Grigore Antipa" 26: 7–10.

Becker K-H (1979) Eidonomie und taxonomie abyssaler Harpacticoidea (Crustacea, Copepoda) Teil II. Paramesochridae, Cylindropsyllidae und Cletodidae. "Meteor" Forschungsergebnisse Reihe D 31: 1–37.

Boeck A (1865) Oversigt over de ved Norges Kyster iagttagne Copepoder henhørende til Calanidernes, Cyclopidernes og Harpactidernes Familier. Forhandlinger i Videnskabs-Selskabet i Kristiania 1864: 226–282.

Boeck A (1872) Nye Slaegter og Arter af Saltvands-Copepoder. Forhandlinger i Videnskabs-Selskabet i Kristiana 1872: 35–60.

Borutzky EV (1931) Materialien zur Harpacticidenfauna des Baikalsees. II. Zoologischer Anzeiger 93: 263–273.

Borutzky EV (1952) 3 Fauna SSSR. Rakoobraznye. Harpacticoida presnykh vod. [Fauna of U.S.S.R. Crustacea. Freshwater Harpacticoida]. Izdatel'stvo Akademii Nauk SSSR, Moscow, 424 pp. [in Russian; English translation by Mercado]

Bowman TE, Abele LG (1982) Classification of the recent Crustacea. In: Bliss DE, Abele LG (Eds) The Biology of Crustacea 1: Systematics, the fossil record, and biogeography. Academic Press, New York, 1–27.

Boxshall GA, Halsey SH (2004) An introduction to copepod diversity. Vols. I & II. The Ray Society, London, 966 pp.

Brady GS (1872) Contributions to the study of the Entomostraca. No. VII. A list of the non-parasitic marine Copepoda of the north-east coast of England. Annals and Magazine of Natural History 4: 1–17. https://doi.org/10.1080/00222937208696629

Brady GS (1880) 2 A monograph of the free and semi-parasitic Copepoda of the British Islands. The Ray Society, London, 182 pp. https://www.biodiversitylibrary.org/item/67810#page/7/mode/1up

Brady GS (1896) On entomostraca collected in the Solway district and at Seaton Sluice, Northumberland, during the summer of 1894. Natural History Transactions of Northumberland 13: 19–33.

Brady GS, Robertson D (1873) Contributions to the study of the Entomostraca. No. VIII. On marine Copepoda taken in the west of Ireland. Annals and Magazine of Natural History 12: 126–142. https://doi.org/10.1080/00222937308680724

Brady GS, Robertson D (1876) Report on dredgings off the coast of Durham and North Yorkshire in 1874. Report of the British Association for the Advancement of Science held at Bristol in August 1875 1 & 2: 185–199.

Brancelj A (1991) *Paramorariopsis anae* gen. n., sp. n. and the female of *Ceuthonectes rouchi* Petkovski, 1984 - 2 Interesting Harpacticoids (Copepoda, Crustacea) from Caves in Slovenia (NW Yugoslavia). Stygologia 6: 193–200.

Brehm V (1936) Mitteilungen von den Forschungsreisen Prof. Rahms. Mitteilung VII. Schlußmitteilung über Cladoceren und Copepoden.-Über den Formenkreis de *Delachauxiella trigonura* (Ekman). *Macrothrix atahualpa* nov. spec. und *Godetella*. Zoologischer Anzeiger 115: 317–325.

Brehm V (1965) Bericht über eine unvollendet gebliebene Untersuchung der Argentinischen Kopepodenfauna. Sitzungsberichte der Mathemathisch-naturwissenschaftlichen Klasse, Abteilung 1 174: 1–15. https://doi.org/10.1007/978-3-662-26601-4_1

Burgess R (2001) An improved protocol for separating meiofauna from sediments using colloidal silica sols. Marine Ecology Progress Series 214: 161–165. https://doi.org/10.3354/meps214161

Chang CY (2013) A new species of *Cletocamptus* Copepoda (Harpacticoida, Canthocamptidae) from salt marshes in Korea. Animal Systematics, Evolution and Diversity 29: 227–237. https://doi.org/10.5635/ASED.2013.29.3.227

Chappuis PA (1924) Descriptions préliminaires de copépodes nouveaux de Serbie. Buletinul Societatii de Stiinte din Cluj, România 2: 27–45.

Chappuis PA (1929a) Die Unterfamilie der Canthocamptinae. Archiv für Hydrobiologie 20: 471–516.

Chappuis PA (1929b) Révision du genre *Canthocamptus* Westwood (Note peréliminaire). Buletinul Societăţii de Stiinţe din Cluj 4: 41–50.

Chappuis PA (1930) Notes sur les copépodes. 4. *Antarctobiotus koenigi* (Pesta). Buletinul Societatii de Stiinte din Cluj 5: 62–64.

Chappuis PA (1932) Canthocamptinae nouveaux d'Afrique occidentale française. (Descriptions préliminaires). Buletinul Societatii de Stiinte din Cluj 6: 413–420.

Chappuis PA (1933) Copépodes (première série). Avec l'énumération de tous les copépodes cavernicoles connus en 1931. Archives de Zoologie Expérimentale et Générale 76: 1–57.

Chappuis PA (1934) Süsswasser Harpacticiden aus dem Hawaiischen inselgebiet. Bulletin de la Société des Sciences de Cluj (Roumanie) 7: 631–635.

Chappuis PA (1936) Brasilianische ruderfusskrebse (Crustacea Copepoda), gesammelt von Herrn Dr. Otto Schubart. IV. Mitteilung. Bulletin de la Société des Sciences de Cluj (Roumanie) 8: 450–461.

Chappuis PA (1957) Les crustacés de la grotte de Gourgue près Montardi (Ariège). Notes Biospéologiques 11: 127–131.

Claus C (1863) Die frei lebenden Copepoden mit besonderer Berucksichtigung der Fauna Deutschlands, der Nordsee und des Mittelmeeres. Verlag von Wilhelm Engelmann, Leipzig, 230 pp. https://doi.org/10.5962/bhl.title.58676

Conroy-Dalton S (2001) Systematics and phylogeny of the Ancorabolidae (Copepoda: Harpacticoida). II. Polyphyly of *Polyascophorus* and description of *Arthuricornua*, new genus. Journal of Crustacean Biology 21: 170–191. https://doi.org/10.1163/20021975-99990115

Coull BC (1973) Meiobenthic Harpacticoida (Crustacea, Copepoda) from the deep sea off North Carolina I. The genera *Hemimesochra* Sars, *Paranannopus* Lang, and *Cylindronannopus* n. g. Transactions of the American Microscopical Society 92: 185–198. https://doi.org/10.2307/3224915

Daday E (1902) Mikroskopische Süsswasserthiere aus Patagonien. Természetrajzi Füzetek 25: 201–310.

Delachaux T (1917) Neue Süßwasserharpacticiden aus Südamerika, gesammelt von Herrn Ingenieur E. Godet in den peruanischen Anden. Zoologischer Anzeiger 49: 315–335.

Dinet A (1976) Sur une nouvelle forme du genre *Pyrocletodes* Coull, 1973 (Copepoda, Harpacticoida) à position systématique incertaine. Bulletin de la Société Zoologique de France 100: 437–442.

Dussart BH (1974) Contribution à l'étude des Copépodes des eaux douces d'Éthiopie. Bulletin de l'Institut Fondamental d'Afrique Noire 36, sér. A: 92–116.

Dussart BH, Frutos SM (1986) Sur quelques copépodes d'Argentine. 2. Copépodes du Paraná Medio. Revue d'Hydrobiologie Tropicale 19: 241–262.

Felsenstein J (2005) PHYLIP (Phylogeny Inference Package) version 3.6. Distributed by the author. Department of Genome Sciences, university of Washington, Seattle.

Fiers F, Rutledge P (1990) Harpacticoid copepods associated with *Spartina alterniflora* culms from the marshes of Cocodrie, Louisiana (Crustacea, Copepoda). Bulletin de l'Institut Royal des Sciences Naturelles de Belgique Biologie: 105–125.

Fleeger JW (1980) Morphological variation in *Cletocamptus* (Copepoda: Harpacticoida) with description of a new species from Louisiana salt marshes. Transactions of the American Microscopical Society 99: 25–31. https://doi.org/10.2307/3226077

Fuentes-Reinés JM, Zoppi de Roa E, Torres R (2015) A new species of *Cletocamptus* Schmankewitsch, 1875 (Crustacea, Copepoda, Harpacticoida) and the description of the male of *C. nudus* from Colombia. Pan-American Journal of Aquatic Sciences 10: 1–18.

Gee JM (1999a) A new species of *Cletocamptus* Schmankewitsch 1875 (Copepoda; Harpacticoida) from a mangrove forest in Malaysia. Hydrobiologia 412: 143–153.

Gee JM (1999b) A revision of *Acrenhydrosoma* (Copepoda, Harpacticoida) with the establishment of *Dyacrenhydrosoma* gen. nov. and *Paracrenhydrosoma* gen. nov. and descriptions of two new species. Cahiers de Biologie Marine 40: 337–357.

George KH (2020) Restructuring the Ancorabolidae Sars (Copepoda, Harpacticoida) and Cletodidae T. Scott, with a new phylogenetic hypothesis regarding the relationships of the Laophontoidea T. Scott, Ancorabolidae and Cletodidae. Zoosstematics and Evolution 96: 455–498. https://doi.org/10.3897/zse.96.51349

George KH, Schminke HK (2003) *Isthmiocaris longitelson* gen. et sp. nov., a strongly derived harpacticoid (Copepoda) from the Magellan region, and its systematic affinities to certain "canthocamptid" taxa. Journal of Crustacean Biology 23: 119–130. https://doi.org/10.1163/20021975-99990321

Gómez Noguera SE, Fiers F (1997) Two new species of *Mesochra* Boeck, 1865 (Copepoda: Harpacticoida) from a costal lagoon in Sinaloa State, Mexico. Bulletin de l'Institut Royal des Sciences Naturelles de Belgique 67: 39–56.

Gómez S (2005) New species of *Cletocamptus* and a new and fully illustrated record of *C. sinaloensis* (Copepoda: Harpacticoida) from Brazil. Journal of Natural History 39: 3101–3135. https://doi.org/10.1080/17415970500264335

Gómez S (2020) On some new species of Stenheliinae Brady, 1880 (Copepoda: Harpacticoida: Miraciidae) from north-western Mexico, with the proposal of *Lonchoeidestenhelia* gen. nov. Zookeys 987: 41–79. https://doi.org/10.3897/zookeys.987.52906

Gómez S, Fleeger JW, Rocha-Olivares A, Foltz D (2004) Four new species of *Cletocamptus* Schmankewitsch, 1875, closely related to *Cletocamptus deitersi* (Richard, 1897) (Copepoda: Harpacticoida). Journal of Natural History 38: 2669–2732. https://doi.org/10.1080/0022293031000156240

Gómez S, Gee JM (2009) On four new species of *Cletocamptus* Shmankevich, 1875 (Copepoda: Harpacticoida) from inland waters of Argentina. Journal of Natural History 43: 2853–2910. https://doi.org/10.1080/00222930903374171

Gómez S, Gerber R, Fuentes-Reinés JM (2017) Redescription of *Cletocamptus albuquerquensis* and *C. dominicanus* (Harpacticoida: Canthocamptidae *incertae sedis*), and description of two new species from the US Virgin Islands and Bonaire. Zootaxa 4272: 301–359. https://doi.org/10.11646/zootaxa.4272.3.1

Gómez S, Ingole B, Sawant M, Singh R (2013) *Cletocamptus goenchim* sp. nov., a new harpacticoid (Copepoda: Harpacticoida) from India. Proceedings of the Biological Society of Washington 126: 259–275. https://doi.org/10.2988/0006-324X-126.3.259

Gómez S, Scheihing R, Labarca P (2007) A new species of *Cletocamptus* (Copepoda: Harpacticoida) from Chile and some notes on *Cletocamptus axi* Mielke, 2000. Journal of Natural History 41: 39–60. https://doi.org/10.1080/00222930601141476

Gurney R (1927) Prof. Labbés Copepod 'Allomorphs'. Nature 120: 295–296. https://doi.org/10.1038/120295b0

Gurney R (1932) The British fresh-water Copepoda. II. Harpacticoida. The Ray Society, London, 336 pp. https://doi.org/10.5962/bhl.title.82138

Hamond R (1973) The harpacticoid copepods (Crustacea) of the saline lakes in Southeast Australia, with special reference to the Laophontidae. Records of the Australian Museum 28: 393–420. https://doi.org/10.3853/j.0067-1975.28.1973.406

Hamond R (1987) Non-marine copepods of Australia. I. Canthocamptidae of the genus *Canthocamptus* Westwood s. lat. and *Fibulacamptus*, gen. nov., and including the description of a related new species of *Canthocamptus* from New Caledonia. Invertebrate Systematics 1: 1023–1047. https://doi.org/10.1071/IT9871023

Herbst VH V (1960) Copepoden (Crustacea, Entomostraca) aus Nicaragua und Südperu. Gewasser und Abwasser 27: 27–54.

Herrick CL (1894) Microcrustacea from New Mexico. Zoologischer Anzeiger 18: 40–47.

Huelsenbeck JP, Ronquist F (2001) MRBAYES: Bayesian inference of phylogeny. Bioinformatics 17: 754–755. https://doi.org/10.1093/bioinformatics/17.8.754

Huys R (2009) Unresolved cases of type fixation, synonymy and homonymy in harpacticoid copepod nomenclature (Crustacea: Copepoda). Zootaxa 2183: 1–99. https://doi.org/10.11646/zootaxa.2183.1.1

Huys R, Boxshall GA (1991) Copepod evolution. The Ray Society, London, 468 pp. https://doi.org/10.4319/lo.1993.38.2.0478

Huys R, Conroy-Dalton S (2006) Revision of the genus *Evansula* T. Scott, 1906 (Copepoda, Harpacticoida, Cylindropsyllidae) with a description of three new species. Zoological Journal of the Linnean Society 147: 419–472. https://doi.org/10.1111/j.1096-3642.2006.00227.x

Huys R, Gee J, Moore C, Hamond R (1996) Marine and brackish water harpacticoid copepods. Part 1. In: Barnes R, Crothers J (Eds) Synopses of the British fauna (New Series). Published for The Linnean Society of London and The Estuarine and Coastal Sciences Association by Field Studies Council Shrewsbury, London, 352 pp.

Huys R, Kihara TC (2010) Systematics and phylogeny of Cristacoxidae (Copepoda, Harpacticoida): a review. Zootaxa 2568: 1–38. https://doi.org/10.11646/zootaxa.2568.1.1

Huys R, Thistle D (1989) *Bathycamptus eckmani* gen. et spec. nov. (Copepoda, Harpacticoida) with a review of the taxonomic status of certain other deepwater harpacticoids. Hydrobiologia 185: 101–126. https://doi.org/10.1007/BF00010809

Itô T, Burton JJS (1980) A new genus and species of the family Canthocamptidae (Copepoda, Harpacticoida) from a hot spring at Dudun Tua, Selangor, Malaysia. Zoologische Jahrbücher, Abteilung für Systematik 107: 1–31.

Jakobi H (1956) Novas espécies de Harpacticoidea (Copepoda-Crustacea) provenientes de regiões de água salobra da costa São Paulo-Paraná. (Neue Harpacticoiden-Arten (Copepoda-Crustacea) aus den Brackwassergebieten der Küste São Paulo-Paraná). Dusenia 7: 159–171.

Karanovic T (2004) Subterranean copepods (Crustacea, Copepoda) from arid Western Australia. Crustaceana Monograph, Brill, Leiden, 366 pp. https://doi.org/10.1163/9789047412779

Karaytuğ S, Huys R (2004) Taxonomic position of and generic distinction between *Parepactophanes* Kunz, 1935 and *Taurocletodes* Kunz, 1975 (Copepoda, Canthocamptidae *incertae sedis*), with description of a new species from the Black Sea. Zoological Journal of the Linnean Society 140: 469–486. https://doi.org/10.1111/j.1096-3642.2003.00101.x

Kiefer F (1929) Eine neue Harpacticoiden-Form aus Südafrika: *Cletocamptus trichotus* n. sp. Zoologischer Anzeiger 84: 21–23.

Kiefer F (1933) Über zwei Arten der Gattung *Cletocamptus* Schmankewitsch (Copepoda Harpacticoida). Zoologischer Anzeiger 105: 141–144.

Kiefer F (1934) Neue Ruderfußkrebse von der Insel Haiti. Zoologischer Anzeiger 108: 227–233.

Kiefer F (1936) Freilebende Süß- und Salzwassercopepoden von der Insel Haiti. Mit einer Revision der Gattung *Halicyclops* Norman. Archiv für Hydrobiologie 30: 263–317.

Kiefer F (1957) Freilebende Ruderfußkrebse (Crustacea Copepoda) aus einigen ostanatolischen Seen. Zoologischer Anzeiger 159: 25–33.

Klie W (1929) Die Copepoda Harpacticoida der südlichen und westlichen Ostsee mit besonderer Berücksichtigung der Sandfauna der Kieler Bucht. Zoologische Jahrbücher, Abteilung fur Systematik, Ökologie und Geographie der Tiere 57: 329–386.

Kornev PN, Chertoprud EC (2008) Copepod crustaceans of the order Harpacticoida of the White Sea: morphology, systematics, ecology. Biology Faculty MSU (Ed.) Tovarishchestvo Nauchnikh Izdanii KMK, Moscow, 379 pp.

Kunz H (1935) Zur Ökologie der Copepoden Schleswig-Holsteins und der Kieler Bucht. Schriften des Naturwissenschaftlichen Vereins für Schleswig-Holstein 21: 84–132.

Kunz H (1975) Harpacticoiden (Crustacea, Copepoda) aus dem Küstengrundwasser der französischen Mittelmeerküste. Zoologica Scripta 3: 257–282. https://doi.org/10.1111/j.1463-6409.1974.tb00822.x

Labbé A (1927) Contributions à l'étude de allélogénèse. III-memoire. L'histoire naturelle des copépodes des Marais Salants du Croisic. Essai de phylogénie expérimentale. Archives de Zoologie Expérimentale et Générale 66: 135–290.

Labbé MA (1926) Les Rhyncoceratinae, groupe nouveau de copépodes harpacticides (note préliminaire). Bulletin de la Société Zoologique de France 51: 441–444.

Lang K (1936) Beiträge zur Kenntnis der Harpacticiden. 6. Bemerkungen über die Familie der Ameiridae Monard. Zoologischer Anzeiger 114: 133–136.

Lang K (1944) Monographie der Harpacticiden (vorläufige Mitteilung). Almqvist & Wiksells Boktryckeri AB, Uppsala, 39 pp.

Lang K (1948) Monographie der Harpacticiden. Vols. I & II. Nordiska Bokhandeln, Stockholm, 1682 pp.

Lang K (1965) Copepoda Harpacticoidea from the Californian Pacific coast. Kungliga Svenska Vetenskapsakademiens Handlingar (4)10: 1–560. http://www.vliz.be/imis/imis.php?refid=78667

Löffler H (1961) Beiträge zur Kenntnis der Iranischen Binnen-gewässer II. Regional-limnologische studie mit besonderer Berücksichtigung der Crustaceenfauna. Internationale Revue der Gesamten Hydrobiologie 46: 309–406. https://doi.org/10.1002/iroh.19610460304

Löffler H (1963) Zur Ostrakoden- und Copepodenfauna Ekuadors. Archiv für Hydrobiologie 59: 196–234.

Loftus WF, Reid JW (2000) Copepod (Crustacea) emergence from soils from Everglades marshes with different hydroperiods. Journal of Freshwater Ecology 15: 515–523. https://doi.org/10.1080/02705060.2000.9663774

Mielke W (1975) Systematik der Copepoda eines Sandstrandes der Nordseeinsel Sylt. Mikrofauna des Meeresbodens 52: 1–134.

Mielke W (2000) Two new species of *Cletocamptus* (Copepoda: Harpacticoida) from Galapagos, closely related to the cosmopolitan *C. deitersi*. Journal of Crustacean Biology 20: 273–284. https://doi.org/10.1163/20021975-99990039

Miura Y (1969) Results of the speleological survey in South Korea 1966. XIV. Subterranean harpacticoid copepods of South Korea. Bulletin of the National Science Museum, Tokyo, Series A, Zoology 12: 241–254.

Moeschler P, Rouch R (1984) Un nouveau genre de Canthocamptidae (Copepoda, Harpacticoidea) des eaux souterraines de Suisse. Revue Suisse de Zoologie 91: 959–972. https://doi.org/10.5962/bhl.part.81592

Monard A (1927) Synopsis universalis generum Harpacticoidarum. Zoologische Jahrbücher, Abteilung für Systematik 54: 139–176.

Monard A (1928) Les harpacticoïdes marins de Banyuls. Archives de Zoologie Expérimentale et Générale 67: 259–443.

Monard A (1935) Étude sur la faune des harpacticoïdes marins de Roscoff. Travaux de la Station Biologique de Roscoff 13: 5–88.

Mrázek A (1893) Beitrag zur Kenntniss der Harpacticidenfauna des Süsswassers. Zoologische Jahrbücher. Abteilung für Systematik, Geographie und Biologie der Tiere 7: 89–130.

Noodt W (1958) Die Copepoda Harpacticoidea des Brandungsstrandes von Teneriffa (Kanarische Inseln). Abhandlungen der Mathematisch-Naturwissenschaftlichen Klasse, Akademie der Wissenschaften und der Literatur in Mainz 1958: 53–116.

Oliveira LP, Krau L, Miranda ASA (1971) Plâncton poluído da Guanabara com copépodos *Cletocamptus* e rotíferos Rotaria. Archivos do Museu Nacional do Rio de Janeiro 54: 55–56.

Özdikmen H (2008) Nomenclatural changes for nine crustacean genera (Crustacea: Copepoda). Munis Entomology and Zoology 3: 265–275.

Özdikmen H (2009) Substitute names for two genera of Harpacticoida (Crustacea: Copepoda). Munis Entomology & Zoology 4: 297–298.

Pesta O (1932) Krebstiere oder Crustacea. I: Ruderfüsser oder Copepoda. 3. Unterordnung: Harpacticoida (1. und 2. Hälfte). In: Dahl F (Ed.) Die Tierwelt Deutschlands und der Angrenzenden Meeresteile nach Ihren Merkmalen und nach Ihrer Lebensweise. Verlag von Gustav Fischer, Jena, 1–164.

Philippi A (1840) Zoologische Bemerkungen. Archiv für Naturgeschichte 6: 181–195. from: https://www.biodiversitylibrary.org/page/7203160

Por F (1960) *Mesopsyllus atargatis* n. g., n. sp., ein neuer Harpacticoide (Crustacea, Copepoda) aus dem Schwarzen Meere. Travaux du Museum d'Histoire Naturelle "Grigore Antipa" 2: 177–181.

Por FD (1968) Copepods of some land-locked basins on the islands of Entedebir and Nocra (Dahlak Archipelago, Red Sea). Sea Fishery Research Station in Haifa Bulletin 49: 37–41.

Por FD (1986) A re-evaluation of the family Cletodidae Sars, Lang (Copepoda, Harpacticoida). Proceedings of the Second International Conference on Copepoda, Ottawa, Canada, 13–17 August 1984, Schriever G, Schminke HK, Shih C-t (Eds) Syllogeus 58: 420–425.

Ranga Reddy Y, Radhakrishna Y (1979) A new record of *Cletocamptus deitersi* (Richard, 1895) (Copepoda: Harpacticoida) from India. Current Science 48(1): 45–45.

Richard J (1897) Entomostracés de l'Amérique du Sud, recuellis par MM. U. Deiters, H. Von Ihering, G. W. Müller et C. O. Poppe. Mémoires de la Société Zoologique de France 10: 263–301.

Ringuelet RA (1958a) Los crustáceos copépodos de las aguas continentales en la República Argentina. Sinopsis sistemática. Contribuciones Científicas de la Facultad de Ciencias Exactas y Naturales de la Universidad de Buenos Aires, Serie Zoología 1: 1–120.

Ringuelet RA (1958b) Primeros datos ecológicos sobre copépodos dulciacuícolas de la República Argentina. Physis 21: 14–31.

Ringuelet RA (1960) Datos de fecundidad en copépodos dulciacuícolas. Physis 21: 316–317.

Ringuelet RA (1962) Rasgos faunísticos de las reservas naturales de la Provincia de Buenos Aires. Physis 23: 83–91.

Ringuelet RA, Moreno I, Feldman E (1967) El zooplancton de las lagunas de la Pampa deprimida y otras aguas superficiales de la llanura bonaerense (Argentina). Physis 27: 187–200.

Rohal M, Thistle D, Easton EE (2016) Extraction of metazoan meiofauna from muddy deep-sea samples: operator and taxon effects on efficiency. Journal of Experimental Marine Biology and Ecology 502: 105–110. https://doi.org/10.1016/j.jembe.2017.01.006

Ruber E, Gilbert A, Montagna PA, Gillis G, Cummings E (1994) Effects of impounding coastal salt marsh for mosquito control on microcrustacean populations. Hydrobiologia 292–293: 497–503. https://doi.org/10.1007/BF00229977

Sars GO (1906) Copepoda Harpacticoida Parts XV & XVI Diosaccidae (concluded), Canthocamptidae (part). An account of the Crustacea of Norway with short descriptions and figures of all the species 5: 173–196.

Sars GO (1909) Copepoda Harpacticoida. Cletodidae (concluded), Anchorabolidae, Cylindropsyllidae, Tachidiidae (part). An account of the Crustacea of Norway with short descriptions and figures of all the species 5: 305–336.

Sars GO (1911) Copepoda Harpacticoida Parts XXXIII & XXXIV Supplement (continued). An account of the Crustacea of Norway with short descriptions and figures of all the species 5: 397–420.

Sars GO (1920) Copepoda Supplement. Parts V & VI. Harpacticoida (continued). An account of the Crustacea of Norway with short descriptions and figures of all the species 7: 53–72.

Schmankevitsch VI (1875) Nekotoryya rakoobraznyya solyano-ozernykh' i presnykh vod' i otneshenie ikh' k' srede. Some Crustacea of salt and freshwater lakes, and their relation to the surrounding environment. Zapiski Novorossiiskago Obshchestva Estestvoispytatelei (= Mémoires de la Société des Naturalistes de la Nouvelle Russie, Odessa) 3: 1–391.

Schmeil O (1894) Einige neue Harpacticiden-Formen des Süsswassers. Zeithschrift für Naturwissenschaften 67: 341–350.

Schriever G (1983) New Harpacticoidea (Crustacea, Copepoda) from the North-Atlantic Ocean. III. New species of the family Cletodidae. Meteor Forschungsergebnisse Reihe D Supplement: 65–83.

Scott T (1892) III Additions to the fauna of the Firth of Forth. Part IV. Annual Report of the Fishery Board for Scotland 10: 244–272.

Scott T (1894) II Additions to the fauna of the Firth of Forth. Part VI. Annual Report of the Fishery Board for Scottland 12: 231–271.

Scott T (1902) Notes on gatherings of Crustacea collected by the fishery steamer "Garland", and the steam trawlers "Star of Peace" and "Star of Hope", of Aberdeen, during the year 1901. Annual Report of the Fishery Board for Scotland. 20: 447–484.

Scott T (1904) On some new and rare Crustacea from the Scottish seas. Reports of the Fishery Board for Scotland 23: 141–153.

Scott T (1906a) A catalogue of the land, fresh-water and marine Crustacea found in the basin of the River Forth and its estuary. II: The Ostracoda, Copepoda, and Cirripedia. Proceedings of the Royal Physical Society of Edinburgh 16: 267–386. https://doi.org/10.5962/bhl.title.53706

Scott T (1906b) LXII. Notes on British Copepoda: change of names. Annals and Magazine of Natural History 7: 458–466. https://doi.org/10.1080/00222930608562556

Scott T, Scott A (1893) On some new or rare Scottish Entomostraca. Annals and Magazine of Natural History 6: 210–215. https://doi.org/10.1080/00222939308677499

Seifried S (2003) Phylogeny of Harpacticoida (Copepoda): revision of "Maxillipedasphalea" and Exanechentera. Cuvillier Verlag, Göttingen, 259 pp.

Shen C-J (1956) On a collection of Copepoda from Chinghai Province and inner Mongolia. Acta Zoologica Sinica 8: 1–12. [In Chinese]

Shen C-J, Sung T (1963) Notes on Copepoda collected from Shigatze and Gyangtse regions in Tibet, China. Acta Zoologica Sinica 15: 79–97. [In Chinese, with English sumary]

Sitjar CC (1988) Crustáceos del arroyo Naposta Grande (Provincia de Buenos Aires, Argentina). Spheniscus 6: 63–72.

Smirnov SS (1946) Novye vidy Copepoda Harpacticoida iz severnogo ledovitogo okeana (New species of Copepoda-Harpacticoida) from the northern Arctic Ocean). Trudy Dreif. Eksped. Glav. na ledokol. Parokh. "G. Sedov" 1937–1940: 231–263. [in Russian]

Song SJ, Dahms HU, Lee CR, Ryu J, Khim JS (2014) A new species of *Paracrenhydrosoma* (Copepoda: Harpacticoida: Cletodidae) from a subtidal muddy bottom of southern Korea, with a key to the species of *Acrenhydrosoma*-complex. Journal of the Marine Biological Association of the United Kingdom 94: 981–991. https://doi.org/10.1017/S0025315414000289

Stěrba O (1968) Neue Harpacticoidea (Crustacea, Copepoda) aus dem asiatischen Teil der Paläarktis. Zoologischer Anzeiger 180: 50–68.

Stoch F (1997) A new genus and two new species of Canthocamptidae (Copepoda, Harpacticoida) from caves in northern Italy. Hydrobiologia 350: 49–61. https://doi.org/10.1023/A:1003072813906

Suárez-Morales E, Barrera-Moreno O, Ciros-Pérez J (2013) A new species of *Cletocamptus* Schmankewitsch, 1875 (Crustacea, Copepoda, Harpacticoida) from a high altitude saline lake in Central Mexico. Journal of Limnology 72: 313–325. https://doi.org/10.4081/jlimnol.2013.e25

Suárez-Morales E, Reid JW, Iliffe TM, Fiers F (1996) Catálogo de los copépodos (Crustacea) continentales de la Península de Yucatán, México. Comisión Nacional para el Conocimiento

y Uso de la Biodiversidad (CONABIO) and El Colegio de la Frontera Sur (ECOSUR), Unidad Chetumal, Mexico City, 296 pp.

Tai AY, Song YZ (1979) Harpacticoida Sars, 1903. In: Shen C-J, Ai-Yun T, Chong-Zhou Z, Zhi-Ying L, Da-Xiang S, Guo-Xiao C (Eds) Freshwater Copepoda. Fauna Sinica, Crustacea. Science Press, Beijing, 450 pp.

Wells JBJ (2007) An annotated checklist and keys to the species of Copepoda Harpacticoida (Crustacea). Zootaxa 1568: 1–872. https://doi.org/10.11646/zootaxa.1568.1.1

Westwood JO (1836) *Cyclops* (Muller). In: Partington CF (Ed.) The British Cyclopaedia of Natural History. Orr & Smith, London, 227–228.

Willey A (1930) Harpacticoid Copepoda from Bermuda. Part I. Annals and Magazine of Natural History 6: 81–114. https://doi.org/10.1080/00222933008673192

WoRMS [Editorial Board] (2021) World Register of Marine Species.

Zamudio-Valdéz JA (1991) Los copépodos de vida libre (Crustacea, Maxillopoda) del Valle de Cuatro Ciénegas, Coahuila, México. Autonomous University of Nuevo León, Monterrey, Mexico, 107 pp.